The effect of particle size on the performance of low-smoke fuels in coal stoves

LP Sumbane-Prinsloo

orcid.org/0000-0003-1039-4405

Dissertation submitted in fulfilment of the requirements for the degree *Master of Engineering* in Chemical Engineering at the North-West University

Supervisor:	Prof JR Bunt
Co-supervisors:	Prof SJ Piketh
	Prof HWJP Neomagus

Graduation May 2018

Student number: 22063560

NWU®
NORTH-WEST UNIVERSITY
NOORDWES-UNIVERSITEIT
UNIBESITI YA BOKONE-BOPHIRIMA

Declaration

I, Lungile P. Sumbane-Prinsloo, hereby declare that this dissertation titled: **"The effect of particle size on the performance of low-smoke fuels in coal stoves"**, submitted in fulfilment of the requirements for the degree Master of Chemical Engineering, is my own work and that where the published work of others has been consulted, appropriate references have been provided. Furthermore, this work has not been submitted to any other tertiary institution and copies submitted for examination are the property of the University.

Signed at Potchefstroon on March 7, 2018

_____

LP Sumbane-Prinsloo

Abstract

The effect of particle size on the performance of low-smoke fuels in coal stoves

The link between exposure to household air pollution (HAP) and ill-health has been consistently drawn in the literature. The World Health Organisation (WHO) places the burden of disease from HAP at an estimated 4.3 million premature fatalities a year; almost 600 000 of these occur in Africa. The 2011 South African census reported that approximately 3.9 million households in the country rely on a form of solid fuel as their primary energy source, despite interventions by government, including the policy of universal electrification. For low-income households in the colder climates of the Highveld, coal is the most common solid fuel which is burnt in a variety of devices, including cast iron stoves. This persistent use of coal is not only associated with poor health, but has also been identified as a major source of local ambient air pollution. A low-smoke fuel (LSF) has been previously considered, at government level, as a way to quell the effects of domestic coal use. This work aimed at determining the effect of the fuel particle size on the performance of such a low-smoke fuel when used in a common cast iron stove.

A bulk coal sample was acquired from one such community and was segregated into its constituent sizes then subjected to partial devolatilisation at 550°C to produce an LSF. Four fuel sizes - 15, 20, 30, and 40 mm, as well as a composite of the sizes - were tested, against their untreated coal analogues, in pre-set combustion tests to evaluate the thermal- and emissions performance of each fuel. Thermal performance assessment metrics included ignition time, water boiling time, and heat transfer- and combustion efficiencies, while the emissions considered were CO, SO_2, NO_x, particulate matter (PM) and volatile organic compounds (VOCs).

Ignition times were found to decrease from coals to LSFs, and to decrease with increasing particle size; the 40mmLSF (a 40 mm devolatilised coal or LSF) ignited twice as fast as the 15mmLSF. The effects of fuel type on the water boiling time were only observed in the later stages of the burn cycle, with the LSF boiling a 2 L batch of water in an average 20 minutes, while the coals reported an average boiling time of 24 minutes. In addition to boiling water faster than the coals, the LSF boiling times were found to decrease with increasing particle size. Heat transfer efficiencies showed no significant variation with fuel type or particle size, with the average efficiency for the coals being 66.4 %, while that of the LSFs was 65.8 %. The fuels' performance was better gauged by the combustion efficiency, which was found to improve marginally from the coal fuels to the LSFs, and to increase with increasing particle size.

Emission factors (EFs) for NO_x and SO_2 were found to depend on the fuel nitrogen and sulphur content as well as the combustion conditions. Increased combustion efficiency, which increased with particle size, was found to lead to higher SO_{2EF} and NO_{xEF}. The PM and VOC emissions showed a strong dependence on the ash content and volatile matter yield, which both increased with increasing particle size. The emission factors of both VOCs and PM were found to be inversely correlated with particle size, and decreased from coals to LSF as a result of the pretreatment.

This work contributes to the emissions and performance inventories from South African domestic coal combustion. The insight gained lends itself to the production of coal alternatives, the pairing of these fuels with suitable combustion devices, and may be consulted as part of the growing body of literature which impacts on low-income household energisation policies and interventions.

Keywords: particle size, coal combustion, low-smoke fuels, cast iron stove, heterogeneous testing protocol

Acknowledgements

I wish to acknowledge the following for their contributions towards the completion of this work:

- My supervisors Professors John Bunt, Hein Neomagus and Stuart Piketh for their guidance and advice over the course of my work. It was a comfort knowing that their combined expertise and guidance was at my disposal.
- The National Research Foundation, which has funded my studies through the free-standing innovation bursary as well as through Prof. Bunt's SARChI chair in coal research,as well as Eskom who have contributed through Prof. Piketh's EPPEI chair.
- Dr. Tafadzwa Makonese whose help with the processing of the combustion test experimental results according to the HTP was invaluable. Dr. Henry Matjie for his assistance in interpreting the mineralogical analyses. Dr D. Branken, Prof. Ray Everson and Dr Oupa for their contributions and advice during our meetings.
- Mr Richhein du Preez, Dr. Roelof Burger of the Climatology Research Group for all their help with building and equipping the testing facility and the patience with which they helped me address the challenges of running a lab. Mr. Joe Mahlalela from the same group who drove all the way to Kwadela on two occasions to fetch my sample, and helped with the weighing of the quartz thimbles prior to and after the combustion tests.
- The fourth years students who had a role in producing the LSFs, Ms Leora Gouws, Mr George Louw, and Mr Ettiene Hattingh, I am very grateful for your coming at awkward hours of the night to babysit the furnace and for your company and assistance during the long combustion tests campaigns.
- Messrs Adrian Brock, Jan Kroeze, Elias Mofokeng, Ted Paarlberg and Jakob Thlone for their involvement in the technical aspects of my work from changing gas cylinders to the production of custom parts for the testing facility. A special thank you to Mrs Rene Bekker, as well as Mrs Erika du Toit, and Mrs Sanet Botes, for their efficient handling of administrative matters over the last two years.
- All my colleagues in the Coal Research Group, for the discussions, especially Mrs Mosele Tsemane and Mr Jandri Ribberink for keeping the office jovial.
- My Mom and Dad for their support and encouragement and for being patient with my absence from home. My darling husband, Phillip, for his help with writing up my MATLAB scripts for the data processing and for proof-reading some of the earlier chapters, but most importantly for his patience and care during the writing up, and the invaluable support for the last two years.

Conferences

2016

L.P., Sumbane, J.R., Bunt, H., Neomagus, S.J., Piketh. Evaluation of a Domestic-Use Low-Smoke Fuel Produced via the Pyrolysis of Lump Coal. *33rd Annual Pittsburgh Coal Conference*, 8-12 August 2016, Cape Town, South Africa

2017

Sumbane, L.P., Piketh, S.J., Bunt, J.R.and Neomagus, H.W.J.P. Evaluating the performance and emission reductions of a coal-derived low-smoke fuel in a conventional household stoves. *25th International Domestic Use of Energy Conference.* 3-5 April 2017, Cape Town, South Africa.

Sumbane-Prinsloo, L.P., Bunt J.R., Neomagus, H.W.J.P., Piketh S.J. Particle size and its effect on the performance of a coal-derived low smoke fuel in a conventional household stove. *Fossil Fuel Foundation Conference on Sustainable Development of Southern Africa's Energy Resources.* 29-30 November 2017, Johannesburg, South Africa.

Contents

Nomenclature

Abbreviations and Acronyms

BLUD	Bottom-lit Updraft fire lighting method
BNM	Basa Njengo Magogo fire-lighting method.
CCT	Controlled Cooking Test
CFB	Circulating Fluidised Bed
CV	Calorific Value
DME	Department of Minerals and Energy of South Africa
EA	Excess Air
EF	Emission Factor
HAP	Household Air Pollution
HTP	Heterogeneous Testing Protocol: see Makonese [2011]
ICS	Improved Cook Stove
KPT	Kitchen Performance Test
LHV	Lower Heating Value
LPG	Liquid Petroleum Gas
LRI	Lower Respiratory Infections
LSF	Low-smoke Fuel
NDIR	Non-Dispersive Infra-red Absorption
NGO	Non Governmental Organisation
PAH	Polycyclic Aromatic Hydrocarbons
PIC	Product of Incomplete Combustion
PM	Particulate Matter
PSD	Particle Size Distribution
TGA	Thermogravimetric Analysis

TLUD	Top-lit Updraft fire lighting method
VOC	Volatile Organic Compounds
WBT	Water Boiling Test
WHO	World Health Organisation
XRD	X-ray Diffraction
XRF	X-ray Fluorescence

Mathematical Symbols

η	Efficiency	%
Cp	Specific Heat Capacity	$J.kg^{-1}.°C^{-1}$
H_{vap}	Latent heat of vapourisation	$kJ.kg^{-1}$
M	Mass	g
P	Power	W
S	Siegert Efficiency	%
T	Temperature	°C
t	time	s

List of Figures

List of Tables

Chapter 1

Introduction

The study will be introduced and framed in this chapter via a review of the issues pertaining to the use of coal as a domestic energy source in the developing world, and in South Africa. Steps taken to reduce the impact of domestic coal use on health and the environment, including previous attempts of producing a low-smoke fuel, will also be reviewed. From this background, the problem statement is presented, along with the aims, objectives, scope and limitations. Lastly, the organisation and structure of the dissertation is presented.

1.1 Introduction and Background

1.1.1 A Portrait on Domestic Coal Combustion in the Developing World

An estimated 2.8 to 3 billion people, globally, do not have access to clean energy sources [Wang *et al.*, 2016; Bruce *et al.*, 2015; Jeuland *et al.*, 2015; Makonese, 2015; Kshirsagar and Kalamkar, 2014; Ezzati, 2005]. Over half of these live in China and India and a fifth in Sub-Saharan Africa [Jeuland *et al.*, 2015; Smith *et al.*, 2013]. Their search for alternatives inadvertently exposes them to household air pollution (HAP). Fuel types used differ between and within countries subject to availability and cost. Coal is a typical choice in China, while charcoal used in East Africa's urban areas. Dung, wood, and, to a lower but still significant degree, coal are used in India [Jeuland *et al.*, 2015; Smith *et al.*, 2013]. This *status quo* is unlikely to change in the near future [Wernecke *et al.*, 2015; Jeuland *et al.*, 2015; Kumar *et al.*, 2013; Ezzati, 2005], making the use of such fuels among the most urgent problems in the developing world [Khandelwal *et al.*, 2016; Naz *et al.*, 2016; Gulia *et al.*, 2015; Smith and Mehta, 2003]. The fuels are burnt in anything from the traditional three-stone fire to rudimentary, and even efficient, cook stoves [Martin *et al.*, 2014]. Exposure to products of incomplete combustion is common when these fuels are used [Gordon *et al.*, 2014; Smith *et al.*, 2013; Smith, 1994], especially in inefficient or badly maintained cooking devices [Martin *et al.*, 2014; Scorgie *et al.*, 2003; Balmer, 2007]. Pollutants such as particulate matter (PM), carbon monoxide (CO), carbon dioxide (CO_2), nitrogen oxides (NOx), sulphur dioxide (SO_2), organic pollutants (*e.g.* benzene, formaldehyde, and poly-aromatic hydrocarbons) and other chemicals are of interest in pollution reduction studies and interventions [Naz *et al.*, 2016; Jeuland *et al.*, 2015; Smith and Mehta, 2003]. HAP-

related pollutants have been consistenlty linked to ill-health in both developed and developing countries [Naz *et al.*, 2016; Muller *et al.*, 2015; Jeuland *et al.*, 2015; Martin *et al.*, 2014; Mabahwi *et al.*, 2014; Barnes *et al.*, 2009; Kampa and Castanas, 2008; WHO, 2002]. Exposure to these pollutants has been shown to cause a host of diseases, including lower respiratory infections (*e.g.* pneumonia), chronic obstructive pulmonary and cardiovasular diseases, and some cancers [Jeuland *et al.*, 2015; Gordon *et al.*, 2014]. Exposure can start in utero (due to the role of women in cooking and other household tasks), and can continue through childhood (Naz *et al.* [2016] report that children are usually with their mothers in the kitchen), and into adulthood [Jeuland *et al.*, 2015]. The World Health Organisation (WHO) reporting on the annual global burden of disease cites 4.3 million premature deaths resulting from HAP [WHO, 2014]. This accounts for 2% of the global burden of disease , or 4% in the developing world, [Kshirsagar and Kalamkar, 2014; Ezzati, 2005] with most of these being in the South East Asian and Western Pacific regions, followed by Africa [Rohra and Taneja, 2016; WHO, 2014].

The domestic energy scenarios in developing countries such as China and India have been extensively covered in the literature. China, with the largest population, accounts for an approximated 25% of global athropogenic carbon-based emissions. A large majority of this, (approximately 70% according to Bi *et al.* [2008] is directly from domestic activites. Lu *et al.* [2011] report that, in 2001, Chinese domestic consuption of coal accounted for only 18% of total coal consuption yet was responsible for 10%, 50%, and 69% of total anthropogenic SO_2, black carbon, and organic carbon emissions repsectively Liu *et al.* [2016]. Some solutions proposed and implemented by the Chinese government include the provision of central heating systems in cities, the replacement of conventional stoves with natural- and liquid petroleum gas stoves with improved cook stoves, or ICSs, [Wang *et al.*, 2016; Hao *et al.*, 2015; Martin *et al.*, 2014], as well as the introduction of more stringent policies on residential coal properties [Li *et al.*, 2016; Muller *et al.*, 2015]. This dependence on solid fuels, wood in this case, is also found in India, the second-most populous country. Among the rural population, over 90% relies on biomass fuels. The use of biomass fuels is also significant in the urban areas; 31% of the urban population use biomass fuels as a primary energy source [Naz *et al.*, 2016]. India bears 28% of the burden of disease from HAP among developing countries, accounting for 4 million HAP-related deaths and about a quarter of the ambient $PM_{2.5}$ (fine particles with diameters less than 2.5 micrometers) emissions [Rohra and Taneja, 2016]. ICSs have been researched, developed, and disseminated in India with a lesser degree of success than in China, owing to low public demand, low adoption rates, and the popularity of the traditional stoves [Khandelwal *et al.*, 2016; Rohra and Taneja, 2016; Martin *et al.*, 2014]. Other interventions involve cleaner fuels such as cow dung used to produce a clean gas for cooking [Kankaria *et al.*, 2014]. Electrical induction cookers have been suggested by Smith [2014], who further cite the high cost as a possible drawback.

1.1.2 Domestic Coal Combustion: A South African Perspective

The energy landscape of South Africa is dominated by coal [Okolo, 2010; Balmer, 2007; Mdluli, 2007; Sowazi and Maake, 2001], which is still an important commodity to the majority of low-income households, where it is used as a primary energy source for cooking, space-, and water heating [Makonese, 2015; Lloyd, 2014]. Wenzel [2006] reports that there are approximately

eighteen million people living in three million informal dwellings, and relying on affordable fuels such as wood and coal, to meet their basic energy needs. Anywhere between one and three million tons of coal are burnt in homes every year [Lloyd, 2014; Sowazi and Maake, 2001]. This data is confirmed by the 2011 census [StatsSA, 2012] which reports approximately 3.9 million of the surveyed households using coal as a primary fuel for cooking and heating. Wenzel [2006] further states that even communities with formal housing and access to electricity will still use these fuels in conjuction with the electricity, mostly due to affordability and multiple utility (a biomass stove can simulataneously cook a meal and heat the room). The use of multiple fuels has been noted by others as well [Lloyd, 2014; Balmer, 2007; Mdluli, 2007; van Niekerk, 2006; Sowazi and Maake, 2001]. The burning of coal in these homes takes place in fixed-bed devices ranging from the simple *"imbaulas"* [Makonese, 2011; Le Roux *et al.*, 2004; Kimemia *et al.*, 2010] and artisan stoves, produced within the communities, to cast iron stoves. The *imbaula* is lit outside the home, brought inside for cooking and heating once the smoke has subsided [Lloyd, 2014; Kimemia *et al.*, 2010]. In most cases the cast iron stoves are in bad repair [Nkosi *et al.*, 2017; Balmer, 2007; Wagner *et al.*, 2005], having been one of the first purchases made by rural migrants upon arival in the city [Balmer, 2007; Mdluli, 2007], and holding a socially important role in the family [Mdluli, 2007]. Nkosi *et al.* [2017] reports an average age of 25 years for stoves used in the Kwadela township in Mpumalanga, leading to inefficient combustion and the associated HAP. It is also worth noting that cast iron stoves are no longer produced in South Africa, thus new stock and spare parts are not avaialble for maiantaiing the stoves currently in homes. According to Lloyd [2014], the cast iron stoves available on the market today were originally designed to burn wood, but are also able to burn coal cleanly after the coals are flaming; however, during the ignition phase, the stove emits a considerable amount of smoke, exposing the users to HAP. It is further stated that a stove fitted with a chimney aids significantly in managing the smoke [Taylot, 2009].

The major problem with coal burning in the home is the emission of pollutants which have been associated with health effects such as acute and respiratory infections, cancers, and increased childhood mortality [Gordon *et al.*, 2014; Lockwood *et al.*, 2009; Friedl *et al.*, 2008; Scorgie *et al.*, 2001]. Source apportionement studies [Friedl *et al.*, 2008; Mdluli, 2007; Scorgie *et al.*, 2003, 2001; Sowazi and Maake, 2001] report that the domestic burning of coal is the single greatest contributor to aerosol pollution in the coal burning communities, and that these emissions pose a far greater threat to the residents of these communities than emissions from motor vehicles and adjacent industries. Furthermore, emissions are at their worst in the colder winter months where temperatures can drop to -5°C. Scorgie [2012] studied the ambient air pollution of the Gauteng province; the author reports that domestic activities contribute 65% of the pollution, while the rest is due to electricity generation (5%) and industrial and commercial applications (30%). Domestic activities were also shown to be the greatest contributor to PM emissions. A study by Mathee [2004] allots 48% of the quantifiable PM emissions in the city of Johannesburg to domestic fuel burning and only 22% to scheduled processes. Lloyd [2014] found a similar trend on a larger scale, reporting that 40% of the total PM in the country is due to domestic activities, a value of 20% is reported by Wagner *et al.* [2005]. Other pollutants of concern were studied by Scorgie [2012], who reported that SO_2 measurements were frequently below the SANS limit of 124 $\mu g.m^{-3}$ daily due to the relatively low sulphur content of the coal. Volatile organic

compounds (VOCs) were found to consist mainly of benzene, toluene, ethyl-benzene, and xylene (BTEX) compounds.

As a response to the overwhelming evidence of the link between the domestic burning of biomass fuels, and the emission of pollutants which have a negative impact on the health of users and the environment, the South African government undertook policies that would improve access to electricity and limit the use of "dirty" fuels. The former Department of Minerals and Energy (DME) undertook the policy of universal electrification by 2012, under which a significant number of homes were connected to the grid between the mid-90s and mid-2000s [Pretorius *et al.*, 2015; Balmer, 2007]. However, despite the accelerated electrification and the monthly subsidy of 50 kWh of electricity to poor households from 2001 [Pretorius *et al.*, 2015; Inglesi and Pouris, 2010], the use of coal and wood still persisted because of perceptions about the reliability of electricity, and the availability and affordability of coal sold through well-established networks [Nkosi *et al.*, 2017; Mdluli, 2007; Balmer, 2007; van Niekerk, 2006; Qase *et al.*, 2000]. The dissemination of the *Basa Njengo Magogo* (BNM) fire-lighting method was another intervention taken on as a means to reduce the emissions from coal burning. Numerous programmes by governmental and non-governmental organisations were carried out in various coal burning communities, including those by the NOVA Institute. NOVA has successfully demonstrated and monitored the use of the BNM method in over 13 communities [NOVA Institute, 2017], including Embhalenhle in the Highveld and Zamdela in the Free State [Wagner *et al.*, 2005]. The use of this method to reduce emissions from coal burning in *imbaulas* has been addressed in the literature [Masondo *et al.*, 2016; Kimemia *et al.*, 2010; Le Roux, 2009; Wenzel, 2006], and reports indicate a decrease in PM emissions of over 50%, using this method alone. However, few studies directly address the use of the BNM method in a conventional cast iron stove. An attempt to introduce new technology in the form of an ICS was made under the DME in the 1960s and 1970s, however the project was discontinued due to the rather large subsidy required to disseminate the stove. The idea of a low-smoke stove has been put into practice elsewhere in the world, as illustrated by the Chinese and Indian programmes, and it is clear that its success is highly dependent on government funding. It was not until the development of a mud stove by NOVA, who have successfully piloted their clay stove for wood burning in the rural community of Molati, that the idea of an South African ICS was explored again [NOVA Institute, 2017]. This stove has not yet been commercialised.

The low-smoke fuels (LSF) programme, a DME-sanctioned enterprice, launched in the 1990s under which the production of a low-smoke fuel that would meet the same needs as coal, but without the disadvantage of excessive HAP was investigated on several levels, namely: techincal performance, *in situ* improvements in ambient air pollution, and social accpetability. The programme was divided into two pilot projects in 1992/1993 [Dickson *et al.*, 1995] and 1997 [Asamoah *et al.*, 1998]. Technical assesmments of potential LSFs produced from colliery discards [Horsfall, 1994], a coal-cement composite [Tait and Lekalakala, 1993], and briquetting of devolatilised fine coal [Le Roux *et al.*, 2004; Mangena and Korte, 2000] were part of the technical assessments. Reports from the programme, including those of Dickson *et al.* [1995], Hoets [1995], and Asamoah *et al.* [1998] provide a good indication of the criteria that need attention should such a project be attempted: a suitable LSF is one that is tailored to each community in terms of the results of user consultation, technical evalautions, and emissions monitoring. In terms of

the technical evaluations of the potential LSF, Le Roux *et al.* [2004] highlighted the lack of a simple "standardised" method of testing and validating a potential low-smoke fuel; until that point potential LSFs were produced and tested at the discretion of those involved, and results from different tests and fuels could not be compared. The method developed by Le Roux *et al.* [2004] was used to test a LSF produced by devolatilisation in an *imbaula*. So far this method has been used to evaluate the performance of LSFs lit using the BNM method in these devices [Le Roux, 2009]. No reports including the use of this evaluation method for cast iron stoves have been found. To asses the distribution potential of a LSF in the coal network, Qase *et al.* [2000] conducted an in-depth study of the country's coal sales networks. The authors reported that based on the widespread recognition of the health hazards related to coal use, there exists a "reasonable degree of acceptance that an alternative is desirable". Furthermore, they support devolatilisation as the correct method of LSF production, but lament the lack of satisfactory demonstrations of a LSF in South Africa. They also state that particle size in this context also remains largely unexplored, though it is agreed on that larger sized fuels are better suited for use in *imbaulas*, which allows for a satisfactory performance of the fire in natural draft conditions. It is this gap that this study aims to fill. As a first attempt at this, the North West University conducted experiments with LSFs in cast iron stoves in order to determine the optimum LSF production temperature. The LSF was produced via the devolatilisation of coal lumps of size ranging from 10-60 mm at 450, 550, 650 and 750°C. Results for the LSF produced at 550°C had the best overall performance, boiling 1L of water in approximately 30 minutes, and providing up to 8 hours of useful heat. PM and VOC emissions were also reduced by 80% and 90% respectively when compared to the untreated coal. The fuel recorded a combustion efficiency of only 72%, and ignited after 30 min, using LPG. Though this study showed that a coal-derived LSF can perform satisfactorily in a cast iron stove, there is ample room for improving the ignitability and combustion efficiency of such a fuel in order to meet the criterion of equal performance. A general economic analysis was done to estimate the potential for commercialisation. It was found that with industry collaboration, it will be possible to produce and retail a LSF in communities adjacent to these industry collaborators [Kühn, 2015].

The case of the BNM method makes it clear that solutions that do not require a significant change in the habits of the user were most successful. The use of ICS as a means to reduce HAP is not likely as there is no evidence that an ICS for coal has been successfully distributed in South Africa; furthermore, previous attempts were burdened by the high costs associated with dissemination. There is a lack of information on how solutions that have been successful in the *imbaula*, such as the BM method, or the use of low-smoke fuels, will perform in the conventional cast irons stoves that are still being used in many homes. Before a devolatilised-coal LSF can be piloted or marketed, further study into improving the performance of the fuel, especially in conjunction with current stoves, is warranted.

1.2 Problem Statement

Domestic coal burning in low-income communities, as a primary source of energy or in conjunction with other sources, will persist as long as coal stays competitive against other fuels in

terms of its utility, cost, and accessibility [Nkosi *et al.*, 2017; Balmer, 2007; Mdluli, 2007; van Niekerk, 2006]. The importance of improving household air quality has been illustrated well in the literature and in the updated SANS air quality standards [SANS1929:2011] which requires ever-lower limits of common pollutants. Based on previous programmes aimed at reducing HAP by introducing coal alternatives, a simple set of requirements for any such alternative can be deduced. The alternative should be technically viable, it should neither require drastic changes in user habits, nor be out of the end user's reach in terms of availability and cost. In this study, the suitability of a low-smoke fuel, produced from locally-sourced coal which can be used in the stoves currently available in the homes, is assessed.

The coal used in this study was obtained from the coal-burning community of Kwadela in the Mpumalanga Highveld. According to Nkosi *et al.* [2017], Kwadela is located close to coal mines and the N17 highway, both of which could be sources of the ambient air pollution experienced by residents. Despite 97% of the community having access to electricity, 76% still make use of solid fuels burnt in cast iron stoves (61%) and welded artisan stoves (11.4%) [Language *et al.*, 2016]. Coal, wood, animal dung, paraffin, and LPG have been found in varying frequencies of use. Coal is sold in Kwadela through a well-establised network. The typical home in Kwadela is the government subsidised four-room house; a study by the Nova Institute reported that these houses are too cold in winter [NOVA Institute, 2017] due to poor energy planning when the houses were built, prompting the use of solid fuels for heating. A seasonal variation in use has been reported [Nkosi *et al.*, 2017; Language *et al.*, 2016; Wernecke *et al.*, 2015] with peaks in PM emissions being reported for winter. Language *et al.* [2016] further identified two daily peak times for coal burning, that is, in the morning from 4 AM and in the evenings from 4 PM. The location of Kwadela in the Highveld, in close proximity to coal mines, the availability of ambient and household air quality data, and the well-documented coal-use patterns, including the predominant use of the cast iron stove, make it an ideal case study for the possible implementation of a low-smoke fuel for use in such stoves.

1.2.1 Aim and Objectives

This study aims to determine the effect of fuel particle size on the performance and emissions reductions of a low-smoke fuel when used in a conventional domestic coal stove.

In order to achieve the above aim, the following objectives were set out:

- The low-smoke fuels required for the combustion tests will be produced via the pyrolysis of the parent coal in atmosphere of nitrogen. The parent sample will be treated in such a manner as to produce five different "fuels" distinguished from one another by their sizes: 15mm, 20mm, 30mm, 40mm, and composite of all the sizes. These fuels, as well the untreated coal analogues, will be characterised according to known standards. Conventional chemical, mineralogical, and petrographic characterisations will be performed.
- Thermogravimetric analyses (TGA) will be used to study the combustion properties of the various fuels. These analyses will offer some insight into the following:
  - the combustion (or burning) phases
  - approximate burning rates of of the fuels

- Combustion tests in a Falkirk Union 7, a commonly used household stove, will be carried out, according to an acceptable protocol, in order to determine the effect of fuel particle size on the practical performance and emissions released during the combustion of LSFs. Results from the LSF combustion will be compared to those of untreated coal in each size fraction.

1.2.2 Relevance of the Study

This work contributes to the body of knowledge of domestic coal combustion in South Africa in a few ways. Firstly, the work builds on the strategic goals for pollution reduction and community uplifment of coal-burning communties, as set out by Kühn [2015], by developing and evaluating a low-smoke fuel suitable for use in current coal-burning stoves. Furthermore, this work seeks to improve on the efficiency of the fuel by manipulating the particle size, which has been shown to affect the perfomance and emissions released from coal and other biomass fuels in the literature (*e.g.*Masondo *et al.* [2016],Li *et al.* [2016]), Kumar *et al.* [2013]).

Secondly, by conducting the combustion tests in the stoves currently used in coal-burning homes, this study will contribute to the existing knowledge of the combustion vessels used in coal-burning communities, and the performance of these, since many studies reported have been based on the "imbaula" or brazier [Masondo *et al.*, 2016; Le Roux *et al.*, 2004; Mangena and Korte, 2000].

Furthermore results from this work may inform policy on alternative fuel production and dissemination projects should such a project be undertaken by the South African government. Overall, this work seeks to contribute to our understanding of fuel/stove compatibility in the search for cleaner burning fuels and stoves in communities where the use of coal or biomass is still dominant, while keeping costs to the consumer at a minimum.

1.3 Scope of the Study

1.3.1 General Approach and Limitations

The arguments and results presented herein are limited to coal and coal-derived LSF burnt in a cast iron stove, fitted with a chimney. The cast iron stove is also unique in the sense that it is the "most advanced" device available currently in homes, however, these stoves are found to be in bad repair as there are no new stoves or spare parts because production of cast iron stoves has stopped. Along with these stoves *imbaulas* are also found in coal-burning household. However, while the latter has enjoyed ample coverage in the literature, while the former has not.

Emissions sampling is done according to the "hood method", aided by the portable dilution sysytem illustrated by the SeTAR Centre at the University of Johanessburgs[Makonese, 2015]. The method for low-smoke fuel testing and validation suggested by Le Roux *et al.* [2004] is used in conjustion with the heterogeneous testing protocol (HTP) developed by the SeTAR centre, to quantify the thermal and combustion efficiency and emission factors (EF) of pollutants. The

HTP, primarily a stove testing tool, is unique in that it allows for the systemic testing of a fuel/stove combination and is well suited to this study as we seek to assess the performance of the LSF when used in the stoves currently employed in coal-burning homes. The development of a standard testing method for low-smoke fuels which combines the emissions reductions and practical performance of the fuels in different devices should be considered in future, but is not within the scope of this study.

Measurement of emissions were carried out for a pre-set period of time where the major phases of combustion can be observed. While most work in the literature reports emissions for H_2S and CH_4, these could not be monitored in this study due to instrumental limitations. Only emissions of CO, CO_2, SO_2 and NO_x are reported. For the same reason, total PM is measured and not size-specified fractions (*i.e.* $PM_{2.5}$ or PM_{10}). Emission factors are reported on an energy basis in order to allow for "task based" comparison of the performance between fuel types.

Only fuel type and particle size were varied. Other important variables such as fuel loading, fuel bed dimensions, and the flow rate of the ignition LPG, were kept constant. The flow of air into the stove was neither controlled nor monitored as unregulated air-flow is characteristic of household usage.

1.3.2 Dissertation Outline

This dissertation brings together the objectives listed in Section 1.2 and the findings of the study over six chapters as shown below.

- The present chapter, provides a background on issues pertinent to the study such as the combustion of coal in households, the resultant pollution, and its effect on the users. The problem statement is formulated, and the the aim, objectives, scope, and relevance of the study are presented.
- In order to build a sound theoretical knowledge base, topics pertinent to the study will be reviewed in Chapter 2.
- The characteristics of the parent coal, and resultant fuels will be covered in Chapters 3 and 4. Chapter 3 presents data on chemical, mineralogical and petrographic characteristics of the parent coal sample and the resultant fuels, while Chapter 4 will discuss the combustion characteristics of the fuels as informed by thermogravimetric analyses.
- The materials, methods, and equipment used to conduct the experiments in the study are presented in Chapter 5. This includes technical information regarding the equipment, measurements taken, quality control procedures, and the set up for monitoring emissions and performance.
- Chapter 6 will present and discuss the results of the experiments.
- Finally, Chapter 7 will summarise the most important results, show how the objectives stated in Chapter 1 have been fulfilled. Recommendations for further work, needed to address outstanding issues identified during the course of the study, will also be presented here.

Chapter 2

On the Combustion of Coal and Low-smoke Fuels in Household Devices

The aim of the study is to determine the effect of fuel particle size on the combustion of a low-smoke fuel in a household stove, with a particular focus on practical performance metrics and reductions in emissions. In order to achieve this, an understanding of the combustion process and especially of pollutant formation and emission is required. This literature survey aims to address this in two parts. The first, will provide a background into the fundamental concepts and theory underlying the formation (Section 2.1) and combustion (Section 2.2) of coal , as well as the formation and release of pollutants (Section 2.3). The second part will apply this theory to common household devices (Section 2.4), and in the assessment and characterisation of their performance (Section 2.5). Lastly, the developments in the production of a low-smoke fuel (Section 2.6) intended for use in low-income areas will be discussed.

2.1 The Properties of Coal

Knowledge of the structure and properties is important in understanding the transformations of the coal particle during conversion processes. In this section, the general nature and formation of coal, and of coal from the Highveld coalfield in particular, are discussed.

2.1.1 Coal Formation and Composition

Physically, coal can be viewed as porous, mostly organic rock. Chemically, it is a collection of ”islands” of aromatic ring clusters held together by aromatic-, hetero-atomic- and other ”bridges”, whose relative sizes are related to the rank and behaviour of the coal during conversion processes [Svoboda, Hartman and Cermák, 2000]. The formation of coal via the accumulation and alteration of organic material in sedimentary strata, accompanied by chemical, biological, bacteriological, and meta-morphological activity on the vegetable- and mineral debris, is referred to as coalification [Flores, 2014; Roets, 2014; Schobert, 2013; Nel, 2011; Crowell *et al.*, 2008; Hlatshwayo, 2008; England *et al.*, 2012; Falcon and Ham, 1988]. The rank of the coal is an

indication of the advancement of this process [England *et al.*, 2012; Gupta, 2007; Falcon and Ham, 1988; Falcon and Falcon, 1987].

The organic fraction, or coal maceral, is formed from the remnants of the original vegetable matter [Roets, 2014; Scott, 2002; Stopes, 1935]. Vitrinite, formed from cellulose and lignin, liptinite from the waxes and oils, and inertinite, from oxidised plant material, are the three major maceral groups. Subgroups within each of the main macerals have been identified [Roets, 2014; England *et al.*, 2012; Beukman, 2009; Crowell *et al.*, 2008; Scott, 2002; Falcon and Ham, 1988; Falcon and Falcon, 1987; Stopes, 1935, 1919]. The grouping is done on the basis of common chemical, physical, optical, and technological properties [Falcon and Ham, 1988], according to which the macerals can be identified and classified using advanced techniques [Gupta, 2007; Speight, 2005; Falcon and Snyman, 1986]. The composition of the macerals significantly affects the behaviour of the coal in terms of swelling propensity, composition of evolved volatiles, as well the structure and composition of the post-pyrolysis char and residual ash [White, 2015; Gupta, 2007; Benfell, 2001]. Upon heating, vitrinite and liptinite combust easily due to their moderate-to-high volatile content. Inertinite, as the name implies, is relatively inert and is responsible for the formation of the carbon-rich products such as chars during pyrolysis [Falcon and Ham, 1988]. Cloke and Lester [1994], however, warn against the absolute "reactive versus inert" classification, stating that "not all vitrinites are reactive and not all inertinites are inert". The type of char formed by vitrinite is dependant on temperature and rank: higher temperatures result in thicker-walled spheres and lower rank coals are associated with pore-networks. Liptinite is linked with flame stability due to its high volatile matter content. Furthermore, liptinite starts burning and vapourising at ~300 °C and is thus significant only during pyrolysis, and does not contribute to the char combustion behaviour of coal. Inertinite can form any type of char, including networks, spheres, and dense solids. Similar to vitrinite, inertinite behaves according to its rank: lower rank inertinites may swell during combustion and have been shown to produce porous chars [Cloke and Lester, 1994 and references therein].

The inorganic fraction, consisting mainly of mineral matter, occurs as randomly dispersed mineral inclusions, dissolved salts, or as inorganic species which are chemically bound to the organic structure [White, 2015; England *et al.*, 2012; Gupta, 2007; Speight, 2005; Ward, 2002; Williams *et al.*, 2000; Smoot and Smith, 1985]. Over 125 minerals, including those found in trace amounts have been identified [Vassilev and Vassileva, 1996; Finkelman, 1980], and can be divided into two distinct groups: (1) inherent, or included, minerals that occur as infillings in the cavities and fractures, and (2) adventitious, or excluded, minerals, which are discrete particles occurring mostly as silicates, sulphides, sulphates, phosphates, carbonates and other minerals, and are external to the coal matrix [Matjie *et al.*, 2016; Roets, 2014; Matjie *et al.*, 2011; Speight, 2005; Ward, 2002]. Matjie *et al.* [2016] state that the mineral matter within macerals, especially non-mineral organic elements, is the dominant contributor to the formation of ultra-fine ash particles and condensed metallic vapours during combustion [Matjie *et al.*, 2011; Ward, 2002; Davidson *et al.*, 1974]. The catalytic nature of minerals in thermal processes has been discussed in detail by Roets [2014], who studied the effects of minerals on the products of Highveld coal pyrolysis. Highveld coal have shown to be rich in kaolinite, followed by lesser amounts of quartz, calcite and dolomite [Matjie *et al.*, 2016; van der Merwe, 2011; Hattingh, 2012; Wagner and Hlatshwayo, 2005]. Cloke and Lester [1994] insist that mineral effects should be considered when assessing

char formation and reactivity, as certain minerals can affect the type and reactivity of the char, flame stability, as well as char burnout efficiency. Particle heating, for example, can be delayed by the high heat capacity of minerals, causing poor burnout.

2.1.2 The Properties of South African Coals

The characterisation of South African coals according to their organic- and inorganic properties, and their applicability to various conversion processes, has been covered widely in the literature, with the report of Hancox and Gotz [2014] being the most recent and comprehensive account. Resource and reserve surveys have been reported by *e.g.* Jeffrey [2005] and Eberhard [2011]. Falcon and Ham [1988] provide a good basis of the characteristics of South African coals in terms of their properties as they apply to combustion and other conversion processes, while Falcon and Falcon [1987] present findings linking maceral content to physical properties of coal. Matjie *et al.* [2016] provide insight into the mineral matter composition of Highveld coals, while Everson *et al.* [2013] reported on the coals' amenibility to gasifiation. In their study of the Witbank coalfield, Holland *et al.* [1989] found the coals to be rich in inertinite (20-80%), with values >55% being common. Vitrinite was reported to vary between 0% and 10%, while liptinite was found to be less than 10%. Matjie *et al.* [2016] found similar results for a selection of Highveld coals. von Holt [1992] states that local variations in maceral composition are not uncommon, for example, the coal within the Witbank coalfield fit the inertinite-rich generalisation, while those in northern Natal are typically vitrinite-rich. This is corroborated by Snyman and Botha [1993] and Hancox and Gotz [2014]. In general, the Permian-aged South African coals are found to have higher inertinite content (consisting of a significant amount of reactive semifusinite) when compared to their carboniferous counterparts in the Northern hemisphere, despite the high petrographic variability [Snyman and Botha, 1993; von Holt, 1992].

The composition of sulphur and its effects on the properties of coal are covered extensively by Kalenga [2011], whose work aids in the prediction and mitigation of the emission of sulphur-related pollutants, as these are linked to the distribution, nature, and forms of sulphur within the coal. In general, South African coals are of low sulphur content, and average values of 0.5% to 1.0% are not uncommon [Hancox and Gotz, 2014]. Sulphur thus poses a low risk of pollution when proper mitigation measures are taken [Williams *et al.*, 2000]. Though not covered extensively in the literature, trace elements are a concern with regards to pollution emission during coal conversion processes, as these have been reported to be a great contributor to the health impacts of particulate matter [Davidson *et al.*, 1974], and of fly ash especially. The trace element chemistry of South African coals is covered in publications such as those of Cairncross [1989] and Wagner and Hlatshwayo [2005]. The former provides a more general account of the trace elements in South African coal, while the latter focusses on the coals of the Highveld coalfield. They report that despite having higher *in situ* ash, Highveld coals have lower concentrations of sulphides, halogens and trace elements compared to their northern hemisphere counterparts. Furthermore, the concentrations of most trace elements (As, Cd, Co, Cu, Hg, Mo, Ni, Pb, Sb, Se, V, and Zn) fall below global averages presented in literature. This, the authors state, indicates that the emissions from Higveld coal, as far as trace elements are concerned, do not pose a health risk.

The Highveld Coalfield

The Highveld coalfield has 5 seams and is situated in south-eastern Gauteng and Mpumalanga, extending over a distance of 95 km from Nigel in the west to Davel in the east, and 90 km from north to south [Hancox and Gotz, 2014]. This coalfield is of economic importance as the second largest productive coalfield of the 19 South African coalfields [Roets, 2014; Eberhard, 2011; Jeffrey, 2005; Wagner and Hlatshwayo, 2005] and is important to the long-term function of Sasol Synthetic Fuels (SSF). This coalfield is also in close proximity to the Eskom Kriel, Matla and Tutuka power stations [Hancox and Gotz, 2014].

Highveld coal is typically of low-grade bituminous quality [Jeffrey, 2005]. A general proximate analysis would classify it as a medium-to-high volatile (12-32%), low moisture (2-6%), and high ash (8-35%) coal on an air-dry basis [Roets, 2014; Hancox and Gotz, 2014; Pinetown *et al.*, 2007; Wagner and Hlatshwayo, 2005; Jeffrey, 2005]. Some seams have been found to have ash yields of up to 40% [Matjie *et al.*, 2015]. The mineralogical assay of a typical Highfield coal (on a mineral matter only basis) has been reported to be predominantly koalinite (~40%), followed in decreasing order by quartz, pyrite, calcite and dolomite [Matjie *et al.*, 2016; Roets, 2014; Pinetown *et al.*, 2007]. Calorific values reported for Highveld coal range from 15-25 $MJ.kg^{-1}$ on a dry basis [Jeffrey, 2005]. The characterisation of the coal sample used in the current study is presented in Chapter 3, and due to the location of the Kwadela community within the Highveld coalfield, it is expected that the coal will have properties akin to those of Highveld coals.

2.2 Combustion Processes for Coal

Coal combustion involves both physical and chemical processes that can occur chronologically or simultaneously [Makonese, 2015; Goshayeni and Sutherland, 2014; Kosowska-Golachowska, 2010; Basu, 2006]. These are divided into two main stages: (1) devolatilisation and (2) char combustion [Ramabuda, 2015; van der Merwe, 2011; Kosowska-Golachowska, 2010; Williams *et al.*, 2000; Kök *et al.*, 1997; Morgan *et al.*, 1986; Smoot and Smith, 1985; Smith, 1982]. Stage 1 starts with the removal of free moisture, followed by the pyrolytic devolatilisation of the coal and the subsequent combustion of the volatile matter. The latter process involves the release, and subsequent oxidation, of flammable gases and the generation of heat flux. Depending on the size of the particle, these processes may occur consecutively or simultaneously, and possible fracturing and/or fragmentation may result from pressure build-up within the particle. This is particularly true for larger (>3 mm) particles [Kosowska-Golachowska, 2010; Svoboda, Hartman and Cermák, 2000]. It should be noted that devolatilisation in an inert atmosphere, such as that employed in this study to produce the LSF, is not the same as that which occurs during combustion [Svoboda, Hartman and Cermák, 2000]; differences in temperatures at which reactive intermediaries such as HCN form, are cited by Varey *et al.* [1996] as indicative of the distinction between the two processes. The second stage is characterised by a mixture of heterogeneous char-consuming reactions taking place alongside gas phase oxidation reactions [Wielgosinski, 2012; Li *et al.*, 2009; Smoot and Smith, 1985]. These processes, with regards to domestic coal combustion, and related gases, are illustrated in Figure 2.1 for a single coal particle.

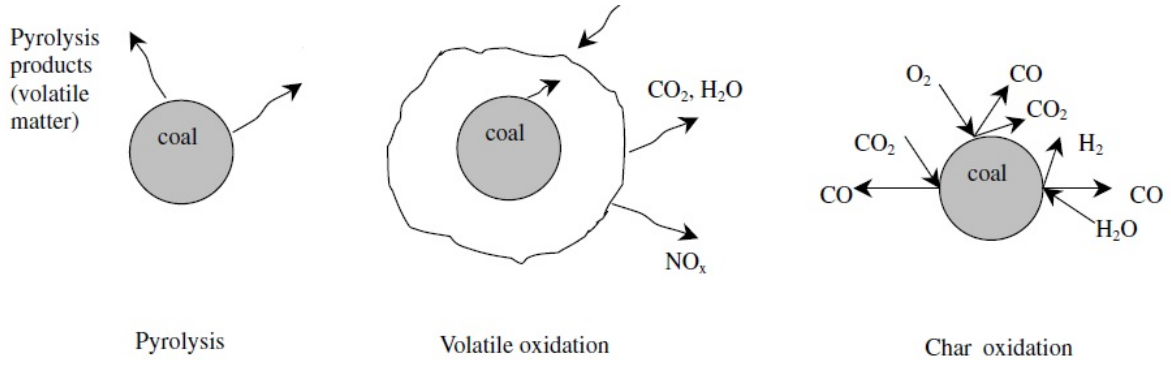

Figure 2.1: Schematic of Coal Combustion Mechanisms. Adapted from Sami *et al.* [2001]

Coal combustion can be studied in three configurations, (1) single coal particles, (2) coal piles or layers and (3) coal clouds. Single coal particles are used in fundamental studies to provide basic data and practical insights in dilute flame applications. Coal layers occur in fixed or moving beds and storage piles where the fuel particles are closely packed. Coal clouds are typical of pulverised coal applications, such as boiler burners where the pf coal is dispersed in a stream of air [Makonese, 2015; Sami *et al.*, 2001; Smoot and Smith, 1985]. Single particle studies, especially of pulverised (pf) coal, have received the majority of attention due to the simplicity of experiments and the ability to isolate properties of interest. In its simplest form, the combustion process for a single particle can be studied in terms of ignition, volatile release and combustion, and char burn-out [Makonese, 2015; Ramabuda, 2015; Kosowska-Golachowska, 2010; Sami *et al.*, 2001; Williams *et al.*, 2000; Smoot and Smith, 1985].

These processes will be reviewed in this section, based largely on single particle studies, keeping in mind the call to caution by Marek and Stanczyk [2013], who warn that conclusions drawn from single particle combustion may differ from those for a packed bed, owing to features such as oxygen competition and temperature variation.

2.2.1 Heating and Drying

Moisture makes up between 2 to 15% of the mass of a coal particle [Speight, 2005]. During heating this moisture is released, and may cause fragmentation in lower rank coals [Makonese, 2015; Kosowska-Golachowska, 2010; Miller and Tillman, 2008]. Drying is an endothermic process and is limited by heat transfer to and within the particle. The evolution of steam from drying keeps the particle temperature low, delaying the devolatilisation step [Makonese, 2015; Miller and Tillman, 2008; Kosowska-Golachowska, 2010; Winter *et al.*, 1997]. Yu *et al.* [2005] studied the effect of particle size on mass loss during TGA experiments and reported that heating rates increase with decreasing particle size.

2.2.2 Particle Ignition

Smoot and Smith [1985] describe ignition as the process through which a sustained reaction between the fuel and oxidising agent is achieved, often identified by a visible flame. Ignition can also be characterised as the time taken to achieve a visible flame, a certain temperature, or

consumption of fuel for a set of conditions. Several theoretical and experimental studies have been undertaken with the aim of identifying a mechanism for particle ignition [Essenhigh *et al.*, 1989; Du and Annamalai, 1994; Markos *et al.*, 2001; Zhu *et al.*, 2009]), from which three modes of ignition have been identified:

- Homogenous Ignition occurs via ignition of the volatile matter released, as a result of pre-ignition pyrolysis from coal. Such ignition takes place when the mixture of volatiles and oxygen (the oxidising agent) is at a temperature higher than the self-ignition temperature of the coal [Marek and Stanczyk, 2013].
- Heterogenous Ignition occurs as a result of the direct contact between the oxidising agent and the coal particle surface.
- Hetero-homogenous Ignition refers to the simultaneous and competing ignition of the volatile matter and the coal particle surface.

Of importance in determining the ignition temperature and time, are coal type, particle size, moisture-, volatile-, and mineral matter content, as well as gas-phase composition and temperature. An increase in coal rank from lignite to anthracite was found by Chen *et al.* [1996] to move the ignition scheme from homogenous to heterogenous. In their review of combustion studies, Essenhigh *et al.* [1989] report that large particles (>100 μm) undergo homogenous ignition via pyrolysis, of the coal surface and the subsequent volatile ignition, while small particles are easier to ignite heterogenously via direct attack. These findings are also reported by Kosowska-Golachowska [2010] who states that ignition temperature decreases with increasing particle size, oxygen concentration, and volatile matter content. Figure 2.2 shows an agreement in the results of different authors who found that the ignition temperature decreases as a function of increasing volatile matter content in coal.

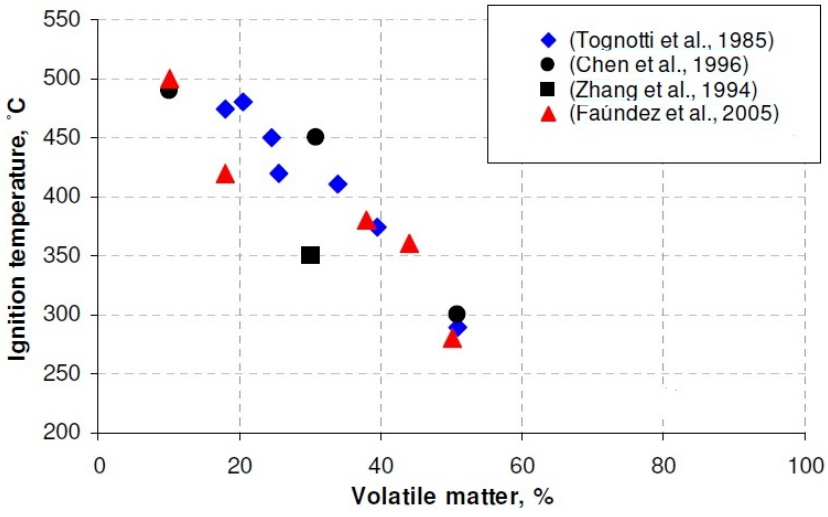

Figure 2.2: Results obtained for 5-10 mg samples heated at 2-10° C.min^{-1} in an oxygen atmosphere under atmospheric pressure, volatile matter is given on a dry basis; Adapted from Kosowska-Golachowska [2010]

In their TGA study of the effect of coal particle size on combustion and thermal properties, Kök *et al.* [1997] found that as particle size decreased, peak temperatures (the point at which mass loss is at its highest) and burn-out temperature (the point at which char oxidation is essentially

complete) decreased slightly while ash residue increased. Shen [2009] reported estimated ignition temperatures for different coal ranks. Their results, shown in Table 2.1, echo the relationship between increasing volatile matter and decreasing ignition temperature shown in Figure 2.2, and confirmed the increase in ignition temperature with rank [Chen *et al.*, 1996], as well as the shift of the ignition scheme from exclusively via volatiles to a combined ignition scheme.

Table 2.1: Ignition temperatures for coals of different ranks from Shen [2009]

Coal Type	Ignition Temperature ° C	Initial VM Release Temperature ° C
Lignite	250-450	130-170
Bituminous	400-500	200-300
Antracite	700-800	380-400

Li and You [2010] employed Equation 2.1,

$$\frac{dT_s}{dt} = 0 \tag{2.1}$$

where T_s is the temperature on the surface of the particle, to define ignition as the point where the particle's temperature is constant. They too reported that smaller particles will require higher temperatures to ignite and maintain combustion, due to the high heat loss per unit area in smaller particles, requiring higher temperatures to offset this loss and cause ignition. Once ignited, the combustion rate of smaller particles will be higher than larger particles, resulting in a higher particle temperature during combustion.

2.2.3 Devolatilisation

When the coal particle is heated to high (>300° C) temperatures in an oxygen-free environment, it decomposes into a hydrogen-rich volatile fraction and a carbon-rich solid fraction, called char. This occurs through the breaking of covalent carbon bonds (with, for example, oxygen, nitrogen, and sulphur) within the coal matrix [Roets, 2014; Makonese, 2015; Kosowska-Golachowska, 2010; Beukman, 2009; Miller and Tillman, 2008; Chen *et al.*, 1996; Matzakos, 1992]. The volatile matter fraction comprises mainly of light gases (CO_2, CO, H_2, H_2O), hydrocarbon gases (CH_4, C_2H_4, C_2H_6) and liquids, as well as polycyclic aromatic hydrocarbons, or PAHs [Wijayanta *et al.*, 2010; Wendt, 1980]. The aromatic and hydro-aromatic building blocks that make up a coal particle are shown in Figure 2.3a. The building blocks are held together by bridging groups (alkyl- and ethereal oxygen and sulphur) and functional groups at their periphery [Roets, 2014; Borah *et al.*, 2005]. In this context, devolatilisation can be defined as the simultaneous de-polymerisation and thermal decomposition of coal, where these reactions compete for the H_2 released from the breaking down of stable building blocks.

The onset of pyrolysis is characterised by the cleavage of hydrogen bonds and the vaporisation and migration of non-covalently bonded molecules through the coal matrix. Upon further heating, the peripheral groups are evolved as volatiles, the bridge bonds (shown in Figure 2.3a) are

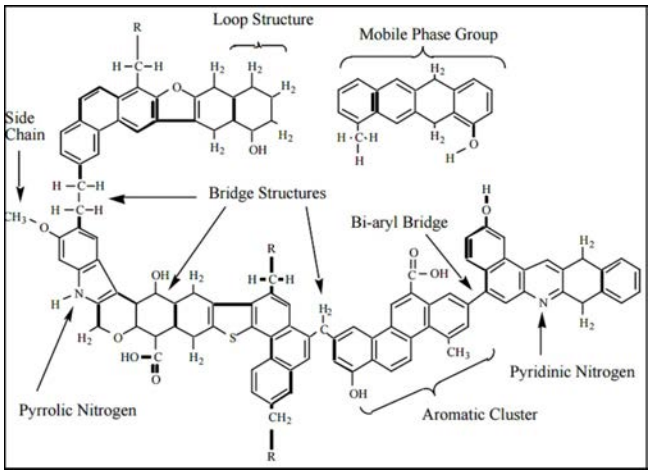

(a) Chemical bonds in coal, showing the aromatic and hydro-aromatic building blocks along with the bridging and peripheral groups, adapted from Fletcher [2005]

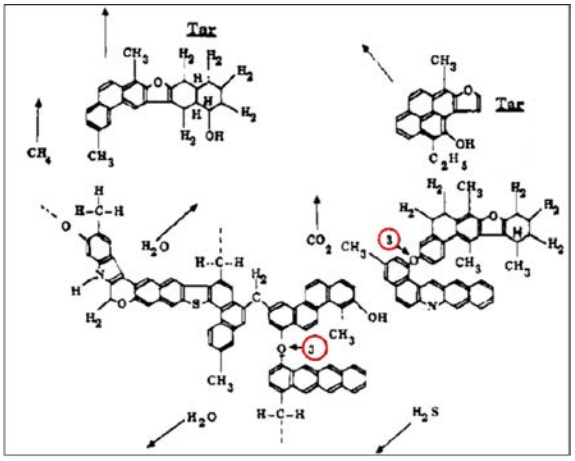

(b) Coal structure during primary pyrolysis showing the evolution of tars, water and lower chain hydrocarbons, adapted from Hattingh [2012]

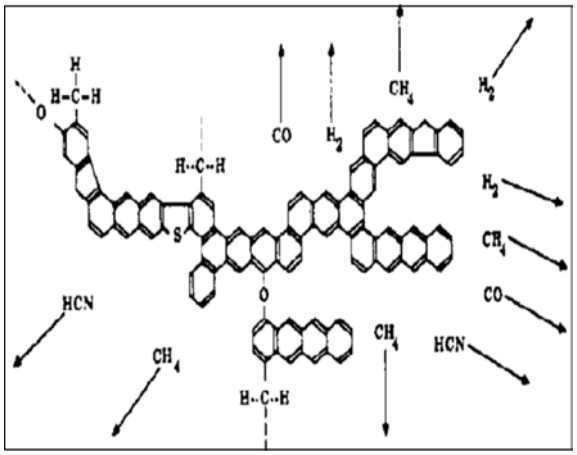

(c) Coal structure at secondary pyrolysis showing the carbon-rich char, adapted from Hattingh [2012]

Figure 2.3: Changes in the Structure of Coal during Pryloysis

cleaved, and the hydro-aromatic blocks are converted to aromatic blocks via dehydrogenation and condensation reactions. Figures 2.3b and 2.3c show the two stages of pyrolysis; an in depth discussion was published by Solomon *et al.* [1992] and Solomon and Hamblen [1985]. Primary pyrolysis (Figure 2.3b) begins at ~350° C, ends at ~550° C, is associated with the rapid release of volatiles, and is characterised by the following processes: [Roets, 2014; Fadeela, 2012; Hattingh, 2012; van der Merwe, 2011; Borah *et al.*, 2005]

1. The conversion of hydro-aromatic building groups to aromatic blocks, adding to the aromatic hydrogen content of the coal.
2. The cross-linkage of remaining building blocks occurs. This step is associated with the release of H_2O, CH_4 and CO_2 and its subsequent effect on the O/C and H/C ratios of the char. The faster these gases are released, the higher the rate of cross-linkage reactions.
3. The lighter fractions are released as oils or condensible tar if they are of low enough mass to vapourize, and not undergo secondary decomposition, during transit to the surface of the particle. If this occurs, re-polymerisation will lead to char formation.

4. The formation of char, *i.e.* the condensible tars that were too large to escape the coal matrix start to condense and solidify into the carbon-rich fraction.
5. The functional groups of oxygen are released as water or carbon oxides.
6. Sulphur and nitrogen functionalities play a minor role. Nitrogen will form part of the oil and tar fractions with additional releases as HCN and NH_3. Aliphatic- and heterocyclic sulphur only becomes reactive at temperatures above 750° C and 950° C respectively.
7. Primary pyrolysis ends when all the available hydrogen has been depleted.

Secondary pyrolysis, taking place at temperatures above 600 ° C, is associated with a slower release of volatiles. This process starts with the release of gases from the decomposition of functional groups and the condensation reactions. The hydrogen used in these reactions originates from the aromatic hydrogen formed from the the decomposition of hydro-aromatic blocks during primary pyrolysis [Roets, 2014; Hattingh, 2012]. Heteroatom decomposition during secondary pyrolysis leads to the evolution of nitrogen and sulphur volatiles: nitrogen, released initially as HCN and then as NH_4 and other nitrogen species, and sulphur, released as H_2S [Makonese, 2015; Miller and Tillman, 2008; Sami *et al.*, 2001], are a concern from a pollution reduction viewpoint, and will be discussed in a later section. The resultant solid fraction is of interest in this study, as it can be used as a low-smoke fuel [Kühn, 2015; Qase *et al.*, 2000].

The exact products and rates of devolatilisation are dependant on coal types, coal composition, particle size, and heating conditions [Shen, 2009; Sami *et al.*, 2001; Chen *et al.*, 1996]; these are discussed at length by Kühn [2015]; Roets [2014]; Fadeela [2012]; Cai *et al.* [1996] and Smoot and Smith [1985]. The effect of particle size (the main concern of the current study) on pyrolysis products is embedded most clearly in the secondary chemical reactions that lead to the deposition of volatiles on the char surface. These reactions take place on the internal char surface, which provides the reaction sites. Pyrolysis products formed near the centre of the particle must travel to the surface, and may crack, condense, or polymerise during this migration, lowering the volatile yield. The larger the particle, the greater is the degree of deposition [Roets, 2014; Hattingh, 2012; Smoot and Smith, 1985; Stubington, 1984]. This delays the homogeneous ignition of particles, because the release of volatile material is slow. The devolatilisation of bituminous coal was studied by Anthony *et al.* [1976] under varying heat rates (65 - 10 000 $°C.s^{-1}$), final temperature (400-1100 °C), and particle size (70-1000 μm); their results confirm that volatile yield increases substantially with decreasing particle size. Yang *et al.* [2013], who studied Australian coal particles, ranging from 3-11 mm, with varying volatile matter content, reported that the development of a temperature gradient within the larger particles led to variations in volatile yield amounts and composition. This is because larger particles require more time to stabilise the internal temperature.

2.2.4 Volatile Combustion

The subsequent combustion of volatiles released during pyrolysis contributes largely to the heat release - up a half of the coal's specific energy, according to Eslami *et al.* [2012] - as well as the formation of pollutants and soot during coal combustion [Makonese, 2015; Li and You, 2010; Marlow *et al.*, 1992; Wendt, 1980]. Volatile combustion involves the homogeneous reaction of

the pyrolysis products with oxygen in the vicinity of the char particle, resulting in the increase of temperature and the depletion of the oxidizer [Smoot and Smith, 1985]. Howard and Essenhigh [1967] suggested a relation between the quantity of evolved volatiles and their combustion scheme. Their results showed that for a low surface flux of volatiles, the combustion of volatiles occurs parallel to that of the char, whereas a high flux of volatiles moved the reaction zone away from the solid surface, shielding it from oxygen attack. The former case can be associated with a homo-heterogenous reaction scheme, and the latter with a homogenous ignition scheme, as well as a lower particle temperature [Li and You, 2010]. Others have since modeled the combustion of coal particles in this manner; a review of these works is presented by Vamvuka and Woodburn [1998]. Apart from being involved in the ignition of the particle, volatile matter, is also responsible for further increasing the temperature of the char particle, according to Li and You [2010], even after the ignition flame has been extinguished.

Effective combustion of volatiles is important from a pollution emission perspective, since ineffective volatile combustion leads to the emission of hydrocarbon pollutants, such as low-molecular mass hydrocarbons, PAHs, and VOCs. Soot formation also takes place in this step [Williams *et al.*, 2000]. The exact pathways will be discussed in a later section.

2.2.5 Char Combustion

From a kinetics viewpoint, the combustion of the char is essentially a group of heterogeneous exothermic reactions between the solid carbon and gaseous oxygen. This is coupled with the homogeneous exothermic oxidation of CO to CO_2 and the heterogeneous endothermic CO_2 and steam gasification reactions [Makonese, 2015; Miller and Tillman, 2008; Markos *et al.*, 2001; Sami *et al.*, 2001; Matzakos, 1992; Smoot and Smith, 1985]. Chemically, this can be viewed as the non-catalytic gas-solid reaction of carbon-rich char and oxygen, and is usually described from a reaction-diffusion mechanistic standpoint using one of several models. This section will review the chemical reaction and mechanistic aspects of char combustion. Modelling the kinetics is outside the scope of this study and the reader is directed to the vast literature on the subject [Ramabuda, 2015; Kaitano, 2007; Everson *et al.*, 2006; Zhang *et al.*, 2006; Zajdlik *et al.*, 2001; Levenspiel, 1999; Molina and Mondragon, 1998; Bhatia and Perlmutter, 1980].

Char Combustion Regimes

The char structure is highly porous - an artefact of the evolution of gases during the devolatilisation step [Ramabuda, 2015; van der Merwe, 2011; Kosowska-Golachowska, 2010; Markos *et al.*, 2001]. Char combustion can thus take place on the surface of the particle or inside the pores. Depending on the relative rates of oxygen transfer (diffusion rates) and chemical reaction (kinetic rates), three combustion regimes have been identified. At low temperatures (below 900-1000 °C) char combustion is limited by the kinetics of the oxidation reaction, and at high temperatures (>1000-1200 °C), either diffusion of reactants though the gas film around the particle and/or pore diffusion become the controlling step [Ramabuda, 2015; Kosowska-Golachowska, 2010; Svoboda, Hartman and Cermák, 2000]. These regimes are implicitly functions of temperature, heating rates, particle size, pressure, oxygen access and diffusion. The regimes are

shown qualitatively in the Arrhenius plot in Figure 2.4 along with an approximate distribution of oxygen around and inside the particle [Kosowska-Golachowska, 2010].

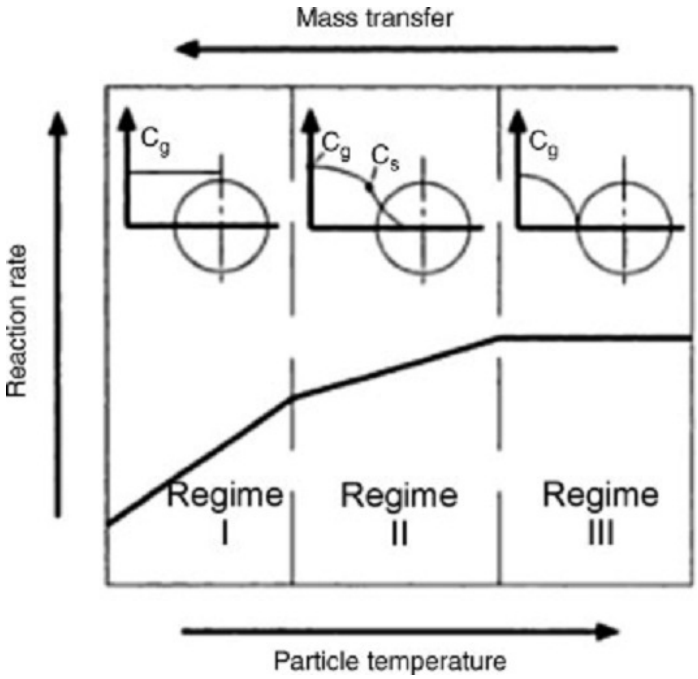

Figure 2.4: Rate controlling regimes for char combustion. From Kosowska-Golachowska [2010]

Regime I occurs when the reaction rate is slow relative to the diffusion rate. Regime II occurs when pore diffudion is the limiting step (*i.e.* the reaction rate is greater than the rate of diffusion into the particle). Regime III occurs when the diffusion of gases to the surface of the particle is hindered and the reactions take place in the gas layer around the particle [Ramabuda, 2015; Basu, 2006; Kosowska-Golachowska, 2010; Svoboda, Hartman and Cermák, 2000; Smoot and Smith, 1985]. Svoboda, Hartman and Cermák [2000] further split up the third regime into two sub-regimes: one where the diffusion through the gas film around the particle is the controlling step, and the other where the ash layer around the particle poses a hindrance for diffusion. Table 2.2 shows the important features and observations for the three regimes. Initial particle size, as seen in Table 2.2, is an important factor in determining the regime in which the char combustion will take place. A bed of smaller particles is more likely to burn in the reaction controlled regime, whereas larger particles will experience diffusion limitations to char combustion.

Table 2.2: Qualitataive Description Char Combustion Regimes, adapted from Ramabuda [2015]; Kosowska-Golachowska [2010] and Svoboda, Hartman and Cermák [2000]

	Description	Observation
Regime I	***Chemical Reaction Controlled***	
	Low temperature combustion.	Oxidation time decreases with increase in temperature and pressure.
	Large and small particles, but predominantly in smaller particles, where diffusive resistance is negligible	Coal type significant insofar as it effects char reactivity and mineral catalysis.
	Free diffusion of gas into particle interior.	
	O_2 concentration and reaction uniform throughout.	
	May be observed during the initial stages of domestic use,when the particles are heating up.	
Regime II	***Pore Diffusion Controlled***	
	Combustion at intermediate temperatures.	Oxidation rate decreases with increase in temperature, pressure and gas flow rate.
	Large and small particles.	Coal type has a moderate effect.
	Gas does not diffuse into particle interior; reactants are consumed on the surface, leaving behind an uncreated core.	
Regime III	***Gas Film Diffusion Controlled***	
	Combustion at high temperatures.	Oxidation time decreases with increasing gas flow rate.
	Small particles, or large particles,with flaking ash.	Coal rank and type has no effect.
	Gas diffusion into particle interior is hindered; reaction occurs on the particle surface.	Flaking ash layer may develop.
	decreasing d_P; constant density.	
	Ash Layer Diffusion Controlled	
	Combustion at moderate/high temperatures.	Temperature increase may cause decrease in oxidation time.
	Large particles, high ash coals, lignites.	Coal type has an effect: ash content and ash diffusivity.
	Ash layer retards the diffusion of gas to the surface.	

Char Combustion Reactions

Oxygen for the char-oxidation reactions is supplied via O_2, CO_2 and/or H_2O, while the CO taking part in the homogeneous reactions is released from the heterogeneous reactions. The general reactions are shown below.

Combustion:

$$2C + O_2 \longrightarrow 2CO \tag{R.1}$$

$$C + O_2 \longrightarrow CO_2 \tag{R.2}$$

Gasification:

$$C + CO_2 \longrightarrow 2CO \tag{R.3}$$

$$C + H_2O \longrightarrow CO + H_2 \tag{R.4}$$

Homogeneous CO oxidation:

$$CO + \frac{1}{2}O_2 \longrightarrow CO_2 \tag{R.5}$$

The reaction rate for the char-O_2 reactions is far higher than that of the gasification reactions; 10^5 times faster at temperatures of about 500-700 °C, where the CO_2-formation reaction (R.2) is more dominant. At higher temperatures (>1000 °C), the CO-forming reaction (R.1) becomes dominant and CO_2 is formed through the oxidation of CO according to Reaction R.5. At these temperatures, the ratio of the rates of CO production to CO_2 production is about 1:2 [Williams *et al.*, 2000] and increases exponentially with temperature. This ratio, according to Pemberton-Pigott *et al.* [2009] is ideal for complete combustion. The gasification reactions (R.3 and R.4) are endothermic and substantially slower, at temperatures below 1000 °C, than the combustion reactions (R.1 and R.2), and become comparable at temperatures above 1200 °C. The presence of alkaline compounds (K_2O, CO_2, CaO, $CaCO_3$) and some metals (Fe) in the ash can catalyse these reactions [Svoboda, Hartman and Cermák, 2000]. Temperatures over 1000°C have been reported by Kühn [2015] in household stoves.

2.3 Formation of Pollutants during Coal Combustion

In this section, the formation of pollutant species during combustion is discussed. Typical coal combustion pollutants of interest include gases, mainly CO and the oxides of sulphur and nitrogen, particulate matter, and organic compounds [Makonese, 2015; Uski, 2014; Williams *et al.*, 2000; Kim and Chun, 1998]. The volatile and tar fractions from pyrolysis contain light gases and condensible organic compounds, whereas the char fraction contains organically bound nitrogen and sulphur, as well as some trace elements, all of which are pollutant sources [Williams

et al., 2000]. The compositions and forms of these pollutants are dependant on the combustion temperature and combustion conditions.

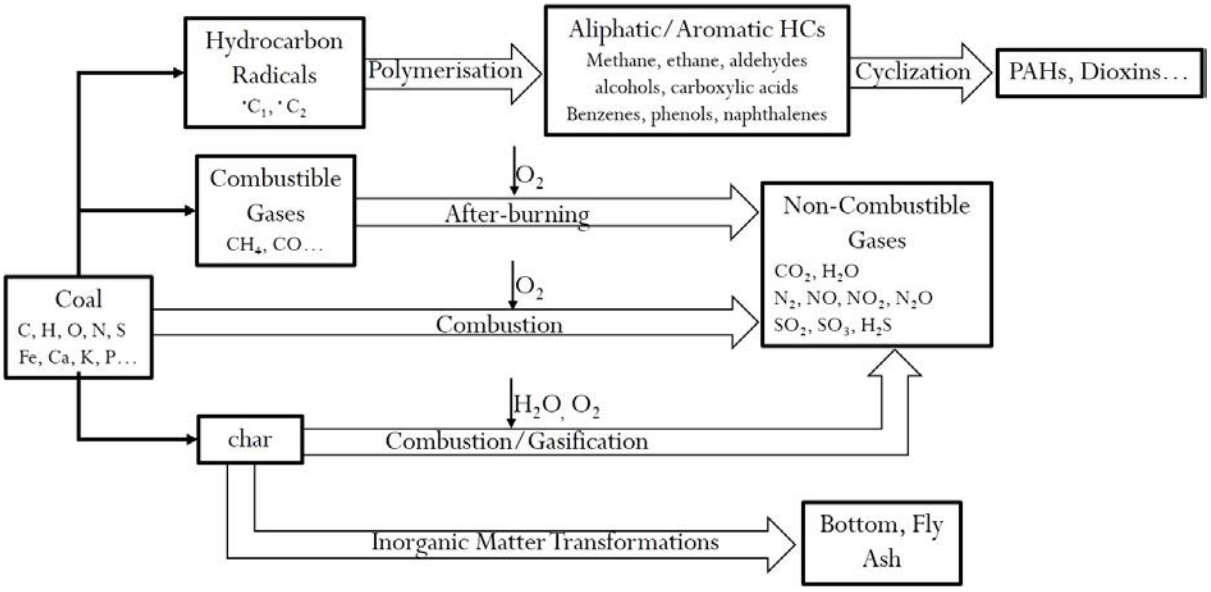

Figure 2.5: Key Pollutants of Coal combustion, Adapted from Krawczyk *et al.* [2013]

Figure 2.5 shows simplified formation pathways for common pollutants. Particles and aerosols form from the incomplete combustion of hydrocarbons and from the transformation of mineral matter associated with the coal. CO forms when there is insufficient oxygen to allow for the complete oxidation of carbon to CO_2, or when the heterogeneous oxidation of CO to CO_2 is inhibited by insufficient temperatures. SO_2 is a direct product of the oxidation of the sulphur within the fuel. The most dominant oxide of nitrogen, NO, is formed mostly via the reactions of nitrogen within the fuel. Some fixation of N_2 from the air may also occur.

2.3.1 Sulphur Dioxide

Sulphur appears in three forms in coal. (1) Organic sulphur exists as aromatic rings or aliphatic functional groups, whereas inorganic sulphur appears mostly as (2) pyrrite, and as (3) sulphatic salts of iron and calcium [Müller *et al.*, 2013; Johnson and Glarborg, 2000; Williams *et al.*, 2000; Calkins, 1994]. Distribution of sulphur within the coal depends on the rank and total sulphur content of the coal. Bituminous coals have comparable amounts of all forms, whereas anthracites have significantly less pyritical sulphur [Johnson and Glarborg, 2000].

The release of sulphur from coal starts during pyrolysis and extends through the char combustion process. Typically, the organic compounds are less stable than their inorganic counterparts, and are mostly released during pyrolysis, however a fraction is retained in the char and is released during char combustion [Krawczyk *et al.*, 2013; Müller *et al.*, 2013]. The main sulphur-bearing pyrolysis product is H_2S [Müller *et al.*, 2013; Button, 2010], formed from the decomposition of the organic components. Aliphatic species and sulphatic salts decompose at 700-850 °C, aromatic compounds at ~900 °C, and thiopenic species at ~950 °C [Fadeela, 2012; Johnson and Glarborg, 2000; Gryglewicz and Jasienko, 1992]. Pyrrite decomposes to pyrrhotite, which is further oxidised to magnetite and converted to haematite and SO_2 [Krawczyk *et al.*, 2013;

Müller *et al.*, 2013; Wielgosinski, 2012]. Sulphur-bearing products of pyrolysis and combustion are quickly oxidised to SO_2 via Reaction R.6, where RS is any sulphur-containing radical (HS, CS, CH_3S or S) [Johnson and Glarborg, 2000; Cullis and Mulcahy, 1972]. SO_2 is thus the overall main product of sulphur during combustion [Müller *et al.*, 2013; Williams *et al.*, 2000; Levy *et al.*, 1970]. A small percentage (1-5 %) of SO_2 is converted, via Reaction R.7, to SO_3 [Sternling and Wendt, 1972; Coykendall, 1962] and the remainder is retained as solids in the ash.

$$\text{Fuel}-\text{S} \longrightarrow \text{RS} \longrightarrow \text{SO} \longrightarrow \text{SO}_2 \tag{R.6}$$

$$\text{SO}_2 + \frac{1}{2}\text{O}_2 \rightleftharpoons \text{SO}_3 \tag{R.7}$$

Studies focussing on the gas phase oxidation of SO_2 to SO_3 [Johnson and Glarborg, 2000; Sternling and Wendt, 1972; Levy *et al.*, 1970; Coykendall, 1962], and its retention in the ash via natural mechanisms [Krawczyk *et al.*, 2013; Ilic *et al.*, 2003; Grubor *et al.*, 1999] or aided by the addition of absorbents [Zielke *et al.*, 1970; Liu *et al.*, 2002] as a form of SO_2 emission control, have been published widely. Cheng *et al.* [2003] offers a comprehensive review of the latter subject. The majority of these have been framed from the point of view of pollution reduction from industrial processes. The reader is referred to the literature for fundamental studies focused on the existence of the different forms of sulphur in raw coals [Hittle *et al.*, 1993; Kelemen and George, 1990], and their transformation during pyrolysis [Button, 2010; Olivella *et al.*, 2002; Chen *et al.*, 1998; Liu *et al.*, 2007; Shao *et al.*, 1994] and combustion [Yi *et al.*, 2007].

The effect of particle size on SO_2 is indirect. Since particle size plays a role on the release of volatiles during pyrolysis [Roets, 2014; Yang *et al.*, 2013; Hattingh, 2012; Anthony *et al.*, 1976], it may affect the rates at which the sulphur-bearing gases are converted. Particle size has been linked to the self-retention efficiency of a coal by Grubor *et al.* [1999] and Grubor and Manovic [2002], although the results from the two studies are contradictory. In the former study, the coal was sieved into 4-7, 7-10, and 10-13 mm size fractions and introduced to an electric fluidised bed reactor at various temperatures. Sulphur retention in the ash was found to increase with increasing particle size. However, in the latter study, where even smaller particle size fractions (1-1.6, 2.5-3.15, and 4.76-7 mm) are used, the authors reported no effect of particle size on sulphur retention, pointing to the non-uniformity of mineral matter distribution as the cause of the differences in sulphur capture.

2.3.2 Nitrogen Oxides

Nitrogen occurs in coal primarily as heteroatoms in aromatic rings or clusters [Baxter *et al.*, 1996; van Krevelen, 1981] and can be released during combustion as nitrogen (N_2), nitrogen oxide (NO), nitrogen dioxide (NO_2), and nitrous oxide (N_2O). NO_x species are formed according to three mechanisms, namely (1) Thermal-NO_x, (2) Fuel-NO_x, and (3)Prompt-NO_x [Wielgosinski, 2012; Bowman, 2000; Williams *et al.*, 2000; Flagan and Seinfeld, 1988]. The NO_x grouping is variable: some authors include all three species into the grouping [Kim *et al.*, 2011], while others

exclude N_2O. NO is the most dominant nitrogen oxide and has received a lot of attention in the literature; indeed the mechanisms listed above are for the formation of NO. Mechanisms for N_2O formation are discussed by Bowman [2000] and Svoboda, Cermák and Vesely [2000]. The Fuel-NO mechanism is responsible for the most NO (up to 90%), while the thermal mechanism only takes effect at high temperatures (>1400 °C) and produces no more than 10-20% of the NO. The prompt mechanism is responsible for the least amount (1-5%) of NO [Wielgosinski, 2012; Bowman, 2000; Baxter *et al.*, 1996].

The thermal mechanism involves the direct synthesis of NO from molecular O_2 and N_2 in the air at high reaction temperatures. This process is essentially a chain reaction initiated by the formation of an active oxygen atom, via reaction R.8, with a high-energy inert molecule, which can be a molecule or the hot metallic wall of the combustion chamber. Propagation occurs through alternative reactions of active O atoms with molecular nitrogen (R.9) and active N atoms with molecular oxygen (R.10) [Wielgosinski, 2012]. In fuel-rich conditions, when the $OH^{\bullet}$ is in abundance, Reaction (R.11) terminates the chain reaction.

$$O_2 + M \longrightarrow O + O + M \quad \text{(R.8)}$$

$$O + N_2 \longrightarrow NO + N \quad \text{(R.9)}$$

$$N + O_2 \longrightarrow NO + O \quad \text{(R.10)}$$

$$N + OH \longrightarrow NO + H \quad \text{(R.11)}$$

The prompt mechanism is prevalent in the flaming stages of combustion. Hydrocarbon radicals, formed from the reaction of hydrocarbons and molecular nitrogen, are oxidised to NO in the flame:

$$CH_2 + N_2 \longrightarrow HCN + HN \quad \text{(R.12)}$$

$$CH + N_2 \longrightarrow HCN + N \quad \text{(R.13)}$$

$$C + N_2 \longrightarrow CN + N \quad \text{(R.14)}$$

Oxidation occurs via:

$$HCN + O \longrightarrow NCO + H \quad \text{(R.15)}$$

$$NCO + O \longrightarrow NO + CO \quad \text{(R.16)}$$

The fuel mechanism is directly related to the nitrogen content of the coal. Figure 2.6 shows how NO is formed from fuel-bound nitrogen as conceptualised by Miller and Bowman [1989].

The source of nitrogen for this mechanism is the fuel itself. Hydrocarbons containing nitrogen are pyrolysed to release HCN, which is oxidised to $NCO^{\bullet}$ radicals, which are, in turn, reduced to a nitrogen atom. There are three possible routes for this N-atom, namely (1) reduction by an existing NO molecule to form elemental N_2, (2) oxidation to form NO, and (3) reaction with a hydrocarbon radical which returns the process to the start. Reburning and subsequent

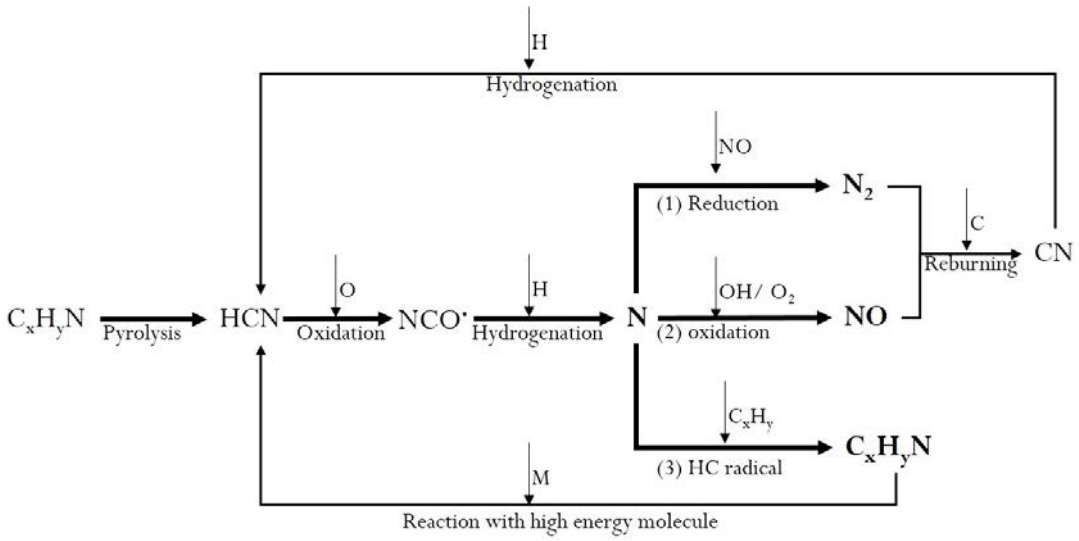

Figure 2.6: NO formation accorfing to Fuel Mechanism, Adapted form Wielgosinski [2012]

hydrogenation of the N_2 and NO formed from the first and second paths produce HCN, which also restarts the process [Wielgosinski, 2012].

NO_x and N_2O emissions from fuel-bound nitrogen during pulverised fuel processes, in predominantly fluidised beds, have been reported in the literature. Factors of interest are temperature, atmosphere, O_2 concentration, as well as coal properties, including particle size. Zhou *et al.* [2013] studied the variations of NO_x and N_2O emissions between combustors of different scales. They reported, from single particle TGA studies, that less than 8% of the nitrogen is released as N_2, while up to 85% reports to the NO_x fraction. This result is consistent with convention reported in literature. In larger scale combustors, *i.e.* pilot-scale and industrial scale reactors, the authors found that as the size of the application increases, more N_2O is released. Coal rank was found to have a positive effect on the conversion of fuel-N to NO_x [Kim *et al.*, 2011; Baxter *et al.*, 1996]. Liu *et al.* [2005] studied a wider range of coal properties and their effect on the NO_x and N_2O emissions; fuel carbon and nitrogen content was found to be the most important properties, as the emissions of NO_x and N_2O increased with an increase in the amounts of nitrogen and carbon in the coal. Operating conditions in a circulating fluided bed (CFB) were studied by de Diego *et al.* [1996] who reported that both NO_x and N_2O increased with temperature, which was positively correlated with the emissions of both species, depending on the excess air. The authors also studied the response of the system to the addition of limestone: a decrease in N_2O emission was noted while NO_x emissions increased. This result indicates an interplay between the emissions of NO_x and SO_x since both these species can interact with limestone. This idea is discussed at length by Johnson and Glarborg [2000].

A comprehensive account of the effect of particle size is given by Jiang *et al.* [2010] who studied pf particles smaller than 20μm in a fixed bed reactor, and monitored the emissions of the three species (NO, NO_2, and N_2O) individually. N_2O emission was found to increase with an increase in mean particle size, while NO emission decreased. Their findings were consistent with those of de Diego *et al.* [1996]. The authors assign the ease with which volatile species are able to escape the smaller particles as the main cause. The greater fraction of NO_x emissions are from

volatile-N [Wendt, 1980]. Smaller particles facilitate the release of volatiles from within the coal during combustion. This affords the nitrogen species sufficient time in the combustion chamber to convert to NO_x and further to N_2O. The delay of volatile release in larger particles may delay ignition and consumption of the char,which may cause some char-N to remain in the solid phase and thus decrease the formation of NO_x.

2.3.3 Particulate Matter

Particulate matter emissions can appear in various ways [Ninomiya *et al.*, 2004; Williams *et al.*, 2000; Flagan and Seinfeld, 1988; Damle *et al.*, 1982]: (1) Soot, or black carbon, is produced from the incomplete combustion of the coal (*i.e* instead of forming CO_2). Soot is made up of chain-like aggregates of primary carbon-enriched particles, or poly-aromatic hydrocarbons [Mastral *et al.*, 1999]. (2) Mineral matter associated with the coal can form ash particles depending on the mode of occurrence. Included minerals become free after the carbon structure around them burns and coalesce in the liquid or solid phase [Liang *et al.*, 2017]. Excluded minerals, especially those having size of less than 10 μm, can escape the char when it fragments [Makonese, 2015; Liu *et al.*, 2008], and transfer to PM without phase change. This mechanism is called the *solid-to-particle* pathway and is associated with particles in the 2.5-10 μm size range and the presence of refractory elements (Si, Al, Ca, Fe *etc.*) in the PM [Lui *et al.*, 2007; Tomeczek and Palugniok, 2002; Linak *et al.*, 2000; Lui *et al.*, 2007]. (3) Heavy metals in the coal may vapourise in the flame and subsequently undergo homogeneous and/or heterogeneous nucleation to form ultrafine (10-30 nm) aerosols which can condense and coagulate in the post flame region, where temperatures are low [Linak and Wendt, 1993]. This *solid-vapour-particle* pathway results in particulate agglomerates of the 1-2 μm size range and is associated with the presence of volatile elements in the PM [Senior *et al.*, 2000; Clarke and Sloss, 1992].

The formation of soot from hydrocarbon agglomeration is shown in Figure 2.7, and described by Bockhorn [2000] as the conversion of a hydrocarbon fuel containing a few carbon atoms to a carbonaceous conglomerate containing millions of carbon atoms. Hydrocarbons released during the devolatilisation step may themselves be pyrolyzed in the oxygen-poor conditions, depending on their chemical structure: aliphatic compounds may pyrolyse to form ethyne, which, via polymerisation reactions, become polyethynes, whereas aromatic hydrocarbons undergo pyrolysis and becomes PAHs. The latter species is of particular concern since PAHs have been associated with ill health effects [WHO, 2014]. The coagulation of these products results in the formation of soot particles [Williams *et al.*, 2000]. The types, amounts, and size distributions of soot depend on the combustion temperature, residence time [Williams *et al.*, 2000], as well as the composition of the volatiles. These are especially dependant on the presence of aromatic hydrocarbons, which are, themselves, related to the rank of the parent coal: an increase in rank is linked to an increase in aromaticity, which increases the soot yield [Buhre *et al.*, 2006]. Soot is known to increase the heat transfer via radiation [Bockhorn, 2000; Vovelle and Delfau, 2000], a desired effect when coal is burnt for space heating. Failure to oxidise soot within the flame zone leads to its emission in the flue gas [Bockhorn, 2000].

Ash was not considered as one of the species of interest from a pollutions point of view until it

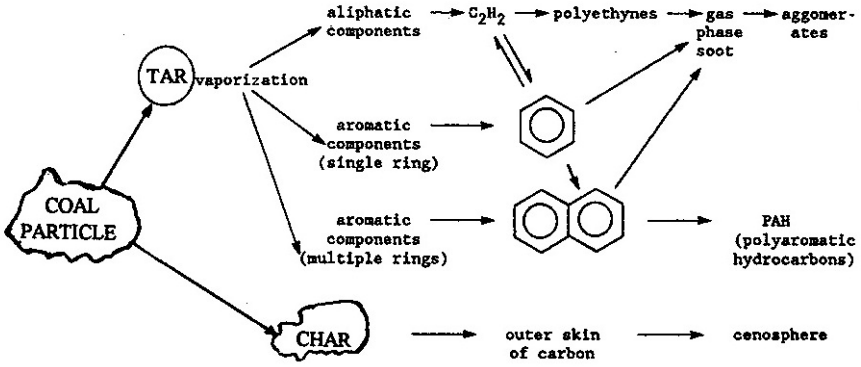

Figure 2.7: Soot Formation Pathways during Coal Combustion from Williams *et. al.,* [2000]

was pointed out by Davidson *et al.* [1974] to be a carrier of many toxic metallic species [Flagan and Seinfeld, 1988]. Ash forms primarily from the inorganic matter associated with the coal. Larger ash particles are usually left over at the end of combustion and are termed bottom ash, whereas smaller particles that become entrained in the gas flow are called fly ash [Flagan and Seinfeld, 1988]. Entrainment occurs due to the air flow through the coal bed [Wielgosinski, 2012].

In epidemiological studies, particulate matter is divided into classes according to their size. Particles with diameters less than 1 μm (PM_1) are termed submicron. Those whose diameters are less than 2.5 μm ($PM_{2.5}$) are termed fine particles, whereas coarse particles are those with diameters greater than 10 μm, (PM_{10}). All particles larger than 1 μm are called supermicron [Uski, 2014; Buhre *et al.*, 2006]. Studies linking various coal characteristics and reaction conditions yield a few generalisation regarding the mechanisms [Xu *et al.*, 2011; Damle *et al.*, 1982], size distribution [Lui *et al.*, 2007; Yu *et al.*, 2007; Liu *et al.*, 2008], chemistry and morphorlogy [Liang *et al.*, 2017; Ninomiya *et al.*, 2004] of PM from coal combustion. Submicron particles form primarily from the vapourisation and homogeneous condensation of heavy metals, are perfect spheres with smooth surfaces, and are rich in sulphates, sodium, phosphorus, and heavy metals. Fine particles are formed from the heterogeneous condensation of metallic vapours on larger particles such as the refractory elements, and are rich in these elements. Coarse particles mostly form via the transformation of the mineral matter and account for the majority of PM.

The studies of Ninomiya *et al.* [2004] and Liu *et al.,* [2007, 2008] are good illustrations of the relation of raw coal particle size and properties on the size and type of PM emissions. The latter authors studied the influence of mineral matter transformations on the formation of PM. Their 2007 study involved the firing of pf coal particles in a drop-tube furnace at 1100, 1250, and 1400 ° C in 20 or 50% O_2. This work revealed two peaks in emissions, at 4 and 0.1 μm respectively. The $PM_{0.1}$, formed from the vapourisation and condensation of heavy metals, was found to be rich in sulphates, while the PM_4, formed from char fragmentation and the coalescence of included minerals, was rich in aluminosilicates. The increased reaction temperature, they found, led to more PM emissions, possibly due to increased fragmentation causing more mineral matter to be freed from the char and forming PM via the solid-to-particle pathway. The Liu *et al.* [2008] study further elucidates the roles of included and excluded mineral transformation in PM formation: a Chinese bituminous coal was separated into light (-1.4 $g.cm^{-3}$), medium (+1.4-2.0

g.cm^{-3}) and heavy (+2.0 g.cm^{-3}) fractions, which were pyrolysed (at 1 atm and 1400 ° C in a mostly N_2 atmosphere) and combusted (at 1400 ° C and 20% O_2) in a drop-tube furnace. From this work, the authors found that the light fraction, having the smallest sized minerals, the majority of which were excluded, had the highest emissions of PM_1 and PM_{10}, while the heavy fraction, consisting of larger-sized, mostly included minerals, had the lowest emissions. This, they ascribed to a three-fold effect of the increasing density: (1)The smaller-sized minerals in the light fraction were more amenable to particle formation, (2) The strong difference in mineral modes had an effect on the mineral transformation- and PM formation mechanisms for each fraction: the included minerals of the light fraction formed finer particles through coalescence, while the excluded minerals from the heavy fractions formed particles through fragmentation. (3) Char fragmentation was more pronounced in the chars formed from the lighter fraction, resulting in more PM from this fraction.

Ninomiya *et al.* [2004] sought to describe the effect of coal particle size and PM emission. Their study involved firing of three Chinese pf coal samples with varying ash content, separated into small (-63 μm), medium (+63-125 μm) and large (+125-250 μm) particle size fractions, in a drop-tube furnace at 1200 °C and 20% O_2. The most pronounced effect of particle size, they found, was in the dependance of the modes of occurence of the mineral matter on the particle size. Similar to the resuslts of Liu *et al.* [2008], PM formation was found to be greater as size, and with it the concentration of included minerals, decreased. Other studies have shown that PM emssions increase with increasing reaction temperature [Lui *et al.*, 2007; Yu *et al.*, 2007; Zhang *et al.*, 2006], inherent moisture [Liang *et al.*, 2017] and O_2 concentration [Yu *et al.*, 2007].

2.3.4 Organic Pollutants

The organic fraction of coal contains volatile aliphatic and aromatic hydrocarbons, such as tuluene, xylene, ethylbenzene, benzene, and aldehydes, as well as the heterocyclic compounds of nitrogen and sulphur [Chmielewski *et al.*, 2003]. These structures can be seen in Figure 2.3a. If the combustion conditions are such that complete combustion takes place, hydrocarbons are oxidised to CO_2 and H_2O [Wielgosinski, 2012; Williams *et al.*, 2000]. Practical applications present a scenario where the conditions lead to incomplete combustion, resulting in the partial oxidation of the hydrocarbons. Volatile organic compounds (VOCs) are defined as organic compounds which, once released into the atmosphere, can remain there sufficiently long enough to participate in photochemical reactions [Jaecker-Voirol, 2000]. Though the emissions of VOC are low compared to the other pollutants [Chmielewski *et al.*, 2003], it is significant as some VOCs are complicit in the negative health and environment effects of coal combustion [Jaecker-Voirol, 2000], particularly in the home. PAHs are the subject of much research as they have been linked to lung cancer and other debilitating diseases [WHO,2014; WHO,2002]. PAH formation via polymerisation of acetylene is discussed above and shown in Figure 2.7. At typical ambient temperatures, lower mass PAHs, with 2-4 rings, are found in the vapour phase, while heavier PAHs occur in the particle phase [Makonese, 2015; Forbes, 2010].

Kühn [2015] reported that the majority of VOCs from domestic coal combustion in a household stove were the BTEX compounds (benzene, toluene, ethybenzene and xylene). This result was

consistent with those reported by Sloss [2001], who studied VOC emissions from coal powered stations. Gulyurtlu *et al.* [2004] measured the VOC emissions from coal co-firing with waste material and found that the coal was responsible for the majority of the VOC emissions. The authors also reported that important parameters are temperature, excess air, and effectiveness of mixing, stating that high temperatures (>1000 °C) give rise to significant reduction of VOC emissions. Regardless of the fuel type, CO emissions were found to be correlated with VOC emissions, as both species are an indication of incompleteness of the combustion [Gulyurtlu *et al.*, 2004]. In their study of VOC emissions from coal combustion, Chagger *et al.* [1999] reported that as combustor size increased, VOC emissions decreased, since a larger combustion chamber allows for better mixing [Gulyurtlu *et al.*, 2004]. Makonese [2015] supports this view, stating that the use of simple devices, typical in households, makes it difficult to burn coal without producing substantial amounts of smoke, since providing the requisite pre-mixing of air and combustion gases is difficult in these devices. This results in the emissions of products of incomplete combustion such as CO, VOCs, and PAHs.

2.4 Coal Combustion in Household Devices

The combustion of coal can be undertaken in a fixed bed of large particles on a grate, a fluidised bed of smaller particles, or in high-intensity combustion applications as a cloud of even smaller pulverised coal particles. This section will review, briefly, the issues relevant to coal combustion in the home.

2.4.1 Characterisation of Common Household Combustion Devices

Characterisation of combustion devices

Combustion devices used in the home vary according to location, fuel availability and income. Taylot [2009] provides a basis for the classification of devices according to (1) fuel used, (2) fuel feeding procedure, (3) ignition front propagation, (4) combustion regime, (5) dominant heat transfer mechanism, (6) the fate of stove exhausts, and (7) the type of airflow into the device. In the developing world, liquid petroleum gas (LPG), kerosene (or paraffin outside the U.S), or some form of solid fuel are the common choices, striated according to income and location [Nkosi *et al.*, 2017; Naidoo *et al.*, 2014; Balmer, 2007; Mdluli, 2007]. This fuel can be fed into the device at any time in continuous-feed systems such as open fires, and only at the beginning of a burn cycle in batch-fed systems, *e.g.* kerosene stoves. Mixed-feed systems accommodate batch feeding but also allow for refuelling during the cycle. This type of feeding scheme can be employed in cast iron stoves where the combustion chamber is accessible. Ignition propagation can occur in concurrent flow where the propagation of the ignition front and the air flow are in the same direction (as in open fires) and counter-current flow where the ignition front propagates in the opposite direction to the airflow. This propagation behaviour is typical of the top-lit updraft method applicable to cast iron stoves and *imbaulas*, where the fuel bed is ignited at the top and propagates downward, but air flow begins at the bottom of the bed. The heat transfer method, determines where the cooking pot is placed to allow for maximum efficiency.

Convection-dominated devices require the pot to be placed directly in the path of the combustion products. Conduction-dominated stoves have the pot placed on a griddle, which is first heated by the combustion gases and then heats the pot via conduction. Radiation-dominant devices work by suspending the pot directly over the hot coals, such is the case in many charcoal-fuelled stoves. Convection- and radiation-dominant stoves usually vent exhaust gases to the outside of the room, whereas conduction-dominant devices exhaust combustion products into the room. Finally, devices can operate using a natural- or forced draft to facilitate airflow. Below follows a short review of the most common devices used in a South African context.

Common Household Combustion Devices

The open, or three-stone, fire is the most common "cooking device", and is used in rural, wood-burning communities [Jetter *et al.*, 2012; Ballard-Tremeer and Jawurek, 1996], including sub-Saharan Africa [Robinson *et al.*, 2011]. This system consists of three irregular stones, supporting a single pot over an open fire burning locally sourced wood [Preble *et al.*, 2014; Jetter *et al.*, 2012; Taylot, 2009; Bussmann, 1988]. An "improved" fire was studied by Ballard-Tremeer and Jawurek [1996] who raised the fire on a grate. The elevation is said to improve heat transfer efficiency (defined as the ratio of energy transferred to the pot to energy released via combustion) by limiting heat losses to the ground. The completeness of combustion is improved in this design by supplying primary air through the bottom [Ballard-Tremeer and Jawurek, 1996]. The three-stone fire has been used as a baseline for the assessment of biomass ICSs such as the Berkely-Dafur Stove [Preble *et al.*, 2014; Jetter *et al.*, 2012] in predominantly controlled laboratory settings. Robinson *et al.* [2011], however, warn that due to significant effect of user behaviours such as how the fire is ignited and tended to, *in situ* testing of the three stone fire is favourable over controlled testing.

Makonese [2011] used three different paraffin stoves, found in South African suburban homes to develop the HTP: (1) paraffin wick stove, (2) the improved wick stove, (3) and the pressurised paraffin stove (see also Makonese *et al.* [2012]). The wick stoves are barrel-shaped with a series of slots along the sides, as well as the characteristic twin woven fibre-glass wicks submerged into the fuel tank and fitted into bent aluminium retainers. The cooking surface has three pot supports. The improved wick stove was brought out to meet new SABS standards on paraffin stove safety and contains improved safety features such as better separation of the fuel tank from the combustion zone to keep the fuel from reaching flash point. The pressurised paraffin stove operates using the "roarer" type burner, so named due to the distinct jet-like noise it makes when in use, and operates via a combination of building and releasing pressure in the fuel tank, causing paraffin to flow out of the tank. This fuel is subsequently vapourised, mixed with air and combusted around the burner head [Makonese, 2011].

The majority of reports in a South African context involve the use of *imbaulas*, metal drums (20 or 25 L) with holes punched into the sides. These are used extensively in suburban communities [Kimemia *et al.*, 2010; Balmer, 2007], and can burn coal, wood, and even waste in some cases [Makonese, 2015; Masekameni *et al.*, 2014]. There is no standardised *imbaula* and variations in the number and size of holes, the presence and position of a grate, and the size of the drum

used are common. Improvements on efficiency and pollution reduction in *imbaulas* have been achieved by (1) adding a grate [Kimemia, 2009], (2) adjusting the ventilation rates by increasing or decreasing the size and number of holes [Masondo *et al.*, 2016; Kimemia *et al.*, 2011], and (3) changing the ignition method [Masondo *et al.*, 2016].

Cast iron stoves are also common for burning coal. In their survey of the household energisation scenario in the Kwadela community, Nkosi *et al.* [2017] reported that cast iron stoves were the most common device. Cast iron stoves were also found in the townships of Tembisa and Zenzele [Makonese *et al.*, 2015; Naidoo *et al.*, 2014]. These stoves are prized possessions and are passed down through families and this, in part, is the reason that the stoves are often in bad wear [1] [Nkosi *et al.*, 2017; Naidoo *et al.*, 2014; Balmer, 2007; Mdluli, 2007]. Families in possession of coal stoves, according to Naidoo *et al.* [2014], preferred to use the stoves in winter for the dual utility of the appliance. Despite the popularity of the cast iron stove, little work has been done to quantify the emissions or performance of cast iron stoves, with many studies simply reporting survey data on fuel usage and stove types found. If emissions results were gathered, they were concerned with the fuel type and less with the type of stove used [Language *et al.*, 2016; Wernecke *et al.*, 2015; Naidoo *et al.*, 2014].

In addition to store-bought cast iron stoves and the *imbaulas*, home-made stoves are also used in coal-burning communities such as Zenzele [Naidoo *et al.*, 2014] and Orange Farm [Balmer, 2007]. Novel devices such as the bottom-lit down-draft stoves of the SeTAR centre have been designed and lab-tested [Makonese, 2015; Ibraimo *et al.*, 2014; Makonese, 2011; Pemberton-Pigott *et al.*, 2009], but have not yet been encountered in homes.

Graham and Dutkiewicz [1999] and Graham [1997] evaluated the thermal and emissions performance of typical devices (and corresponding fuels) used in South Africa, including the *imbaula* and Union cast iron stove. The authors reported the *imbaula* to achieve a higher cooking efficiency than the Union stove, for which a cooking efficiency of 57.4% was reported. The opposite was reported for the combustion efficiency, calculated as the CO/CO_2ratio: the Union stove was reported to have a higher combustion efficiency than the *imbaula* and was found to vary depending on the bed configuration and to be negatively affected by the opening and closing of the side vent to control the power output during simmering. Losses due the thermal inertia of the stove, stack gases, and due to unburnt carbon remaining in the ash residue and char are possible causes of the low combustion efficiency of the appliance. CO_2 and CO emissions were found to be lower for the Union stove than for the *imbaula*. This, the authors explained, may be an indication of large fuel losses through the grate of the stove. In addition to the performance and emissions tests, Graham and Dutkiewicz [1999] determined the cost effectiveness of the different devices, concluding that the stove and *imbaula* were more cost effective than electricity in the Highveld. Interestingly, this varies with location and season: the abundance of coal in the Highveld makes its use more cost effective than in areas where it is scarce, and the longer heating services required in the winter make the coal appliances more cost effective than liquid fuel burning appliances, due to the higher cost of the latter fuel. These results, illustrate the need to assess fuels along with the appliance in which it is burnt as a system, as the two are

[1] It is important to note that union stoves are no longer produced in South Africa and there are not spare parts on teh market.

inextricably bound in terms of performance and cost.

2.4.2 Ignition Methods in Household Devices

Ignition of the coal bed can be done using one of two methods. In the traditional or conventional method, also called the bottom-lit, updraft (BLUP) method, a wood and paper fire is ignited on the grate, once established, coal is added onto this fire. Semi-volatiles released from the heated coal, rise through the cold zone and condense into droplets before escaping. This results in the emission of copious amounts of smoke, especially during the ignition and devolatilisation phases. Alterantively, the top-lit, updraft (TLUD) method, colloquially knowns as the *Basa Njengo Magogo* (BnM) method, can be used to ignite the coal bed. During TLUD ignition, the coal is placed at the bottom of the grid, and the paper and wood placed on top of this. The aim is to have a flame on top of the heating coals available to consume the smoke-causing volatiles released during the pyrolysis phase. This method was piloted by the Nova Institute in a programmed in the eMbalenhle community near Secunda [van Niekerk *et al.*, 1999] and named after granny Mashinini, one of ten participants, who was able to correctly implement the method [Wenzel, 2006]. The structural and observational differences between the traditional method and the BnM method are illustrated in Figure 2.8

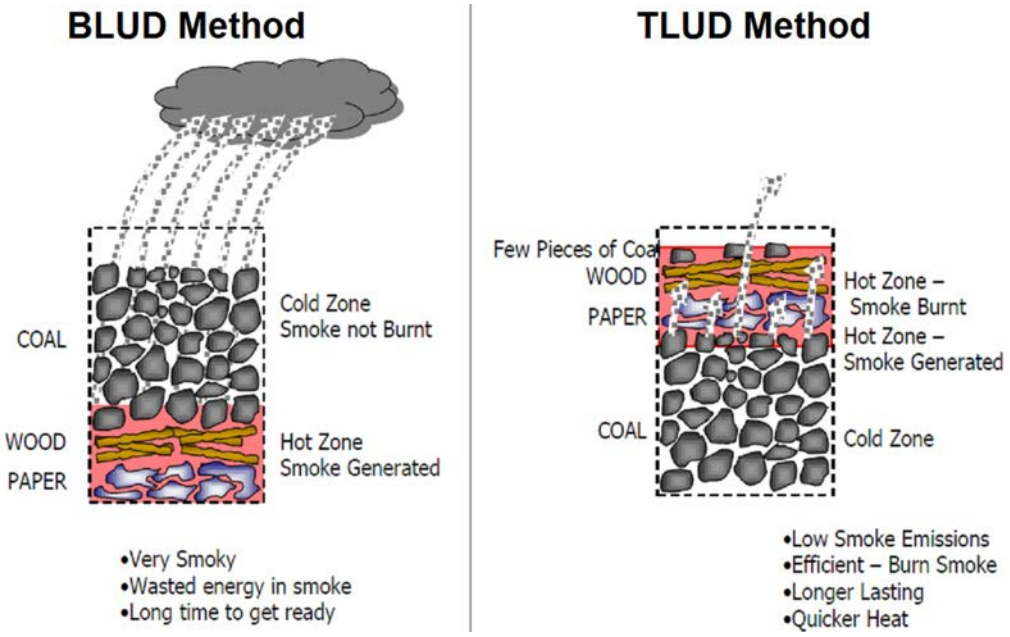

Figure 2.8: Differences between the BLUD and TLUD ignition methods adapted from Makonese [2015]

Since the successful intervention by Nova, several lab scale studies pairing the BnM and *imbaulas* have been published [Masondo *et al.*, 2016; Makonese *et al.*, 2015; Masekameni *et al.*, 2014; Le Roux, 2009], and all results show that using this method alone, leads to a a decrease of gaseous and particulate emissions. Despite this, and its status as a national energy intervention programme [Makonese, 2011] large scale deployment has not been explored beyond the pilot communities. However, this method has the potential to be a low-cost intervention that will not only result in emission reduction, but also has monetary and coal resource savings benefits [Makonese, 2015].

2.4.3 Requirements for Efficient Coal Combustion in Household Devices

There are three requirements for combustion: fuel, oxygen, and heat; the so-called "fire triangle". The fuel is the combustible material that feeds the fire, heat is required to ignite the material and oxygen sustains the combustion [Agee, 1996]. In the coal-burning household scenario, coal is the fuel, heat is provided by using kindling or paper, and the primary airflow into the stove is usually by natural draught through the bottom of the coal bed [Makonese, 2015]. Complete combustion of the fuel is the desired outcome as incomplete combustion is associated with emission of pollutants.

The most important parameters to ensure complete combustion conditions are: high enough combustion temperatures, sufficient primary air supply, and good mixing of fuel and air [Makonese, 2015; Tissari *et al.*, 2008]. High combustion temperatures increases combustion rates. In order to attain this in households, the loss of heat, from the stack gasses, for example, should be minimised [Tajwar *et al.*, 2011]. In *imbaulas* or open fires, much heat is lost to the surroundings, thereby reducing the combustion temperature and oxidation rates, due to the lack of an enclosed combustion chamber [Tissari *et al.*, 2008]. Balmer [2007] reported that stoves used in South African urban areas have had their internal structures and brickwork removed; such alterations can decrease the heat storage capacity of the stove [Tissari *et al.*, 2008]. High moisture content in the fuel can also reduce the combustion temperature as heat is removed from the system during the vapourisation of this moisture. Air supply to the coal is of critical importance and can be controlled via a chimney damper in devices fixed with a chimney. In *imbaulas*, this can be achieved by having fewer or more holes [Masondo *et al.*, 2016; Makonese, 2015]. Insufficient airflow can cause quenching of the fire, whereas an excess airflow (the amount of air supplied to the combustion chamber above the stoichiometric requirement for complete combustion [Felder and Rousseau, 2005]) will result in lower combustion temperatures due to the heat lost to the heating of the inert nitrogen in the air [Tissari *et al.*, 2008]. Most household combustion devices have excess air, measured in %, however, the availability of this air is diminished by poor fuel-air mixing in these devices [Fitzpatrick *et al.*, 2009]. In addition to these three parameters, a long-enough residence time at high temperatures in sufficiently mixed air-fuel conditions is required. [Uski, 2014; Tajwar *et al.*, 2011; Tissari *et al.*, 2008].

2.5 Characterisation of the Performance and Emissions from Coal Combustion Devices

Stove testing can be done in two contexts: (1) lab-based testing is traditionally used for design purposes as a tool for stove designers to assess changes in the performance of stoves, or fuels, due to design features. Data such as efficiency, fuel consumption and CO and PM emissions can be collected during such tests. (2) Field-based tests include prolonged surveys of the real-world use of stoves where data such as fuel savings are collected [Lombardi *et al.*, 2017]. Two case studies: the Lorena stove programme [Taylot, 2009] and the Indian National Programme on Improved Cookstove (NPIC) programme [Khandelwal *et al.*, 2016; Taylot, 2009; Kishore and Ramana, 2002] are commonly cited as evidence supporting the need for controlled testing for

design and optimisation purposes, as well as for comparative analysis of different devices and fuels used around the world [Makonese, 2011; Baldwin, 1987], and the need for field testing to corroborate the lab results in a real-life context. The lack of controlled lab testing could be the lead cause of the erroneous assertions of 50% fuel savings associated with the Lorena stove, and the most important lesson from the NPIC programme is the importance of cross-checking controlled lab test results against field data, since lab conditions are better optimised than the real-world use of the stove or fuel [Taylot, 2009]. This section will discuss the available methods for characterising the performance of and emissions from stoves burning various fuels in the lab context.

2.5.1 Assessing the Emissions of a Stove System

The *chamber-* or *hood method* can be used for measuring and characterisation of emissions during testing [Makonese, 2011].

The hood method, sometimes called the *direct*, was first introduced by Butcher *et al.* [1984] as a means to measure the emissions from unvented cookstoves, based on already existing methods to measure emissions from gas stoves [Davidson *et al.*, 1986] and kerosene heaters [Lionel *et al.*, 1986]. The method comprises of a hood attached to a dilution duct. The device is placed under the hood, the flue gases are extracted, via natural or forced draft at a known dilution ratio, into the duct and the concentrations of pollutants as well as the flue flow rate are measured [Arora and Jain, 2016; Makonese, 2011; Ballard-Tremeer and Jawurek, 1999a; Ahuja *et al.*, 1987]. In addition to the conventional emissions monitoring equipment, this method requires a constant, steady state flue flow rate throughout the burn cycle, as well as isokinetic sampling for sampling and measurement of particulates. Direct measurement of the flue flow rate, or a mass balance taking nitrogen or carbon as baseline species can be used to calculate emission factors [Ahuja *et al.*, 1987].

The chamber method was proposed by Ahuja *et al.* [1987] as a means to address the cost, complexity and to avoid the supposed effects of the extraction on the system, typical of the hood method. The Chamber method, as described by Ballard-Tremeer and Jawurek [1999b] consist of two steps. In the first, the stove is operated according to a predetermined task, such as the boiling of water in a sealed, dilution chamber. The concentrations of pollutants in the chamber are measured. Fans can be used to limit the striation of gases in the chamber [Ahuja *et al.*, 1987]. The calculation of emission factors requires that the air exchange or ventilation rate be measured. This is done in the second step, where the device is removed from the chamber and the measurement of pollutants continues. The air exchange rate is determined from the decay in pollutant measuremnts. Some disadvantages of this method include the assumption of constant emission rates, which, according to the results of Ballard-Tremeer and Jawurek [1999b], can only be achieved by refuelling the devices, thus limiting the use of the method to continuously-fed devices, such as the three stove fire. Secondly, the operator is exposed to the emissions in the chamber.

Opponents of the hood method argue that the method is costly and complex, due mainly to the addition of ducting and of equipment required for measuring the flue flow rate [Arora and

Jain, 2016; Ahuja *et al.*, 1987]. A further concern, raised by Ahuja *et al.* [1987], is that the extraction, especially when forced extraction is used, will change the combustion characteristics of the system under assessment. Furthermore, directly sampling from hood ducting, or from the chimney of a stove fitted with one, may lead to errors since not all the emissions may pass through the hood or chimney, especially in the case of aged stoves. In addition to this, determinations of excess air, which are required for the calculations of EFs and thermal efficiency, are complicated using the hood method as it cannot be known whether the measured O_2 came from the ambient air or went through the stove [Makonese, 2011]. Zhang *et al.* [2000], however, reported no significant differences in measured emissions when one sampled directly from the chimney or over a hood. In their studies of the hood and chamber methods, Ballard-Tremeer and Jawurek [1999a,b] found that even under forced extraction, using the hood method has no significant effect on measured temperatures, fire power, efficiencies or the measured emissions of SO_2 and TSP, and only a minimal effect on CO emission measurements. Their second study also concluded that due to the requirement of constant burn rate and emission factor, the chamber method was inferior to the hood method when comparing emissions of different devices.

2.5.2 Assessing the Performance of a Stove System

The design, use, and dissemination of improved cookstoves can be traced back to the 1970s and 1980s where widespread deforestation due to the overwhelming use of wood as a basic energy source, as well as to the growing attention placed on global warming, and especially of anthropogenic contributions, from as early as the 1990s [Taylot, 2009]. Despite this, Bussmann [1988] laments that even in the late 1980s, stove testing had yet to gain prominence as part of such programmes, and assessments of the efficacy of interventions were done using vague, and often biased, user surveys administered at the family level [Makonese, 2011; Taylot, 2009; Bussmann, 1988].

The advent of the WBT [2] [VITA, 1985] introduced the "efficiency" as a single metric to express the performance of the stove, or the fuel consumption per task [Ballard-Tremeer and Jawurek, 1996]. In the WBT, a pot containing a knwon aount of water is placedon the stove or cooking device and the time taken for this water to reach a rolling boil is measured. Opponents argued that (1) efficiency numbers were ambiguous and gave no background on power, fuel properties, pots used, and the testing conditions [Taylot, 2009], and (2) that efficiency numbers alone are unable to fully describe the complex nature of the biomass-burning system and were of no use to the end-users whom, in most cases, were impervious to their meaning [Makonese, 2011; VITA, 1985]. This initial WBT was far from ideal, and concerns over the failure of the test to explain the variation in the performance of different stoves soon arose. Furthermore, the test was not suitable for design purposes [Bussmann, 1988]. The Controlled Cooking Test (CCT) and Kitchen Perfomance Test (KPT) were introduced as a means to accommodate the variations in user habits and foods prepared in real-world cooking settings [Kipruto, 2011]. Following reports of inconsistencies [Makonese, 2011; Taylot, 2009] between results from three-stone fires tested in the lab [Smith *et al.*, 2000; Zhang *et al.*, 2000] and in the field [Kituyi *et al.*, 2001; Ludwig *et al.*, 2003], various WBT revisions [Bond *et al.*, 2014; GERES, 2010; DeFoort *et al.*,

[2] published along with the Controlled Cooking Test (CCT) and the Kitchen Performance Test (KT)

2009; Bailis *et al.*, 2007] were publshed in aim to address the any concernes. The UJ SeTAR centre recently developed the HTP to address the shortcomings of the WBT and variants such as the failure to simulate the real-world use of the fuel/stove system especially in contexts where boiling water is not an important part of cooking practices [Makonese, 2011; Makonese *et al.*, 2011]. Other reported methods include the Chinese [Bureau of Technical Support Beijing, 2017] and Indian [Kshirsagar and Kalamkar, 2014; Kishore and Ramana, 2002] national standards. Figure 2.9 provides a summary of the historical development of these methods from the reviews of [Lombardi *et al.*, 2017] and Kipruto [2011].

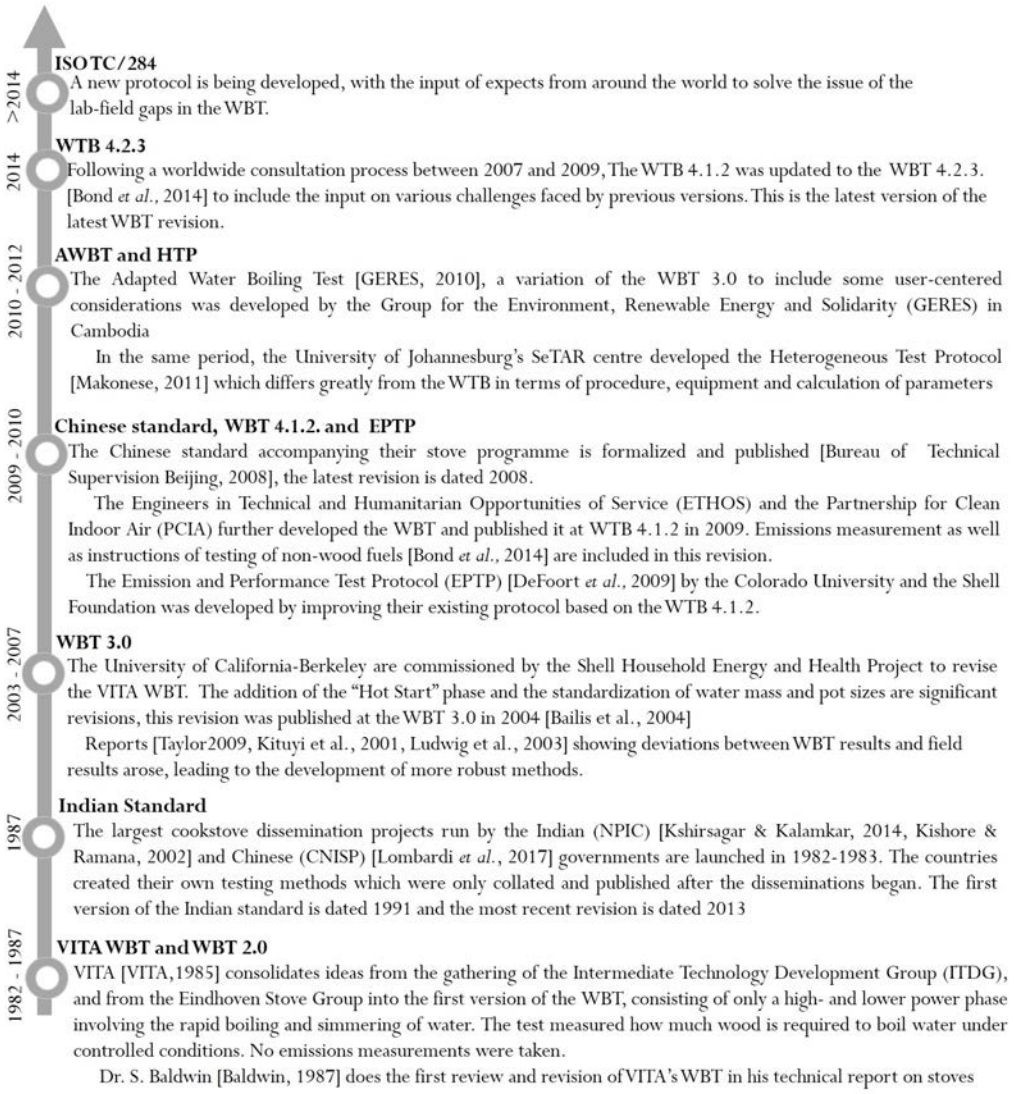

Figure 2.9: The Development of Common Testing Protocols, adapted and compiled from Lombardi *et al.* [2017]

The WBT is treated as the baseline protocol, and indeed many of the protocols above can be viewed as variations of "upgrades" of the WTB [Lombardi *et al.*, 2017]. The WTB comprises of three phases [Bond *et al.*, 2014]:

1. Cold start - the stove is at room temperature when the cold start phase begins, a known amount of fuel is ignited, and a known amount of water is heated and brought to the boil

atop the stove.

2. Hot Start- the stove, still hot from the previous phase, is loaded with a fresh batch of fuel and a fresh batch of water is allowed to boil.
3. Simmering - The stove is maintained (by adding more fuel) in a state where it is able to keep the water from the previous phase at a temperature just below its boiling point for 45 minutes.

There are three important parameters to be measured or determined in all three phases. (1) Thermal efficiency (calculated as the ratio of heat absorbed by the water to the heat produced via combustion), (2) the time taken for the water in phases 1 and 2 to reach boiling point, and (3) emission factors [3] . Some merits of the WTB include [Lombardi *et al.*, 2017; Kipruto, 2011] the application of the WTB to different stove types and non-wood fuels, allowing for the protocol to be adapted to different testing scenarios. The main challenge of the protocol is the concern of its *"real-life relevance"*. Furthermore issues of repeatability of the protocol related to the exclusion of the lid and the accuracy of temperatures of water near the boiling point are still outstanding.

The HTP differs from the WBT in that instead of three discrete phases (cold start, hot start and simmering), the HTP is conducted in one continuous phase where the power (high, medium and low) of the device is varied. This may be difficult to achieve in devices without a method of controlling the power, such as *imbaulas* and cast irons stoves. Furthermore, the HTP attempts to address the challenges faced by the WBT by (1) using a lid and limiting the water temperature to 80 °C, as well as (2)using performance curves to assess the perfomance of the stove under a wider range of applications than achieved with the WBT [Lombardi *et al.*, 2017; Makonese, 2011]. Makonese *et al.* [2011] use ethanol gel stoves as a case study to compare the WTB and the HTP. The conceptual assumptions of each protocol were assessed according to (1)energy efficiency, ability to meet the needs for (2) certification and (3) indoor air quality. The authors concluded that while the two protocols report similar results in thermal efficiency and time to boil, it is the conceptual differences between the protocols that lead to variances in parameters such as fire power, specific fuel consumption, burn rates and turn down ratio. Such differences occur as the result of the calculation and analysis methods, as well as the absence, or presence, of a pot lid. Both Makonese *et al.* [2011] and Lombardi *et al.* [2017] suggest that the HTP is an improvement on the WTB, and add that to fully exploit this advantage, the HTP needs to be applied in the field to determine its applicability in real-world use.

2.6 Low-smoke Fuels: The South African Journey

Following the publishing of several epidemiological studies [van Horen *et al.*, 1996; Terblanche *et al.*, 1993,b] linking the use of solid (wood and coal) and other "non-clean" (paraffin) fuels and the resultant indoor pollution to ill-health in children, low smoke fuels were considered as a possible short-to-medium term solution. This led to the launch of the Low-smoke Fuels

[3](The average mass (in gram) of pollutant emitted per mass (on kilogram) of burnt fuel. These can be on the basis of time, water boiled, test phase, energy produced or delivered to the pot [Lombardi *et al.*, 2017; Bond *et al.*, 2014]

Programme in the early 1990s, where the production, distribution, and impact of LSFs was to be studied. This programme took the form of two pertinent studies, (1) the Evaton field trials of 1992/1993 [Dickson *et al.*, 1995; Grobbelaar *et al.*, 1995], and (2) the Qalabotjha Macro-Scale Experiment of 1997 [Asamoah *et al.*, 1998; Scorgie *et al.*, 2001]. Other studies included, including the Orange Farm BMN campaign and interventions by the Nova Institute on behalf of Sasol Synfuels in eMbalenhle [Scorgie *et al.*, 2001]. Dickson *et al.* [1995] and Grobbelaar *et al.* [1995] provide a chronicle of progress of pre-1990 research. This section will follow the developments in low-smoke fuels research in South Africa since the Low-smoke Fuels Programme, and place the current study within that context.

2.6.1 The Evaton Project

The Evaton study, a multi-disciplinary enterprise, aimed to research all the aspects of introducing a viable low-smoke fuel into the market as a way to combat the HAP from coal combustion and improve air quality in coal-burning comminuities. Studies pertaining to the baseline scenario of solid fuel use in households and the associated health effects [Terblanche *et al.*, 1995], the production and testing of a low smoke fuel [Tait, 1993; Tait and Lekalakala, 1993; Rogers, 1995; Horsfall, 1994], as well as the social acceptability [Hoets, 1995], distribution and impact of the product were conducted [Dickson *et al.*, 1995; Grobbelaar *et al.*, 1995].

Three fuels:[4] (1) a reconstituted briquette produced by the The Council for Scientific and Industrial Research (CSIR), (2) a devolatilised coal produced by the University of Witwatersrand working together with United Carbon Producers (Wits/UCP), as well as (3) a commercial LSF supplied by Ecofuel were studied under controlled lab conditions and in the field. This formed part of the "production" leg of the Evaton Project.

Lab testing was done at the CSIR and University of Witwatersrand. A SABS [SANS-1111, 2008] approved low-smoke stove was used during both tests. Emissions data such as smoke obscuration EF_{PM}, emissions of SO_2, CO, CO_2 and NO_x was collected during the CSIR experiments. In addition to these, performance data such as useful heat provided and water boiling time was collected during the Wits experiments. The performance of the fuels was assessed using the SABS 1111 (now SANS 1111) standard for low-smoke coal appliances [Graham, 1997; Dickson *et al.*, 1995], despite the existence of several testing protocols that could be used. This method only provided a procedure to measure smoke emissions, and was supplemented with the EPA-G5 methodology for the meaurement of gaseous and particulate emissions from small-scale combustion devices [Dickson *et al.*, 1995; Rogers, 1995; Horsfall, 1994]. Rogers [1995], who performed such tests, commented on the unsuitability of this method as a means to characterise the performance of the fuel as it is a certification procdure for stoves designed to burn with limited smoke emissions and not as a design tool. Ten years after the inception of the low-smoke fuels project, Le Roux *et al.* [2004], under instruction of the DME, published a lab test methodology for the evaluation and validation of a low-smoke fuel. This method, developed using an *imbaula* and various coal-based fuels, involves the collection of data such as ignition time (the point where a thermocouple set above the coal bed registered a peak in temperature), water boiling time (the

[4] other proprietary fuels, under devlopment at the time are catalogued by Dickson *et al.* [1995]

time taken, after the smoke subsided, for 1L of water to reach boiling), combustion efficiency (based on the amount of fuel burnt) as well as the emissions of PM (total, $PM_{2.5}$ and PM_{10}) and CO, CO_2, and SO_2. SO_2 emissions were taken as the difference in sulphur content between the raw fuel and the ash, whereas CO and CO_2 emissions were measured continuously using an infra red monitor. It is not stated in the methodology how the method can be adapted for various devices and fuel/stove systems.

Field testing took place in two phases. In the winter of 1992, the CSIR and Wits/UCP fuels were piloted in 30 houses (15 houses per fuel) against a control group of 15 houses using normal coal. This phase was mostly inconclusive and the reader is directed to the report of Dickson *et al.* [1995] for an overview. The second phase, over the winter of 1993, increased the number of households to 90 (30 per fuel), and instead of a control group each household was given the coal along with their respective fuel [Dickson *et al.*, 1995; Grobbelaar *et al.*, 1995; Hoets, 1995]. This, according to Hoets [1995], enabled a direct user-orientated comparison between the fuels. Upon selection, respondents were trained and given a trial batch (two 70 kg bags) of their fuel for a week and then one bag a week for the succeeding two weeks. At the end of this test period, a round of interviews was scheduled, after which they were given a bag of standard township coal to use for a week. At the end of this "control" week, second interviews were scheduled and respondents were asked to comment on their experiences with the two fuels they had used. During each phase of the campaign household and ambient air quality was monitored as a contribution to the "impact" leg of the project. The interviews were used to furnish the "social acceptability" leg [Dickson *et al.*, 1995; Hoets, 1995].

The Evaton Project Fuels

The CSIR briquette is produced by binding coal discards[5] with cement and water in a ratio, in kg, of 100:15:21 [Tait, 1993]. This form of the briquette was lab tested against bituminous lump coal in *imbaulas* and was found to yield less and "whiter" smoke, suggesting, according to Tait [1993], lower sulphur emissions that could be related to the higher quality of the coal used, or the interactions of the sulphur with the lime in the cement [Dickson *et al.*, 1995]. A second, optimised version was produced and included the addition of lime to enhance the sulphur capturing capabilities. This new briquette comprised of coal discard, lime, cement and water in a 100:1:13:15 ratio in kg. This fuel was tested again in the lab against the original briquette and "normal coal" in the low-smoke stove [Rogers, 1995], and used in the 1993 field trials [Dickson *et al.*, 1995].

The Wits/UCP low-smoke fuel is produced by heating washed, bituminous coal discards under controlled conditions for 3 hours, where it is divested of most of the smoke-forming tars [Horsfall, 1994]. The issue of the heat required for the devolatilisation, the second major requirement, was addressed by using waste heat stokers already employed for the production of coke. The modifications required to reduce the heat supply to levels suitable for LSF production were not made to the stokers owing to the high cost. Thus the fuel was produced in a standard,

[5]see Horsfall [1994] and Grobbelaar and Surridge [1995] for an assessment of the availability of coal discard and its amenability for low-smoke production

unmodified stoker, and hence not according to design. The resultant LSF was smaller in size, had lower volatile yield and had a lower outer skin reactivity than the fuel produced under ideal conditions [Mangena and Korte, 2000; Dickson *et al.*, 1995]. The fuel was also tested in a lab and mass produced (100 tons) for each of the Evaton Campaigns.

Ecofuels' "Wandafuel" is a tapered, cylindrical briquette with a hollow core. Production methods were not reported, while a minimum retail price of R 45 per kg was indicated [Dickson *et al.*, 1995].

Rogers [1995] reported the following characterisation of the fuels as used in the lab tests.

Table 2.3: Characteristics Evaton Project LSFs

Fuel	CV [MJ/kg]	Size [mm]		Composition [%]			
		Min	Max	Ash	Moisture	Volatile Matter	Suphur
Bit. Coal*	≥24	6	70	10-30	1-5	17-30	0.6-2.7
Wits/UCP	21.4-24	20	90	<30	n.s	12	n.s
CSIR**	16.3	20	70	30-40	7.1	15	0.76
Ecofuel^{o}	24.5	40	45	24.3	8.3	24.3	0.84

* bituminous coal characteristics in line with SANS 1111 requirements
** version 2 of CSIR fuel
^{o} Ecofuel briquette ID=13mm, OD=45, annulus length=40mm

Results of the Evaton Project

Table 2.4, [Dickson *et al.*, 1995; Rogers, 1995], shows the results of the CSIR lab tests. Ignition of the fire was not standardised, but optimised to each fuel. The coal ignited easily using wood and paper as normally done (it is not specified which ignition method was used), as did the Wandafuel briquette. The CSIR briquettes required compressed air to be blown into the chamber and the Wits/UCP fuel required additional wood and paper. Refuelling was done 3 times for each burn cycle.

The gaseous emissions were not related back to the amount of fuel burnt, no provision for this is made by the test procedure used, and results can thus not be directly compared across fuels. The PM results for the coal and Wandafuel briquettes agree with the statement that emissions are highest during the ignition phase of combustion. Furthermore, the Wandafuel had the highest reduction, with regards to the coal, in PM emissions. The reduced SO_2 emissions achieved by the CSIR briquettes were attributed to the presence of lime. It was recommended that the Wits/UCP fuel be used in conjustion with coal once an established fire bed is in place [Rogers, 1995]. Dickson *et al.* [1995] commented that these results present a best case scenario as the tests were done in a good quality stove, optimised for low smoke emission, and pointed out the inseparable nature of a fuel and the device in which it is burnt, stating that "results of a particular fuel in a particular stove, cannot be automatically applied to another combination". This is of particular importance as the low-smoke stove used in the lab experiments was not used during the field trials.

According to Figure 2.10, showing some of the results from the Wits experiments as reported by

Table 2.4: CSIR Lab Test Results from Rogers [1995]

	Emission	EF_{PM}	Average gas composition [ppm vol.]				
	Period	[g/kg]	SO_2	CO	CO_2*	HC**	NOx
Bituminous Coal	Start-up	13.0	80	1490	2.7	406	64
	Refuel	8.11	101	724	2.5	71	58
WandaFuel	Start-up	3.19	12	945	3.2	128	68
	Refuel	1.34	16	922	2.1	21	30
CSIR briquette	Start-up	x,o					
	Refuel	2.16	9	935	1.05	56	13.4
Wits/UCP fuel	Start-up	o					
	Refuel	3.31	60	825	2.3	32	35

*CO_2 expressed as %Vol, ** HC = total hydrocarbons
[x]1993 CSIR fuel used
[o] start-up data was not meaningful for CSIR and Wits/UCP fuels due to ignition methods

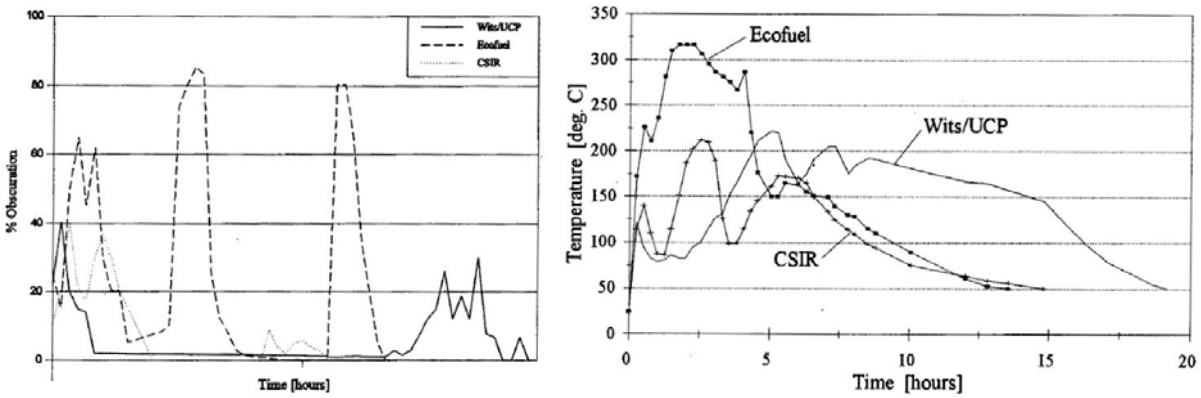

(a) Smoke obscuration

(b) Plate temperature

Figure 2.10: Results from the Wits Lab Test of the Evaton LSFs Dickson *et al.* [1995]

Horsfall [1994], the Wandafuel emitted high degrees of smoke at the start of the burn and after refuelling. The CSIR and Wits/UCP fuels behaved similarly, *i.e.* peaks in smoke emissions were observed at the start and after refuelling, however, the emissions were lower than the Wandafuel. Rogers [1995] found similar results from his study at the CSIR. Time-temperature relationships were also monitored during this study, and results found that due to its fast burn rate, the Wandafuel was able to: (1) boil water quicker (no times provided), (2) achieve the most complete combustion and (3) provide the most "useful heat" than the other two. Similar to the obscuration results, the Wits/UCP and CSIR fuels' temperature behaviour was similar to one another, with the former providing usable heat for a slightly longer period of time.

Household air quality monitoring in the 90 houses was reported by Terblanche *et al.* [1995] who monitored the emissions of particulates, CO, NO_x and SO_2. Monitoring was done over a 22 day period for 8-12 hours a day, including the peak cooking time. Table 2.5 shows the maximum peaks in SO_2, NO_2, and CO emissions from the field trials.

SO_2 exceedences increased in the order CSIR<Wandafuel<WIts/UCP<coal. The author con-

Table 2.5: Evaton Field Trials: Hourly average emission peaks

	Pollutant Emission [ppm]		
	SO_2	**NO_2**	**CO**
WHO hourly exposure limit	0.40	0.60	35
Coal	1.83	0.45	145.22
WandFuel	3.29	0.19	15.86
CSIR Briqutte	3.35	0.005	55.29
Wits/UCP LSF	3.91	0.18	83.15

firmed that the LSFs produced less smoke than the coal. Average SO_2 emissions, in the case of Wandafuel and the CSIR briguettes, were lower than the coal. NO_2 and CO emissions, however, remained unchanged. Particulate emissions from all three LSF were reported to be *always* over the 12-hour (260 $\mu m.m^3$) and 24-hour (180 μm^3) limits, while the coal passed these thresholds 96 % and 85 % of the time respectively. This, could be due to the high background levels in the township.

A direct comparison between lab and field data cannot be done due to: (1) the use of a stove designed for lower emissions during the lab tests, while regular household stoves were used in the field, and (2) field data reported emissions in the home while lab data reported values directly from the stove. The ignition methods, which have a significant effect on the emissions [Masondo *et al.*, 2016; Le Roux, 2009], used in the lab may have differed from those used in the field, emphasising the point made by Kipruto [2011] that provision must be made in lab testing protocols, for user-centred variability. It should be noted that the Terblanche *et al.* [1995] study aimed to determine the impact of the LSF on domestic air quality and was thus intended for comparison with previous housed monitoring data and not necessarily the lab tests.

From the interviews conducted as part of the 1993 campaign, Hoets [1995] reported multiple fuel usage in Evaton, including the selective use of electricity, echoing the findings of many a fuel use survey in the literature. When asked what was the largest concern regarding coal use, two thirds of the respondents reported that they worry "a lot" about coal smoke. Only 11% responded, after the three week period, that they were not likely to convert to LSFs. This low number indicated a satisfaction with the test fuels. When pressed to say what they "liked" about the respective fuels, all respondents noted the decreased smoke emissions. Wandafuel users considered the rapid burn rate both an advantage and a disadvantage and were satisfied with the ease with which the fuel could be ignited. Users of the Wits/UCP fuel were dissatisfied with the ignition, stating that too much wood was required to ignite the fuel, whereas CSIR-fuel users lamented the weak structure of the fuel, while they were pleased with the cleaner handling. These resuslts are consistent with the lab observations of Rogers [1995] and Hoets [1995]. Based on these responses, Hoets [1995] then concluded that the LSFs had an adequate acceptance and commented that further lab work be done to improve on the grievances.

2.6.2 Lessons from the Evaton Project: The Qalabothja Macro-scale Experiment

The Evaton Project was followed by the Low-smoke Fuels Macro-Experiment[6] which saw three "commercially-produced" LSFs being tested over the winter of 1997 in the Free state community of Qalabothja. Qalabotjha is a more isolated location than Evaton, ideal for reducing the interference from other pollutant sources as experienced by Terblanche *et al.* [1995]. Furthermore, Qalabotjha is a small-enough community to allow for a community-wide switch to LSF, instead of a selected number of homes. This too reduces the interference from homes who continued to burn coal during the study. Only three fuels were evaluated in the Evaton study, despite there being others on the market at the time; seven more fuels were considered in the lab test phase of this study in order to assess a wider range of choices [Scorgie *et al.*, 2001]. Furthermore, the use of *imbaulas* and a typical coal stove was an improvement to the lab tests as the results could be compared to those form the field tests, though it is not clear, from this report, what method was used during the lab test and whether this method was better suited to evaluating the performance of a LSF. The economic analysis and social acceptability was also assessed during the field trials.

Lab tests on 10 LSFs, in addition to "normal coal" were conducted by the Atomic Energy Corporation of South Africa (AEC). Scorgie *et al.* [2001] report that based on these experiments the LSFs performed better overall in *imbaulas* than in the Dover88 coal stove, due possibly, to the lower combustion efficiencies achieved by these fuels in the Dover stove. Only one of the ten fuels, a devolatilised coal, was able to achieve emissions equivalent to or lower than the baseline coal in the Dover stove. Fuel size and strength, the authors reported, strongly influenced the combustion efficiency, and as a result, the emissions of CO, VOC, and NO.

Scorgie *et al.* [2001] compared the reduction in emissions with those reported from the Evaton project. This data is found in Table 2.6, and show that overall, LSFs were able to reduce the emissions of pollutants and improve the air quality.

Ambient PM emission concentrations were greatly reduced by the use of LSF in Qalabotjha and Evaton, while CO emissions increased as a result of poorer combustion efficiency. Ambient NOx emissions, showed only a marginal decrease, despite all expectations that NO emissions from the LSFs would be reduced. Similarly, no significant change was observed for ambient SO_2 measurements despite the fuels having a lower sulphur content (17 - 53% lower than the lowest measured for coal) than for the baseline coal. The results from the Qalabotjha study confirmed that the only pollutants than can be reduced by changing fuel are PM, SO_2 and to an extent CO which is a function of the efficiency of combustion of the fuel/stove system. Reports on the socio-economics of LSFs, based on the acceptability studies in Evaton, Soweto, Kagiso (done by the NOVA institute under contract to Sasol) and Qalabotja, are mostly congruent with one another, despite some discrepancies of the technical studies [Scorgie *et al.*, 2001]. Overall, users stipulated that fuels must: (1) ignite easily, (2) burn effectively, and (3) produce sustained heat, this achieved by a fuel of the correct size and strength. Respondents in the Qalabotjha study showed a willingness to pay prices in the same range as coal for LSFs, a tall order considering

[6] Scorgie *et al.* [2001] report that the Low-smoke Fuels Programme included other similar studies in Soweto in 1996 [Hoets, 1996] and Kagiso in 1994 [van Niekerk *et al.*, 1994]

Table 2.6: Changes in ambient air quality due to the use of LSFs, from Scorgie *et al.* [2001]

Project	Fuel	Change in ambient Concentration LSFs compared to Coal							
		TSP	PM10	PM2.5	NO	CO	SO2	HC	VOC
Evaton Study [A]									
*	CSIR	↑			↓	↓	↓		
	Wits/UCP	↑			↓	↓	↓		
	WandaFuel	≈			↓	↓	↓		
1997 Macro-Scale Experiment [B,C]									
**	AFC		↓	↓					
	Chartech		↓	↓					
	Flame Africa		↓	↓					
*	AFC	↓			↓	↓	≈	↑	↑
	Chartech	↓			↓	↓	↓	↑	↓
	Flame Africa	↑			↓	↓	↑	↑	↑

A = Terblanche *et al.* [1995], B = Engelbrecht *et al.* [2001], C = Taljaard [1998]
* = indoor monitoring, ** = outdoor monitoring
↑ = increase in pollutant level
↓ = decrease in pollutant level
≈ = no significant change in pollutant level

that LSF can can cost between 65-900% as much as coal. The Wits/UCP fuel and the CSIR were found to be in the acceptable price range. Overall replacement of coal, a 3.3Mt per year market, will require production plants with very high throughput. Small, isolated markets, *e.g* communities with a significant reliance on coal over the winter, may be a better alternative. A comprehensive study of the market potential of low-smoke fuels was done by Qase *et al.* [2000], where the role of the merchants is highly emphasised [Scorgie *et al.*, 2001]. Considering all these factors, devolatilisation appears to be the most feasable production method. Devolatised coal is: (1) in the same price class as coal, (2) can be produced in large enough quantities, and (3) is able to provide the heat content required [Scorgie *et al.*, 2001; Qase *et al.*, 2000]. Lastly, the engagement of the community [7] is vital as fuel switching by isolated households, while beneficial to reducing HAP, is unlikely to achieve significant improvement in ambient air pollution [Scorgie *et al.*, 2001].

2.6.3 The North West University study on LSF Production

In 2015, the North west Univeristy undertook to produce a LSF via coal devolatisation and test the fuel's performance in a typical coal stove. The effect of production temperature on the fuel (and associated products) was investigated [Kühn *et al.*, 2017; Kühn, 2015]. LSF was produced at 450, 550, 650, and 750 °C and combusted in the Union 7 stove, typically used by the residents of Kwadela. Combustion tests were done in accordance with the method of Le Roux *et al.* [2004].

Results showed that final temperature had a significant effect on the fuels. LSF produced at 550°C, while found to yield a fuel that achieved significant reductions in the emissions of SO_2,

[7] See Asamoah *et al.* [1998] for a discussion on the community involvement from the Qalabotja study

PM, and VOCs, reported poor ignition, low burning rates and inefficient combustion. The study supported, once again, the use of devolatilisation as a production method and the economic evaluation, based on a scenario where the minimal amount of capital is required, showed that a low-smoke fuel produced in this manner at 550 °C could be sold at the same price as the baseline coal. It was recommended that particle size be studied as a potential avenue for improvement on the fuel's performance.

2.7 Summary

This chapter discussed the fundamentals of coal combustion, and the associated emission of pollutants, as well as their applications in household devices. The effect of fuel properties, especially particle size, and process conditions on the combustion of coal, the devices in which such combustion takes place, as well the emission and measurement of the associated pollutants, were of particular interest.

An overview of coal formation and the resultant properties was provided in order to develop an understanding of the structural and chemical components of coal, and the role these play in the description of the combustion process and the emission of pollutants. Two distinct combustion steps were identified: (1) a rapid devolatilisation step, followed by (2) a slower char burnout step. The former step involves the release of free moisture, the release, ignition and subsequent combustion of volatile gases, some of which are emitted as pollutants, whereas the latter is characterised by the reactions of carbon and oxygen resulting in the formation of more pollutants and the release of heat. Both steps are significantly affected by the fuel particle size. Building further on this basis, the formation mechanisms of pollutants such as SO_2, NO_x, CO, CO_2 particulate matter, and organic species were identified and related to the fuel properties, especially to fuel particle size, and the combustion step mentioned above. No direct links between raw coal particle size and SO_2 emission have been reported whereas, the effect of raw coal particle size on the emission of PM is embedded in its effect on the composition and forms of mineral matter. Smaller raw coal particles are said to contain more excluded minerals which are linked to the formation of submicron PM. It was also found that PM and SO_2 emissions are strongly dependant on fuel properties, lending themselves to control via LSF production, whereas the emissions of CO_2, CO and NO_x are dependant on the combustion conditions.

Previous work into the production and distribution of a LSF to low-income households concluded that devolatilisation is the most promising method for producing a fuel that is: (1) able to improve household- and ambient air quality, (2) is acceptable to the user, and (3) shows economic potential.

While the work done has added value to the the knowledge base of household energisation and the properties of the fuels used in low-income households, and the evaluation of proposed coal alternatives little attention was given to properties of the fuels, such as particle size, that can be controlled without subjecting the fuel to any chemical or thermal procedure. The myriad of pf coal studies in TGA have indicated that particle size plays a role in determining combustion properties such as ignition and peak temperature: larger particles are prone to heat and

mass diffusion limitation, while the former may be beneficial for ignition by trapping heat from combustion reactions with the particle and causing the particle to ignite, the latter may restrict reactions to the surface of the particle, leaving behind an unrestricted core, which may result in lower burning rates and combustion efficiencies. There is also ample evidence of the link between particle size and the formation mechanisms of pollutants such as sulphur and particulate matter. Despite all this, there is, however, no evidence of work done to systemically evaluate how the size of the fuels will affect its performance in a conventional packed bed household coal stove.

Chapter 3

Coal and Low-smoke Fuel Characterisation I: Conventional Analyses

The chemical structure and composition, mineralogy, and petrography of coal are of interest from an "initial properties and conditions" view point. This also allow for the characterisation of the transformations of organic- and inorganic matter and pollutant emissions during combustion. The low-smoke fuels (chars) used in this study are produced via the partial devolatilisation; the release of volatiles, condensible tars and reactivity of char is dependant on these initial properties. It is thus of importance to understand these properties and their implications for the LSF production- and combustion behaviour. This chapter presents the results of the conventional characterisation analyses.

3.1 Sample Selection and Origin

It is of importance that any stove test reproduce, as closely as possible, the real life use of the stove [Makonese, 2011]. From this viewpoint, the coal sample used in this study was procured from the Kwadela township through the same network as would its residents. The specific origins of the coal are unknown, however, the location of Kwadela, *i.e* within the Mpumalanga Highveld, suggest that it may be from a mine situated in the Highveld coalfield and it is anticipated that the coal sample will show similar traits to Highveld coals.

3.2 Sample Preparation

3.2.1 Size Separation and Representative Samples

The parent coal sample was left to air-dry in order to bring it to an equilibrium with the environment. A representative sample, to be used for characterisation, was extracted using the cone-and quarter method [England *et al.*, 2012].

The aim of the study is to evaluate the effect of fuel particle size on the combustion of coal and a coal-derived low-smoke fuel in a conventional household coal stove. It was thus necessary to separate the sample into its constituent sizes. To this end, the remainder of the parent sample was manually dry-screened and separated into its constituent size fractions. The screens were arranged in order of decreasing aperture size in millimetres: 53.0>37.5>26.5>19.0>13.2>9.5. Figure 3.1a shows the size distribution histogram for the parent sample. The size fractions in Figure 3.1b were obtained by normalising the total mass of the sample after the fines (<9.5 mm) particles were removed. Fine particles are susceptible to falling through the grate of the stove and are unlikely to be used in the home, these particles were thus excluded from the study. The x-axis in Figure 3.1b further shows the size designations, or classes, that will be used in the dissertation, for example, particles passing through the 37.5 mm screen but not the 26.5 mm screen are termed "30mm", those passing through the 26.5 mm screen, but not the 19 mm will be referred to as "20mm" and so forth. The type of fuel, *i.e* coal or LSF, will be appended to the size designation in order to distinguish the different fuels from one another. For example, the 30mm LSF will be referred to as 30mmLSF.

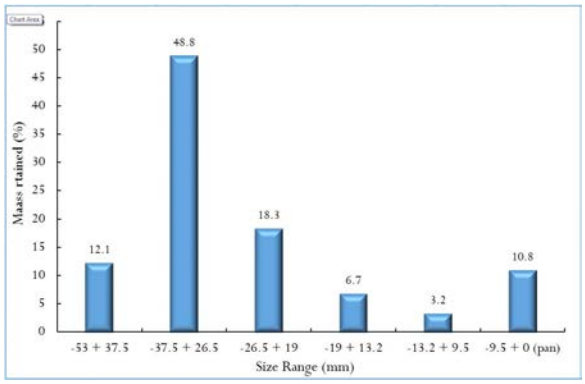

(a) Parent sample particle size distribution histogram

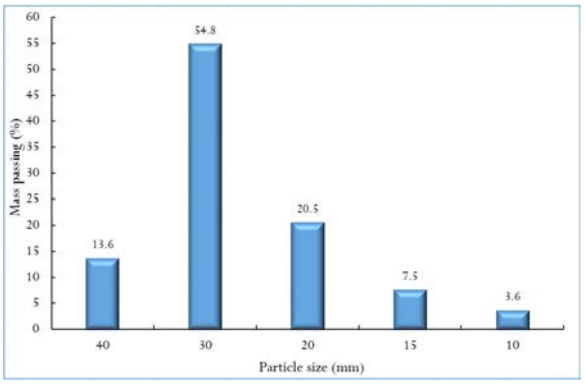

(b) Working particle size distribution histogram

Figure 3.1: (a) The particle size distribution of the parent coal sample showing the aperture sizes of the screens used. (b) As in (a) but normalised to a total mass excluding the fines (<9.5mm) which were not included in the study.

Similar to the parent sample, a representative sample of each size class was sought for characterisation purposes. The cone-and-quarter method was once again employed to this end. In addition to the size classes shown in the particle size distribution (PSD) in Figure 3.1b, a composite class was created by reconstituting the separated sizes in the mass fractions as shown in Figure 3.1b. The remainder of each size class was reserved for the production of LSF and subsequent combustion tests discussed in Chapters 4 and 6.

Further treatment of these representative samples is shown in Figure 3.2. Half of each representative sample was subjected to devolatisation at 550 °C to produce representative samples of the LSF to be used in the study. The work of Kühn *et al.* [2017] indicated that devolatilisation at 550 °C delivered a fuel that was able to meet the heating and cooking needs of the home, while achieving significant reductions in the emissions of SO_2, PM, and VOCs. The coal and LSF representative samples, in all the size classes, were then used for TGA analysis (discussed in chapters 4 and 5) as well as prepared for the conventional characterisation analyses. Preparation for mineralogical analyses, performed by the North West University Geology Department,

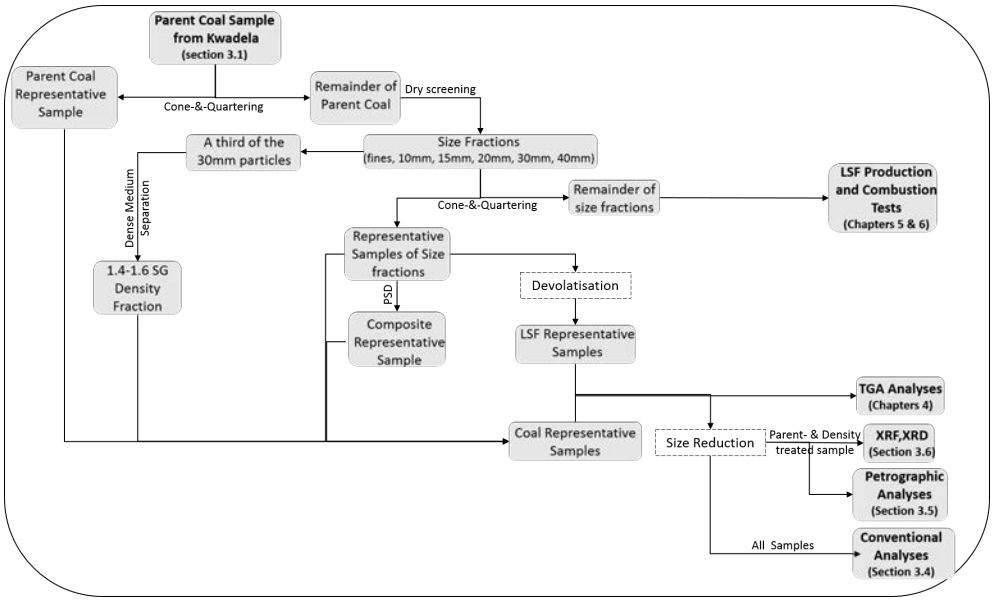

Figure 3.2: Treatment of parent coal sample for characterisation purposes.

involved crushing in a jaw crasher (Samuel Osborne (SA) LTD, Model 66YROLL) to reduce the size to <3mm and further reduction via milling (rotary mill: Wenaman Willian & Co. (PTY) LTD. 503A) and sieving to a pass size of -75 μm. Preparation for the chemical and petrological analysis was limited to jaw crushing and mixing (rotary sample splitter: SMH model:50/1A, serial no: 09/01/005) as the contracted lab, Bureau Veritas, performed further preparations on site.

3.2.2 Density Separation

Coal properties such as ash content (wt%) and maceral composition of a coal particle are related to its relative density [England *et al.*, 2012]. Separation of a sample by density then results in fractions with homogeneous properties. For the calibration of instruments and determination of the repeatability of results during the combustion tests, such a sample was required.

The 30mm size fraction was found to be the most abundant, accounting for over 50% of the parent sample; this fraction was chosen for dense medium separation. A large enough "homogenised" sample was obtained by subjecting the 30mm size fraction to dense medium separation, contracted to SGS Laboratories.

Float and sink analysis was performed to determine the density distribution of this size fraction. Float and sink analysis refers to the consecutive immersion of a coal sample into a series of liquids of different relative densities; coal particles of densities lower than the liquid float to the top and those of higher densities sink, the two fractions can then be separated mechanically [England *et al.*, 2012]. A densimetric curve, such as the one shown in Figure 3.3 can be constructed from the float and sink analysis and be used to determine how much coal will float at a given relative density, and this method was used to determine which relative density range would yield a sample large enough for the aforementioned purposes. Figure 3.3 indicates that close to 70% of the particles will float at a relative density of 1.6. From this information, the "homogeneous"

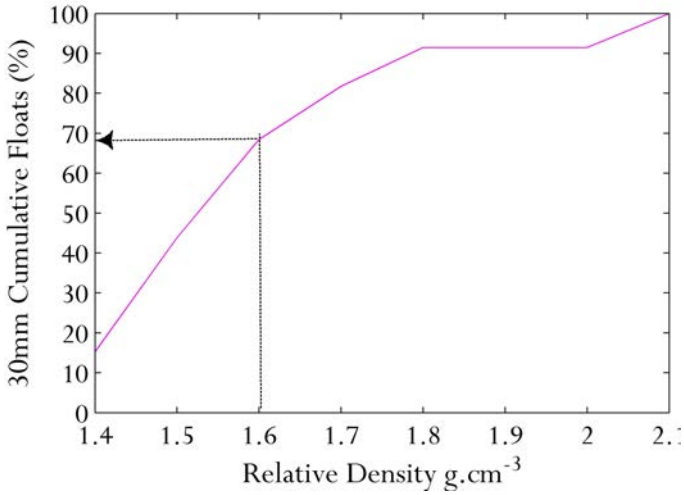

Figure 3.3: Densimetric curves of the the 30 mm size fraction. Such curves from the other size fractions can be found in Appendix A.

sample was created out of 30mm particles of relative density between 1.4 and 1.6. This sample was prepared for characterisation following the procedure outlined above.

3.2.3 Low-Smoke Fuel Production

Devolatilisation is considered as the correct method of producing a LSF from coal [Qase *et al.*, 2000]. In this study, this was done in a tube furnace, (Lenton:Model TMH16/75/610 3x3216+3216i), shown in Figure 3.4. The reducing atmosphere was created by feeding nitrogen, at a flow rate of 3 L.min^{-1}, into the furnace. A kilogram of coal, already prepared into the different size classes, placed in a stainless steel sample "boat", was heated from ambient temperature to 550 °C at a rate of 5 °C.min^{-1} and held for two hours. This process was repeated enough times to create the characterisation samples as mentioned above, as well as three 4-5kg batches of LSF for each fuel size class. The 550 °C maximum temparature was based on the work of Kühn [2015] who concluded that 550 °C was the optimum production temperature for a LSF that is able to perform typical household tasks, while emitting significantly less pollutants when compared to the untreated coal.

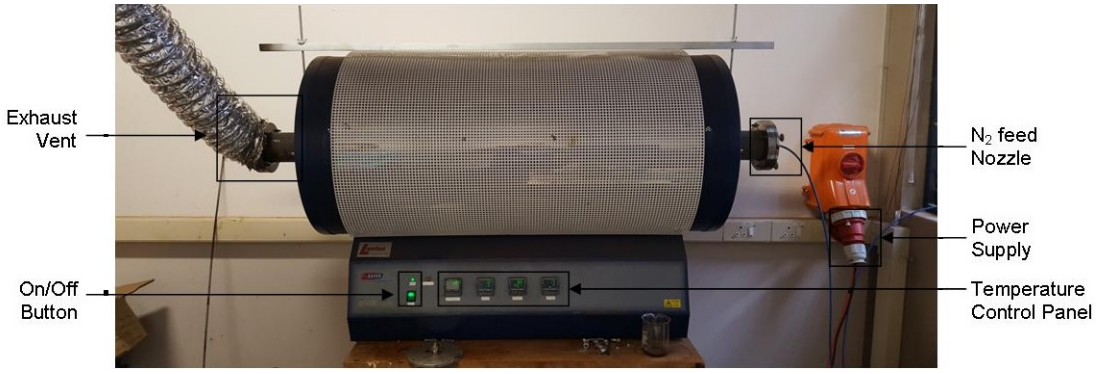

Figure 3.4: Tube furnace used for coal devolatisation. Nitrogen was fed to the system at a rate of 3 $L.min^{-3}$; the coal was heated up to 550 °C at 5 °C.min^{-1} and held for 2 hours.

3.3 Characterisation Analyses Overview

The suite of analytical methods used to characterise the coal and LSF used can be split into three groups: (1) chemical-, (2)mineralogical-, and (3) petrographic analyses. The chemical analyses aim to provide information regarding the composition of the coal in terms of carbon, hydrogen, nitrogen, oxygen and sulphur and include the thermal properties such as the calorific value (CV) and the swelling number. Mineralogical analyses provide information on the inorganic matter composition, and petrographic analyses, the organic matter composition and rank of the coal.

Table 3.1 shows the tests conducted as well as the standards used. Only the results for the parent sample and the size fractions will be discussed. The results for the density separated fraction can be found in Appendix B.

Table 3.1: List of characterisation analyses and standards

	Analysis/Procedure	**Standard**
Chemical Properties	Proximate Analysis	
	% Inherent Moisture	ISO 11722: 1999
	% Ash content	ISO 1171: 2010
	% Volatile matter content	ISO 562: 2010
	% Fixed carbon content	By difference
	Ultimate Analysis	ISO 29541: 2010
	% Total Sulphur	ISO 19579: 2006
	% Forms of Sulphur	ISO 157 (subcontracted)
	Calorific Value	ISO 1928: 2009
	Free Swelling Number	ISO 501: 2003
Mineralogical Properties	Ash Analysis (XRF)	ASTM D4326:XRF
	Mineral Matter (XRD)	Rietveld Method
Petrographic Properties	Maceral Composition	
	Vitinite Reflectance	ISO 7404 (3 to 5): 1994

3.4 Chemical Analyses

The proximate- and ultimate analyses, and the determination of the forms of sulphur as well as the CV and swelling index constitute the chemical analyses. The proximate analysis is an assay of the moisture, ash, volatile matter and fixed carbon of the coal. The ultimate analysis reports the composition of carbon, nitrogen, hydrogen as well as sulphur and oxygen in the coal. The CV is a thermal property of the coal and is a direct indication of the heat content of the coal and represents the combined heats of combustion of the elemental species identified in the ultimate analysis. [England *et al.*, 2012; Kosowska-Golachowska, 2010; Speight, 2005; Williams *et al.*, 2000].

Table 3.2: Results of Chemical Analyses. All % are given on a mass basis

	Parent Coal	MixedCoal	15Coal	20Coal	30Coal	40Coal	MixedLSF	15LSF	20LSF	30LSF	40LSF
Proximate Analysis (a.d)											
% Inherent moisture content	2.6	3.1	2.2	2.3	2.3	2.2	1.0	0.6	0.7	0.7	0.6
% Ash content	24.0	24.1	26.8	23.4	23.3	25.5	28.6	33.3	25.8	30.5	32.8
% Volatile Matter	24.4	28.5	24.3	23.9	25.9	27.3	9.1	9.8	9.5	10.9	12.4
% Fixed carbon (by calculation)	49.0	44.3	46.7	50.4	48.5	45.0	61.3	56.3	64.0	57.9	54.2
Total	**100.0**	**100.0**	**100.0**	**100.0**	**100.0**	**100.0**	**100.0**	**100.0**	**100.0**	**100.0**	**100.0**
Ultimate Analysis (d.a.f)											
% Carbon	79.0	78.1	78.5	79.8	78.1	77.3	86.9	87.6	89.0	86.3	85.9
% Hydrogen	4.4	4.6	4.2	4.3	4.3	4.2	2.7	2.3	2.3	2.3	2.7
% Nitrogen	1.9	1.8	1.9	1.9	1.9	1.9	2.1	2.2	2.2	2.3	2.0
% Sulphur	0.5	1.5	1.7	1.5	1.9	3.0	1.2	1.3	0.8	1.3	2.6
% Oxygen (by calculation)	14.2	14.0	13.7	12.5	13.8	13.7	7.0	6.6	5.8	7.8	6.8
Total	**100.0**	**100.0**	**100.0**	**100.0**	**100.0**	**100.0**	**100.0**	**100.0**	**100.0**	**100.0**	**100.0**
Forms of Sulphur (d.a.f)											
% Pyritical Sulphur	0.08										
% Sulphatic Sulphur	0										
% Organic Sulphur	0.42										
Gross Calorific Value (MJ/kg, a.d.)	22.8	22.1	21.9	23.2	23.2	21.9	23.2	21.8	24.5	22.0	21.8
Crucible Swelling Number (CSN, a.d)	0										
Calculated Properties											
Fuel ratio	2.01	1.55	1.92	2.11	1.87	1.65	6.74	5.74	6.75	5.31	4.38
Atomic H/C ratio	0.67	0.71	0.64	0.64	0.65	0.66	0.38	0.31	0.31	0.32	0.38
Atomic O/C ratio	0.14	0.13	0.11	0.12	0.13	0.11	0.06	0.05	0.04	0.08	0.03

a.d = air dry basis, d.a.f = dry ash free basis.

3.4.1 Proximate Analysis

On an air dry basis, the proximate analysis (in Table 3.2) of the parent and size fractions adhere to the expectations for a Highveld bituminous coal. The coal has low moisture content (2-3%), high ash yield (up to 30%), and medium to high volatile matter yield (up to 30%) [Matjie *et al.*, 2016; Kühn, 2015; Speight, 2005].

Studies that have characterised the effect of particle size on the proximate composition [Yu *et al.*, 2005; Mathews *et al.*, 1997], and the behavior of coal during pyrolysis and combustion [Kök *et al.*, 1998, 1997] have been in the form of TGA studies of fine (-400 to -60 μm) particles. Fixed carbon was reported to decrease [Kök *et al.*, 1998], while volatile matter yield increases [Yu *et al.*, 2005] with decreasing particles size. Ash yield, as reported by Yu *et al.* [2005] and Mathews *et al.* [1997], decrease with decreasing particle size, to a point, whereafter the opposite trend was noted. This, the authors, attribute to the variance in mineral matter content; larger particles, they said, is likely to be associated with more mineral matter. The results of Kök *et al.* [1998] omit the initial decrease and report only that ash yield increases with decreasing particle size due to mineral matter content. These trends are not obvious in the results in Table 3.2. There is indeed a decrease in ash yield, for both untreated coal and LSF fuels, as the particle size decreases, down to the 20mm particles, followed by a rise for the 15mm particle, mimicking the trend reported by Yu *et al.* [2005] and Mathews *et al.* [1997], albeit for pf sized particles. As expected, the volatile matter yield of the LSF chars is lower than that of the untreated coal fuels, consistent with devolatisation. Both fuels, however, show trends opposite to that observed by Yu *et al.* [2005], *i.e.* volatile matter yield decreased with decreasing particle size. Mathews *et al.* [1997], who studied the variability of volatile matter with particle size, concluded that any variability is due almost entirely to maceral effects and not a direct result of particle size.

The fuel ratio is an indication of the fuel's behaviour during combustion. A high fuel ratio indicates a fuel that is difficult to ignite, that will burn for longer with a short, clean flame; whereas a low fuel ratio is indicative of a rapidly igniting fuel, with a short burn out time and long, smoky flame [Schobert, 2013]. The fuel ratios for the untreated coals are similar to that of the parent coal sample: an average of 2. This value was also reported by Kühn [2015] and Hattingh [2012] for coals from the Highveld. The LSFs have fuel ratios three times higher than those of the untreated coals, this is consistent with the decrease in volatile matter from coal to LSF. Furthermore, the increase of the fuel ratio indicates an increase in aromaticity, which is related to rank [Yu *et al.*, 2005].

The swelling number gives an indication of the swelling propensity of the coal during conversion processes. The Kwadela coal parent sample was found to have a swelling number of 0, indicating that it is a non-swelling coal. This is of significance in cast iron stoves as swelling particles could block the flow of air through the bed [Svoboda, Hartman and Cermák, 2000]

3.4.2 Ultimate Analysis

The elemental assay of the parent coal, the untreated size fractions as well as their corresponding LSFs is shown in Table 3.2. Carbon occurs in coal as organic carbon and as mineral carbonates.

The untreated coals reported, on a dry ash free basis, an average carbon content of 78%. Similar results were obtained by Wagner and Hlatshwayo [2005]; van Niekerk *et al.* [2008]; Nel [2011] and Kühn [2015] in their characterisations of coals from the Highveld. The LSFs reported an average carbon content of 87% (10% higher than the untreated coals), which is consistent with the increase in fixed carbon seen in the proximate analysis. The mechanisms of the release of carbon in the fuel as part of short hydrocarbon chains, CO, CO_2 and black carbon or soot, and its role in the characterisation of combustion efficiency during combustion were discussed in Chapter 2.

The parent coal reports a sulphur content of 0.5% d.a.f (0.4% a.d), this is on the lower margin of the normal range of 0.4-1.27% a.d for Higveld coal [Wagner and Hlatshwayo, 2005] and fits the description of South African coal being of low sulphur content [Hancox and Gotz, 2014; Kalenga, 2011; Scorgie *et al.*, 2003]. The values for the different size fractions, averaging 1.9 % d.a.f, are more in line with the normal range. There is no clear trend in the wt% sulphur and particle size in either fuel. Considering the connection between sulphur and mineral matter, the expectation is that the sulphur content would show a similar size dependence as the ash in the proximate analysis. The decrease in sulphur content from untreated coal to LSF in each size corresponds with the release of sulphur-bearing gases during pyrolysis. During combustion, sulphur is emitted mainly as SO_2 through the combustion of organic sulphur as well as the decomposition (to Fe_2O_3), and subsequent oxidation (to SO_2 and, to a lesser degree, SO_3) of pyritical sulphur. Only a small fraction remains in the ash [Krawczyk *et al.*, 2013]. The total sulphur (determined through the amount of SO_2 released when the coal is combusted at 1350 °C [ISO19579:2006, 2011]) is thus a good indication of the potential SO_2 emissions during combustion. Chapter 5 will present more details on this.

The hydrogen content of the parent coal and untreated coal fuels is approximately 4% (d.a.f), this value is within the 2-6% range for bituminous coals [Speight, 2005]. The LSFs report about half the amount of hydrogen compared to the untreated coals. Hydrogen is lost as moisture and as part of low-chain hydrocarbons during primary (at temperature below 600 °C) pyrolysis [Roets, 2014; Fadeela, 2012; Hattingh, 2012; Solomon *et al.*, 1992]. Nitrogen content, as shown in Table 3.2 stays constant at about 2% across all sizes and fuel types. Since almost all nitrogen is bound to the organic coal matrix and play a minor role during primary pyrolysis, it is to be expected that the amount of this element remain essentially unchanged.

3.4.3 Calorific Value

The amount of heat that can be released when coal is burnt is designated by its CV. Highfield coal results from elsewhere [Kühn, 2015; Hattingh, 2012; Jeffrey, 2005; Wagner and Hlatshwayo, 2005] indicate a range of 15-35 $MJ.kg^{-1}$ (a.d) for the gross calorific value. All the fuels tested fall within this range. There is a positive correlation between the elemental carbon content of a coal and its CV [Vargas-Moreno *et al.*, 2012; Kosowska-Golachowska, 2010]. Based on this, the expected increase in CV of the LSFs (average 33 $MJ.kg^{-1}$ d.a.f) from that of the untreated coals average (31 $MJ.kg^{-1}$ d.a.f) is met, however, this increase may be too low considering the ~10% increase in carbon content. The increase in ash yield, which is negatively correlated to the CV,

from untreated coal to LSF, could be a possible reason for the deviant relationship between the elemental carbon and CV. The similar CV values suggest that if the same mass of any of the fuels is used, the potential energy released will be the similar. This will be further explored in Chapter 5.

Apart from giving an indication of the thermal potential of a coal, the calorific value, as well as the %FC and %VM, can be used to classify the coal by rank according to the ASTM D388 standard. The parent coal, and untreated coals fuels can be classified as high-volatile bituminous coals and the LSFs rank ranges from low-volatile bituminous to semi-anthracite.

3.5 Mineralogical Analyses

Mineral matter refers to the inorganic constituents of the coal and is the principal source of the elements that make up the ash when the coal is combusted [Speight, 2005]. Minerals can be roughly grouped as clays, carbonates, silica, sulphides, sulphates and salts. Clays (illite, kaolinite) can account for up to >50% of minerals in coal and contribute aluminium and silicon to the ash. Carbonate (calcite, siderite, dolomite) contribute iron, calcium and magnesium to the ash. Quartz (the primary silica mineral) can account for up to 20% of minerals and contributes silicon to the ash. Sulphides (mostly pyrite) make up less than 5% of minerals, convert to SO_2 during combustion, and contribute iron to the ash. Sulphate minerals (gypsum for example) occur in very low concentrations, if at all, in coal. When heated, these inorganic components undergo transformations an reactions that yield a mixture of solid, and volatile products which pose a pollution concern [Matjie *et al.*, 2016; Schobert, 2013; Huffman and Huggins, 1984].

For this study, the inorganic constituents of the parent coal sample were investigated by performing X-ray diffraction (XRD) and X-ray florescence (XRF) analyses. XRD analysis provides information about the mineral compounds (present as crystalline phases) in the coal, whereas XRF analysis provides information on the composition of elements (presented as oxides) in the ash formed after the coal is burnt in oxygen.

3.5.1 Mineral Matter Composition: XRD

The results of the mineral matter analysis are shown in Table 3.3. Matjie *et al.* [2016] studied several Highveld coals and found that kaolinite, quartz and dolomite accounted for the largest proportion of the minerals. This is the case with the Kwadela coal. A trace amount of iron-bearing minerals (pyrite and siderite) were found in the coal. The results for this coal sample are in agreement with those of Kühn [2015] who studied a sample from the same community and of others who studied Highveld coals.

Roets [2014] found that adding kaolinite to de-mineralised coal resulted in an increase in char yield during pyrolysis at 520 °C, whereas quartz caused a decrease in the char yield at the same temperature. From the relative amounts of kaolinite (12.8%) and calcite (<2%), it is expected that the effect of the latter will be insignificant in determining LSF yields during devolatilisation. During combustion, mineral matter can cause a lowering in the heat release and burn-out times

Table 3.3: Parent Sample XRD Mineral Matter Results. The difractogram for the parent coal sample can be found in Appendix A.1

Mineral Species	Composition by wt. %	
	Parent Coal	**Kuhn (2015)**
Amorphous Content	75.87	68
Kaolinite	12.8	14.1
Quartz	7.9	4.4
Dolomite	2.04	7.4
Calcite	1.28	3.6
Siderite	0.04	n.r
Pyrite	0.06	0.5
Graphite	n.r	0.8
Micricline	n.r	0.4
Goyazite	n.r	0.4
Muscovite	n.r	0.3
Anatase	n.r	0.2
Total	**100**	**100**

n.r=not reported

of coal; *e.g.* a study by Sentorun *et al.* [1996] found that demineralised Turkish lignite coals, showed an increase in burnout times and heat released during combustion. The modelling work of Shirazi *et al.* [1995] support this finding, reporting a decrease in the calorific value as mineral matter increased. This, the authors stated, is due mostly to the endothermic nature of the mineral decomposition reactions. This suggests that high fractions of minerals in coal lead to poor combustion efficiency.

3.5.2 Ash Composition Analysis: XRF

The composition of the ash reflects the changes that the mineral matter has undergone during the combustion process [van Dyk *et al.*, 2009; Vorres, 1986]. For example calcite decomposes at 800 °C to form calcium oxide CaO and CO_2 [Schobert, 2013; Speight, 1994]. Ash is a health concern due to: (1) the presence of trace elements such as mercury, selenium and arsenic [Vejahati *et al.*, 2010; Wagner and Hlatshwayo, 2005], and (2) the ability of finer particles to enter the lungs [Makonese, 2015; Davidson *et al.*, 1974].

Table 3.4 shows an abundance of SiO_2 (55%), Al_2O_3 (23%), a significant amount of CaO (12%), and trace amounts of MgO (4%), SO_3 (2%), TiO_2 (1%), and Fe_2O_3 (1%). These results are in agreement with reported ash constituent analyses of Highveld coals [Matjie *et al.*, 2016; Kühn, 2015; Matjie *et al.*, 2011; van Dyk *et al.*, 2009]. The high fractions of SiO_2 and Al_2O_3 is consistent with the dominance of kaolinite and quartz reported in the mineral matter (XRD) analysis. Likewise, CaO is the direct result of the presence of calcite. The presence of Mg, Ti, V species may also be due to the clay minerals as these elements have been shown to occur in trace amounts in clay minerals, the same applies for Fe and S species and sulphide minerals such as pyrite. [Vejahati *et al.*, 2010; Querol *et al.*, 1995]. These results also compare well, qualitatively, to those obtained by Kühn [2015], who also studied coal from Kwadela and concluded that the

sample, may indeed be from a Highveld coal mine.

Table 3.4: Parent Sample XRF Ash Composition Results

Ash Species	wt. % L.O.I.-free basis	
	Parent Coal	**Kuhn (2015)**
SiO_2	55.24	49.01
Al_2O_3	23.25	31.38
CaO	11.92	5.70
MgO	3.79	0.76
SO_3	2.27	6.65
TiO_2	1.33	1.94
Fe_2O_3	1.10	1.24
P_2O_5	0.60	0.92
K_2O	0.39	2.13
MnO	0.04	0.03
V_2O_5	0.03	n.r
Cr_2O_3	0.03	n.r
Na_2O	n.r	0.19
Total	**100**	**100**

n.r=not reported, L.O.I.=Loss of ignition

3.6 Petrographic Analyses

The organic content of coal, termed macerals, includes the fragmented and partially decomposed organic remains of the original vegetation. These can be ordered into three main groups: vitrinite, exinite (or liptinite) and inertinite [England *et al.*, 2012; Hlatshwayo, 2008; Falcon and Ham, 1988]. Petrographic analyses carried out in this study (*i.e.* maceral point-count analysis shown in Table 3.5, and vitrinite reflectance tests, in Table 3.6) were conducted in order to provide information regarding the organic composition and rank of the coal, as discussed below.

Table 3.5: Parent Sample Maceral Composition

Maceral Specie	**vol. % (m.m.b)**	**vol. % (m.m.f.b)**
Mineral Matter (calculated)	**13.1**	
Vitrinite	**23.1**	**26.6**
Liptinite	**1.9**	**2.2**
Inertinite	**61.9**	**71.2**
Reactive Semifusinite	31.1	35.8
Inert Semifusinite	28.9	33.3
Fusinite + Secretinite	1.9	2.2
Micrinite	0.0	0.0
Vitrinite Classification	**Low**	-

Highveld coals are characteristically inertinite rich and low in vitrinite [England *et al.*, 2012; Falcon and Ham, 1988]; this is true for the parent coal sample (see Table 3.5) with an inertinite content of over 70% on a mineral matter free basis and vitrinite content of only ~27% by volume.

Similar results have been reported by Wagner and Hlatshwayo [2005] for Highveld coals. This high inertinite coal is expected to form a relatively low-pore (denser), low-reactivity char characterised by a slow burn, 2-4 times slower than vitrinite-rich chars according to Cloke and Lester [1994]. The low liptinte content (2% m.m.f.b) is typical for the Permian-aged South African coals [Holland *et al.*, 1989] and is in agreement with previous reports on Highveld coals [Kühn, 2015; Roets, 2014]. Liptinite is linked with flame stability due to its high volatile matter and hydrogen content. Liptinite is only of importance during the devolatisation stage of combustion due to its low-temperature (~300°C) vapourisation that leads to the formations of pores on the surface of the softened char [Cloke and Lester, 1994]. The effect of liptinite is not expected to play a significant role during combustion of Kwadela coal due to its relatively low content in comparison to the vitrinite and inertinite.

Vitrinite is used to determine the rank of the coal sample, due to the linear relationship between vitrinite content and coal rank [England *et al.*, 2012; Cloke and Lester, 1994]. The reflectance range for the Kwadela sample is between 0.5-0.9% distribution with an RoV (vitinite reflectance) max of 0.68. Wagner and Hlatshwayo [2005] reported RoV max values ranging from 0.58 to 0.64 for their Highveld coal samples. The rank classification for the Kwadela coal, deduced from the vitrinite reflectance results, is Medium rank C bituminous coal, which differs slightly from the ASTM classification as a high-volatile A bituminous coal.

Table 3.6: Parent Sample Vitrinite Reflectance Results

Vitrinite Reflectance Distribution	**Rr %**
V5 (0.50 - 0.59)	17
V6 (0.60 - 0.69)	42
V7 (0.70 - 0.79)	35
V8 (0.80 - 0.89)	6
V9 (0.90 - .99)	-
V10 (1.00 - 1.09)	-
Rov(max)	0.68
Rank Category	Med. Rank C

3.7 Summary

The preparation and characterisation of the parent coal sample, the size fractions and corresponding LSFs were done, employing the conventional sampling and analysis techniques. Overall, results obtained for the Kwadela coal sample are consistent with those of Highveld coals.

All coals were found to be of high ash, and medium to high volatile content. Ash content showed an initial decrease, followed by an increase with size; this trend was found to be consistent with previously reported studies on the effect of size on coal properties. From the elemental composition, all coals and LSFs can be further classified as low sulphur. Lower sulphur content values were reported for the LSFs compared to the corresponding coals, consistent with the release of sulphur-bearing gases during devolatilisation. The calorific values were found to be within the expected range for Highveld coals and no significant difference in CV was found

between the different size fractions.

The parent coal sample was found to be rich in kaolinite and quartz with smaller amounts of dolomite and calcite and trace amounts of iron-bearing pyrite and siderite. The ash composition, was found to be rich in aluminium and silicon elements, reaffirming the mineral composition results. Characterisation of the coal's macerals revealed an inertinite-rich, low vitrinite, medium rank C bituminous coal.

Chapter 4

Coal and Low-smoke Fuel Characterisation II: Thermogravimetric Analyses

The parent coal was dry-screened into its constituent sizes, and from each of these, a representative sample was drawn for the purposes of studying the characteristics of each fuel. This chapter continues the aim of the previous one by reporting on the pyrolysis and combustion profiles of each of the fuels.

4.1 Operation Conditions

The use of thermogravimetric analyses for characterisation of coal is is not new and has been employed in many a fundamental study to determine the pyrolysis [Hattingh, 2012; Beukman, 2009; Zhu *et al.*, 2008; Kök *et al.*, 1998] and combustion [Sonibore *et al.*, 2005; Yu *et al.*, 2005; Davini *et al.*, 1990; Morgan *et al.*, 1987, 1986] properties of coal and other solid materials. Many of these studies have been concerned with the behaviour of fine coal particles under conditions typical of industrial conversion processes. Figure 4.5 shows a schematic of the purpose-built large particle TGA used in this study to characterise the pyrolysis and combustion behaviour of the fuels.

The experimental set-up consists of a vertical tube furnace (LentonTSV 15/50/180), with an internal diameter of 50 mm and a length of 500 mm, able to deliver heating rates of up to 25°C.min^{-1}, temperatures up to 1250°C, and accommodate particles of up to 40 mm diameter, suspended over the coal sample. The sample is placed in a quartz sample holder which is mounted on a mass balance (Radwag PS 750/C/2) able to measure mass with an accuracy of 0.001g. The flow rate of the process gas, fed to the top of the furnace, is controlled by a mass flow controller, to allow for one to two volume changes per minute. The temperature just above the sample is measured by a K-type thermocouple. The rise in temperature and change in mass are measured and logged in real time.

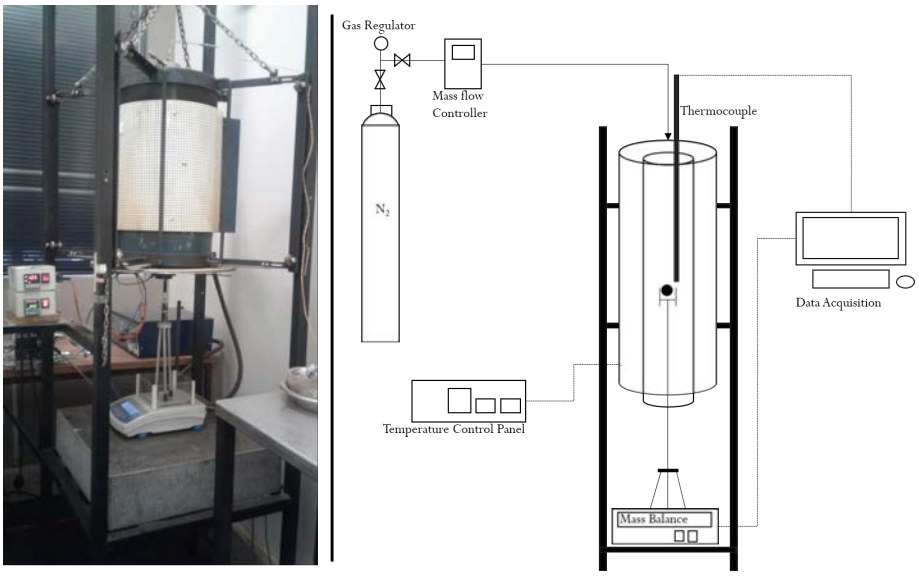

Figure 4.1: TGA Experimental Setup

During a typical experiment, the sample is placed in the holder and the initial mass of the particle is recorded once the balance is equilibrated. The furnace is lowered onto the sample and purged with the process gas, after which the temperature is allowed to rise to 1000°C at the set heating rate and held at that temperature for 2 hours to allow the mass loss to became asymptotic. Pyrolysis experiments were conducted in order to determine the degree of devolatilisation at 550°C, and the combustion experiments provided information regarding the expected burning profiles of the fuels. Table 4.1 summarises the experimental conditions for the TGA experiments.

Table 4.1: TGA Experiment Operating Conditions

	Pyrolysis	**Combustion**
Gas flow rate [L.min^{-1}]	2	1.5-2
Heating rate °C.min^{-1}	5	10
Final Temperature °C	1000	
Holding time [min]	120	
Sample mass [g]	single particles of 5-40 g	

These experimental conditions have been based in previous studies [Kühn, 2015; Yu *et al.*, 2005; Zygourakis, 2000; Kök *et al.*, 1998, 1997; Davini *et al.*, 1990]. In their study of the effect of coal size on its pyrolysis behaviour, Kök *et al.* [1998] employed a heating rate of 10 °C.min^{-1} and a final temperature of 900°C. Similar conditions were used by Morgan *et al.* [1987, 1986] during their twin study of the combustion of coal and char. The authors warn that, for combustion experiments, the heating rate ought to be such as to avoid ignition of the sample. Furthermore, final temperatures were suitable for the combustion experiment as Kühn [2015] reported temperatures around 1000 °C, for his experiments in common household stoves.

4.2 Standardisation of Procedure

Since single coal particles are used for each experiment, it was necessary to repeat each experiment to obtain a representative result. Therefore experiments were repeated at least twice. In order to determine whether two repetitions were enough to produce a reliable result, the combustion of 20 mm particles was repeated five times to establish the typical span of results. In order to avoid interference from fragmentation, the subsequent settling of the resultant fragments, or contact with the sides of the furnace wall, the larger particles, which are more likely to fragment, were not chosen for repeatability tests. Figure 4.2 shows the spread of the data, along with the typical temperature profile for these tests.

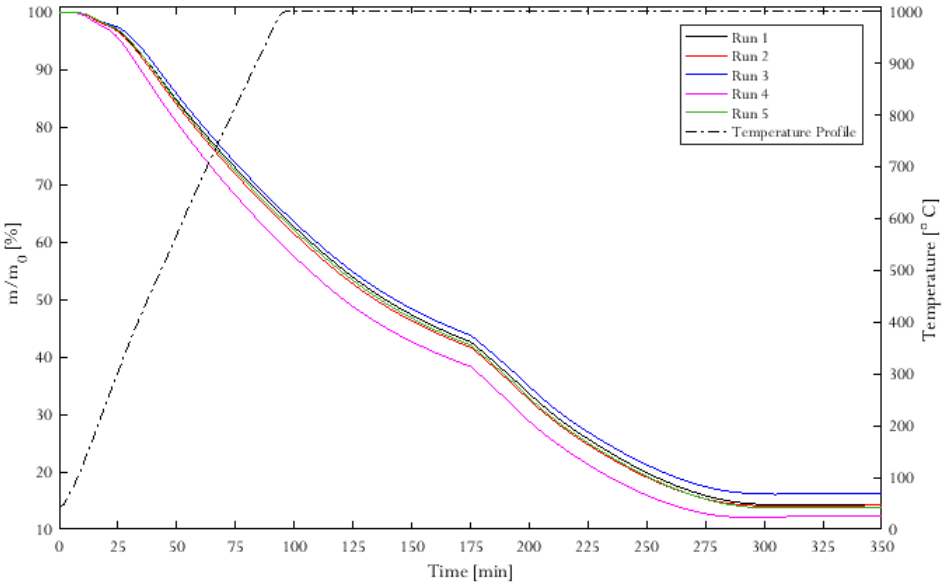

Figure 4.2: Repetition results for the 20mmCoal combustion experiments

The span of mass loss for the single particle tests in Figure 4.2 ranges between 84 and 87%, with an average of 85.8%. It was deduced from this result that two repeats per fuel would be sufficient to deliver a representative result. The repeats of the other tests can be found in Appendix B.

The selection of particles for the test was also an important consideration. Chapter 3 details the preparation of representatives samples for each fuel and size, as well as the use of some of this sample for float-and-sink analyses - densimetric curves can be found in Appendix A. Particles for the thermogravimetric experiments were limited to a narrow density range of 1.4-1.6 SG. The use of density separation as an additional preparation step is supported by Hattingh [2012], who used mercury submersion to separate the particles of his study according to density, as a means to increase the repeatability of results. The initial mass of the particle was found to have an effect on the result. This was particularly true for the larger particles, which tended to make contact with the side of the furnace, causing the mass readings to destabilise. Furthermore, the larger particles were more likely to fragment, in a random, unrepeatable manner. To limit these effects, particles of similar masses were selected for each size.

4.3 Pyrolysis Characteristics of Coal Sample

Figures 4.3 and 4.4 show respectively the thermogravimetric (TG) and differential thermogravimetric (DTG) curves for the pyrolysis experiments. Two distinct regions can be clearly identified in Figure 4.3. A short region of rapid mass loss extending from the beginning of the experiment until roughly 300 °C. This is followed by steep loss of mass ranging from ~350 to above 600 °. These regions can be seen for all the fuels with steeper slopes being observed for the larger (30 and 40 mm) particles. The corresponding DTG curves, from which the rates of mass loss can be observed, are shown in Figure 4.4.

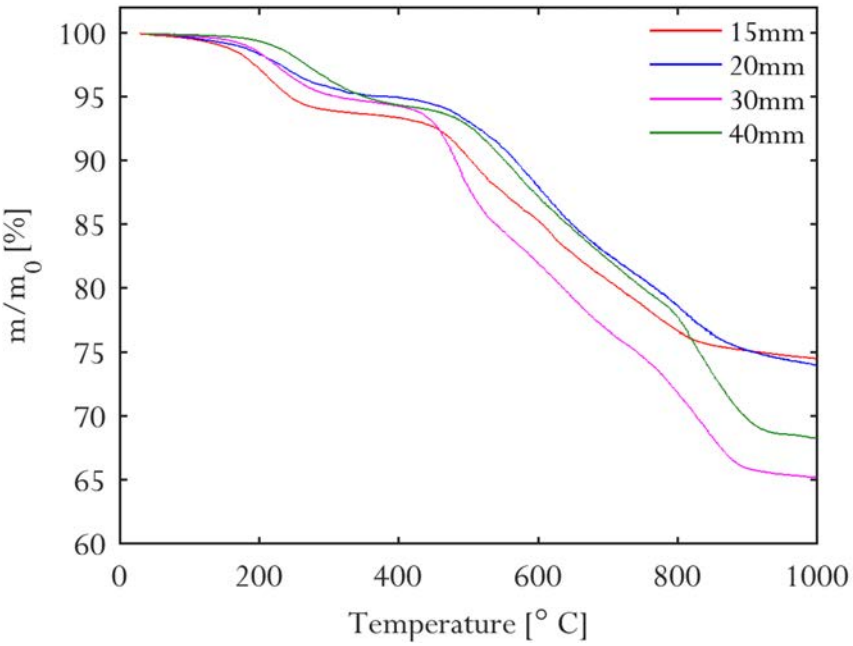

Figure 4.3: Coal Pyrolysis TGA Curves

The initial peak, occurring between 200-280 ° C corresponds to drying and loss of moisture. The temperature at which this peak occur increases with increasing particle size, indicating that water mass loss occurs at a higher temperature for larger particles, possibly due to the thermal resistance and diffusional resistance of water vaoour experienced by the larger particles, or the diffusional resistance to wtare vapour through these particles. This observation is consistent with that of Yu *et al.* [2005], who observed an increase in the rate of particle heating with decreasing particle size. The second peak occurs in the range between ~350-600 ° C. Mass lost during this period is due to primary devolatilisation [Roets, 2014; Fadeela, 2012; Hattingh, 2012; Borah *et al.*, 2005]. The trend observed is an increase in peak temperature, from 570 ° C for the 15 mm particles to about 600 ° for the 20 and 40 mm particles. Lastly, a third peak occurs at ~800 ° C for the larger particles. This third region was also observed by Rosenvold and Dubow [1982], who associated temperatures above 550 ° C with cracking and coking processes [Kök *et al.*, 1998].

Compared to the proximate analyses, the residue masses, seen in Figure 4.3, of the smaller particles (~25% for both) are consistent with the proximate analysis in Chapter 3. The larger particles, however, report volatile mass losses (>30%) which are between 4-7 % higher than those reported by the proximate analysis.

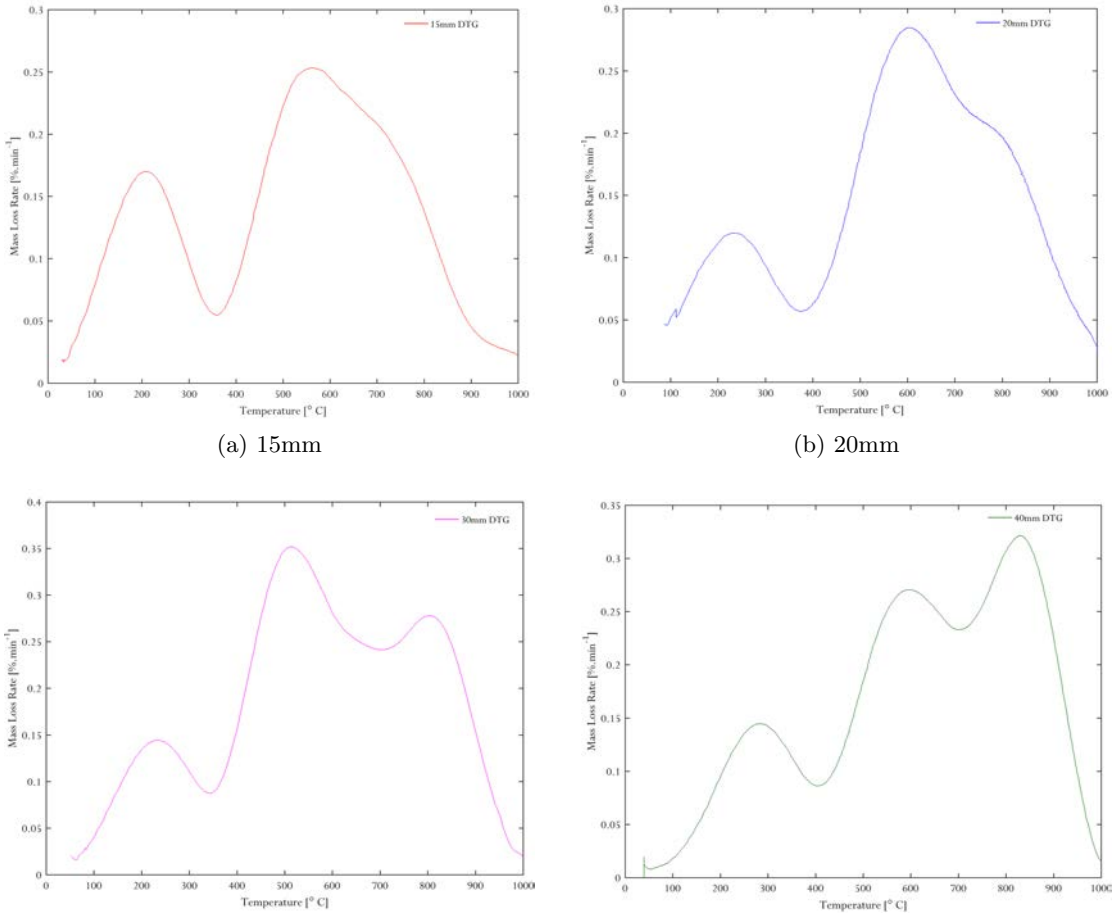

(a) 15mm

(b) 20mm

(c) 30mm

(d) 40mm

Figure 4.4: Coal Pyrolysis DTG Curves

The aim of the pyrolysis experiments was to ascertain that a fuel produced at the proposed temperature has not lost all its volatile matter and will be able to support ignition; inspection of Figures 4.3 and 4.4 shows that, at 550 °, the particles have not yet entered the secondary pyrolysis regime and, although the maximum rate of primary devolatilisation has been reached, it is not complete. This indicates that the devolatilisation should not affect the LSF's ability to ignite via volatile evolution.

4.4 Combustion Characteristics of Coal and LSFs

The contact between oxygen and a fuel is enough to initiate its combustion. However, properties of the fuel, oxygen supply and temperature are vital in determining the nature and extent of this reaction [Kök *et al.*, 1997]. It is the aim of this thermogravimetry study to determine the thermal properties of the fuels under study in order to inform practices during the combustion tests.

4.4.1 Combustion Profiles

The thermograms for the coal combustion experiments, their corresponding differential TG curves as well as a summary of the thermal properties of the fuels are shown in Figures 4.5, 4.6 and Table 4.2 respectively. A typical thermograph consists of the following features: An initial mass loss, associated with the loss of volatiles and surface char combustion, a second stage, starting at ~750 ° C, and is characterised by mass loss from char combustion in the interior of the particle, and a final stage occurring at temperatures above 900 ° C corresponding to residual char combustion [Zhou *et al.*, 2016; Yu *et al.*, 2005; Kök *et al.*, 1997].

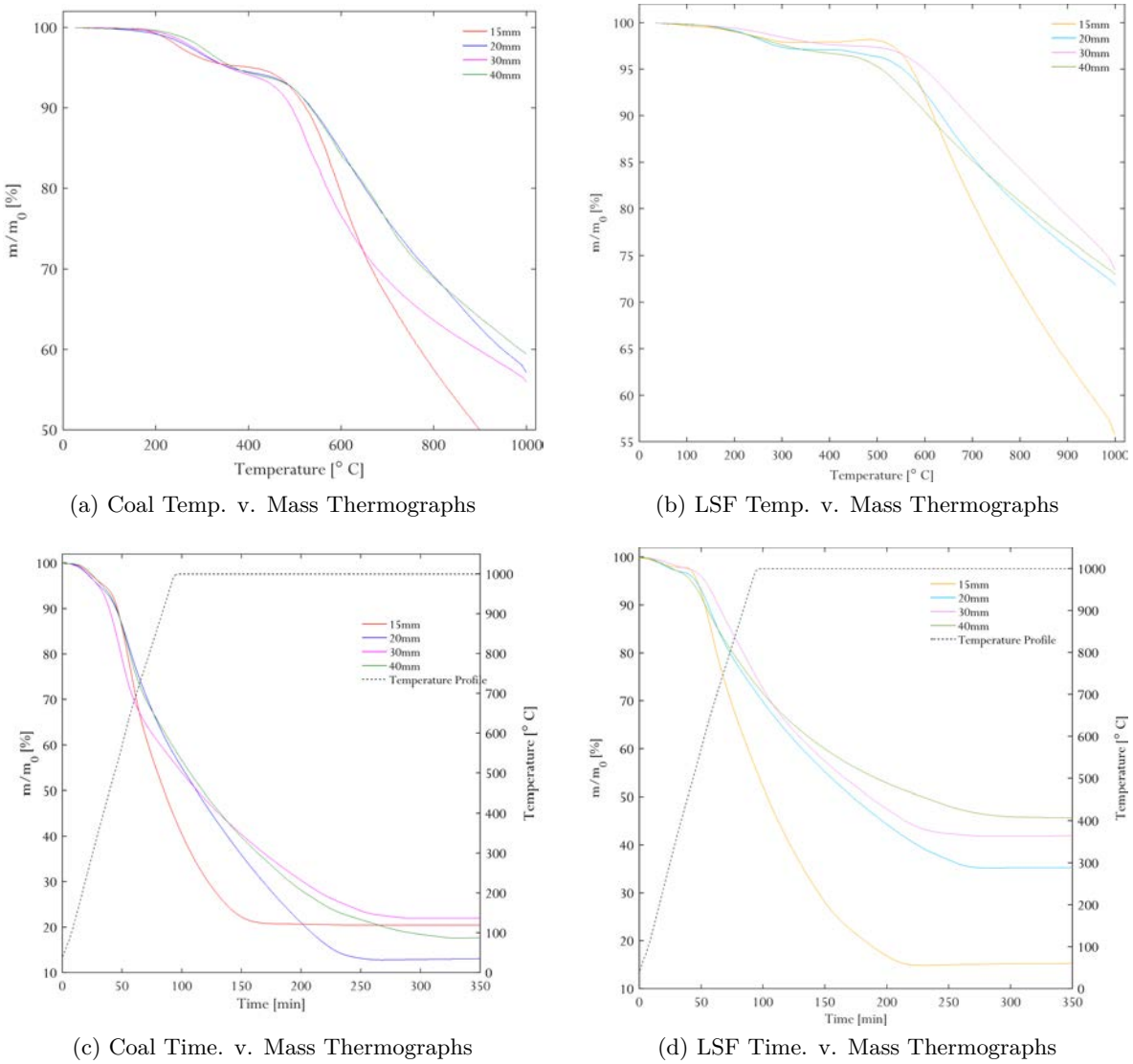

(a) Coal Temp. v. Mass Thermographs

(b) LSF Temp. v. Mass Thermographs

(c) Coal Time. v. Mass Thermographs

(d) LSF Time. v. Mass Thermographs

Figure 4.5: Combustion TGA Curves

The curves in Figure 4.5 show no appreciable difference in the inception point of each stage with particle size, however, a more pronounced difference occurs across fuel types. In general for the coals, the volatile combustion stage begins at ~160-180 °C and ends at 350 ° C - with the exception of the 40mmCoal particles which continue until 400 ° C. The second stage occurs between 450 ° C (470 ° C for the 40mmCoal particles) and is essentially complete at around 650-700 ° for all sizes, whereupon the final stage begins. The LSF volatile combustion also begins in the region of ~180 °C, and continues to 350 °C, while the internal combustion stage starts

slightly later at 530-560 °C and continues until about 720 °C. The final stage is thus also delayed and begins only at temperatures above 800 °C. These results are consistent with the report of Shen [2009] who site a volatile initiation temperature of 130-170 °C for bituminous coals[1]. The larger coal particles (30 and 40 mm) show these stages in a more pronounced manner than their smaller (15 and 20 mm) counterparts. This may be a direct result of the dependence of combustion regime (see Section 2.2.5) on particle size: smaller particles experience less diffusion resistance and the char consumption reactions are limited by reaction kinetics, whereas larger particles have a distinct separation for surface- and internal char reactions due to limitations on the diffusion of gas and heat [Kosowska-Golachowska, 2010].

4.4.2 Combustion Parameters

The combustion behaviours of the different fuels and sizes are more apparent on the differential thermographs, such as shown in Figure 4.6, and will be characterised by the ignition (T_i), peak (T_p), and burnout (T_b) temperatures or times, using techniques from the literature [Zhou *et al.*, 2016; Li *et al.*, 2007; Yu *et al.*, 2005; Kök *et al.*, 1997; Davini *et al.*, 1990; Morgan *et al.*, 1987, 1986]. The method used here is similar to that used by Zhou *et al.* [2016] and Li *et al.* [2007]. It is not possible to obtain the burnout temperature from the TG curves in Figure 4.5a; this indicates that the test range (the 96 minute period where the temperature is raised from ambient temperature to 1000 ° C) is insufficient for complete combustion. However, a burnout time (t_b) can be determined from Figures 4.5b and 4.5d which includes data for the holding period of two hours at 1000 ° C.

Factors known to effect the ignition temperature of a coal include: sample mass, volatile matter yield, oxygen concentration, and rank. The ignition times in Table 4.2 are consistent with generalisations in the literature regarding the dependence of the ignition temperature on volatile matter yield and coal rank classification [Kosowska-Golachowska, 2010]. Figure 2.2 shows that a coal with a volatile matter yield of ~25% (dry basis) will have an ignition time of between 400-450 ° C, this is true for the fuels under study. Furthermore, the recorded ignition temperatures are consistent with the expected ignition temperature (400 to 500 °C) for bituminous coals [Shen 2009].

Similar to the combustion regions, the ignition temperature, and time, show no strong dependence on particle size, with the majority of the particles reporting an ignition temperature of 420 °C, corresponding to a time of 36 minutes at the 10°C.min^{-1} heating rate employed. This is counter intuitive as it is expected that the smaller particles should show signs of volatile initiation and ignition sooner than their larger counterparts.

[1] The rank classification for the fuels used in this study is discussed in Chapter 3 and Appendix A

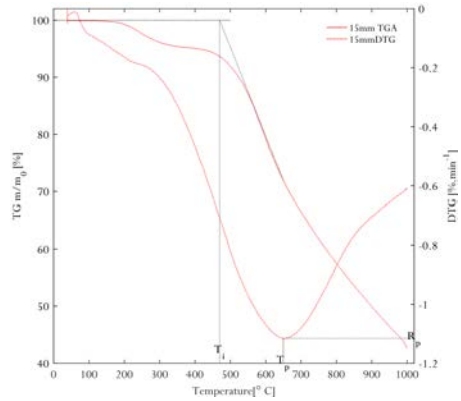

(a) 15mmCoal

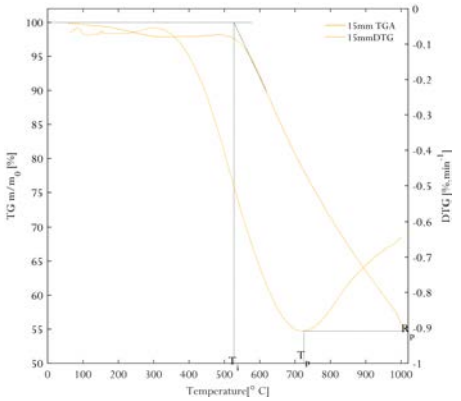

(b) 15mmLSF

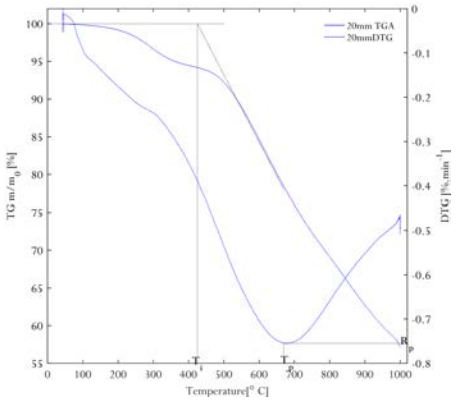

(c) 20mmCoal

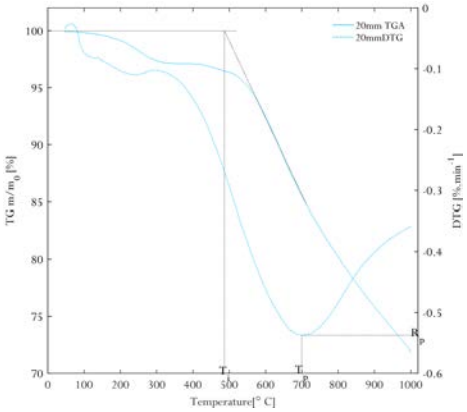

(d) 20mmLSF

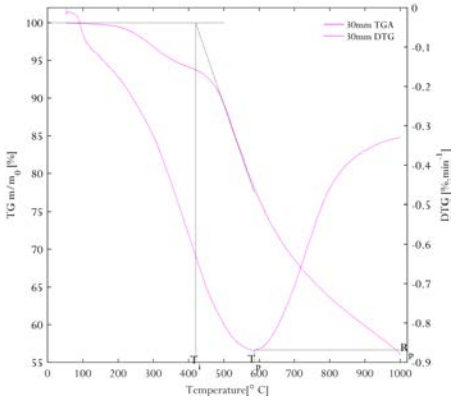

(e) 30mmCoal

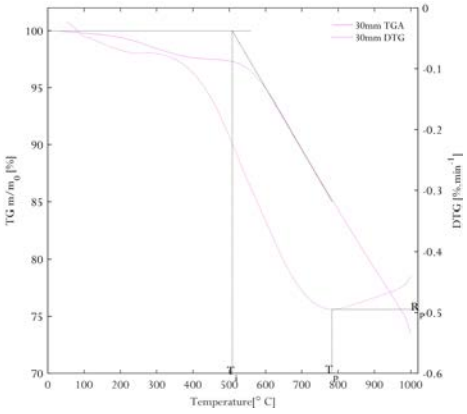

(f) 30mmLSF

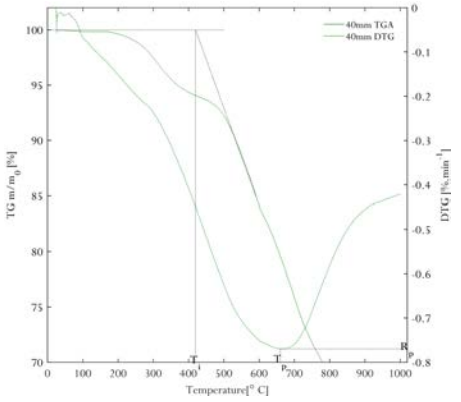

(g) 40mmCoal

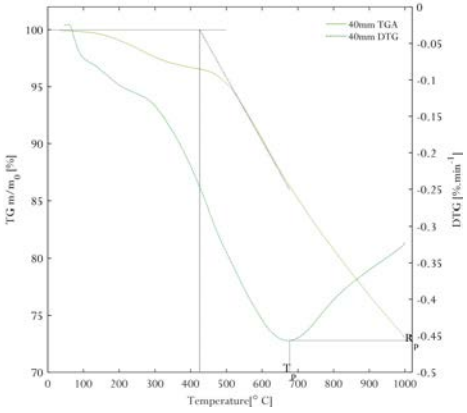

(h) 40mmLSF

Figure 4.6: Coal Combustion DTG Curves

Table 4.2: Coal and LSF Combustion Characteristics

Fuel] Size [mm]	**Av. Particle Mass [g]**	**VM [%]**	**T_i [° C]**	**t_i [min]**	**T_p [° C]**	**t_p [min]**	**$(m/m_0)_{max}$ [%.min^{-1}]**	**t_b [min]**
15mmCoal	4.0	24.3	470	40.9	650	57.1	1.115	172
20mmCoal	7.4	23.9	425	36.7	670	59.0	0.755	230
30mmCoal	23.9	25.9	420	36.3	585	51.5	0.866	280
40mmCoal	50.0	27.2	420	36.3	660	58	0.7694	322
15mmLSF	4.2	9.8	527	46.4	725	65.4	0.908	224
20mmLSF	11.7	9.5	490	42.9	700	62.7	0.537	270
30mmLSF	16.4	10.9	510	44.8	785	72.3	0.495	260
40mmLSF	31.5	12.4	426	35.8	680	61.7	0.456	290

The studies of Kök *et al.* [1997] and Yu *et al.* [2005] on the effect of particle size on the combustion profiles of pf coals report a slight increase in peak and burnout temperatures with an increase in particle size. These results were echoed by the parameter study of Morgan *et al.* [1986]. The characteristic DTG peak temperatures for the coals in Table 4.2, are consistent with these observations. Increasing the particle size increases the reactivity of the coal due to an increase in surface area and thus higher temperatures can be achieved. The increase in reactivity with increasing size can be confirmed by inspection of the peak mass loss rates. The results for the LSFs are inconclusive in this regard. The burnout times, used in lieu of the temperatures do indeed increase with increasing particle size for both fuels as observed in the literature.

4.4.3 Summary Applications to Combustion Tests

Thermogravimetry was used, in this chapter, to study the combustion behaviour of the fuels and to gain insights that will inform the practices of the combustion tests to follow.

Pyrolysis experiments were done to determine the extent of devolatilisation achieved at the proposed LSF production temperature of 550 °C. It was found that at 550 °C, all particles had:

- not yet entered into the secondary pyrolysis regime. This has implications for the expected emissions of sulphur and nitrogen oxides. Nitrogen functional groups are not engaged at the production temperature, while sulphur is only marginally engaged through the decomposition of pyrite. This means that NO_x emissions may not be controlled by pre-treating the fuels and will be dependant on the combustion conditions. SO_2 emissions may be marginally reduced by the pre-treatment.
- only lost ~20% of their mass. This includes the loss of moisture and volatiles. This reduction in volatile matter content will have implications for the ignitability of the LSF.

The combustion experiments were used to determine the expected combustion profiles of the fuels. The effect of particle size on the ignition and peak temperatures was not as pronounced as expected from a study of the literature on the subject; only slight variances were noted and no distinct trends could be found. The ignition temperatures were found to decrease with increasing particle size, and volatile matter content. Ignition temperatures for the coals (425-475 °) and LSFs (~420-520 °) were found to be consistent with expectations considering volatile matter

content (24-24 and 9-12 %, a.d. for the coals and LSFs respectively) and fuel rank (coals were ranked as semi-anthracite and LSFs as high volatile bituminous according to the ASTM D388 standard).

The proposed ignition scheme is thus to supply heating gas to the coal bed until the temperature measured at the center of the bed reaches the upper margin for the expected ignition point, 500 °C, despite the coals reporting ignition temperatures lower than that. This is done to compensate for any possible profile changes resulting from the use of a bed of particles instead of a single particle in an controlled environment that may lead to poor ignition and render the experiment inconclusive in terms of thermal perfomance and emissions monitoring. Furthermore, observation from the Kühn [2015] study indicate that the coal bed will be self-sustaining at 500 °C.

Chapter 5

Experimental Methods and Materials

The aim of the study is to determine the effect of the fuel particle size on the combustion and pollutant emissions of a low-smoke fuel in a conventional, domestic cast iron stove. To this end, a set of combustion tests were performed for the evaluation of the thermal and combustion efficiencies, as well as to monitor the emissions of gaseous, particulate, and organic pollutants. This chapter details the experimental- and data analysis procedures.

5.1 Stove Characterisation and Operation

The Falkirk Union No 7 cast iron stove was used for the combustion tests. Cast iron stoves, as discussed in Chapter 2, are commonly used in coal-buring communities. This particular stove, according to Nkosi *et al.* [2017], is abundantly available in the township of Kwadela and has been used before by Kühn *et al.* [2017] and Kühn [2015] in similar combustion tests. Graham [1997] and Graham and Dutkiewicz [1999] used a different model of the Union stove in their evaluation of the emissions, efficiencies and cost-effectiveness of different appliances.

In order to best simulate the *real world use* of the proposed fuel, the stove was sourced, with the aid of the NOVA institute, from a coal burning home, and is in a fairly used condition. The inner components had been removed, as noted by Balmer [2007] in his study of urban township energisation. Figure 5.1 shows the main components of the stove. The stove is fitted with a chimney, has a cooking surface with five removable hob rings and a small oven. The pot was placed on the hob marked "1" on the figure during the combustion tests. Primary air is supplied via a hatch below the coal bed. The hatch was kept open for all tests. Secondary air supply is controlled via the louvre on the side of the stove; this was kept in the "closed" position during the tests. The exhaust system consists of a purpose built steel chimney (1.59 m, 11cm ID), the dilution system (see Makonese [2015]) and an aluminum extension (1 m), together comprising a ~2.6 m "chimney". This length is similar to the 2.7 m minimum length prescribed by Rogers [1995], and stipulated by the SABS 1111 methodology, for good combustion.

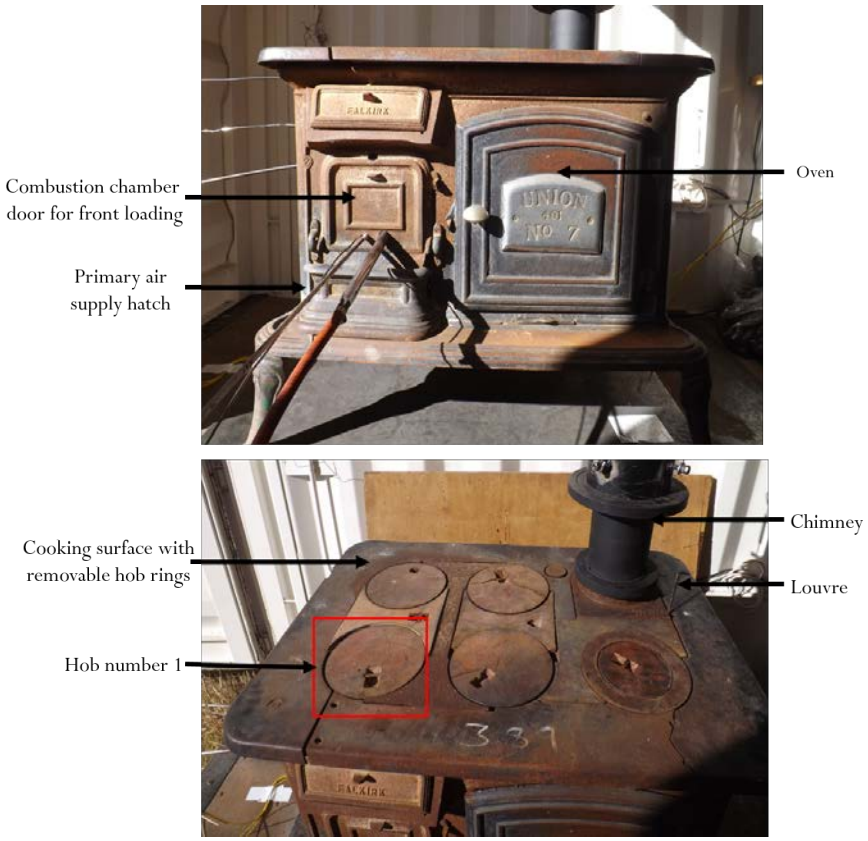

Figure 5.1: Union No. 7 Stove used during Combustion Tests

5.2 Fuel Characterisation

Two fuel types: coal and LSF in five sizes (15, 20, 30, 40 mm, and a composite of these sizes) are used, with the coals serving as the baseline scenario.

Fuel loading was between 4 and 5 kg. Some of the LSFs experienced fragmentation during preparation, storage and handling, and were hand screened before use to remove fragments, resulting in the lower fuel loading.

All the fuels can be classified as high ash with the LSFs having a slightly higher ash yield than the corresponding coal. Furthermore, all the fuels have a calorific value of ~22 MJ.kg^{-1}. The proximate- and elemental composition of the LSF is consistent with pyrolysis: *i.e.* the LSFs have a lower moisture content (<1% (a.d)), volatile matter yield (~20% (d.a.f) less), and sulphur composition (between 0.4-1% (d.a.f) less) than the coals, while the carbon content increases. Chapter 3 provided an in-depth account of the characteristics of the fuels being considered.

5.3 Experimental and Data Acquisition Procedures

This section will discuss the experimental set-up, procedures, and data collection. The combustion experiments are performed largely in accordance with the heterogeneous testing protocol [Makonese, 2015, 2011] supplemented with the test for LSF validation by Le Roux *et al.* [2004].

The thermal performance is characterised by the water heating test and the flue gases are monitored in order to characterise the emissions, while the *post hoc* analysis of the ash and residue provides information regarding the overall combustion efficiency.

5.3.1 General Start-up Procedure

Three experiments are conducted for each fuel type. The third experiment is allowed to burn until extinction to provide the ash residue for the characterisation of the overall combustion efficiency. Each experiment is divided into 3 segments: (1) ignition, (2) cooking, and (3) heating. The ignition segment involves the lighting and development of the coal fire, the cooking segment involves the heating and boiling of two pots of water, and the heating segment simulates the use of the stove for heating purposes by allowing the fire to progress to a point where refuelling would occur. In total, each experiment runs for two hours. After the two hours have expired, the bed of coals was removed, along with the ash, and the mass was recorded. The stove was quenched with water and cooled with compressed air to a temperature below 50 °C in order to simulate a consistent cold start for each experiment.

During operation, the fuel is arranged manually on the grate. In order to keep the fuel bed dimensions consistent, a steel grid (270x260x150 mm) was placed on the grate and the coal arranged within this grid. The conventional fire lighting method was simulated by igniting the bed from the bottom using LPG supplied at at a flow rate of 4.5-5 $L_N.min^{-1}$. The ignition gas system consists of an LPG cylinder and a high pressure regulator attached to a rotameter. The gas is delivered to the bottom of the bed via a stainless steel gas burner. The rotameter was calibrated using a bubble flow meter and typical calibration curves can be found in Appendix C. The amount of gas used was determined by weighing the gas bottle prior to and after each experiment. Conventionally the fire is ignited using paper and wood kindling. Other methods found in the literature include commercial firelighters: The significance of the contribution of the firelighters to the emissions and combustion behavior was noted by both Mitchell *et al.* [2016] and Le Roux *et al.* [2004]. Due to the difficulty in characterising this contribution, the former excluded results collected over the early ignition phase of the tests, while the latter subsequently switched to ignition by LPG. The LPG was also used by Kühn [2015] in order to avoid the complications of the use of kindling.

5.3.2 Thermal Performance

Figure 5.2 shows the subsystem for monitoring the thermal performance of the system. It consists of a set of 3 mm K-type thermocouples measuring the temperature in the coal bed, the cooking surface, the stack, the water in the pot, as well as the temperature within the testing facility. All temperatures are recorded, at one second intervals, using a PICO Logger (TC-08) connected to the computer via USB. Mass loss is measured on a balance (Satorus Combics 1:CAISLLO.A7.M41Z 33166583) and logged on a purposed-programmed Raspberry Pi computer connected to a Campbell (CRC100) serial logger.

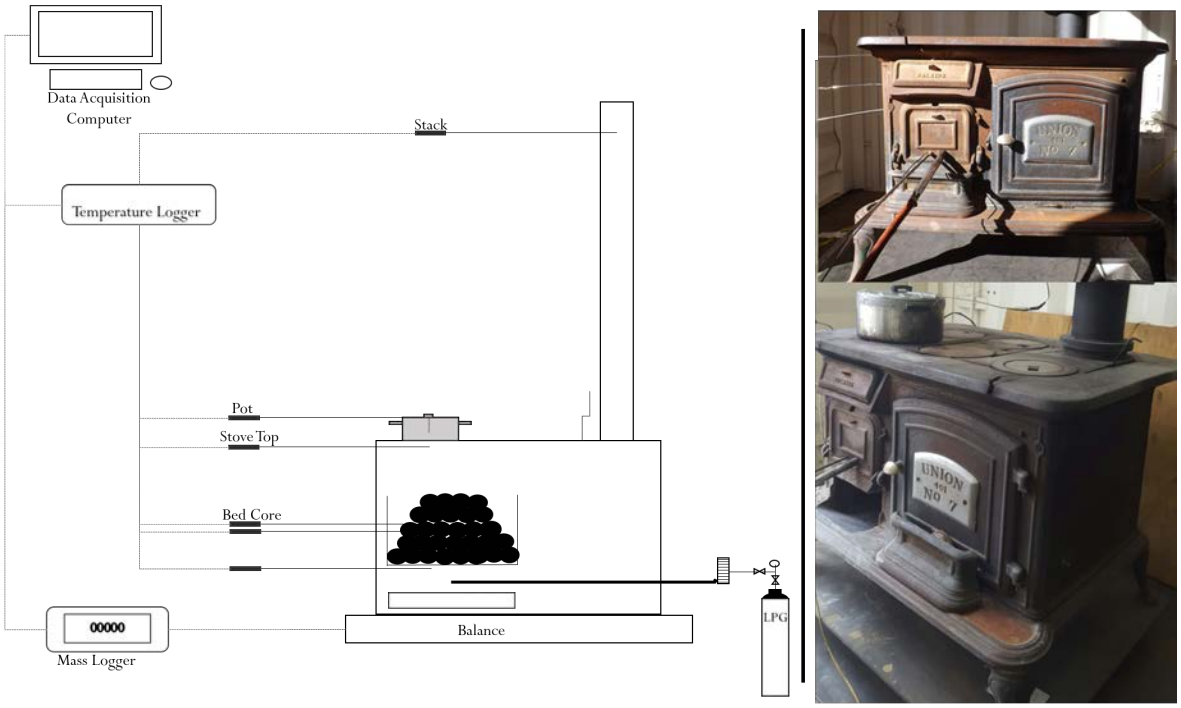

Figure 5.2: Schematic diagram showing set-up for mass and temperature monitoring. There is an additional thermocouple (not shown on schematic) measuring the temperature within the testing enclosure. The ignition gas supply is also shown.

Water Heating and Boiling. Figure 5.3 shows the Hart^{TM} aluminium, 3 L capacity pots, used for the water heating and boiling procedure. Hart^{TM} pots are readily available and are used widely for cooking in South African homes. The water boiling procedure is necessary to determine two parameters: the boiling time, according to the test for LSF validation, and the thermal, or cooking, efficiency achieved by the fuel/stove set-up.

During the experiment, a pot, containing 2 L of water, is placed on the appropriate hob ring and the water is heated from ambient- to boiling temperature. A second, identical pot is placed on the hob and the procedure is repeated once more. The HTP standard operation prescribes that water not be heated higher than 70°C to avoid the complications rising from the evaporation losses. However, in this study, the water is heated to boiling point as described above. In order to limit the amount of evaporation, the pot's lid was fixed tightly on the pot, which is removed from the stove immediately after reaching the boiling point. The water temperature was measured, as per HTP guidelines, at the center of the pot, 50mm from the bottom. To ensure this, a hole just big enough to fit the 3 mm thermocouple was drilled into the center of the pot lid. The thermocouple was then submerged into the water with the tip 50 mm from the bottom. Duct tape is used to keep the thermocouple in place.

The water boiling time is determined by measuring the time elapsed between setting the pot on the stove and the when the pot reaches boiling point.

Fuel Burning Rates. The continuous measurement of the mass loss is an important part of the procedure as it enables the determination of: (1) fuel burn rate, (2) energy output, (3) heat

Figure 5.3: The pots used for the water heating/boiling procedure. Two pots, filled with 2 L water, are sequentially allowed to reach boiling point. The lids and thermocouples are secured by duct tape in order to minimise evaporation losses.

transfer efficiencies, as well as (4) the expression of emissions on a mass-consumed or energy-released basis.

There are a few considerations regarding the monitoring of the change in mass. In order to ensure that the logged mass is only that of the fuel, the stove is loaded with fuel only after the coal bed grid, the thermocouples, and gas supply burner are in place and the balance is tared. Secondly, the positive mass gain registered when the pot is placed on the stove is accounted for as follows: the mass of the pot, water and thermocouple is taken before each experiment, the mass of the fuel prior to the placement of the pot is also noted. The former is subtracted from the latter to account for the positive gain in mass resulting from the introduction of the pot. Since this operation assumes negligible evaporation, the measures discussed above are taken in order to ensure that evaporation is limited. Indeed, an average evaporation mass loss of less than 100 g was found, by weighing the pot, water and thermocouple after boiling for each experiment. A loss of 100 g (or 5%) over the average 25 minutes spent on the stove per pot is insignificant compared to the mass reductions of the fuel.

Ignition Time. The Le Roux *et al.* [2004] study defined ignition as a sudden peak on a temperature curve measured by a thermocouple suspended just above the coal bed. The Le Roux *et al.* [2004] experiments were conducted in an *imbaula* and this procedure could not be followed in the Union stove as the analogous thermocouple is inserted into the fuel bed. For this study, the ignition point is defined at the time where the temperature at the core of the fuel bed is 500°C. This is based on observations made by Kühn *et al.* [2017], Kühn [2015], and on the results of the TGA experiments discussed in Chapter 4.

After all the loggers have been initiated and proper logging has been confirmed, the LPG is ignited and the start time is recorded. When the bed core temperature reaches 500 °C, the time is noted and the LPG is extinguished. The time elapsed between these points is taken as the ignition time.

5.3.3 Emissions Measurements

Apart from being able to perform the common household tasks of cooking and space heating to a satisfactory degree, the proposed LSF must also achieve an appreciable reduction in emissions. Part of the objectives of this study is to quantify this reduction. The HTP has been used to characterise the emissions from the combustion of coals [Masekameni, 2015] of various quality and moisture content, ignited using different methods, in *imbaulas* with different ventilation rates using different fire-lighting methods [Makonese, 2011]. This protocol is thus suitable for the characterisation of emissions from different fuels types. The emission of gases (CO, CO_2, SO_2, and NO_x)and particulate matter are of particular interest. CO poses a health risk due to its toxic interactions in the body. Furthermore, as a product of incomplete combustion, CO gives an indication of the quality of combustion achieved. SO_2, NO_x, and suspended particles are known environmental pollutants. Figure 5.4 shows a schematic of the experimental set-up used for the monitoring and recording of emissions data, and is discussed in the following subsections.

The hood method was employed and samples were drawn directly from the chimney, a meter above the stove. The chimney is fitted with a portable diluter system consisting of high purity nitrogen, fed into the diluter [see Makonese [2015]], from a gas cylinder, at a rate that is sufficient to prevent the saturation of the particle monitor.

Gaseous Emissions. There are two sample configurations for gases: (1) An undiluted flue train consisting of a stainless steel channel routed through a heating gun (not shown on schematic) at 80 °C, followed by Teflon^{TM} tubing, which feeds the sample to a conditioning unit that removes any excess moisture and particles from the stream, before being routed to the gas analyser (Horiba PG250, HGS No:N7ChM47E). (2) The diluted flue train configuration consists of the dilution system, Teflon^{TM} tubing routing the sample through two HEPA filters, a moisture trap (not shown on schematic), and then into the gas analyser (Horiba PG350: HGS No. SPFFF0B6).

Both analysers draw flue samples at 0.4-0.5 L.min^{-1} and measure CO (limit 5000 ppm), CO_2 (limit 20 vol%), SO_2 (limit 1000 ppm), NO_x (2500 ppm), and O_2 (limit 25 vol%). A chemiluminescence detection method that involves the low-temperature conversion of NO_2 to NO is used for NO_x measurements. A non-dispersive infra-red absorption (NDIR) detector is used to measure SO_2, CO, and CO_2, and a galvanic cell is used for O_2 detection. Response time, from the sample inlet, for SO_2 is 240 seconds and 180 seconds for the PG 250 and PG 350 respectively, and 45 seconds for the remaining gases.

For data logging and storage, the PG 250 requires a computer with the appropriate software (LabView Run Time Engine) and a serial interface (COM) port. The PG 350 logs data onto a memory card; at the end of each experiment, the memory card is removed from the analyser and the data is stored on the computer. Logging is initiated after the fuel bed has been packed, prior to ignition, and occurs at one second intervals.

Particulate Matter Emissions. Particulate mass concentration is measured in two ways: (1) a continuous method employing a particulate monitor (DustTrak II: 8530, Serial:8530152405), and (2) using a gravimetric method.

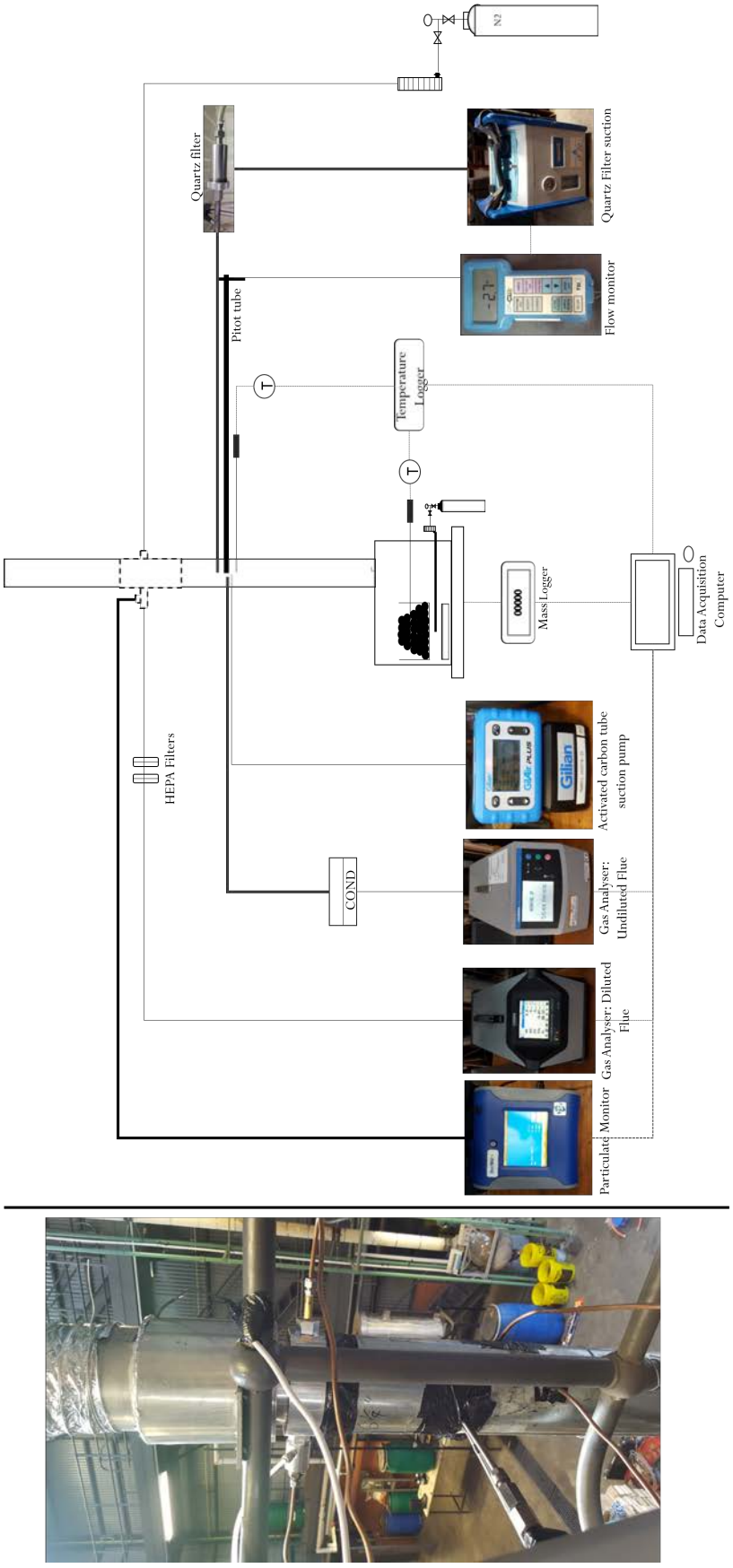

Figure 5.4: Schematic showing the suite of equipment used to monitor the emissions of gases, particles and organic components. The temperate and mass logging subsystem from the previous discussion is also shown. The dilution system is shown in dashed lines on the schematic.

The sampling configuration for the continuous monitoring includes the dilution system, connected to copper tubing that routes the sample to the DustTrack. The DusTrack draws a sample at 2 L.min^{-1}, and records the total concentration of particles over a range of 0.001 to 400 mg.m^{-3} at one second intervals. The dilution N_2 prevents the overloading of the Dustrak, and the copper tubing is used to prevent particle entrainment due to static. Particle concentration detection is based on optical light scattering. The flue sample, containing particles, is drawn into the instrument's sensor chamber by a diaphragm pump. This sample is then split into two streams: (1) a sheath flow stream that goes through a HEPA filter inside the instrument before being rerouted into the sensor chamber, and (2) the sample flow stream, which is directed straight into the sensor chamber. Upon entering the chamber, the sample encounters a thin sheet laser light, from a laser diode, causing scattering of this light. The majority of this scattered light is captured on a gold-plated spherical mirror and then focused onto a photo-detector [Makonese, 2015]. This model of the DustTrak, unlike others, cannot distinguish between the various sizes ($PM_{2.5}$, PM_{10}, *etc.*)

The Dustrak stores data on an internal memory which can be accessed via USB and stored on the computer. Logging begins a few minutes before the fire is lit, to determine the ambient PM concentration before the experiment, and carries on a few minutes after the two hours have expired to measure the ambient PM concentration after the experiment.

The sample for the gravimetric method is drawn from the stack through a stainless steel channel connected to a filter holder containing a quartz thimble filter supplied by Envirocon Instrumentation. Suction is achieved by using a pump (Aquaria CF20, Serial:ABML005). A pitot tube, inserted into the stack at the same level as the gas sampling train, attached to a hand-held differential flow meter, is used to determine the flow rate in the stack. The suction pump is then adjusted manually to match this flow, as required for the isokinetic sampling. A flow reading is taken every two minutes and the pump suction adjusted accordingly. The thimble is inserted into the holder just before the fire is ignited, removed immediately after the two hours has expired, and stored in an airtight container in a climate controlled laboratory. Only two such measurement are taken per fuel.

The suction pump is started at the same time that the fire is lit. The mass of the particulates is determined by measuring the difference in filter mass before and after the experiment.

Volatile Organic Compounds. Volatile organic compounds are emitted when hydrocarbon combustion is incomplete and some species have been shown to be carcinogenic. VOCs are measured by using activated carbon tubes. The sample is drawn directly from the stack, upstream from the diluter and routed, via Teflon^{TM} tubing, to an activated carbon tube, supplied by Biograde. Suction is provided by a small pump drawing a sample at 2 L.min^{-1}. The suction pump is started at the same time that the fire is lit. At the end of the experiment the final volume sampled is noted, in order to convert results to a volume basis, and the activated carbon tubes are labelled and stored in an airtight container. Only two VOC tubes were used per fuel type.

Post-experiment Analyses The residue from the third experiment for each fuel, which was left to burn until extinction, is collected and analysed. Analyses to determine the proximate- and

elemental composition, as well as the LOI and calorific value are carried out by the same lab that performed the analyses on the raw fuel. Preparation of the residue sample is carried out as described in Chapter 3.

The activated carbon tubes are sent to the supplier, Biograde, who performed the analysis for the VOC components.

5.4 Data Processing and Analysis

The HTP calculation spreadsheet version 3.0692 is used in this study to determine the thermal performance metrics (power output, heat transfer efficiencies) and to characterise the emissions, whereas the more practical metrics (ignition and water boiling time) and overall combustion efficiency are reported as per the guidelines of the test for LSF validation. The advantage of the HTP as a fuel/stove performance characterisation method is that results can be viewed as performance curves covering the entire duration of the test (121 minutes in this study), or single "task" segments (in this study: ignition, cooking, and heating). The ignition segment covers the time form the start of the experiment to the ignition point, whereas the cooking segment covers the water heating section, and the heating segment covers the reminder of the test.

5.4.1 Thermal Performance

The thermal performance of the system is rated according to energy, or power, output, system efficiency (η_{sys}) which quantifies the total usable energy delivered, and the efficiency of cooking (η_{therm}), which quantifies the energy delivered to the pot, and heating (η_{heat}), which measures the energy delivered into the room for space heating. An additional parameter is the combustion efficiency (η_{comb}) which takes into consideration the combustible fraction remaining in the residue after the fire has gone extinct.

Fire Power. Stove power output (P), or fire power, measures the total heat energy released by burning the fuel per interval of time. The fire power is determined by measuring the change in fuel mass per interval and determined mathematically as:

$$P = \frac{LHV_f.\Delta M_f}{\Delta t}, \tag{5.1}$$

where the numerator is the heat released form combustion, with LHV_f [MJ.kg $^{-1}$,(d.a.f)] being the lower heating value of the fuel determined from the gross calorific value, and M_f [g], the mass of the fuel. Δt [s] is the time interval, taken as 10 seconds-or 121 minutes for the entire test.

System Efficiency. The total system efficiency determines the usable heat delivered by the system. This takes into account the dual usage of the stove as a heating and cooking appliance. Thus, only heat lost through the stack is considered as energy loss, since heat lost to the

environment, *i.e.* into the house, is used for heating. The system efficiency is thus the ratio of the energy delivered to the pot and into the room to the energy released via combustion. According to the HTP calculation worksheet, the system efficiency is determined by first quantifying the energy lost through the stack: The Siegert efficiency [TSI, 2004] is used to characterise this loss:

$$S = 100 - \left[\left(\left(\frac{A1}{CO_2} + \beta\right)(T_{stack} - T_{room})\right) + \left(\frac{\alpha CO}{CO + CO_2}\right)\right], \tag{5.2}$$

where S [%] is the Siegert efficiency, and CO and CO_2 are the measured emissions in vol%. T_{stack} and T_{room} [°C] are the stack and room temperatures. A1, α, and β are coefficients based on the fuel properties [TSI, 2004].

The system efficiency is then calculated as:

$$\eta_{sys} = \left[\left(\frac{S}{100}\right)(LHV_f.\Delta M_f)\right] \times 100, \tag{5.3}$$

where η_{sys} is the system efficiency in %, LHV [$MJ.kg^{-1}$ (d.a.f)], M_f and S are as defined above.

Thermal Efficiency. Also referred to as the cooking efficiency, is the ratio of energy used to heat and evaporate the water in the pot to energy released by combustion of the fuel. This follows mathematically as:

$$\eta_{therm} = \left[\frac{M_w Cp_w \Delta T + M_e H_{vap}}{M_f LHV_f - M_r LHV_r}\right] \times 100, \tag{5.4}$$

where M_w,M_e, M_f, and M_r represent the mass, in gram, of the water in the pot, the amount of water evaporated, the mass of fuel, and the mass of the residue, respectively. ΔT [° C] is the change in the water temperature. Cp_w [$J.kg^{-1}.°C^{-1}$] and H_{vap} [$kJ.kg^{-1}$] are the specific heat capacity and latent heat of vapourisation of water, and LHV [$MJ.kg^{-1}$] is as described above. M_e is taken as 0 as already discussed.

Heating Efficiency. Just as the cooking efficiency measures how efficiency energy from the fire is transferred to the pot, the heating efficiency rates the efficiency of heat transfer for space heating as the ratio of heat delivered to the room to heat released from combustion. Mathematically:

$$\eta_{heat} = \left[\frac{\left(\frac{S}{100}\right)(LHV_f.\Delta M_f) - \left(\frac{M_w Cp_w \Delta T + M_e H_{vap}}{M_f LHV_f - M_r LHV_r}\right)}{LHV_f M_f}\right] \times 100, \tag{5.5}$$

where the numerator is the difference between the total heat delivered to the system and the energy used for cooking (i.e. the energy used for heating) and the denominator is the total heat released from combustion. η_{heat} [%] is the heating efficiency and all variables are as defined above.

Combustion Efficiency. The HTP uses the ratio between CO and CO_2 to determine the combustion efficiency and this is easily done once the emission factors are calculated. However, the

test for LSF validation offers an alternative method of determining how well the fuel burnt in the stove by examining the "combustible" carbon still remaining in the fuel after it has been left to burn until extinction. After burning to extinction, the residue was analysed for LOI (loss on ignition), which can be used as an estimate of the carbon still left in the residue. The LOI is determined according to the ASTM D7348 standard which involves the two-step combustion of a known amount of sample. The LOI is the difference in sample mass before and after being subjected to drying (Step 1) and combustion (step 2). The combustion efficiency is then calculated as [Le Roux *et al.*, 2004]:

$$\eta_{comb} = \left[\frac{32.8 M_r \left(\frac{LOI}{100} \right)}{M_f C V_f} \right] \times 100, \tag{5.6}$$

where 32.8 [MJ.kg^{-1}] and CV$_f$ [MJ.kg^{-1}] are the gross calorific values of carbon and of the fuel respectively, and LOI [%] is the LOI as determined by the ASTM D7348 standard. M$_f$, M$_r$ are as defined above.

5.4.2 Emissions Characterisation

The emissions profile of a fuel consists of the emission factors of CO, SO_2 and NO_x gases, particulate matter and volatile organic compounds. Emission factors, on an energy basis, will be used to compare the emissions between the various fuels. This section will describe the data processing for the measured emissions.

Excess air. While care is taken to ensure the repeatability of the operation of the stove, dynamic factors such such as the dilution of the emission plume by an unknown amount of excess air (EA) renders the comparison of results from different experiments difficult. In order to standardise results from different experiments, this dilution has to be quantified and eliminated [Makonese, 2015, 2011]. EA measures the amount by which the air (or O_2) available is in excess of that required for stoichiometric combustion. Comparison of results between different fuels and experiments is thus not possible without first accounting for and removing the influence of the excess air flow. For the HTP, which was designed to handle a range of fuel chemistry, the quantification of the EA is done via an oxygen balance approach [Makonese, 2011]. This approach determines the actual amount of excess O_2 relative to that used in the fire by taking into account the chemistry of the flue gases, and considering oxygen in the fuel as an oxygen source in addition to the air. Equation 5.7 shows the operation to determine the EA factor as used in the HTP:

$$\lambda = 1 + \left(\frac{O_{2_{meas}} - \Sigma G_{op}}{\Sigma O_{2_{det}} - (O_{2_{meas}} - \Sigma G_{op})} \right), \tag{5.7}$$

where λ is the EA factor, O_{2meas} is the O_2 measured, ΣG_{op} is the oxidizing potential of all measured gases and $\Sigma O_{2\text{det}}$ is the total oxygen detected from the O-bearing gases. All gas concentrations are in ppm.

This EA factor can then be used to yield a normalised emission concentration upon which the results from different experiments can be compared.

Emission Factors. When the measured pollutant concentration has been corrected for the EA, the resultant figure, when expressed in grams of pollutant on a mass of fuel consumed [g.kg^{-}], or energy released [g.MJ^{-}] basis, is termed the emission factor (EF). The measured pollutant concentrations are converted (See Makonese *et al.* [2017] for the calculation scheme), using the fuel properties from Chapter 3, to their mass in grams. A MATLAB$^{\text{TM}}$ programme of these calculations can be found in Appendix C. The emission factors are then determined by simply dividing by the relevant basis, for example:

$$CO_{2_{EF}} = \frac{CO_2[\text{g}]}{E_{heat}[\text{MJ}]} \tag{5.8}$$

$$PM_{EF} = \frac{PM[\text{mg}]}{E_{heat}[\text{MJ}]}, \tag{5.9}$$

for CO and PM on an energy basis, where E_{heat} is the energy released. EFs can be expressed in terms of mass (*i.e.* g.kg^{-1}). This is most useful when the aim is to develop emission inventories. The energy based EFs, are more readily applied during a comparative study of pollution potentials of different devices Zhang and Morawska [2002]. In this study, the aim is to evaluate and compare the pollution potential and thermal performance, on a task completed basis, of different fuels. EFs on an energy basis are thus better suited.

5.5 Quality Control and Data Verification

This sections outlines the measures taken in order to minimise variations in results due to operator behaviour or instrumental deviation.

5.5.1 Burn Cycle Standardisation

Two practice experiments were done in order to limit the variability of procedure due to operator behaviour and to arrive at a standard procedure to be followed for the remaining burn cycles. The flow rate in the stack was monitored closely during these experiments to determine an average flow rate to be used for the DustTrak particle monitor and VOC suction pump. A standard start up and shut down procedure, with a check list was developed from the observation made during these commissioning trials.

5.5.2 Instrument Response Accuracy and Delay

The time it takes a sample element to travel through the sampling train, to the instrument probe and into the sensing chamber causes a delay in the real-time measurement of continuous data [Wang *et al.*, 2012]. Since many of the metrics, such as the ignition time and the placement and removal of the pots on the stove, in this study are time dependant, it is important to quantify and account for the delay between the event and the detection of the response on the instruments.

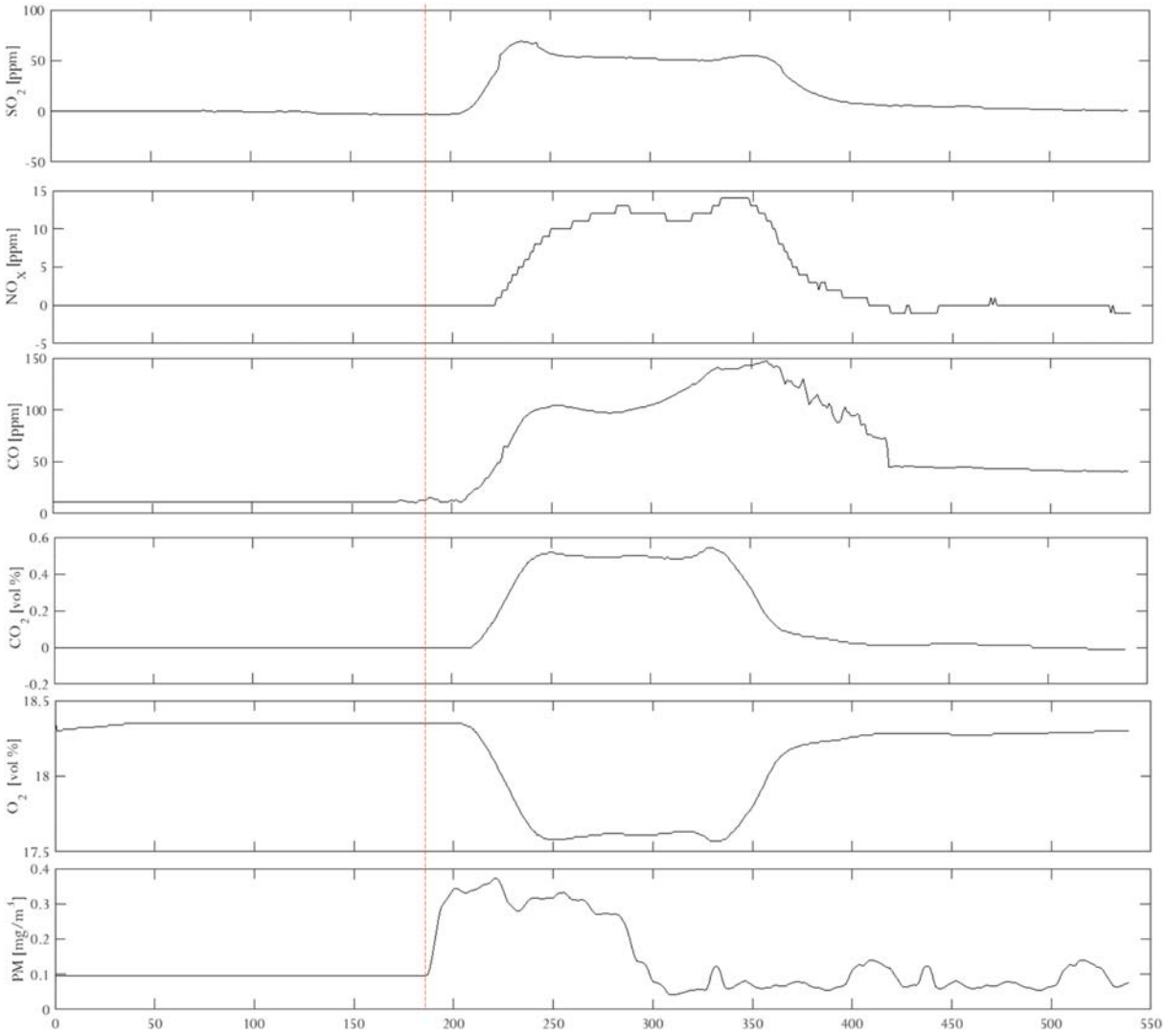

Figure 5.5: Time series of instrument responses to a kindling fire being held (shown by the dotted line) at the base of the chimney. The gas concentrations are measured by the PG 250 analyser and the PM by the DustTrak.

All channels leading from the sampling port on the chimney to the instrument inlets were kept as short as possible in order to minimise the delay. Wang *et al.* [2012] outline a procedure that can be used to determine the delay in response for the various instruments and detectors within the instruments. According to this method, a burning match can be held at the sample entrance of each instrument and the response measured. The gas analysers have a delay time spanning from 45 seconds to 240 seconds after the sample element has reached the inlet as reported above. These values, and the method proposed by Wang *et al.* [2012] do not account for the time taken to reach the inlet. To account for this time, a small batch of kindling was lit at the base of the chimney and the time between ignition and detection of gases and particles was measured, the fire was removed and the response of the instruments was logged. The PG250, has a slower response time (up to 240 seconds for SO_2 according to the manual) and was thus used to measure the longest time delay. Furthermore, since the dustrak is already logging the ambient PM levels before begining the experiments and has been reported by Makonese [2015] to have a response time of less than 5 seconds, it will be used as the reference. Figure 5.5 shows the response for the kindling fire.

The NOx signal appears to take the longest (35 seconds after the DustTrak) to log a change in concentration, while all the other gases adjust almost simultaneously (~20 seconds after the DustTrak) to the change. Outputs from the analysers were adjusted accordingly to arrive at the real-time response of each species.

5.5.3 Instrument Calibration

Gas and particulate matter monitoring instruments were taken to the manufacturer for calibration prior to the experimental campaign. Manual calibrations and start-up procedure included:

1. Cleaning of the sample lines by blowing high pressure compressed air compressed air through the sampling train before starting each experiment.
2. Cleaning of the filter holder was done prior to inserting the thimble filter by wiping it down using ethanol.
3. Zero and span calibration of the gas analysers was done using calibration gases. Calibration gas analysis certificates for the gases can be found in appendix C. Gas analysers were calibrated after every three experiments.
4. Zero calibration of the DustTrak instrument was done using a zero air filter as per the user manual. DustTrak zero calibration was done before each experiment.
5. LPG flow calibration was done, after every third run, by means of a bubble flow meter. Calibration curves can be found in Appendix C.

An element balance on the measured stack gases can be used to determine if the gas analysers have drifted from their calibration. According to the HTP, the curves of the sum of all carbon detected in the stack, when plotted along with the sum of all oxygen detected should track one another. Figure 5.6 shows such a plot for the commissioning trial samples.

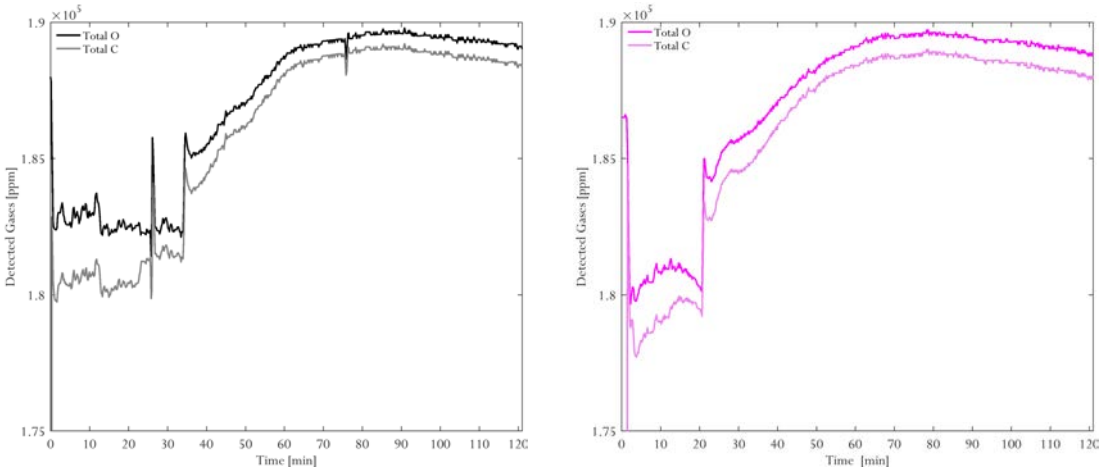

(a) DSCHR Run 1

(b) DSCHR Run 2

Figure 5.6: Gas analyser data quality check. Deviation from the parallel tracking is an indication of deviant analyser behaviour. Makonese [2015] discusses how these curves should behave for various fuels and how the occurrence of the water-gas shift reaction under poor combustion conditions will affect the appearance of these curves.

5.5.4 Treatment of Activated Carbon Tubes and Quartz Thimble Filters

Copper tubing was used for the sampling train to the thimble filter. The line was cleaned, after each cycle, by blowing high pressure compressed air through. Weighing of the thimble prior and after exposure was done in a controlled environment. Thimbles were kept in sealed containers before and after exposure.

Teflon tubing was used for all non-particulate sample lines, These were also purged after each run using compressed air. Activated carbon tubes were kept in a sealed container prior to and after exposure. The seal on the tubes was broken immediately prior to sampling and the tubes were resealed after exposure. Analysis of the VOC components was done by the supplier, Biograde.

5.6 Commissioning Experiments

A set of two commissioning experiments were done, following the procedures outlined in this chapter, to (1) ensure the operator is accustomed to the procedure, (2) determine the repeatability of the procedure. These experiments were done using a density washed char (DSCHAR, S.G. 1.4-4.6) produced from 30 mm particles. The preparation of this char sample is discussed in Chapter 3. The density washed sample is ideal for commissioning experiments since it allows for the evaluation of the experimental set-up and results without significant variations in the fuel properties so that any variability is due to the operator's behaviour or due to equipment faults. The experiments were left to run until extinction. This section reports the results and error margins as determined from these experiments for the first two hours.

5.6.1 Thermal Performance Measurements

The thermal performance of the fuel and stove is largely dependant on two measurements, *i.e.* the mass of the fuel and the temperature of the water. Other important parameters are the ignition time, the heat lost through the chimney, and the mass of residue leftover after the experiment.

Ignition Gas Supply and Ignition Times

As defined above, the ignition time is determined by taking the time taken to raise the temperature at the coal bed to 500 °C from a steady gas supply. It is important to keep the mass flow rate, and thus the amount, of gas used constant to avoid supplying the fire with too much gas too quickly, or too slowly, which may affect the combustion. Table 5.1 shows the ignition-related variables of the commissioning trials.

Table 5.1: DSCHR Ignition Gas Supply and Time

Run	Gas used [g]	Gas flow rate [L.min^{-1}]	Ignition Time [min]
1	240	4.0	32.5
2	220	6.2	19.3
Mean	230	5.0	26.0
Std. Dev	14.1	1.5	9.2
Std Error	-	-	6.5

From Table 5.1, it is clear that keeping the gas flow rate constant is important in limiting the variances in the ignition time. The results show that a 2.1 L_N/min^{-1} difference in gas flow resulted in a difference of 13 minutes in the ignition time. Variances in gas flow may be caused by a difference in ambient temperature as well as the temperature of the gas itself. It was noted that in general, the gas flow for experiments undertaken during the morning hours, (08h00-09h00) was slightly (1.5 $L_N.min^{-1}$) lower than for those taken later in the day. In cases where the "morning experiment" differs significantly in terms of flow rate and ignition time, it is eliminated as an outlier.

Measurement of Mass Loss

The energy released from the combustion is directly linked to the mass of fuel consumed - See Equation 5.1. This is monitored in real time as described in the sections above. The resultant mass curves are shown in Figure 5.7.

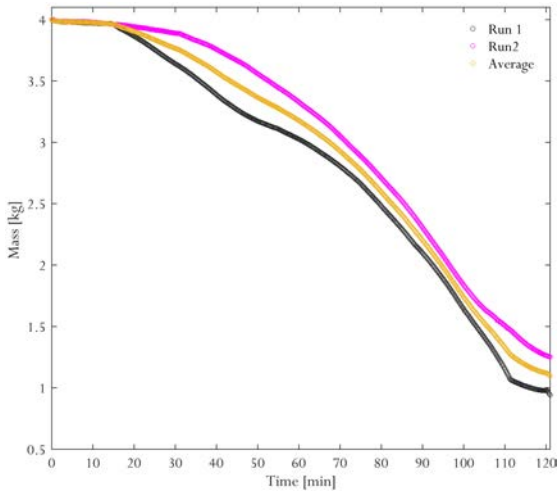

Figure 5.7: DSCHR Repeatability of Mass Monitoring

The mass remaining at the end of the run is 1.19 and 1.25 kg for the first and second trials respectively, corresponding to standard error of 0.03 kg. It is likely that the largest variation in fuel consumption occurs due to the varying rates of absorption of oxygen the initial stages of the burn.

Combustion Efficiency

Paired with the mass consumption is the combustion efficiency, which, for the calculation schemes of this study, depends on the mass and composition of the residue. Both trial runs were left to burn until extinction. The residue from both runs was analysed for ash yield, caloric value and LOI. These results were used to determine the combustion efficiency as shown in Table 5.2. The combustion efficiencies do not differ from one run to the next regardless of the method uses, the method based on the ash yield and CV predict efficiencies slightly higher (87.4%) than using the LOI (85%), but the standard error for both is rather small (< 1 %).

Table 5.2: DSCHR Combustion Efficiency

Run No	**LOI Method**				**CV-Ash Method**				
	Mass [kg]		LOI[%]	η_{comb} [%]	Ash [%]		GCV [MJ.kg^{-1}]		η_{comb} [%]
	RF	Res			RF	Res	RF	Res	
1	4.0	1.19	32.89	85.1	23	68.4	24.62	9.14	87.5
2	4.0	1.25	34.83	84.9	23	67.1	24.62	9.17	87.2
Mean				85					87.35
Std. Dev				0.14					0.21
Std Error				0.1					0.15

RF = Raw Fuel, Res.=Residue
Ash yield and GCV values given on an air dry basis

Water Boiling Time and Thermal Parameters

Second to the mass consumed, the water boiling times, are the most important measurements required to characterise the thermal performance of the fuel. The water boiling procedure is used to determine the thermal, or cooking, efficiency.

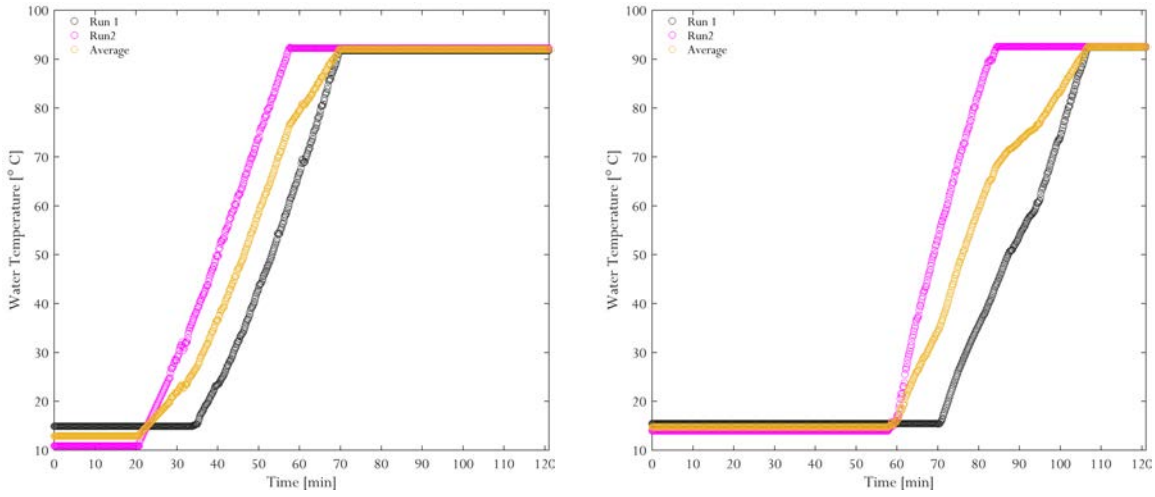

(a) Pot 1 (b) Pot 2

Figure 5.8: DSCHR Water Boiling Test

Figure 5.8 shows the recorded data from the water boiling tests for the DSCHR trials, and Table 5.3 shows the pertinent water boiling test information. The ignition times for pot 1 were found to be stable only differing by a minute, while the boiling times for the second pots differs by a much more significant 11 minutes.

Table 5.3: DSCHR Water Boiling Test

Run No.	**Mass Evaporated [g]**		**Boiling Time [min]**	
	Pot 1	**Pot 2**	**Pot 1**	**Pot 2**
1	40	80	34.5	36.0
2	40	100	35.5	25.0
Mean	-	-	35.0	30.5
Std. Dev	-	-	0.70	7.78
Std. Error	-	-	0.5	5.5

The observations in mass of water evaporated echoes those of the boiling times. As discussed in Section 5.3, the maximum mass loss due to evaporation is 100 g and only occurs in 3 out of the 30 experiments conducted, with the average mass loss being 9 and 16 g for the first and second pots respectively. These masses, corresponding to less than 1 ‘% of the water in the pot are negligible. It is possible that the quicker boiling times (and higher water mass loss) occurs with the second boiling experiment as the fire reaches its maximum burning rate at this time. The standard errors calculated for the boiling times are less than 10 % and would result in a 95% confidence interval of 34 -36 [min] and 19.7-41.3 [min] for the first and second pots respectively.

Temperature Measurements

Temperatures of interest include those of the fuel bed, the stack, and cooking surface. The former two being important in the determination of the ignition time and system efficiency, respectively.

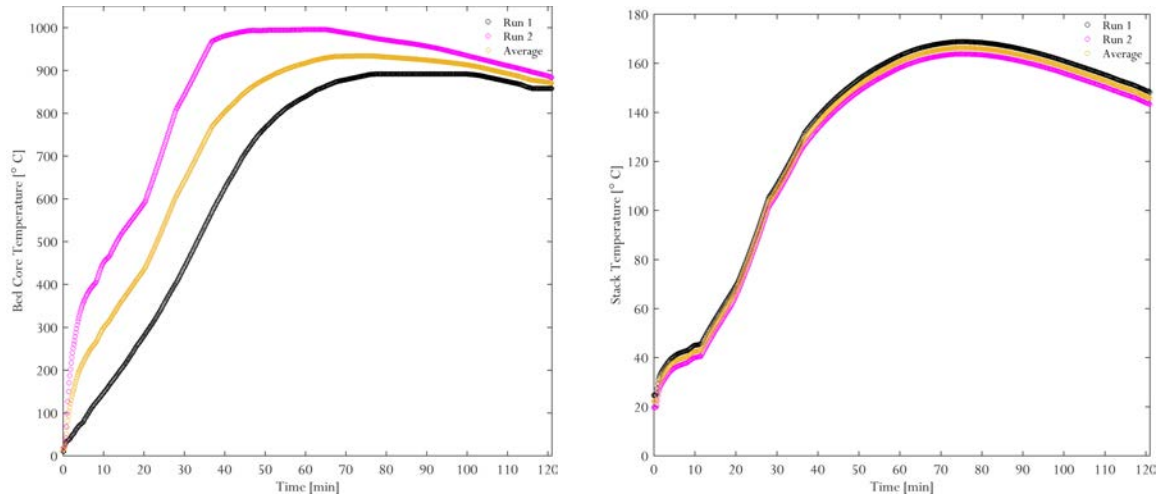

(a) Bed Core

(b) Stack

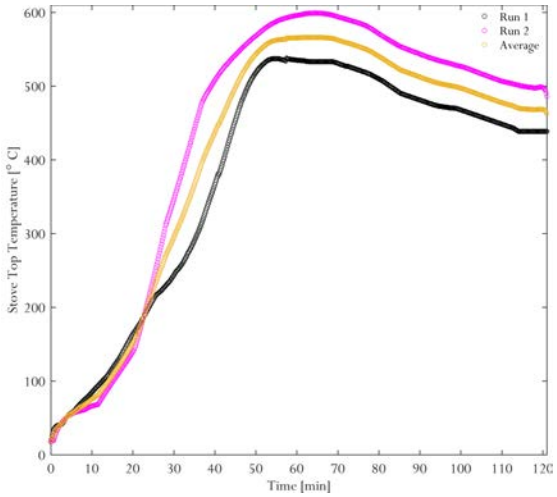

(c) Stove Top

Figure 5.9: DSCHR Temperatures

Figure 5.9 shows the measured temperatures for the DSCHR trials. Figure 5.9a shows the fuel bed temperatures from the two trials along with the average. It is clear that Run 2 has benefited from the increased gas flow and shows a quicker burning fire which not only ignites quicker, but reaches its peak temperature (990 °C, 10°C higher than for the first run) ~30 minutes before the first run. The stack temperatures (Figure 5.9b) show less of a response to the initial conditions, while the stove top temperatures (Figure 5.9c) follow those of the fuel bed. There is a 100 °C difference in the peak stove top temperatures, reached at roughly the same time: ~an hour into the run.

5.6.2 Emission Measurements and Characterisation

The second assessment of the fuels is that of the emissions. The measurement of the gaseous and particulate emissions are important because (1) the SO_2 and PM emissions are related directly to the fuel properties (see Section 2.6 of the literature review), (2) the quality of combustion can be determined from the CO and CO_2 emissions; the latter of which is used to determine the dilution ration required to determine the PM emitted, (3) the excess air is determined from the recorded emission data, and (4) the total oxygen and carbon detected are used to detect deviant instrument behaviour (See Section 5.5.3 of this chapter).

Gas Monitoring

Figure **??** shows the measured gases for the DSCHR trials. Similar to the recording of the mass, the ignition stage of the burn presents the most variation in behaviour. Both trials, however, equilibrate to one point once the fire is self sustaining.

The second-to-last column in Table 5.4 shows the expected emissions if all the loaded fuel was consumed while the emissions in the last column are based on the average mass consumed between the two trials. The combustion calculations assume 100 % efficient combustion, thus not CO is presented.

Table 5.4: Typical combustion calculations were performed on the DSCHAR ultimate analyses (a.d. basis) to determine the amount of each of the measured pollutant that would form in the entire combustible fraction of the fuel was consumed.

	Ultimate Analysis			**Predicted Emission [g]**		
	[% a.d]	*[% a.f.]*	*[g/kgFuel]*	*per kgFuel*	*Fuel Loaded*	*Fuel burnt*
C	65.5	85.06	850.65	3 119.05	12 476.19	8 666.27
S	0.68	0.88	8.83	17.66	70.65	49.07
H	1.92	2.49	24.94	224.42	897.66	623.54
N	1.65	2.14	21.43	45.92	183.67	127.58
M	1.4	1.82	18.18	18.18	86.75	60.26
O	5.91	7.68	76.75	-	-	-
A	23.0	-	-	-	-	-
	100	**100**	**1000**	**3 425.23**	**12 714.93**	**9 526.73**

M*=Fuel Moisture
a.f.=ash free, not to be confused with d.a.f.
fuel loaded refers to the 4 kg fuel load while fuel burnt refers to the actual fuel consumed

The measured pollutants differ from the predicted masses by significant amounts in the case of the NO_x and SO_2, and to a lesser degree for the other components. CO emissions were calculated using the CO\CO_2 from the trial experiments. The difference in emissions may be due to the difference in mass consumed for the fuels; 2.81 kg of fuel was consumed during the first experiment while only 2.75 kg were consumed for the second. This is evident from the LOI in Table 5.2. The prediction for SO_2 overshot the measured amount by 15-25 g and the NO_x ~by 124 g. The assumption of complete combustion may be the cause of the over-estimation. Both the nitrogen and sulphur can interact with CaO in the coal, resulting in their retention in the ash. Jiang *et al.* [2010] reported that NO_x emissions were lowered due when limestone was added to the reaction vessel. With the exception of these two components, the predicted emissions fall within the 99 % confidence interval for the mean of the two trials.

Table 5.5: The Predicted emission mass as determined in Table 5.4, the CO emission is based on the 85% combustion efficiency determined using the LOI method in Table 5.2

	Mass Emitted For Fuel Burnt [g]						**99% CI**	
	Predicted	*Run 1*	*Run 2*	*Mean*	*Std. Dev*	*Std. Error*		
CO2	8 188.79	8 863.26	8 031.40	8 447.33	588.21	415.93	7 374.23	9520.43
SO2	54.40	39.11	28.49	33.80	7.51	5.31	20.09	47.51
Nox	141.43	18.09	16.65	17.37	1.02	0.72	15.51	19.23
CO	477.48	509.55	423.28	466.41	61.00	43.14	355.12	577.70
H2O	691.20	687.28	617.36	652.32	49.44	34.96	562.13	742.51
M	66.80	66.72	59.94	63.33	4.80	3.39	54.57	72.09
Total	**9620.10**	**10184.02**	**9177.12**	**9680.57**	**711.99**	**503.45**	**8381.66**	**10979.47**

* M=Fuel Moisture

Particulate Emission Measurement and Collection

Particulate matter measured in real time for the two trials is shown in Figure 5.10, while the results for the whole burn are shown in Table 5.6.

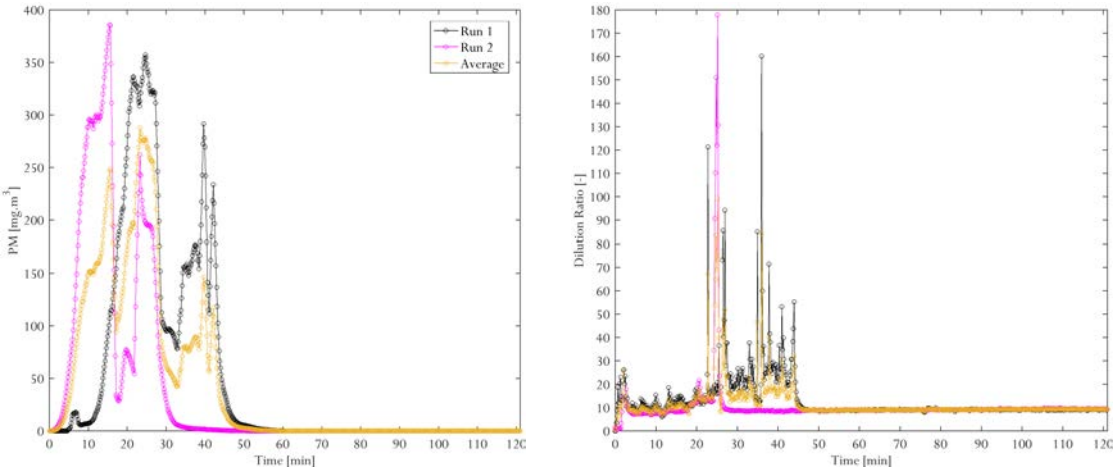

(a) Recorded PM (b) Dilution Ratio

Figure 5.10: DSCHR PM Time Series Plot

The measured, uncorrected PM emissions are shown in Figure 5.10. For each trial, there is a steady increase in the PM emitted which drops suddenly when the "ignition" conditions are reached. This drop is due to the over saturation of the analyser which was countered by engaging the nitrogen dilution as seen in Figure 5.10b. This dilution is accounted for as described above. PM Emissions, become insignificant, for the LSF fuel used here, at the same point the fire reaches its peak bed core temperature (See Figure 5.9a) and the CO\CO$_2$ ratio is reaching its minimum ratio (this can be seen by inspection on Figures **??**a and b), indicating that the combustion is becoming more efficient.

Table 5.6: DSCHR Total PM measured by DustTrak

Run No	**Stack Gas Produced** $[m^{-3}.kg^{-1}]$	**Mass consumed** $[kg]$	**Stack Gas** $[m^{-3}]$	**TSP** $[mg.m^{-3}]$	**TSP** $[g]$
1	8.92	2.80	25.01	36 513.12	913.25
2	8.95	2.88	25.73	27 794.13	715.18
Mean	8.94	2.84	25.37	32 153.63	814.22
Std Dev.				6 165.25	140.06
std error				4 359.49	99.04

The total PM measured for the second trial is over 200 g lower than for the first trial, possibly due the better ignition and combustion. The longer "active emission region", the interval within which the emissions are highest, is longer for the first trial (~45 minutes) compared to the 30 minutes for the second. This too may lead to a higher total in PM emission. This results in a large standard error (99 g). The results of PM emissions are reliant on the ignition and development of the fire being repeatable. As discussed earlier in this section, this relies on the gas flow rate being kept constant.

5.7 Summary Experimental Schedule

There are two variables in the tests, the type of fuel (coal of LSF) and the size of the fuel (5 sizes). Three experiments were done for each fuel/size permutation and the average of the three runs, if there were no outliers, was reported. In total, thirty experiments were carried out in addition to the commissioning experiments discussed above. The Thermal performance was characterised by the (1) fire power output, (2)the cooking-, (3)heating-, and (4) system efficiency. The use of emission factors (EF) ensures that emissions results (CO, O_2 and NO_x, and PM) from different experiments are normalised to a similar reference point so that they may be compared with one another. In this study, and as prescribed by the HTP, 0% excess air is used as the reference point, accounted for by determining the access air (EA) factor and adjusting the emissions measurements accordingly. Pollutant emissions were reported as emission EFs on an energy basis. Combustion efficiency can be expressed as the ratio of CO to CO_2 detected, as done in the HTP, or by analysing the residue of the experiment that was left to run until extinction as prescribed by the test for LSF validation. Both methods were used. Results from the LSFs were compared to their coal counterparts to determine the effect of fuel type and across the various sizes to determine the effect of particle size on the performance of the proposed LSFs. Lastly, each experiment is divided into three sections, ignition, cooking and heating so that results can also be reported on a "task basis".

An evaluation of the reproducibility of the procedures and results was done using a density screened, 30 mm char (DSCHR). The ignition times, mass consumption curves, water boiling times, bed core, stove top and stack temperatures, emissions of gases and particulates were considered. It was found that the ignition gas flow rate was important in ensuring that the fire ignites and develops in a reproducible manner. This LPG flow rate has an effect on the mass consumption and temperature of the fire, which in turn has an effect on the emissions, especially the PM emissions. A 1.2 $L_N.min^{-1}$ change in LPG flow rate led to a 13 minute difference in ignition time as well as a 30 minute difference in the time taken to reach the peak bed core temperature and elongated the "active time", that is the time between the start of the run and the end of the cooking segment, by the same amount of time. The PM emissions also showed a strong response to the varying gas flow rate.

The total emissions, in grams, of gases measured was compared to a set of combustion calculations and it was found that the measured gases differed, by varying degrees to the predicted amounts. The assumption of complete combustion was found to be the greatest source of the variability.

Chapter 6

Results and Discussion

The aim of the study, to determine the change in LSF thermal performance and emissions if particle size is increased from small (15 mm) to large (40 mm). The previous chapters established the properties of the fuels and how they were affected by particle size, this chapter will discuss the results of the combustion experiments as laid out in Chapter 5 according to metrics of thermal performance and emissions. The thermal performance is characterised by the ignition time, the time to bring 4 litres (in two batches of 2 L) of water to boiling point as well as the heat transfer- and combustion efficiencies while emissions of gases (NO_x, SO_2, and CO), total particulate matter and volatile organic compounds.

6.1 Thermal Performance

6.1.1 Ignition Times

Ignition, in this study, is taken as the point where the temperature at the core of the fuel bed reaches 500 °C. The ignition times for all the fuels are shown in Figure 6.1 and the calculation of the standard error (shown, in minutes, in Table 6.1) can be found in Appendix D.

Table 6.1: All Fuels Ignition Times

	Ignition Time [min]		**Ignition LPG**	
	TGA predicted	*Stove*	*Mass [g]*	*Flow rate [L.min^{-1}]*
15mmCoal	40.9	50.0 ± 3.00	0.81 ± 0.10	3.92 + 0.0
20mmCoal	36.7	37.9 ± 4.15	0.59 ± 0.04	4.70 ± 0.14
30mmCoal	36.3	29.4 ± 3.45	0.43 ± 0.02	4.98 ± 0.07
40mmCoal	35.8	23.0 ± 4.97	0.34 ± 0.04	4.59 ± 0.41
CompCoal	-	26.9 ± 1.40	0.49 ± 0.05	4.54 ± 025
15mmLSF	46.4	26.9 ± 3.87	0.47 ± 0.12	4.70 ± 0.27
20mmLSF	42.9	25.1 ± 0.96	0.48 ± 0.07	4.59 ± 0.41
30mmLSF	44.8	14.5 ± 1.02	0.31 ± 0.03	4.93 ± 0.00
40mmLSF	36.3	12.7 ± 1.81	0.28 ± 0.05	4.87 ± 0.07
CompLSF	-	26.4 ± 2.04	0.45 ± 0.12	4.59 ± 0.41

Overall the LSFs ignited in a shorter time than their coal counterparts, using a similar amount of LPG. All the coals, with the exception of the 15mmCoal, ignited in 25-35 minutes, while the LSF took between 12-27 minutes to ignite. The anomaly of the 15mmCoal may be due to the lower gas flow used: 3.9 $L_N.min^{-1}$ compared to the average 4.7 $L_N.min^{-1}$ of the other fuels. As discussed in the previous chapter, a lower gas flow will result in an artificially longer ignition time. The ignition times for the CompCoal (26.9 min.) and CompLSF (26.4 min) are consistent with those of Kühn *et al.* [2017] who reported that an untreated coal, of similar properties to that used in this study, and its corresponding LSF, prepared at 550 °C, ignited in ~25 minutes and LPG flow rates[1] of 8.53 and 7.29 $L_N.min^{-1}$. Ignition time estimates from the single particle TGA study were longer than those achieved in the stove. Differences in combustion conditions, for example the advantage of having the LPG instead of relying on self-ignition, is the chief cause of the disparity.

Ignition, as discussed in the literature study is dependent on, among others, the volatile yield and rank of the coal, the combustion environment, as well as the particle size. The fuel ratios, which can be used as a proxy for the volatile yield of the fuels, were found to increase (by up to 3 times) from the coals to the LSFs. This indicated that the LSFs would experience greater difficulty with ignition. Indeed the results of the single particle study in Chapter 4 supported this notion, reporting higher ignition temperatures, and longer ignition times for the LSFs compared to the coals. Quite the opposite is observed in Table 6.1 for the bed of particles. The more porous nature of the LSFs, allowing for better absorption of O_2 may be a possible explanation for the counter-intuitive result. Rank was reported, by [Shen, 2009; Chen *et al.*, 1996], to be linked to approximate ignition temperature of a particle. For example bituminous coal, which was employed in this study, will ignite at ~400 -500 °C. This was explored in Chapter 4 and served as part of the basis for the 500 °C cut-off point for this study.

A definitive decrease in ignition time is observed as the particle size increases for both fuel types. The volatile matter yield was also found to increase with increasing particle size. A combination of three fcators may have benefitted the larger particles in this regard: (1) the failure to eject heat form the interior, (2) the possible increase absorption of O_2 due to increased porosity, and (3) the increased volatile matter yield. This is consistent with the statements made by Kosowska-Golachowska [2010]. By way of explanation, Zygourakis [2000] suggests considering the relation between the rate of heat generation, from the exothermic reactions, within the particle and the rate at which this heat can be expelled. If r is the radius of the particle, then the heat generation is proportional to r^3, and heat removal, to r^2; so that the ratio of the two is proportional to r^{-1}. This implies that larger particles will have more difficulty dissipating the heat generated by reactions in the interior. This will, as a result, cause the internal temperature to increase, along with the possibility for ignition [Zygourakis, 2000]. This result is confirmed by the experimental work of Matzakos [1992], who studied the ignition of different sized particles in a TGA. The LPG may also pay a role as it will cause the overall bed temperature to increase as it burn in the inter-particle space. The exact interactions of the LPG and the fuel bed is outside the scope of his work and may warrant further study.

[1]The gas flow in the Kühn *et al.* [2017] study was not regulated *in situ*, but measured before each experiment using a bubble flow meter

6.1.2 Fuel Burning Rates

The ignition LPG is to ensure that each experiment can reach a state where the fire is self-sustaining. The mass of the fuel in the stove was monitored through the burning cycle and from that data, the burning rates were computed. These are shown, as dashed lines along the left-hand side axes, in Figure 6.1, along with the cumulative power output, while Table 6.2 shows the peak burning rates as determined during the single particle TGA study as well as the burning rates from the combustion tests. Plots showing the mass consumed, in the stove, for each fuel can be found in Appendix D.

Table 6.2: All Fuels Peak Burning Rates

	TGA		**Stove**		
	T_p $[^{\circ}C]$	R_p $[\%.min^{-1}]$	T_p $[^{\circ}C]$	R_p $[\%.min^{-1}]$	R_{mean} $[\%.min^{-1}]$
15mmCoal	650.0	1.115	528.7	0.830	0.391
20mmCoal	670.0	0.755	611.5	1.042	0.467
30mmCoal	585.0	0.866	761.0	0.827	0.581
40mmCoal	600.0	0.769	702.7	0.730	0.480
CompCoal	-	-	548.0	1.150	0.512
15mmLSF	725.0	0.908	429.0	1.182	0.395
20mmLSF	700.0	0.537	523.1	0.678	0.356
30mmLSF	785.0	0.495	836.5	0.559	0.437
40mmLSF	680.0	0.456	702.1	0.625	0.427
CompLSF	-	-	734.0	0.659	0.403

R_P is the peak burning rate R_{mean} is mean burning rate for entire burn cycle

Peak burning rates determined via TGA underestimated the those for the fuel bed; this is more pronounced for the LSFs than the coals. It is likely that phenomena such oxygen competition, and inter-particle interactions, and bed-wide temperature gradients which occur in a bed of particles but are absent in single particle combustion [Marek and Stanczyk, 2013] may be the cause. The corresponding peak temperatures are also incongruent with their TGA counterparts. It is interesting to note that the peak temperatures for the larger particles (30 and 40 mm) exceeded the predicted peak temperatures while the opposite is observed for the smaller (15 and 20 mm) particles. The occurrence of the peaks for the smaller particles, for both fuel types, near the ignition point suggests that these may be volatile combustion peaks. Furthermore, the temperatures correspond to those reported in Chapter 4 for volatile and surface char combustion. This would be in agreement with the reports that smaller particles are likely to ignite heterogeneously [Kosowska-Golachowska, 2010; Essenhigh *et al.*, 1989]. Overall, peak combustion rates were found to decrease with increasing particle size, while the temperatures increased. the latter observation is consistent with the literature, larger particle are able to reach higher combustion temperatures due to temperature diffusion limiatations as discussed above [Matzakos, 1992]. In a study of the effect of ignition method in an *imbaula*, Masekameni [2015] found that using the bottom-lit up-draft (BLUD) fire lighting method resulted in higher burning rates caused by the flame front propagating upward through the bed, and engulfing it in a volatile-fire that pyrolyses the fuel quicker. The lower volatile matter content and slower release from the larger parties, may also account for the lower average burn rates of the larger LSFs.

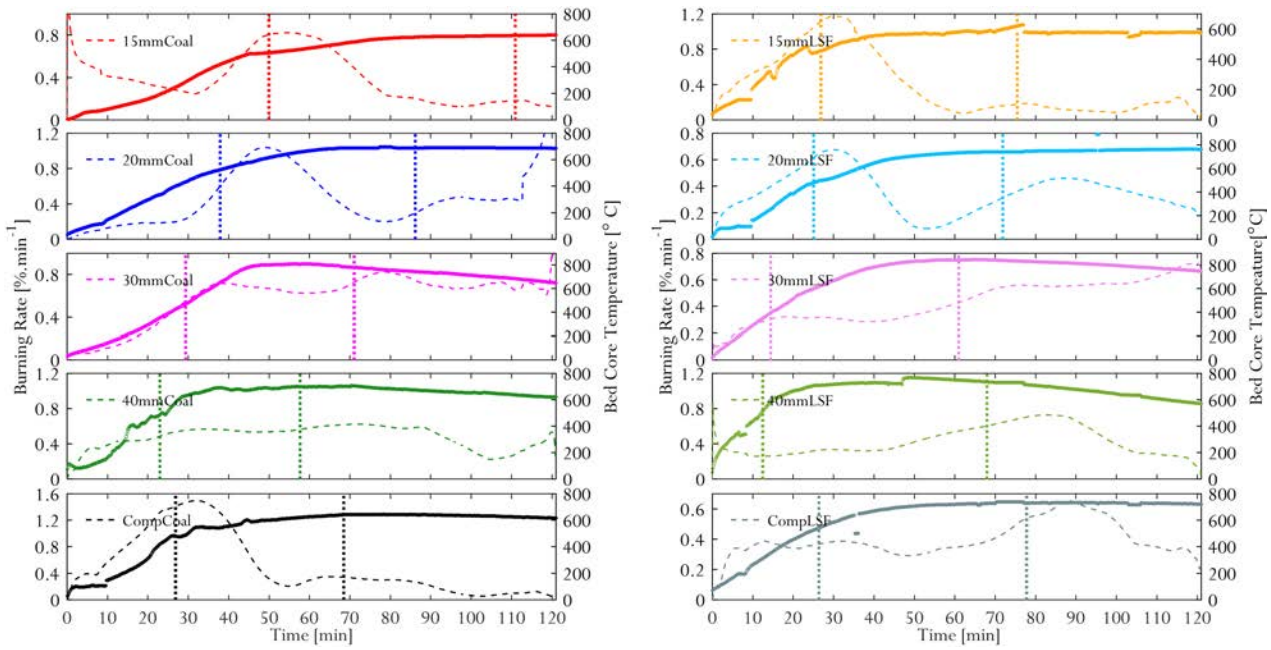

Figure 6.1: **Burning Rates and Bed Core Temperatures.** The mass consumptions rates, in $\%.min^{-1}$, appear on the left-hand side axes as dashed lines while the thick lines on the right-hand side axes show the temeperature at the core of the fuel bed. The figures in the left column are for the coal fuels and those on the right the LSF. The vertical lines indicate the ignition point (leftmost line) and the end of the cooking stage (rightmost line).

The average mass consumption rates, shown in Table 6.1, of the coals are, on average, higher than of the LSFs. However due to the high fuel ratios, the burn rates increase sharply in the first 3-40 minutes of the burn, then dissipate quickly thereafter. This effect is, however, less pronounced for the larger sized fuels. The average burning rates of the LSFs, on the other hand, do not differ significantly from the peak burn rates, indicating a more uniform burning profile. These results are well correlated with the fuel ratios reported in Chapter 3. The fuels' fuel ratio also affects the temperature profiles of the fuels: on average, the LSFs, with the higher fuel ratios reach higher bed core temperatures than the coals. This effect can be seen well in the case of the composite fuels. The CompCoal, with a fuel ratio of 1.55 reaches a maximum temperature ~600 °C, 200 °C lower than the CompLSF (fuel ratio, 6.74). The fuel ratios of the colas increase with particle size in the order 40mm<30mm≈15mm<20mm and their maximum bed core temperatures follow suite with the exception of the 15mmLSF, which was limited by the low burning rate.

6.1.3 Energy and Power Output

Another important parameter dependent on the mass consumption rates of the fuel is the fire power output, which presents the rate at which energy is released from the fuel. Figure 6.2 shows the cumulative fire power output. The fuels have comparable calorific values (~22-23 $MJ.kg^{-1}$, a.d), and it is thus expected that a similar amount of energy will be released per kg of fuel consumed, the power output is thus, in this case, only dependant on the mass consumption rate (see Equation 5.1). The higher the burning rate the higher the power output for that interval.

Nominal values for the ash corrected mass consumed[2], calorific value, total energy liberated, and corresponding power output are shown in Table **??**.

This increased mass consumption of the coals led to a higher average energy yield. Despite having most of the energy released during the cooking segment, as indicated by values in Table **??**, the LSFs still recorded similar cooking times to the coal, for which the most energy is released during the heating segment. This may indicate the the thermal efficiency achieved when using the LSFs is lower than that of the coals as will be explored in a later section.

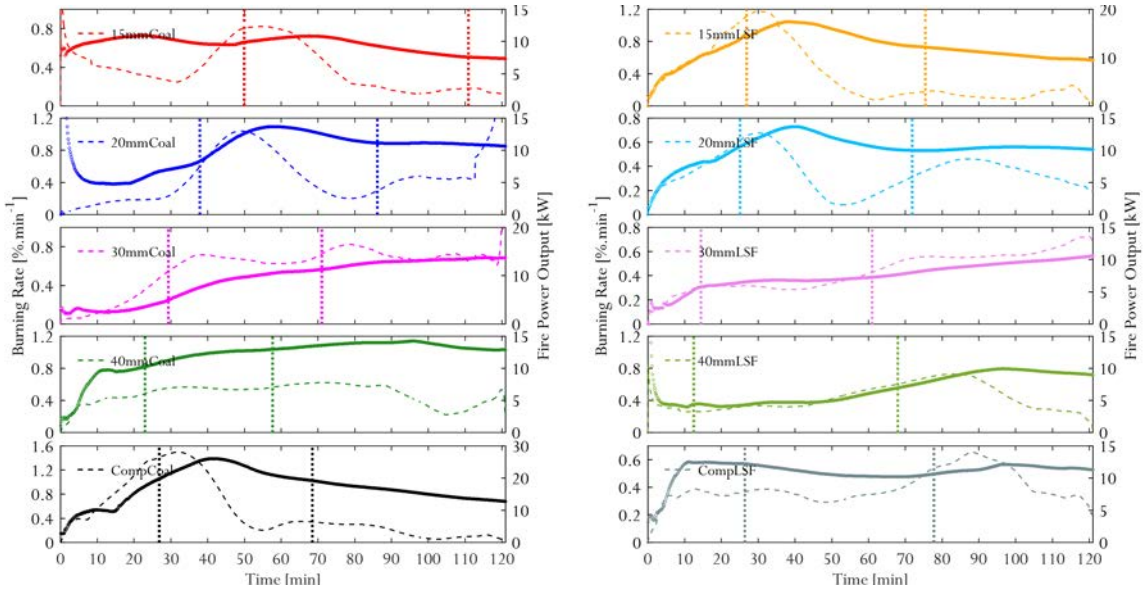

Figure 6.2: **Burning Rates and Power Output.** The mass consumptions rates, in $\%.\text{min}^{-1}$, appear on the left-hand side axes as dashed lines while the thick lines on the right-hand side axes are the cumulative power output.

From their study on the effect of coal properties on the thermal performance of the *imbaula*, Makonese *et al.* [2017b] reported a fire power output of 8 kW for an *imbaula* burning, and this power output deceased to 6.5 kW when the moisture content of the coal increased from 2.4 -8.6. From this it was expected that the LSFs would have a higher power rating than the coal, since the moisture content is greatly decreased from coals to LSFs. This is true for the smaller particles in Table 6.3. For the larger particles, however, the fire power output increases with increasing moisture content. Fuel moisture retards the combustion process by lowering combustion temperatures, leading to lower efficiencies, and requiring more kindling for ignition. This is true for the amount of LPG gas used in this study, more LPG was used for the coals, which recorded longer ignition times. It is possible that the use of the LPG as ignition limited the negative effects of increased coal moisture.

6.1.4 Water Boiling Times

The water boiling procedure is part of both the HTP [Makonese, 2011] and the test for LSF validation [Le Roux *et al.*, 2004] and provides a more practical evaluation of the fuel/stove

[2]the HTP takes into account that the fuels may contain significant amounts of ash, and corrects the "fuel remaining" on the scale for ash composition, yielding a mass value on a "ash-free" basis. This value is used throughout for calculations involving mass

Table 6.3: **Burning Rates and Power Output.** The table shows the combustion heat released by each fuel over the individual segments, as well as over the entire burn cycle.

Fuels	**Mass Burnt**	**Fuel CV**	**Total energy Ouput [MJ]**				**Power Output**
	[kg]	*[MJ.kg^{-1}]*	*Ignition*	*Cooking*	*Heating*	*Overall*	*[kW]*
15mmCoal	1.60	30.82	40.58	9.71	4.38	**54.67**	**7.10**
20mmCoal	2.91	31.21	12.59	40.99	18.57	**72.15**	**8.80**
30mmCoal	3.29	31.13	9.51	46.88	43.58	**99.97**	**13.57**
40mmCoal	2.41	30.37	12.88	40.68	39.92	**93.48**	**12.90**
CompCoal	4.27	30.40	32.98	43.74	16.38	**93.11**	**13.70**
15mmLSF	2.77	33.04	23.55	30.11	4.83	**58.49**	**9.23**
20mmLSF	2.48	33.26	21.88	24.90	25.42	**72.21**	**10.07**
30mmLSF	3.48	31.98	5.27	22.35	49.29	**76.91**	**10.70**
40mmLSF	3.11	32.79	5.15	20.83	36.07	**62.06**	**8.50**
CompLSF	2.94	33.01	7.82	32.55	36.82	**77.19**	**11.27**

Mass reported has been corrected for ash content
CV, d.a.f basis.

system. Pemberton-Pigott [2017] stated that the social life of Mongolian citizens who used a CSI designed for the colder climate, was greatly improved by the ability to boil tea water in a quicker time. As the basis for the *mieliepap* that is a staple food for many South African homes, water boiling provides insight into how a potential user of the LSF may respond to the fuel. The result for the water boiling test is shown in Table 6.4 for each individual pot as well as for the entire cooking segment. The time series plots for the water boiling times can be found in Appendix D.

Table 6.4: All Fuels Water Boiling Times

	Boiling Time [min]		**$T_{initial}$ [°C]**		**Normalised Boiling Time [min]**	
	Pot 1	*Pot 2*	*Pot 1*	*Pot 2*	*Pot 1*	*Pot 2*
15mmCoal	29.8 ± 9.28	31.2 ± 4.73	8.2	9.0	25.7	27.2
20mmCoal	25.1 ± 3.40	23.2 ± 1.10	21.5	18.3	25.6	22.7
30mmCoal	20.7 ± 3.04	20.8 ± 2.59	17.9	17.9	20.3	20.2
40mmLSF	21.3 ± 1.68	23.7 ± 0.78	16.7	12.0	20.4	21.4
CompCoal	19.0 ± 6.45	22.6 ± 5.22	15.8	16.2	18.0	21.5
15mmLSF	31.4 ± 6.39	34.3 ± 4.31	20.8	20.2	31.8	24.3
20mmLSF	24.1 ± 1.93	17.8 ± 1.42	20.2	18.1	24.2	17.3
30mmLSF	28.0 ± 4.33	18.5 ± 1.15	15.5	15.6	26.4	17.5
40mmCoal	25.4 ± 3.35	19.6 ± 1.20	19.8	15.8	25.3	18.6
CompLSF	28.5 ± 4.39	22.9 ± 3.49	19.2	15.3	28.2	21.6

The results in Table 6.4 show a drop in water boiling time from the coals to the LSFs. There is no significant difference in boiling times for the first (23.2 min) and second (24.3 min) pot for the coals, while the LSFs report a decrease in boiling time of 8.5 minutes from the first (24.5) and second (19.0 min) pot. The average boiling times reported for the for the CompCoal (20.8 min) and CompLSF (25.7) are similar to those reported by Kühn [2015] for the composite coal

(16.5 min.) and char (28 min) fuels used in in that study. The Kühn *et al.* [2017] boiling times are for 1 L of water. Since the same amount of water is used, the amount of energy required to reach boiling point, assuming the initial temperatures of the water are the same, is the same for all the pots and fuels. Following on this, the boiling times are only dependent on the rate at which this energy is supplied. For example, the 1L pot of water used in the Kühn [2015] study took the same time to boil as the 2 litres of this study, it may be concluded that, for the former study, the rate of heat transfer was slower, or that the efficiency of the heat transfer was lower. The burning rate gives an indication of the heat is released from the fuel. The boiling time achieved by the 40mmCoal particle does not differ between the two pots, this is due to the more uniform burning profile as seen in Figure 6.1. The burning rate of the 40mmLSF, on the other hand, is still ascending when the second pot is placed on the stove, resulting in the quicker boiling time. Similar connections can be made for the other fuels: the boiling time increases for the CompCoal pots as the burning decreases, while the boiling time for the CompLSF decreases from the first to the second pot due to the increasing burn rate.

The initial temperature of the water also plays a role in the boiling time. The initial water temperatures for each of the pots are shown in Table 6.4. While an effort was made to keep the initial temperatures of the water the same, there are some variances. In order to compare the various tests with one another, the results are normalised to a 75 °C difference in temperature, these normalised boiling times are also shown in Table 6.4. The normalised boiling times do not differ significantly for the majority of the fuels, with the exception of the 15mmCoal, for which the normalised boiling times are 4 minutes shorter than the measured time for both pots. This lag in boiling was exacerbate by the declining burning rate during the cooking segment. However, the initial temperature of the water boiled using the 15mmLSF was comparable to the other LSFs, yet this fuel reported longer boiling times for both pots, and it is clear from Figure 6.1 that the cause is the low burning rate during the cooking segment. Increasing the fuel particle size, it can be deduced from Tables 6.4, decreases the boiling time due to a combination of improved ignition times and increased burning rates.

Another important consideration is the thermal mass of the stove. During a cold start, the heat released from the burning fuel will be absorbed by the stove body before any of it is available for heating and cooking. In this study, the stove was warm at the start of the experiment so the thermal inertia will not play a large role on the boiling times reported. However, since the stove is relatively war when the pot is placed on the stove (this occurs roughly 30 minutes after the fire is lit) heat transfer from the warm hob to the pot may be involved, in addition to the combustion of the fuel, in heating the water and may affect the boiling times. The combustion heat released during the cooking phase, shown in Table 6.3, supports this notion. The 20mmCoal reports that 41 MJ of energy was released from combustion during the cooking segment, while the 15mmCoal only reports 9.7 MJ during the same time. These fuels however report the same boiling time (~25 °C) for the first pot, indicating that other sources of heat must have been available for the pot boiled using the latter fuel.

6.1.5 Heat Transfer Efficiencies

Having discussed the practical metrics (ignition and boiling times) and determined the energy output form each fuel, attention is now turned to the assessment of how efficiently this energy was utilised. These efficiency metrics are not, strictly speaking, a measurement of the fuels' performance, but give an indication of the expected performance of a typical household stove when paired with the proposed fuels.

System Efficiency

The system efficiency measures how much of the liberated energy is lost through the chimney, effectively determining the usable heat delivered by the fuel-stove system. Figure 6.3 shows the system efficiency and Table 6.5 shows the nominal system efficiencies. Plots of the total heat released and heat delivered, for cooking and heating energy, can be found in Appendix D.

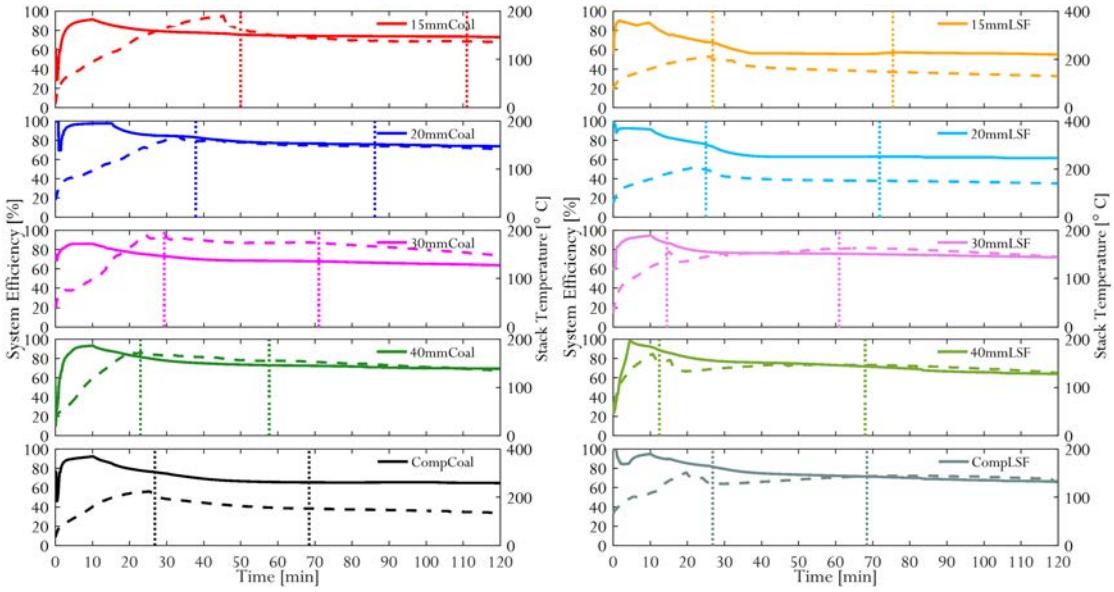

Figure 6.3: **System Efficiency.** The system efficiency is shown on the left-hand side axes as a solid line, while the stack temperature, shown as a dashed line, is on the right-hand side axes.

The initial peak in the system efficiency, occurring in the first ~10 minutes of the burn while, is due to heat is being absorbed by the stove (the stove was at ~50°C at the start of each run) and since the formula used to calculate the system efficiency does not consider heat lost due to the thermal inertia of the stove a "loss", the efficiency is thus overestimated during this period. Following this "inertial period" the system adjusts to the absence of the LPG and reaches an steady state value. This occurs sooner for the LSFs than for the coals.

The system efficiencies shown in Table 6.5 do differ significantly between fuels: there is only a 1% difference in the average system efficiency of the two fuels. Similar to the power output, the efficiency of the coal, the higher moisture fuels, dies not appear to be affected by the moisture content.There does not appear to be a dependence on particle size either, reinforcing the notion that the energy efficiency metrics are not fuel-intrinsic assessments.

Table 6.5: All Fuels System Efficiency

Fuel	Mass Burnt [kg]	Total MJ Yielded	Total Delivered	Fire Power] Output [kW]	η_{Sys} [%]
15mmCoal	1.60	54.67	37.44	7.10	67.34
20mmCoal	2.91	72.15	50.50	8.80	65.84
30mmCoal	3.29	99.97	64.07	13.57	64.99
40mmCoal	3.11	93.48	66.53	12.90	71.05
CompCoal	4.27	93.11	67.27	13.70	67.63
15mmLSF	2.77	58.49	39.13	9.23	53.74
20mmLSF	2.48	72.21	46.40	10.07	63.54
30mmLSF	3.48	76.91	56.13	10.70	72.41
40mmLSFl	2.41	62.06	40.93	8.50	66.43
CompLSF	2.94	77.19	55.73	11.27	68.19

Thermal Efficiency

The thermal efficiency gives the ratio of the heat absorbed by the water to raise the temperature to boiling point and cause some of the water to evaporate. The cumulative thermal efficiency curves are shown in Figure 6.4, along with the temperature at the cooking surface, while the energy delivered to the pots and thermal efficiency are in Table 6.6.

The coals reported higher thermal efficiency that the LSFs as postulated in a previous section. The issues with regards to water evaporation are discussed in Chapter 5 along with the measures taken to limit or avoid, the evaporation of water. It was found (See Appendix D) that the evaporation was greatest for the coal fuels, this is confirmed by the larger amounts of energy delivered to the pots of water boiled using the coal fuels. The exclusion of the evaporation term in the determination of the thermal efficiency has the effect of overestimating the thermal efficiency as the heat lost to the evaporation of water is counted as useful energy.

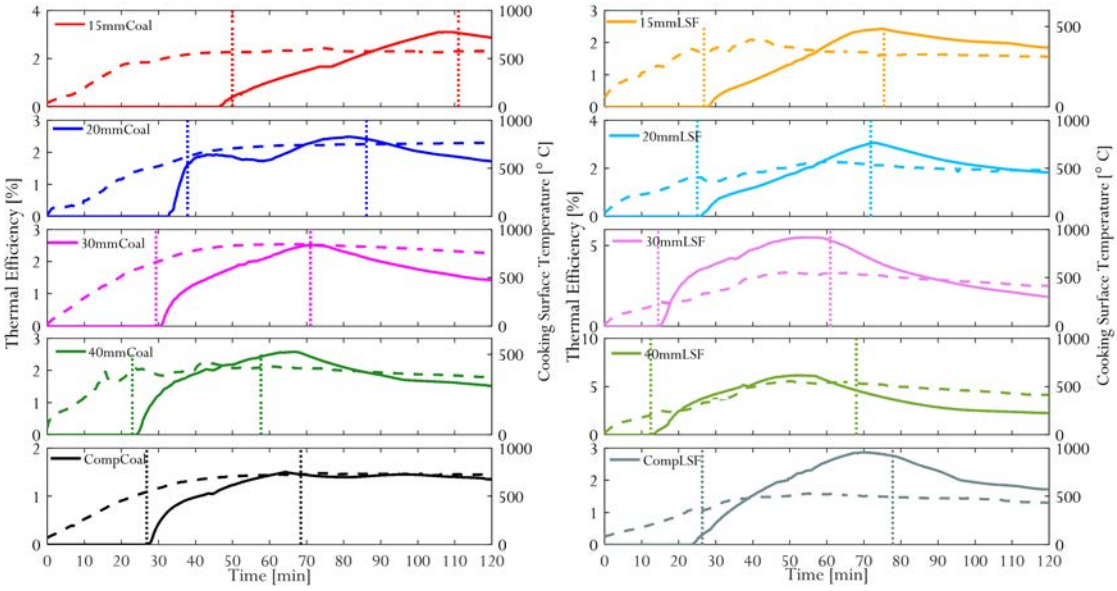

Figure 6.4: **Thermal Efficiency.** The thermal efficiency is shown on the left-hand side axes as a solid line, while the stove top temperature, shown as a dashed line, is on the right-hand side axes.

The average thermal efficiency for the coals is 1.90 % and 1.75 % for the LSFs. These results are consistent with those of Graham [1997] who studied the effeiciency of common household devices, and reported a cooking efficiency of 2% for the Union stove, and a thermal effeiciency of 5.8 % for an *imbaula*, burning a "local coal". Masekameni [2015] and Pemberton-Pigott *et al.* [2009] also reported cooking efficiencies of 5-10% for the imbaulas. The high thermal mass of the Union stove may also be involved in retarding the heating capabilities of the stove. Furthermore, the thermal effeciencies reported in Table 6.6 are consistent with the results of Makonese *et al.* [2017b], who reported that thermal efficiency increased with increasing fuel moisture content. The effect here is not as pronouncced here as in the Makonese *et al.* [2017b] study because the difference in moisture content between the coals (~2.3 % a.d) and the LSFs (~0.7 % a.d) is not as large as in the former study.

The recorded thermal efficiencies decrease with increasing particle size. This follows from the discussion of diffusion limitations, the larger particles increase the amount of energy "lost" to particle drying and delayed volatile evolution.

Table 6.6: All Fuels Thermal Efficiency

Fuel	**Cooking Time**	**MJ in Pots**	**Cooking Power [kW]**	η_{Cook} [%]
15mmCoal	61.0	1.44 ± 0.17	0.34	**2.58**
20mmCoal	48.3	1.40 ± 0.14	0.43	**2.20**
30mmCoal	41.7	1.40 ± 0.0	0.50	**1.35**
40mmCoal	45.0	1.40 ± 0.0	0.51	**2.27**
CompCoal	41.6	1.40 ± 0.0	0.60	**1.41**
15mmLSF	76.3	1.33 ± 0.06	0.41	**2.28**
20mmLSF	42.0	1.37 ± 0.06	0.51	**1.87**
30mmLSF	46.5	1.37 ± 0.06	0.50	**1.76**
40mmLSF	45.0	1.43 ± 0.06	0.53	**1.53**
CompLSF	51.4	1.43 ± 0.06	0.46	**1.75**

Efficiency as a Heater

An advantage of using solid fuels, such as coal, as a household energy source is the dual utility. Many a user survey [Nkosi *et al.*, 2017; Mdluli, 2007; Balmer, 2007] indicate that the continued use of coal is due to this feature. The thermal efficiency measures the ratio of energy liberated to energy "leaked" into the home to provide heat. Table 6.7 contains the overall heating efficiencies. the time series plots for the heating effective can be found in Appendix D.

Mathematically, the heating efficiency is simply the difference between the system- and the cooking efficiency, and there is no pot on the stove during the ignition segment of the run, the heating efficiencies follow those of the system efficiency and then assume a steady state value thereafter. The coal fuels; efficiency is an average 63 % while the low smoke fuels achieved a heating efficiency of 64 %. A slight increase in heating efficiency can be seen as particle size increase; more so for the LSFs than for the coals. The comparable values reported in Table 6.7 confirm that the efficiency metrics are a function of the device rather than that of the fuel within.

Upon finding that the heating efficiency of the Union stove was less than that of the *imbaulas* and three-stone fire, Graham [1997] concluded that the union stove reports low efficiencies due to its thermal inertia. That is, during a cold start (starting a stove at room temperature) the stove absorbs much of the generated heat, thus resulting in lower heating efficiencies. It is unlikey that this happended in this study, since the stove was at a temeperature higher than room temeperature at the start of the runs. Similar to the cooking effeciency, Masekameni [2015] reported much higher heating efficiencies (>90%) for the *imbaula*. This however is weighed down by fact that the *imbaula* is left outside during the initial stages of combustion due to the high levels of smoke and pollutants. During this period,according to Graham and Dutkiewicz [1999], an unknown amount of energy is released that cannot be used, whereas the Union No 7 stove or any device similar, can start heating the room as soon as it overcomes its thermal inertia.

Table 6.7: All Fuels Heating Efficiency

Fuel	**MJ in Home**	**Heating Power [KW]**	η_{heat} [%]
15mmCoal	36.00	4.60	**64.75**
20mmCoal	43.45	6.00	**56.65**
30mmCoal	62.73	8.63	**63.64**
40mmCoal	39.53	5.43	**64.15**
CompCoal	65.87	9.07	**66.22**
15mmLSF	37.80	5.17	**51.91**
20mmLSF	45.03	6.20	**61.66**
30mmLSF	54.77	7.53	**70.64**
40mmLSF	65.10	8.97	**69.52**
CompLSF	54.30	7.47	**66.44**

The efficiency of the stove as a heater is similar to the total system efficiency since the radiant heat makes up the majority of the useful heat delivered. The heating effeciency curves can be seen in Figure 6.5.

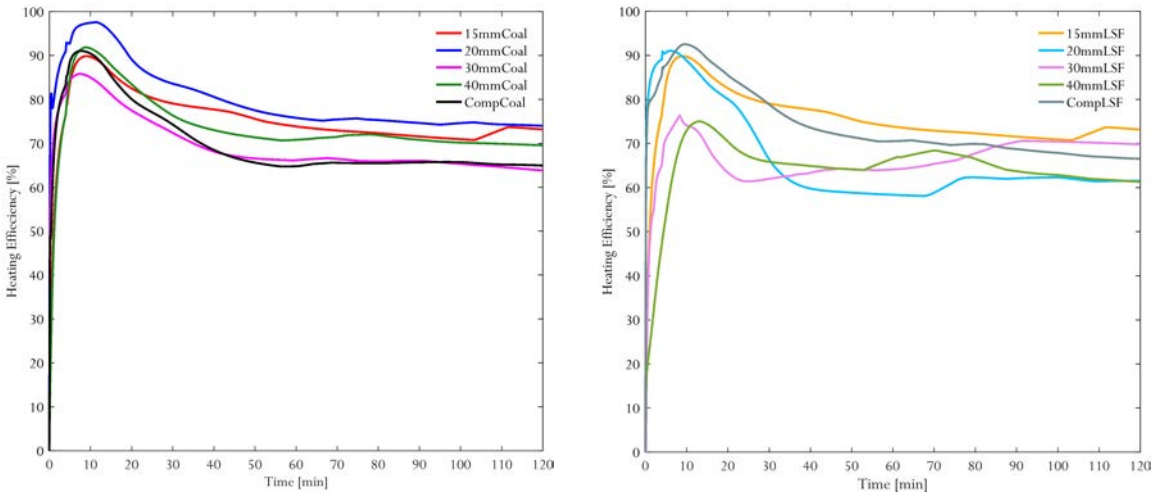

(a) Coals (b) Coals

Figure 6.5: All Fuels Efficiency as a Heater

Combustion Efficiency

The combustion efficiency is the last efficiency metric to be assessed, and unlike the other efficiencies, the combustion efficiency speaks more to the properties of the fuel than those of the stove. The CO\CO$_2$ ratio is used conventionally to indicate the quality of the combustion: a high CO\CO$_2$ indicates a fuel that released more CO, a product of incomplete combustion, than CO$_2$. Figure 6.6 shows the CO\CO$_2$ ratio for all the fuels and Table 6.8 shows the nominal values determined using the results of the proximate and LOI analyses on the residue after the last run of each fuel.

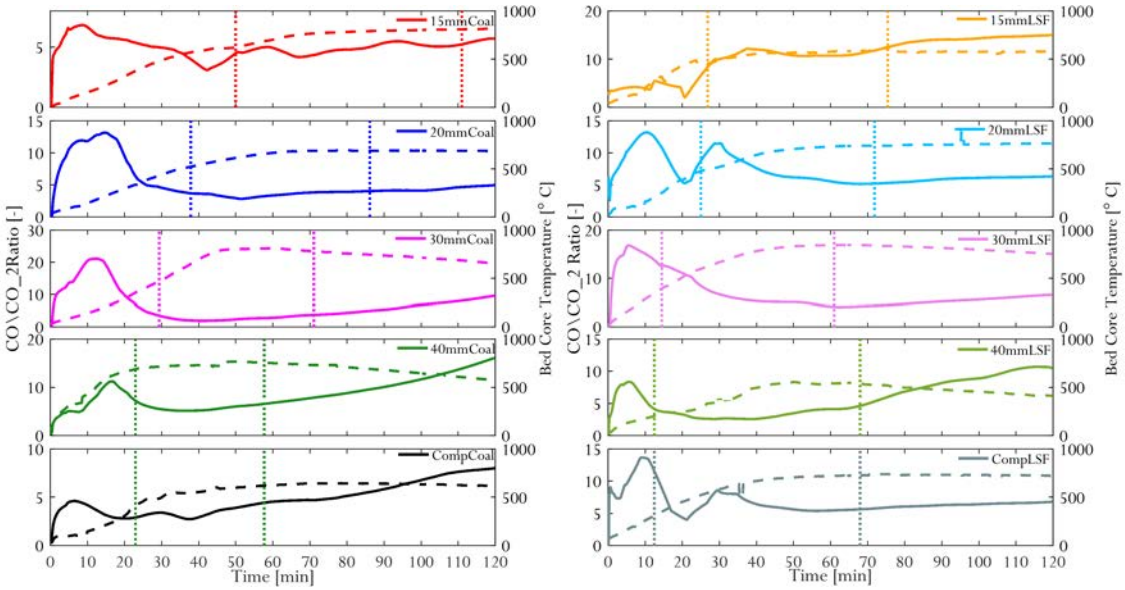

Figure 6.6: **CO\CO$_2$ Ratio.** The ratio of CO to CO$_2$ emitted is shown on the left-hand side axes as a solid line, while the bed core temperature, shown as a dashed line, is on the right-hand side axes.

There is a peak in the ratio of CO\CO$_2$ in the ignition segment, consistent with the ignition process, where the combustion temperatures are low resulting in smoky, inefficient combustion. As the temperature increases, and more of the bed is engaged in the fire, the ratio decreases. All the fuels assume a steady state ratio between 5 and 10 at the start of the cooking segment, where the bed core temperature reaches its maximum. This ratio is maintained throughout the remaninder of experiment. Pemberton-Pigott *et al.* [2009] reports that the ideal ratio of CO to CO$_2$ for efficient combustion is 2, at 5-10, the ratios in Table 6.8, are far outside this prescribed ratio, but are, however, similar to those reported by Masekameni [2015] for an *imbaula*.

Two methods were used to determine the overall combustion efficiency of the fuels, based on the properties of the raw fuel and combustion residue. Overall the coals report higher LOIs than for the LSFs, indicating the the coal residue contains more uncombusted carbon, this is confirmed by the higher calorific values of the coal residue. The higher moisture content, as discussed, has the effect of lowering the combustion temperatures and limitting the efficiency of combustion. For the CompCoal and CompLSF, Kühn [2015] report efficiencies of 69 and 67 % respectively, whereas the results for the same fuels in this study are ~10% higher at 79.8 and 84.9% respectively.

Part of the motivation for this study was to determine if segregating the particle size had an effect

Table 6.8: **The combustion efficiency** as calculated from the LOI as well as using the proximate analysis of the residue.

Fuel	$CO\backslash CO_2$ Ratio	LOI			Proximate Analysis		
		Mass Consumed [kg]	LOI [%]	η_{comb} [%]	Ash *[%]*	Residue GCV *[$MJ.kg^{-1}$]*	η_{comb} [%]
15mmCoal	**5.02**	3.28	31.17	**84.3**	68.8	8.77	**84.4**
20mmCoal	**5.28**	3.36	34.33	**84.4**	66.1	9.72	**85.2**
30mmCoal	**6.58**	3.10	25.57	**87.0**	68.2	9.05	**86.4**
40mmCoal	**5.90**	2.88	22.77	**86.3**	75.4	7.13	**85.8**
CompCoal	**4.85**	3.02	34.38	**79.8**	64.8	9.45	**84.1**
15mmLSF	**10.83**	3.42	27.64	**84.0**	64.6	6.99	**83.5**
20mmLSF	**7.10**	3.00	25.35	**86.5**	70.1	9.07	**86.4**
30mmLSF	**6.97**	2.94	25.86	**84.6**	75.1	7.11	**86.9**
40mmLSF	**8.55**	2.22	33.81	**80.5**	63.0	10.51	**87.5**
CompLSF	**6.75**	3.06	27.58	**84.9**	70.6	8.24	**85.6**

Ash [%] and GCV [$MJ.kg^{-1}$] are given on an air dry basis.
$CO\backslash CO_2$ ratio given is the mean ratio for each burn cycle

on the combuston effeciency of the LSFs. The sample used in the Kühn [2015] study comprised mostly of particles 40 mm and larger, which were not used in this study; comparing the results of the two composite fuels, it can be concluded that lowering the size margin can improve the combustion efficiency. It was reported by Masondo *et al.* [2016], who studied the effect of particle size on the emissions of a typical D-grade coal burnt in an *imbaula*, that the combustion efficiency decreased with an increase in size. Based on these observations, and the decreasing burning rates reported earlier, it was expected that the combustion efficiency would increase as particle size decreased. The results in Table 6.8 do not meet this expectation. Combustion efficiencies, determined by the $CO\backslash CO_2$ ratio or any of the two methods, appear to increase with increasing particle size. It was established based of the work of Zygourakis [2000] and Matzakos [1992], that due to temperature build-up, larger particles will ignite quicker. This improved ignition allows the larger particles to spend more time at higher combustion temperatures. This is especially true for the LSFs which have a higher fuel ratio.

6.2 Pollutant Emissions

One of the major motivators for using a low-smoke fuel as a coal alternative is to decrease the users' exposure the emissions which pose heath risks, and are environmental pollutants. This section will report on the findings from the emissions monitoring during the combustion tests.

6.2.1 NO_x Emission Factors

The emission factors for the release of NO_x are shown in Figure 6.7 and the total emissions are in Table 6.9.

The NO_x emission factors reported in Table 6.9 range between 0.25 and 0.55 $g.MJ^{-1}$, and show

Table 6.9: All Fuels NO_x EF by Task

Fuels	Mass [g] detected				EF [g/MJ]			
	Ignition	*Cooking*	*Heating*	*Overall*	*Ignition*	*Cooking*	*Heating*	*Overall*
15mmCoal	6.41	4.56	1.33	17.58	0.08	0.22	0.22	**0.25**
20mmCoal	4.85	24.67	5.28	40.27	0.39	1.06	0.28	**0.52**
30mmCoal	1.66	16.34	14.24	31.88	0.17	0.68	0.33	**0.32**
40mmLSF	2.73	19.72	14.54	38.35	0.21	0.97	0.36	**0.41**
CompCoal	4.79	23.89	7.21	37.64	0.15	1.05	0.44	**0.40**
15mmLSF	3.89	16.58	10.56	20.97	0.17	0.97	0.36	**0.36**
20mmLSF	2.68	13.99	10.15	26.80	0.12	0.88	0.40	**0.38**
30mmLSF	0.48	8.58	16.27	25.28	0.09	0.76	0.33	**0.33**
40mmLSF	0.84	12.54	21.49	34.12	0.16	1.22	0.60	**0.55**
CompLSF	2.40	16.23	13.02	32.48	0.31	1.00	0.35	**0.40**

no correlation to particle size. These are consistent with the results of Graham [1997] and Graham and Dutkiewicz [1999] who reported an average emissions factor of 0.22 g.MJ^{-1} for the union stove and with those of Makonese [2015] who reported EFs between 0.84 - 0.95 g.MJ^{-1} for an *imbaulas*, while Mitchell *et al.* [2016] reported similar values for a coal (0.2 g.MJ^{-1}) and a "low-smoke coal" (0.29 g.MJ^{-1}) burnt in a fixed-grate stove.

NO_x EFs are influence by fuel nitrogen content, particle size and combustion temperature. The formation mechanisms for NO, the most dominant nitrogen oxide, were discussed in the literature study and it was concluded, that at the temperatures typical of household combustion appliances (<1500°C), the fuel-NO mechanism is the dominant pathway. Thus, NO_x emissions are correlated with the nitrogen content of the fuel which was reported to be ~1.9% for the coals and ~2.2% (d.a.f) for the LSFs. Therefore the different fuels should yield comparable amounts of NO_x and there should be an increase in emissions from the coal to the LSFs. The results in Table 6.9 are consistent with the former statement: the overall amounts of NO_x detected are similar within fuel types, however, only the 15 and 40 mm sized fuels adhere to the latter statement, while while the rest show a decrease in total NO_x emissions from coals to LSF. This may be is a result of the amount of fuel consumed for each fuels, since the more fuel is consumed, the more nitrogen would be available to form NO_x. Table 6.3 shows that, on average, the coals reported higher mass consumption than the LSFs, resulting in the higher NO_x.

The invariant nitrogen content make the fuels ideal to determine the effects of particle size. Wendt [1980] reported that the greater fraction of NO_x comes from volatile-N. Since the rate of the ejection of volatiles from the particle increases with decreasing particles size, it was expeted that the NO_x emissions would follow suit: *i.e.* increase with decreasing particle size. This too is not the case. The LSFs show a steady increase in NO_x emissions with increasing size. A possible explanation for this can be found by considering the combustion efficiency. Higher emissions are an indication of higher combustion efficiency, since the oxidation goes to completion, forming such products as CO_2. SO_2 and NO. The combustion efficiency, shown by the decreasing CO\CO_2 ratio in Table 6.8, is lower for the coal fuels, indicating more complete combustion, and thus more NO_x emission per MJ of energy released. The higher emissions of NO_x correspond with the increasing combustion efficiency. Rogers [1995] made the same

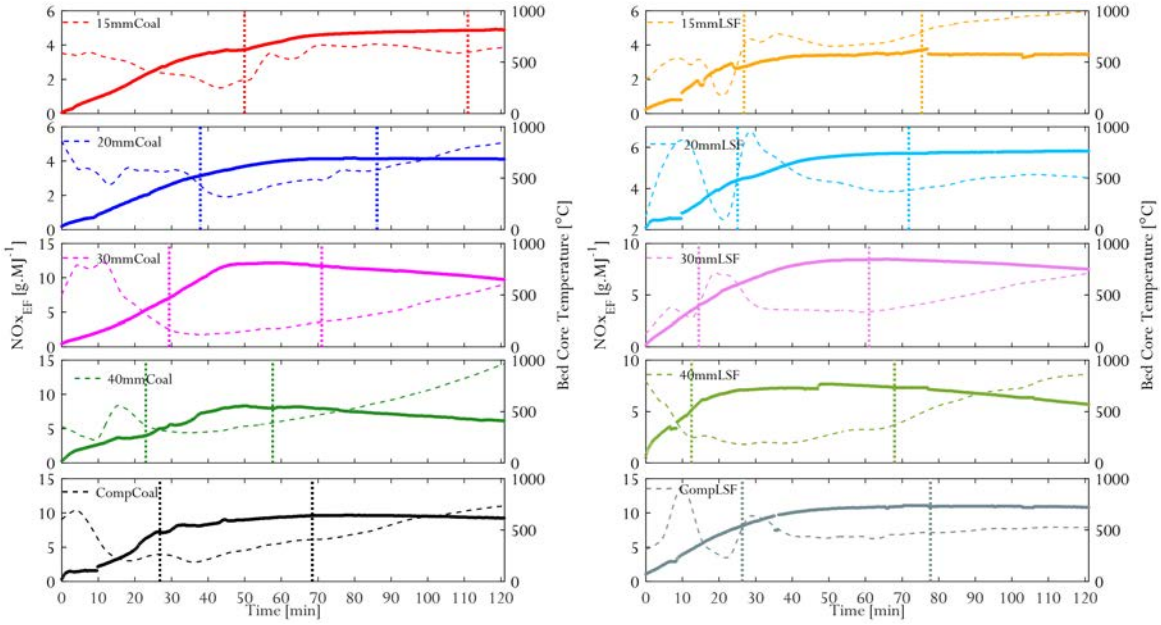

Figure 6.7: **NO_x Emissions Factors.** Time series plots of the NO_x [g/MJ] emission factors. The EFs are shown as the dashed lines against the left-hand side axes and the solid lines along the right-hand side axes are the bed core temperatures.

observation when NO_x during refuelling, characterised by lower fire temperatures and poorer combustion conditions, were lower than the *lighting up* phase of combustion of a community-sourced coal during the Evaton LSF study.

6.2.2 SO_2 Emission Factors

Aside from its direct effects to human health, SO_2 is a known environmental pollutant and is responsible for the formation of acid rain. The emission factors for the SO_2 emissions from all fuels are shown in Table 6.10 and Figure 6.8.

Table 6.10: All Fuels SO_2 EF by Task

Fuels	**Mass [g] detected**				**EF [g/MJ]**			
	Ignition	*Cooking*	*Heating*	*Overall*	*Ignition*	*Cooking*	*Heating*	*Overall*
15mmCoal	21.68	21.25	5.45	77.21	0.32	1.22	0.96	**1.18**
20mmCoal	27.18	76.39	6.84	78.35	2.16	3.04	0.37	**1.01**
30mmCoal	32.89	197.41	188.28	417.44	3.46	8.37	4.32	**4.18**
40mmCoal	14.10	116.69	62.68	182.24	1.09	7.80	2.47	**1.95**
CompCoal	22.31	91.30	33.29	166.31	0.68	4.24	2.03	**1.79**
15mmLSF	17.34	121.53	53.23	237.76	0.74	7.71	4.10	**4.10**
20mmLSF	9.18	84.80	66.13	167.70	0.42	5.26	2.60	**2.39**
30mmLSF	3.18	111.29	136.40	253.92	0.60	9.85	3.21	**3.76**
40mmLSF	2.92	63.39	81.37	150.12	0.57	6.20	2.26	**2.44**
CompLSF	8.21	84.75	64.32	158.76	1.05	5.22	1.75	**1.94**

Similar to the NO_x, the SO_2 emissions can also be linked directly to the sulphur content and the combustion conditions. However, unlike the nitrogen, the sulphur in the LSF can be altered

by the pyrolysis. In Chapter 3, it was found that the sulphur content decreased from coals (1.5-3.0 %, d.a.f) to the LSFs (0.8-2.6%, d.a.f) as a result of the initiation of the reactions of organic and pyritical sulphur at the LSF production temperature. The sulphur content was found to increase with increasing particle size. The larger sized fuels (30 and 40 mm) and the composite fuel results are in agreement with this statement, while the smaller sized fuels show the opposite. The behaviour of the smaller-sized fuel can be explained by consulting the combustion conditions, *i.e.* the LSFs, in both cases, ignite quicker than their coal analogues, and thus have a longer "combustion time" where the sulphur may be oxidised. Rogers [1995] reported similar behaviour for the township coal tested as part of the Evaton LSF study.

An interesting feature shown on Figure 6.8 is the point where the peaks in SO_2 emission occur: at the ignition point for the LSFs and further into the cooking cycle for the coals, with the exception of the 40mmCoal. This, according to Hu *et al.* [2000], gives an indication of the origin of the sulphur that formed the SO_2. The earlier peaks of the LSFs, as well as the CompCoal, 40mmCoal and 30mmCoal are associated with volatile sulphur while the later, less pronounced peaks of the 15mmCoal and 20mmCoal with char-bound sulphur. This could also explain why these two coals recorded lower sulphur values than the others. It also sheds light on the high SO_2 readings for the 30mmCoal, which has both a volatile- and a char-bound sulphur peak.

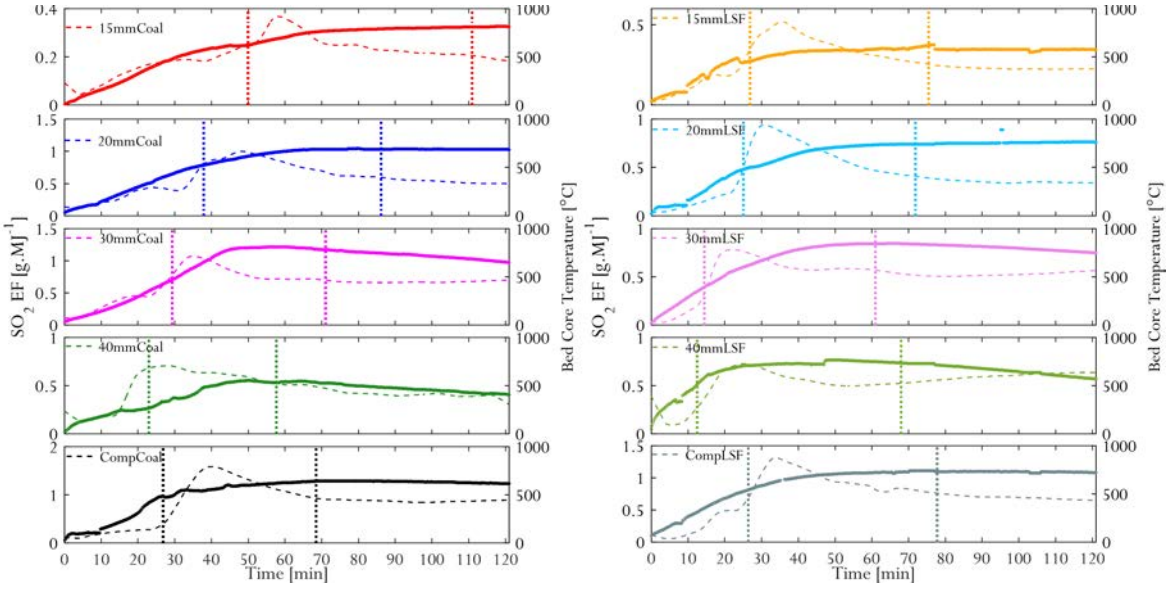

Figure 6.8: **SO_2** Emissions Factors. Time series plots of the SO_2 [g/MJ] emission factors. The EFs are shown as the dashed lines against the left-hand side axes and the solid lines along the right-hand side axes are the bed core temperatures.

6.2.3 CO and CO_2 Emission Factors

The emission factors of CO and CO_2 are not only influenced by the fuel C-content, but by the combustion conditions as well. The relative amounts of these two gases give an indication of the quality of the combustion as discussed. Emission factor plots for CO and CO_2 can be found in Appendix D, while the task-based emissions factors of these gases are shown in Table 6.11.

CO is produced from the incomplete combustion of either the volatiles ejected from the particles during the flaming stages of combustion, or by the combustion of the char in the smouldering

stage. In either case, the CO can be further converted to CO_2 if the conditions allow (See Section 2.4.3) CO emissions for the coals are highest during the ignition segment, which is consistent with the inefficient combustion occurring during this segment. This can be seen clearly in the CO\CO_2 ratios in Figure 6.4. The higher moisture content of the coals, results in low bed temperatures, which causes the increased CO production. The LSFs produce the most CO during the cooking segment, since this is just after the LPG is shut off; it could be that the fuel bed is acclimatising to the absence of the heat source. The reported emission factors, are consistent with those found in the literature [Makonese *et al.*, 2017; Masondo *et al.*, 2016; Mitchell *et al.*, 2016; Makonese, 2015; Graham, 1997]. The stove was operated with the secondary air louvre in the closed position, Mitchell *et al.* [2016] are of the opinion that if the combustion is designed to support secondary inflow of air, then CO emissions can be reduced, especially since the residence time in small combustion devices such as household stoves present a limitation on the CO to CO_2 conversion.

Table 6.11: All Fuels CO and CO_2 Emission Factors

Fuels	**CO2 EF [g/MJ]**				**CO EF [g/MJ]**			
	Ignition	*Cooking*	*Heating*	*Overall*	*Ignition*	*Cooking*	*Heating*	*Overall*
15mmCoal	102.85	188.53	98.10	**98.37**	3.11	5.41	3.71	**3.38**
20mmCoal	150.79	167.22	71.23	**103.24**	6.88	3.39	2.87	**2.72**
30mmCoal	90.04	151.19	94.79	**84.95**	5.89	2.86	3.62	**2.91**
40mmCoal	141.23	252.05	104.14	**106.20**	3.05	8.08	6.89	**5.35**
CompCoal	94.54	189.70	92.45	**93.58**	4.16	3.95	3.57	**3.22**
15mmLSF	94.08	185.28	88.85	**88.85**	1.92	12.86	4.75	**4.75**
20mmLSF	77.17	117.26	119.90	**98.44**	1.72	6.13	4.57	**3.90**
30mmLSF	87.56	174.50	90.52	**88.62**	5.10	5.65	2.84	**3.12**
40mmLSF	106.48	203.48	98.39	**100.52**	2.54	3.91	4.73	**3.44**
CompLSF	62.80	187.81	96.80	**94.94**	6.23	7.31	3.98	**3.73**

Overall, the coals produced more CO_2 than the LSF; this is consistent with the earlier discussion on the CO\$CO_2$ ratio. A cause for the increased CO_2 emission, and thus the lower CO\$CO_2$ ratio, can be found in Figure 6.9, which shows the excess air factor for the different fuels. In the presence of excess air, and sufficient temperatures, the conversion of CO converted to CO_2 is improved. The EA factor for the coals in Figure 6.4 increases during the cooking segment, which enhances the production of CO_2 as seen in Table 6.11.

There is no clear trend of CO_{EF} or CO_{2EF} for either fuel. The total (over the entire burn) emissions in gram, however, does show an increase with particle size. The ultimate analysis in Chapter 3 revealed that the carbon content increased, for both fuels in the order 40mm<Comp/30mm <15mm<20mm: a loose arrangement of decreasing particle size. The arrangement of the total carbon-bearing gases in this order in Table 6.11 support the statement that the CO and CO_2 emission are related directly to the fuel C. Masondo *et al.* [2016] found that a large size difference, *e.g.* from small (20-40 mm) to large sized fuels (60-80mm) showed significant (a threefold increase) in CO_{EF}, while a change from small (20-40 mm) to medium (40-60mm) particles showed no significant increase in the CO_{EF}. This is not strictly true for the results in Table 6.11, where a decrease in CO_{EF} is observed as size increases. This could be due to the

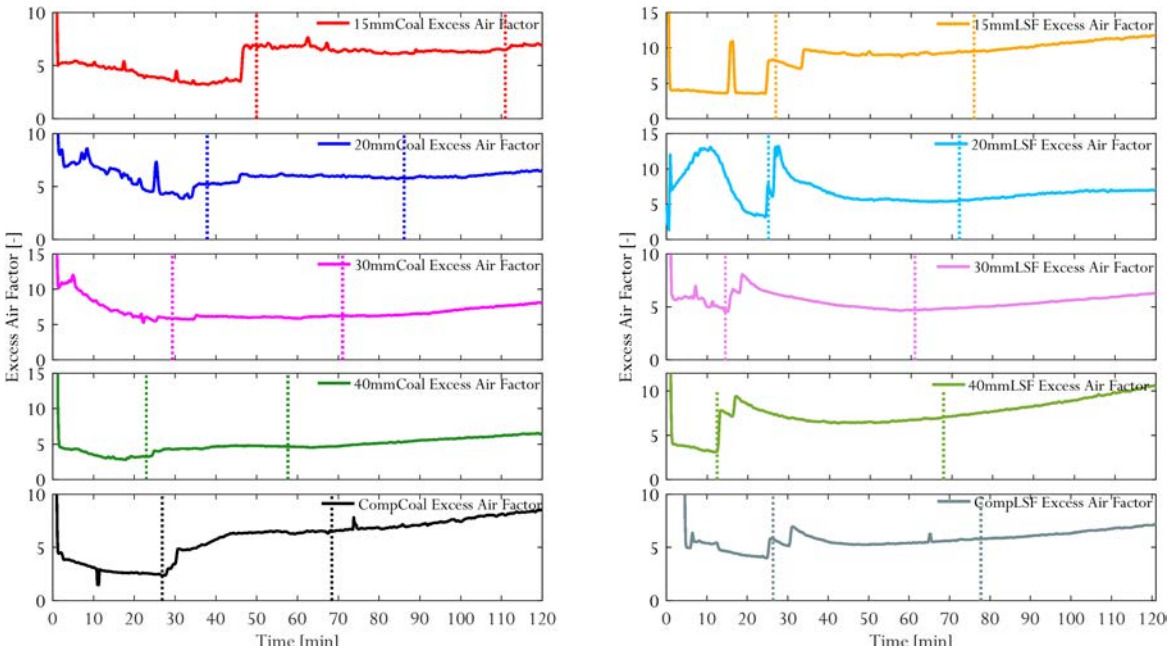

Figure 6.9: All Fuels Excess Air Factor

increase in the energy delivered (See Table 6.5), making the denominator larger, and thus the EF smaller, as size increases. The rise in energy yield, as already discussed is attributed to the faster ignition times.

6.2.4 Particulate Matter Emissions

Many a source apportionment survey [Friedl *et al.*, 2008; Mdluli, 2007; Scorgie *et al.*, 2003, 2001; Sowazi and Maake, 2001] of South Africa's coal-burning communities has revealed that domestic combustion of solid fuels is the highest contributor to local air pollution, accounting for up to 40% of quantifiable PM emissions. It is thus of interest to determine whether the replacement of coal with a LSF will result in a reduction in PM emissions. The time series plots of the PM emission in gram are shown in Figure 6.10 and the emission factors are presesnted in Table 6.12. The time series plots of the PM_{EF} can be found in Appendix D.

As expected, the coals reported higher PM_{EF} than the LSFs: the PM_{EF} for the coals is 2.7 $g.MJ^{-1}$, while that of the LSFs is 0.7 $g.MJ^{-1}$. The recorded values are in agreement with those found in the literature: Graham and Dutkiewicz [1999] reported PM_{EF} of 0.62 and 0.66 $g.MJ^{-1}$ for the Union stove during a cooking and heating procedure respectively, while Makonese *et al.* [2017] reported PM_{EF} between 1.3-2.5 for *imbaulas* with varying ventilation rates.

Kühn *et al.* [2017] noted a decrease of ~80 % in PM emissions when comparing the CompCoal to the CompLSF in their study. A significant drop in PM_{EF} for the same fuels can be seen in Table 6.12. Three out of the five fuels show a decrease in PM_{EF} when the fuel type is changed from coal to LSF. The combined influence of fuel chemical composition, particle size, and combustion conditions are responsible for the differences in PM_{EF} seen in Table 6.12. Li *et al.* [2016] report that the majority of particulate matter forms during the pyrolysis stage of combustion; the early peaks in PM emission seen in the PM emission curves in Figure 6.10

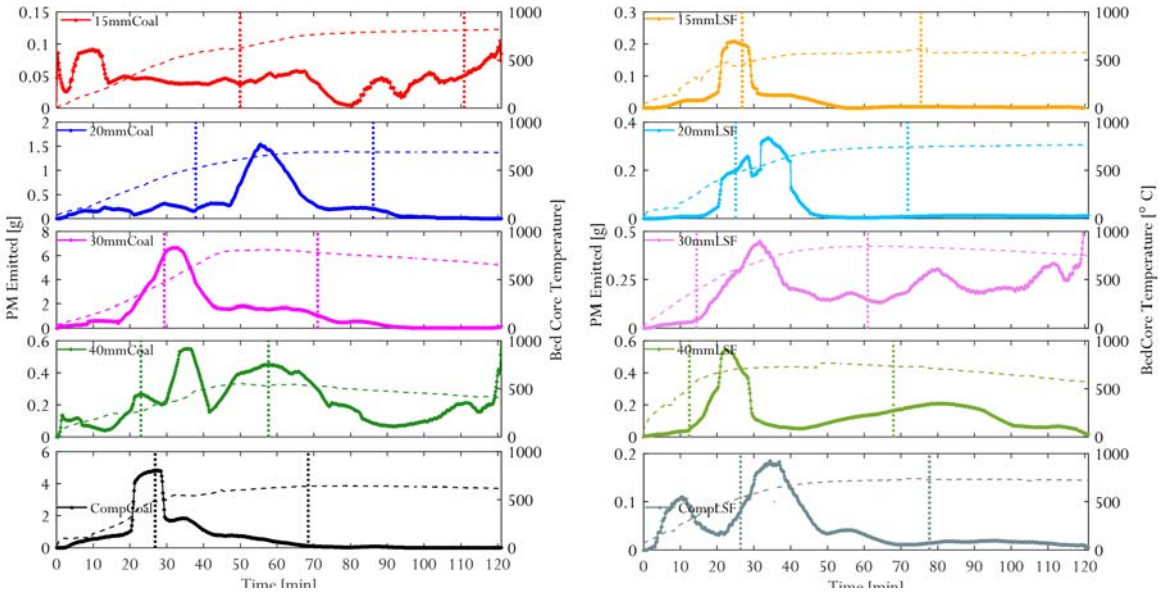

Figure 6.10: **PM Emissions Factors.** Time series plots of the PM [g] emitted. The particle masses per time interval are shown as the dashed lines against the left-hand side axes and the solid lines along the right-hand side axes are the bed core temperatures.

Table 6.12: All Fuels PM EF by Task

Fuels	**Mass [g] detected**				**EF [g/MJ]**			
	Ignition	*Cooking*	*Heating*	*Overall*	*Ignition*	*Cooking*	*Heating*	*Overall*
15mmCoal	14.94	9.23	2.34	26.51	0.37	1.63	1.01	**0.75**
20mmCoal	52.18	193.40	4.41	215.44	4.15	8.40	0.24	**2.79**
30mmCoal	189.48	177.17	31.65	266.57	19.93	8.17	0.73	**2.67**
40mmCoal	49.74	120.92	39.32	184.80	3.86	5.94	0.98	**1.97**
CompCoal	348.11	147.06	8.68	503.85	10.55	4.99	0.53	**5.41**
15mmLSF	13.75	3.72	0.78	15.21	0.58	0.19	0.26	**0.26**
20mmLSF	13.74	14.21	3.31	34.50	0.63	0.79	0.13	**0.49**
30mmLSF	27.47	29.72	44.34	67.54	5.21	2.61	0.90	**0.88**
40mmLSF	2.28	62.50	44.83	116.40	0.44	6.63	1.24	**1.89**
CompLSF	8.16	15.65	3.37	24.46	1.04	0.32	0.09	**0.10**

confirm this. This, the authors state, is why the size of the particle and the volatile matter play a role in the PM emissions. The higher the volatile matter content, the higher the PM emission since more volatiles are available for PM formation. As volatiles escape the pyrolysis particle, they increase the porosity of the particle, which further facilitates the ejection of more volatiles. Once outside the particle, the volatiles may be consumed by a flame where they are oxidised in the temperature and oxygen supply allow. However, household combustion devices are notorious for low temperatures and short residence times, such that the combustion of volatile matter are almost always incomplete. As discussed in Chapter 2, partially combusted organic matter is the precursor to organic PM via agglomeration and coalescence. It can thus be concluded that fuels with higher volatile matter, such as the coals in our study, will contribute to the organic component of PM emissions.

The PM_{EF} is reported by Li *et al.* [2016] and Ninomiya *et al.* [2004], to decrease with increasing

particle size. This is true of the results in Table 6.12, with the exception of the 15mmCoal and 40mmLSF. As particle size increases, the amount of excluded minerals also decrease [Lui *et al.*, 2007; Ninomiya *et al.*, 2004], leaving the particle rich in included minerals which are more prone to PM formation via fragmentation. With relation to volatile matter, the larger particles hinder the ejection of VM, thus reducing the change of the VM going unreacted. From the discussion of mineral interactions, it is clear that the ash yield of the fuel also plays a role in PM emissions. Li *et al.* [2016] tested the effect of mineral additive on PM emissions from high volatile coals and found that minerals hinder the escape of volatiles from the particle via adsorption and reducing diffusivity. Since the ash yield, which can be used as a proxy for mineral matter, was found to increase slightly from coal to LSFs and to increase in the order of 20mm/30mm<40mm<15mm for both fuels, the PM_{EF} should follow the opposite pattern: *i.e.* decrease with increasing ash content. This is true for the coal fuels.

Since the ash content of a fuel can be controlled by using such means as density separation, the particle size can be similarly controlled via screening, and volatile matter content can be controlled by devolatilisation, it follows that, similar to the sulphur related emission, PM emission lends itself to reduction via fuel selection and pre-treatment.

6.2.5 Emission of Volatile Organic Compounds

Volatile organic components, like all the other products of incomplete combustion, are most dominant when the combustion conditions are not conducive to complete oxidation. Furthermore, partially combusted organic species, as previously discussed, are precursors to particulate emissions. In this study, VOC emissions were captured using activated carbon tubes, which were then analysed for a wide range of compounds, the complete list can be found in Appendix D. Figure 6.11 shows the relative amounts of each compound for each fuel and Table 6.13 shows the computed emission factors.

Table 6.13: All Fuels VOC Emission Factors

Fuel	**Total VOC [mg.m^{-3}]**	**Mass Burnt [kg]**	**Stack gas m^{-3}.kg^{-1}**	**Total VOC mg**	**Energy Yiled MJ**	**Total VOC g.MJ^{-1}**
15mmCoal	402.07	1.60	8.17	5 244.29	55.6	**94.33**
20mmCoal	51.64	2.91	8.18	1 230.96	76.7	**16.05**
30mmCoal	1 915.28	3.29	8.08	50 995.16	98.58	**517.31**
40mmCoal	27.90	3.11	8.31	721.61	93.64	**7.71**
CompCoal	54.51	4.27	8.14	1 893.52	99.47	**19.04**
15mmLSF	20.00	2.77	8.50	470.50	72.82	**6.46**
20mmLSF	22.59	2.48	8.71	487.34	73.03	**6.67**
30mmLSF	444.26	3.48	8.24	12 737.65	77.53	**164.30**
40mmLSF	17.15	2.41	8.62	356.68	61.62	**5.79**
CompLSF	27.90	2.94	8.50	697.64	81.73	**8.54**

With the exception of the 30 mm sized fuels, VOC_{EF} decreases from the coal fuels to the LSFs and also decreases with increasing particle size. The effect of volatile yield and particle size with regards to the quantity and rate of volatile ejection was discussed and holds for the results

in Table 6.13: the coal, with the higher volatile content report higher VOC_{EF}, and the larger particles, which are associated with impeded volatile ejection, report significantly lower VOC_{EF}. Kühn *et al.* [2017] reported a ~90 % reduction in VOCs from the CompCoal and CompLSF in their study. The reduction in this study is 45 % for the same fuels. Similar to the Kühn [2015] study benzene, toluene, and xylene are the major species detected.

Reaction chemistry and turbulence are, according to Gulyurtlu *et al.* [2004], the most important parameters in controlling the emission of VOCs. Higher combustion temperatures facilitate faster oxidation reactions, reducing the VOC emissions. Overall, the LFS achieved higher combustion temperatures (see Figure 6.1), and, as a result of the quicker ignition, increased the residence time at those hight temperature, improving the possibility for complete combustion of volatile species. Domestic combustion devices, unlike their industrial counterparts, are usually small and not designed for optimum turbulence inside the chamber. This factor, as stated by Gulyurtlu *et al.* [2004], reduces contact time between the freshly ejected volatiles and the air, lessening the possibility for reaction.

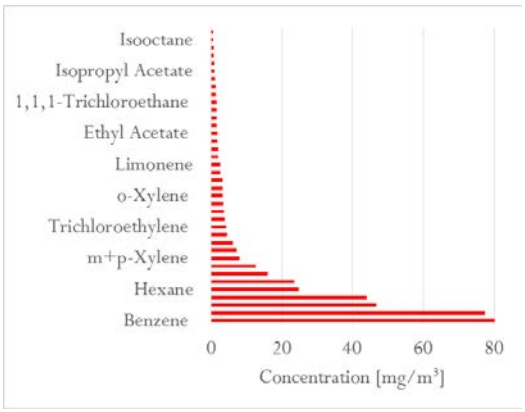

(a) 15mmCoal

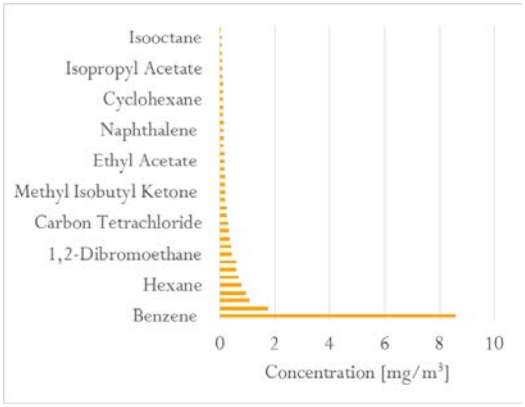

(b) 15mmLSF

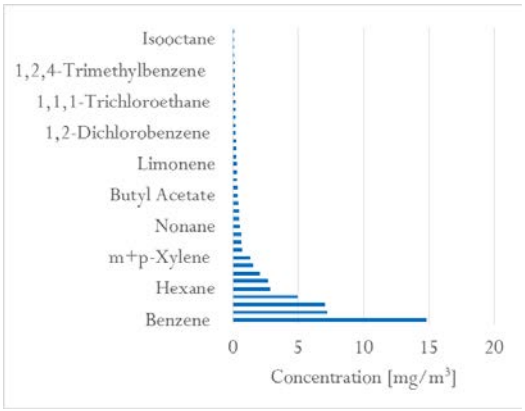

(c) 20mmCoal

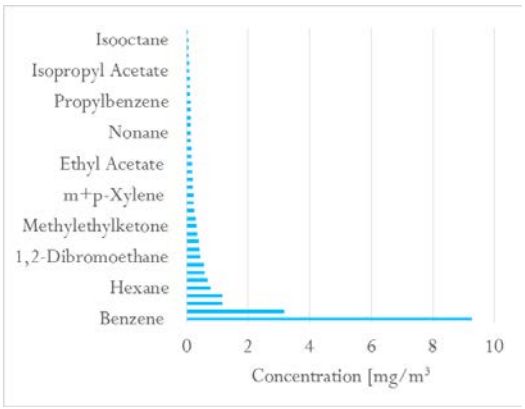

(d) 20mmLSF

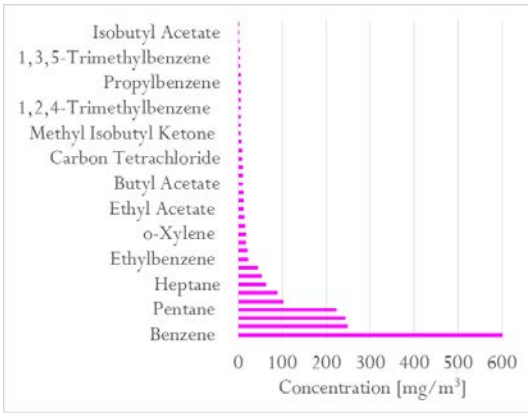

(e) 30mmCoal

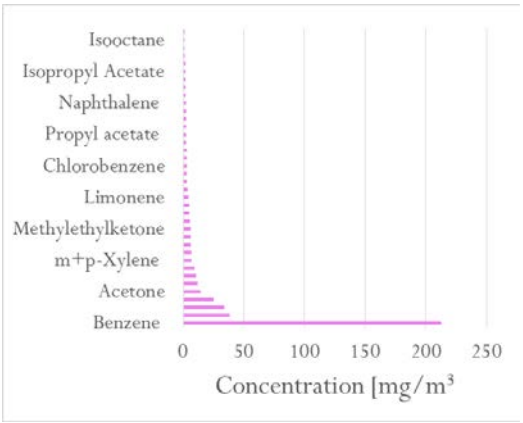

(f) 30mmLSF

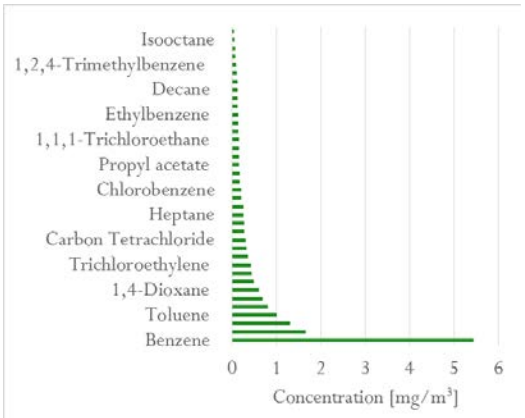

(g) 40mmCoal

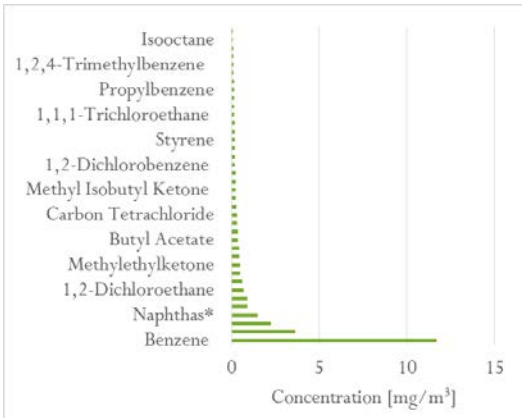

(h) 40mmLSF

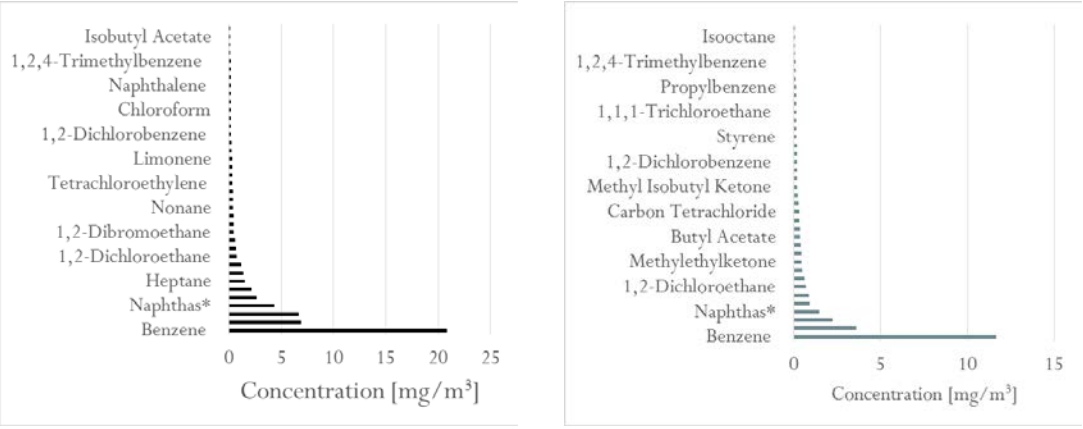

(i) CompCoal (j) CompLSF

Figure 6.11: All Fuels VOC Emission Concentrations

6.3 Summary

This chapter reported the result of the combustion tests in order to determine what effect particle size has on a set of performance metrics used to evaluate the performance of a LSF in a conventional household stove. A known amount of raw fuel (coal of LSF) in a fixed size was batch loaded into the stove and ignited using LPG at a known flow rate. The temperature at the core of the fuel bed was monitored and used as an indicator for the ignition point of the coal. 500 °C was used, based on previous work and a single particle TGA study of the fuels, to be the cut-off point for ignition. A water boiling procedure, along with *in situ* measurement of fuel consumption formed the basis for the evaluation of the thermal performance of each fuel, while real-time monitoring of the gaseous and particulate matter was used to characterise the pollutant emissions.

LSFs reported shorter ignition time compared to their coal counterparts. A decrease in ignition time with increasing particle size was also observed. The shorter ignition times for larger particles can be accounted for by considering the heat transfer limitations experienced in the larger particles, causing an increase in internal temperature which may cause ignition to occur faster. Ignition in the stove may be better understood and assessed if the influence of the LPG, which was found to enhance already present particle size effects, is removed by igniting the fuel bed in the conventional wood-and-paper manner.

Water boiling times were not significantly affected by a change in particle size, but responded to the change in fuel burning rate, which were found to increase with decreasing particle size and were found to be higher for the coals. Cooking times did not differ significantly between fuels, however the LSFs are thought to have benefited from the quick ignition, aided by the LPF.

The thermal efficiency, *i.e.* the ratio of the energy used to heat the water to that released from the fuel decreased with increasing particle size, and were lower for the LSFs than for the coals. Combustion efficiency, on the basis of the LOI and residues proximate analysis were not significantly different between fuels and tended to increase, counter intuitively, with increasing particle size. It was thought that the improved ignition, combined with the higher fuel ratios, may play a role in the improved combustion of the LSFs. The mass consumption rates and ease

of ignition were found to be the most influential as far as thermal performance was concerned.

Along with combustion conditions, the properties of the fuels were found to play a role in the emission of NO_x, SO_2, PM and VOC, while particle size played a role at a mechanistic level. NO_x emissions were found to be higher for the coals than for the LSFs, owing to the increased fuel consumption. In agreement with the combustion efficiency, emissions of SO_2 were found to be higher for the LFS, and increasing with increasing particle size, the combustion temperature history was found to play a role. CO and CO_2 emissions were found to be consistent with the combustion efficiency. PM emissions were found to be highest during the ignition segment, were the fuels are undergoing pyrolysis, and where volatile ejection is highest. The combustion conditions were such that the ejected volatiles were not oxidised. For the coals, this translated into higher CO and PM emissions during the ignition segment. PM emissions were found to be consistent with theory: increasing with increasing volatile yield and decreasing with increasing particle size and ash content. Substantial reductions in VOC emissions were found for the majority of the fuels.

From a performance point of view, larger particles were better suited as these particles ignited quickly and achieved high combustion temperatures which led to higher combustion efficiency. With regards to emissions, only SO_2, PM and VOC emissions can be controlled by particle size screening and devolatilisation. Sulphur reduction via pyrolysis plays an important role in reducing the SO_2 emissions, and smaller particles are better equipped for successful devolatilisation due to the absence of diffusion limitations. However, for the reduction of PM and VOC, which have been linked to adverse environmental conditions and some cancers, larger particles have a natural tendency to lower emissions of PM and VOCs.

Chapter 7

Conclusions and Recommendations

This chapter will summarise the main findings of the study by pointing out the effect of particle size on the thermal performance and pollutant emissions from LSFs combusted in a typical coal-burning household stove. Furthermore, recommendations of how outstanding issues can be addressed by further studies will be discussed.

7.1 Summary of Findings

The copious epidemiological studies in the literature have linked the use of solid fuels in low-income households, especially in developing countries, and the adverse effects on the health of the user and the environment. Lower birth rates, and over 4.3 million premature fatalities per year are attributed to the sustained exposure to the pollutants from solid fuel combustion. HAP has also been linked to various debilitating diseases, such as cancer. The concerns over climate change and the anthropogenic contributions are opening up a new arena for research into the use of fossil fuels in industry as well as in the home. The latter subject has been explored in the South African context since the 1960s and significant strides were made in the early 1990s where government undertook policies to limit the use of solid fuels as a response to the overwhelming cost in healthcare associated with it; *i.e.* the nationwide electrification of urban areas undertaken along with various other initiative by NGOs. Also in this period, the introduction of an alternative fuel, a low-smoke coal-derived fuel, to replace the coal in households was undertaken under the DME's Low smoke Fuels Programme. While a significant amount of progress was made in (1) identifying the optimal production method (devolatilisation of coal), and (2) developing of LSF evaluation procedure, and (3) identifying key role players in a community wide pilot study that spanned two years on 1995 and 1996, little has been done since to produce a technically viable low-smoke fuel with the intent for use in the current combustion devices found in homes. The reports from the DME campaign were lean on details regarding the overall performance of the fuel/stove combination, in terms of heat transfer- and combustion efficiencies, focussing only the emissions of SO_2 and particulates.

The systemic evaluation of the thermal performance and emissions from fixed bed household solid combustion devices has been limited to *imbaulas*, with recent improvements in the reporting

of different types of *imbaulas*. Work on cast iron stoves, even though this type of device has been found in abundance in coal-burning households have been relatively scarce. There is thus a need for an alternative to coal as a solution to the health problems posed by HAP, further investigations into the production of such a fuel and the evaluation of its performance in typical household appliances as a function of its properties, particle size being one of the properties of interest. The aim of this study was to determine, through a systemic testing schedule, the effect of the fuel particle size on the fuel's performance in a conventional cast iron stove.

7.1.1 Production and Characterisation of Low-smoke Fuels

Devolatilisation has been found to be the optimum method for producing a coal-based LSF. This method was used to produce five LSFs of varying particle sizes (15, 20, 30, 40 mm and a composite of the four sizes) by devolatilisation at 550 °C. The resultant fuels, as well as a set of analogous untreated coal fuels were subjected to conventional characterisation analyses. TGA pyrolysis and combustion experiments were used to determine the approximate mass loss to be expected at the production temperature, as well as the combustion properties such as ignition time, combustion rates and burnout times.

Conventional Characteristics

The bulk sample, acquired from a typical coal-burning community was size screened to produce the various sizes for the LSF production, The particle size distribution was found to range between 10-40 mm, the majority of which were the 30 mm (or -37.5 +26.5 mm) fraction.

The raw coal fuels were found to be of high ash (23.4-26.8 %, a.d), medium to high volatile content (23.9-28.5 % a.d), akin to Highveld coals. Ash content tended to increase with increasing particle size. The ash of the LSF did not differ significantly from the coals, ranging between 25.8 - 33.3 %, a.d, and showing a slight positive correlation to increasing particle size. The volatile matter was greatly reduced, an artefact of devolatilisation, from ~24 % a.d. of the coals to an average value of 10.3 % for the LSFs. Since particle size affects the behaviour of the coal during pyrolysis, *i.e.* volatile ejection is hindered in larger particles, there was a stronger correlation with particle size for the volatile matter of the LSFs. The result was that the fuel ratio increased from the coals to the LSFs.

The Ultimate analysis of the two fuels did not show significant variation in nitrogen content, and showed only a decrease in hydrogen content from coals (~4.2 % d.a.f) to the LSFs (~2.2 % d.a.f). Sulphur reduction from coals (~1.9 % d.a.f) to the LSFs (1.5 % d.a.f) was consistent with the reactions of pyritical sulphur at the LSF production temperature.

Calorific values of the fuels did not differ significantly, with both fuels reporting an average CV of 22.5 $MJ.kg-1$.

Based on these analyses, it was concluded that the fuels were similar enough in properties so that any variances in combustion performance would be due to the difference in particle size and combustion conditions.

Thermogravimetric Analyses

Further characterisation of the fuels was done using thermogravimetry. Single particle studies in the TGA were done to determine the combustion characteristics of the fuels and to create a benchmark for the thermal assessment of the fuels. Ignition times were found to vary between 36 and 40 minutes for the coals, and decreasing with increasing particle size, while those of the LSFs were found to be >40 minutes. This was consistent with the increased fuel ratio and diminished volatile matter content of the latter fuels. Ignition temperatures were sought in order to evaluate the cut-off point to be used in the combustion tests. Results were consistent with theory: ignition temperatures were correlated with volatile matter content and were higher for the LSFs (~500 °C) than for the coals (~425 °C). No distinct trend could be drawn between the ignition temperatures and particle size. Peak burn rates were found to be higher for the coals, ranging between 0.7 - 1.2 %,min^{-1}, than for the LSFs, which averaged just 0.6 %,min^{-1} and decreased with increasing particle size. Upon reaching the target temperature, 1000 °C, the fuels had not yet reached burnout, only doing so two hours after reaching the target temperature, however further decreases in mass from this point was less than it had been leading up to that point.

The ignition cut-off time was kept at 500 °C and the test length at 2 hours, as these parameters were used in previous work and showed that the emissions and performance metrics had reached their peaks within this time.

7.1.2 Combustion Testing of LSFs

Following the production and characterisation of the fuels, as well as the single particle study, done to inform experimental practices, a series of combustion tests was undertaken in order to assess the effect of fuel particle size on the performance of a LSF in a conventional coal stove.

Thermal Performance

Thermal performance metrics included the ignition and water boiling time, as well as the power output and heat transfer efficiencies. Ignition times, contrary to the prediction of the single particle study were lower for the LSFs than for the coals, and were found to decrease with increasing particle size. An increase from 15 mm LSF to 40 mm LSF resulted in an ignition time reduction of 14 minutes (or 53 %), which was similar to the difference between the ignition time of the 40mmCoal (23 minutes) and the 40mmLSF (13 minutes). The combined time taken to boil the two batches of 2 L water is referred to as the cooking time. Cooking time did not differ significantly between fuels, with both fuels reporting cooking times in the region of 48 minutes. Single boiling times, especially for the second batch of water was found to decrease from the coals (~24 min) to the LSFs (20 min) and decreasing with fuel particle size. The observations with regards to the ignition and boiling times, may be a result of the interaction between two factors: (1) the larger particles' inability to eject volatiles quickly, thus increasing internal temperature of the particle and, (2) the increased porosity which improves the absorption of oxygen, further increasing the temperature on the inside of the particle. Power output is an all-encompassing

metric that takes into account both the burning rate of the fuels, as well as the energy liberated. The majority of the coal fuels reported power outputs over 10 kW, while the LSFs reported power output ranging between 8.5-10.7 kW. This was found to be consistent with the increased burning rates of the coals.

The system efficiency, which measured the ratio of usable heat delivered to heat yielded from the combustion, did not show any dependence on fuel type or particle, confirming the notion that the heat transfer metrics are more an assessment of the stove than the fuel within. The system efficiency was 66.4 % for the coals and 65.8 % for the LSFs and no trends between the individual efficiencies and particle size were noticed. The thermal efficiency, measuring the energy utilised was higher for the coals than for the LSFs, however it is thought that the exclusion of evaporation losses led to this anomalous result. The coal fuels reported the highest energy losses through evaporation, and thus the reported cooking efficiencies are artificially high. Heating efficiencies were found to be similar to the system efficiency, this is expected since larger devices are better adapted to space heating than cooking. Slight increases in heating efficiency with increasing particle size were observed.

The combustion efficiency was found to be a better gauge of the fuels' performance. The CO\CO$_2$ ratio did not differ significantly between fuels: the coals reported CO\CO$_2$ ratios between 4.9-5.3, while the LSFs' CO\CO$_2$ ratios ranged from 6.7-10.8, indicating lower combustion efficiencies for the LSFs. The combustion efficiency determined via the residue proximate analyses showed the opposite, *i.e.* efficiency of the LSFs was higher than for the coals and tended to increase with increasing particle size. An increase in size from 15mmLSF to 40mmLSF increased the combustion efficiency by 4 %, while changing the fuel type from 40mmCoal to 40mmLSF only achieved an increase of 2 %.

Pollutant Emission

Emissions were found to only depend on particle size on a mechanistic level; this was especially true for the emissions of SO_2, PM and VOCs. All three metrics are related to the fuel's mineral matter composition. Theoretically SO_2 emissions are reduced when the particle size decreases as the included mineral matter content increases, thus increasing the probability for sulphur capture via mineral interactions, however this was not the case in this study. SO_2 emissions were found to be better correlated with fuel sulphur content and combustion efficiency. As the combustion efficiency increased, which, according to the CO\CO$_2$ ratio, decreased with increasing particle size, so did the SO_2 emissions. As a product of complete combustion it is expected that SO_2 emissions increase with increasing combustion efficiency. PM and VOC emissions were found to decrease from coal to LSF, and were inversely correlated to particle size. The combined effect of changing the fuel type from coal to LSF, and segregating the particle sizes saw a reduction in PM from 5.41 g.MJ^{-1} for the CompCoal to to just 1.89 g.MJ^{-1} for the 40mmLSF. VOC emissions, were found to decrease from coals to LSFS, coinciding with a decrease in volatile matter content, and with increasing particle size.

All the metrics discussed are dependant of the combustion conditions in some manner, for example, adding a secondary airflow will increase the combustion efficiency, therby decreasing

the amount of PM, VOCs and CO emitted while increasing the combustion temperature and rate, which will benefit the performance of the fuel-stove system. Furthermore, only the emissions of PM, VOC, SO_2 lend themselves to control via fuel size selection and pre-treatment as particle size affects these on a mechanistic level. It is concluded that the larger particles are better suited for LSF production if the production method is adjusted to accommodate the pyrolysis limitations of larger particles. However, handling and transport of large volatilised particles may be problematic as chars are prone to fragmentation. Furthermore, mineral additives, *e.g.* via impregnation, should be considered as an added feature to limit the emission of SO_2 even at high efficiencies.

7.2 Conclusions and Significance

This study systematically evaluated the effect of particle size on the thermal performance and emission of a coal-derived low–smoke fuel in a typical household stove. There has been a lot of progress in building an inventory of the performance and emissions in a South African context, however most of the work has been limited to *imbaulas*. This work contributes to that inventory by introduction of a different, yet still common combustion device. It has been confirmed that results from the *imbaula* cannot be used as a proxy for cast iron stoves as combustion environment, *i.e.* airflow and ventilation, and the way in which the fire is tended differ.

Low-smoke fuels have not been considered a viable replacement for coal since the last of the work done under the low-smoke fuels programme elapsed. It has been shown here that a devolatilised coal, can perform tasks with comparable efficiency to raw coal while significantly reducing the emissions. Successful validation of the LSFs can lead to their inclusion in the country's energy landscape.

Insight into the combustion environment in this type of stove, as well as how this environment applies to low-smoke fuels, has been gained. These insights can be used: (1)in the development of improved combustion technology, (2) as well as part of intervention policies to reduce the adverse effects of solid fuel use in low-income households.

7.3 Recommendations for Further Work

- **Other Combustion devices.** The experiments conducted as part of this study were focused on cast iron stoves. While this presented a niche in the field, it is suggested that further work consider the inclusion of other combustion technologies, such as *imbaulas* and artisan stoves in conjunction with the low-smoke fuels.
- **Ignition methods.** In this study LPG was used as a repeatable lighting method with the gas was provided at the bottom of the bed in order to simulate the bottom-lit method of fire ignition. The interactions of this ignition LPG and the fuel bed may lend themselves to further study in order to better understand the effect of using LPG as a lighter fuel on the performance and emissions during combustion as explored in this study. Alternative fire lighting methods, *e.g.* the top-lit lighting method, which have been shown to reduce

emissions in *imbaulas* can be applied to cast iron stoves, using regular coal and low-smoke fuels. It is important to note that this study does not suggest that LPG should be adopted, along with the LSFs, as a household ignition fuel due to cost and was used merely as means to ensure repeatability of the ignition stage for all experiments.

- **Fuel Properties.** In attempting to isolate the particle size, the work inadvertently striated the particle properties in terms of mineral matter. An effort should be made in future to use a more homogenised sample in order to limit the variation of results that are not associated with the particle size. The EF factors for sulphur were found to have large variations between fuel types and sizes. A sulphur balance, based on the sulphur content as determined using the ISO 19579 standard, between the raw fuels and residue was attempted but yielded no insight into possible reasons for this variation. A homogenised sample will also help in reducing uncertainties rising form sampling for analysis and from the combustion tests themselves.
- **Development of improved combustion devices.** It was noted during the study that any small improvement in the combustion conditions can improve the overall performance of the fuel-stove system. Apart from the hand-made artisan stoves, there has not been any new technology entering the market targeted at low-income households who use coal, even less so with the intention of reducing emissions and improving performance.
- **Field trails.** One of the lessons from the Evaton/Qalabotjah pilots was the importance of validating lab results in field trials. It is thus recommended that the low-smoke fuel be produced in bulk for field trials which will add user behaviour, and impressions, which should be replicated for in a lab set-up, to the assessment metrics.

Bibliography

Agee, J.,1996. *Fire Ecology of Pacific Northwest Forests*, Island Press, Washington D.C.

Ahuja, D., Joshi, V., Smith, K. and Venkataraman, C.,1987. 'Thermal Performance and Emissions Characteristics of Unvented Biomass-burning Cookstoves: A Proposed Standard for Evaluation', *Biomass* **12**, 247–270.

Anthony, D., Howard, J., Hottel, H. and Meissner, H.,1976. 'Rapid Devolatisation and Hydrogasification of Bituminous Coal', *Fuel* **55**(2), 121–128.

Arora, P. and Jain, S.,2016. 'A Review of Chronological Developments in Cookstove Assessment Methods: Challenges and Way Forward', *Renewable and Sustainable Energy Reviews* **55**, 203–220.

Asamoah, J., Lloyd, P., Hoets, P. and Grobbelaar, C.,1998. 'Low-smoke Fuel Programme: Preliminary Results of the Macro-scale Experiment', *Clean Air Journal* **10**(1), 19–22.

Bailis, R., Ogle, D., MacCarty, N., Still, D., Edwards, R. and Smith, K.,2007. The Water Boiling Test Version 3.0: Cookstove Emissions and Efficiency in a Controlled Laboratory., Technical report, University of California, Berkely.

Baldwin, S.,1987. Biomass Stoves: Engineering Design, Development, and Dissemination, Technical report, Volunteers in Texchnical Assistance (VITA), Arlington, VA.

Ballard-Tremeer, G. and Jawurek, H.,1996. 'Comparison of Five Rural, Wood-burning Cooking Devices: Efficiencies and Emissions', *Biomass and Bioenergy* **11**(5), 419–430.

Ballard-Tremeer, G. and Jawurek, H.,1999a. 'The "Hood Method" of Measuring Emissions of Rural Cooking Devices', *Biomass and Bioenergy* **16**, 341–345.

Ballard-Tremeer, G. and Jawurek, H.,1999b. 'Evaluation of the Dilution Chamber Method for Measuring Emissions of Cooking Stoves', *Biomass and Bioenergy* **17**, 481–494.

Balmer, M.,2007. 'Household Coal-use in an Urban Township in South Africa', *Journal of Energy in Southern Africa* **18**(3), 27 – 32.

Barnes, B., Mathee, A., Thomas, E. and Nigel, B.,2009. 'Household Energy, Indoor Air Pollution and Child Respiratory Health in South Africa', *Journal of Energy in Southern African* **20**(1), 4 – 13.

Basu, P.,2006. *Combustion and Gasification in Fluidised Beds*, CRC Press.

Baxter, L., Mitchell, R., Fletcher, T. and R.H., H.,1996. 'Nitrogen Realease during Coal Combustion', *Energy and Fuels* **10**(1), 188–196.

Benfell, K.,2001. Assessment of Char Morphology in High Pressure Pyrolysis and Combustion., PhD Thesis, University of Newcastle.

Beukman, M.,2009. Coal Pyrolysis Modelling and the Influence of Pyrolysis Conditions on Char Reactivity for Large Particles, Master's thesis, North West Univeristy, South Africa.

Bhatia, S. and Perlmutter,1980. 'A Random Pore Model for Fluid-solid Reaction: Isothermal, Kinetic Control', *American Institute of Chemical Engineering Journal* **26**(3), 379–385.

Bi, X., Simoneit, B. R., Sheng, G. and Fu, J.,2008. 'Characterization of Molecular Markers in Smoke from Residential Coal Combustion in China', *Fuel* **87**(1), 112 – 119.

Bockhorn, H.,2000. Soot Formation and Oxidation, *in* 'Pollutants from Combustion: Formation and Impacts on Atmospheric Chemistry', NATO Science Series C: Mathematical and Physical Sciences, Wiley, chapter 11, pp. 205–240.

Bond, T., Thompson, R., Sherman, D., Naleid, M. and Chiang, R.,2014. The Water Boiling Test version 4.2.3: Cookstove Emissions and Efficiency in a Controlled Laboratory Setting, Technical report, University of California, Berkely.

Borah, D., Barau, M. and Baruah, M.,2005. 'Dependence of Pyrite Concentration on Kinetics and Thermodynamics of Coal Pyrolysis in Non-isothermal Systems', *Fuel Processing Technology* **86**, 977–993.

Bowman, C.,2000. Gas-phase Reaction Mechanism for Nitrogen Oxide Formation and Removal in Combustion, *in* 'Pollutants from Combustion: Formation and Impact on Atmospheric Chemistry', Vol. 547 of *NATO Science Series C: Mathematical and Physical Sciences*, Springer, Netherlands:Dordrecht, chapter 7, pp. 123–144.

Bruce, N., Pope, D., Rehfuess, E., Balakrishnan, K., Adair-Rohani, H. and Dora, C.,2015. 'WHO Indoor Air Quality Guidelines on Household Fuel Combustion: Strategy Implications of New Evidence on Interventions and Exposure–risk Functions', *Atmospheric Environment* **106**, 451 – 457.

Buhre, B., Hinkley, J., Gupta, R., Nelson, P. and Wall, T.,2006. 'Fine Ash Formation during Combustion of Pulverised Coal: Coal Property Impacts', *Fuel* **85**, 185–193.

Bureau of Technical Support Beijing,2017. 'General Specifications for Biomass Household Stoves - China', available online at `http://cleancookstoves.org/binary-data/DOCUMENT/file/000/000/77-1.pdf` Accessed 31 July 2017.

Bussmann, P.,1988. Woodstoves: Theory and Application in Developing Countries, PhD Thesis, Eindhoven University of Technology, The Netherlands.

Butcher, S., Rao, U., Smith, K., Osborn, J., Azuma, P. and Fields, H.,1984. Emission Factors and Efficiencies for Small-scale Open Biomass Combstion: Toward Standard Measurement Techniques, *in* 'Preprints of Symposia, Division of Fuel Chemistry', Vol. 29, American Chemical Scociety, Washiongton DC, p. 122.

Button, S.,2010. The Fate of Sulphur during Pyrolysis and Steam Gassification of High-sulphur South Australian Low-rank Coals, PhD thesis, University of Adelaide, Australia.

Cai, H., Guell, A., Chatzakis, I., Lim, T., Dugwell, D. and Kandiyoti, R.,1996. 'Combustion Reactivity and Morphological Change in Coal Chars: Effect of Pyrolysis Temperature, Heating Rate and Pressure', *Fuel* **75**(1), 15–24.

Cairncross, B.,1989. 'Paleodepositional Environments and Tectonosedimentary Controls of the Postglacial Permian Coals, Karoo Basin, South Africa', *International Journal of Coal Geology* **12**(1), 365 – 380.

Calkins, W. H.,1994. 'The Chemical Forms of Sulfur in Coal: A Review', *Fuel* **73**(4), 475–484.

Chagger, H., Jones, J., Pourkashanian, M., Williams, A., Owens, A. and Fynes, G.,1999. 'Emission of Volatile Organic Compounds from Coal Combustion', *Fuel* **78**, 1527–1538.

Chen, B., Li, B., Yang, J. and Zhang, B.,1998. 'Transformations of Sulphur during Pyrolysis and Hydropyrolysis of Coal', *Fuel* **77**, 487–493.

Chen, Y., Mori, S. and Pan, W.,1996. 'Studying the Mechanisms of Ignition of Coal Particles by TG-DTA', *Thermochimica Acta* **275**(1), 149–158.

Cheng, J., Zhou, J., Liu, J., Zhou, Z., Huanh, Z., Cao, X., Zhao, X. and Cen, K.,2003. 'Sulphur Removal at High Temperature during Coal Combustion in Furnaces: A Review', *Progress in Energy and Combustion Science* **29**, 381–405.

Chmielewski, A. G., Ostapczuk, A., Licki, J. and Kublica, K.,2003. *VOCs Emission from Coal — Fired Power Station Boiler*, Environmental Engineering Studies, Plenum Publishers, New York, chapter 13, pp. 33–42.

Clarke, L. and Sloss, L.,1992. Trace Element Emission from Coal Combstion and Gasification, Technical report, IEA, Coal Research, London (UK).

Cloke, M. and Lester, E.,1994. 'Characterisation of Coal for Combustion using Petrographic Analysis: A Review', *Fuel* **73**(3), 315–320.

Coykendall, L.,1962. 'Formation and Control of Sulfur Oxides in Boilers', *Journal of the Air Pollution Control Association* **12**(12), 567–591.

Crowell, D., Wolfe, M. and Wickstrom, L.,2008. 'Coal: Educational leaflet number 8', Available online at `https://minerals.ohiodnr.gov/portals/minerals/pdf/coal/el08.pdf` Acessed 22 March 2017.

Cullis, C. and Mulcahy, M.,1972. 'The Kinetics of Combustion of Gaseous Sulphur Compounds.', *Combustion and Flame* **18**, 225–292.

Damle, A., Ensor, D. and Ranade, M.,1982. 'Coal Combustion Aerosol Formation Mechanisms: A Review', *Aerosol Science and Technology* **1**(1).

Davidson, C., Borrazzo, J. and Hendrikson, C.,1986. Pollution Emission Factors for Gas Stoves: A Literature Survey, Report CR-812543-01-0, US EPA, Research Triange Park, NC, USA.

Davidson, R., Natusch, D., Wallace, J. and Evans, C.,1974. 'Trace Elements in Fly-ash Dependence on Concentration on Particle Size', *Environmental Science and Technology* **8**, 183–189.

Davini, P., Ghetti, P., Bonfanti, L. and de Michele, G.,1990. 'Investigation of the Combustion of Particles of Coal', *Fuel* **75**(9), 1083–1088.

de Diego, L., Londonot, C., Wang, X. and Gibbs, B.,1996. 'Influence of Operating Paramters on NO_x and N_2O Axial Profile in a Circulating Fluidsed Bed Combustor', *Fuel* **75**(8), 971–978.

DeFoort, M., L'Orange, C. and Kreutzer, C.,2009. 'Stove Manufacturer's Emissions and Performance Test Protocol (EPTP)', Available online at `https://cleancookstoves.org/binary-data/DOCUMENT/file/000/000/73-1.pdf` Acessed 31 July 2017.

Dickson, B., van Horen, C. and Williams, A.,1995. Low-Smoke Fuels as a Solution to Household Problems: A Synthesis of Current Research, Report No. es9406 to the Department of Mineral and Energy Affairs, Energy for Development Research Centre, University of Cape Town, South Africa.

Du, X. and Annamalai, K.,1994. 'The Transient Ignition of Isolated Coal Particle', *Combustion and Flame* **97**(3), 339–354.

Eberhard, A.,2011. The Future of South African Coal: Market, Inverstment and Policy Changes, Technical report, Programme on Energy and Sustainable Development. Available online at `https://fsi.stanford.edu/sites/default/files/WP_100_Eberhard_Future_of_South_African_Coal.pdf` Accessed 20 March 2017.

Engelbrecht, J. P., Swanepoel, L., Chow, J. C., Watson, J. G. and Egami, R. T.,2001. '$PM_{2.5}$ and PM_{10} Concentrations from the Qalabotjha Low-smoke Fuels Macro-scale Experiment in South Africa.', *Environmental Monitoring and Assessment* **69**(1), 1 – 15.

England, T., Hand, P., Michael, D., Falcon, L. and Yell, A.,2012. *Coal Processingin South Africa*, The South African Coal Processing Society.

Eslami, A., Sohi, A., Sheikhi, A. and Sotudeh-Gharebagh, R.,2012. 'Sequential Modeling of Coal Volatile Combustion in Fluidised Bed Reactors', *Energy and Fuels* **26**, 5199–5209.

Essenhigh, R., Misra, M. and Shaw, D.,1989. 'Ignition of Coal Particles: A Review', *Combustion and Flame* **77**, 3–30.

Everson, R., Koekermoer, A., Bunt, J., Neomagus, H. and Schwarz, C.,2013. 'Detailed Characterisation of South African High Mineral Matter Inertinite-rich Coals Density Fractions and Effect on Reaction Rates with Carbon Dioxide: Macerals, Microlithitypes, Carbomineralites and Minerals', *South African Journal of Chemical Engineering* .

Everson, R., Neomagus, H., Kaisani, H. and Njapha, D.,2006. 'Reaction Kinetics of Pulverised Coal-chars derived from Inertinite-rich Coal Discard', *Fuel* **85**, 1076–1085.

Ezzati, M.,2005. 'Indoor Air Pollution and Health in Developing Countries', *The Lancet* **366**(9480), 104 – 106.

Fadeela, S.,2012. Kinetics of Pyrolysis and Combustion of a South African Coal using the Dis-

tributed Activation Energy Model, Masters Thesis, University of the Witswaterstrand,South Africa.

Falcon, M. and Falcon, R.,1987. 'The Petrographic Composition of South African Coals in Relation to Friability„ Hardness and Abrasive Indeces', *Journal of the South African Institute of Mining and Metallurgy* **87**(10), 323–336.

Falcon, R. and Ham, A.,1988. 'The Characteristics of South African Coal', *Journal of the South African Institute of Mining and Metallurgy* **18**(5), 145 – 161.

Falcon, R. and Snyman, C.,1986. *An Introduction to Coal Petrography: Atlas of Petrographic Constituents in the Bituminous Coals of Southern Africa*, Geological Society of South Africa.

Felder, R. and Rousseau, R.,2005. *Elemental Principles of Chemical Processes*, 3 edn, Wiley.

Finkelman, R.,1980. Modes of Occurrence of Trace Elements in Coal, PhD Thesis, Univerisity of Maryland, USA.

Fitzpatrick, E., Bartle, K., Kubacki, M., Jones, J.M. Pourkashanian, M., Ross, A., Williams, A. and Kubica, K.,2009. 'The Mechanism of the Formation of Soot and Other Pollutants during the Co-firing of Coal and Pine Wood in a Fixed-bed Combustor', *Fuel* **88**, 2409–2417.

Flagan, R. C. and Seinfeld, J. H.,1988. *Fundamentals of Air Pollution Engineering*, Prentice Hall: New Jersey.

Fletcher, T. H.,2005. 'Relationships between Coal Chemistry and Decomposition Products'. avaialble online at `https://gcep.stanford.edu/pdfs/RxsY3908kaqwVPacX9DLcQ/fletcher_coal_mar05.pdf` Accessed 31 May 2017.

Flores, R. M.,2014. Coalification, Gasification, and Gas Storage, *in* 'Coal and Coalbed Gas', Elsevier, chapter 4, pp. 167 – 233.

Forbes, P.,2010. Development of a Laser Induced Flourescence Technique for the Analysis of Organic Air Pollutants, PhD Thesis, Univeristy of Pretoria, South Africa.

Friedl, A., Holm, D., John, J., Kornelius, G., Pauw, C., Oosthuizen, R. and van Niekerk, A.,2008. Air Pollution in Dense, Low-income Settlements in South Africa, Report, Royal Danish Embassy.

GERES,2010. 'Group for the Environmet, Renewable Enegy and Solidarity: Adapted Water Boiling Test (AWBT)', available online at `http://cleancookstoves.org/binary-data/DOCUMENT/file/000/000/75-1.pdf.` Acessed 31 July 2017.

Gordon, S. B., Bruce, N. G., Grigg, J., Hibberd, P. L., Kurmi, O. P., Lam, K. H. and Martin, W. J.,2014. 'Respiratory Risks from Household Air Pollution in Low and Middle Income Countries', *The Lancet. Respiratory Medicine* **2**(10), 823–860.

Goshayeni, B. and Sutherland, B.,2014. 'A Comparison of Various Models in Predicting Ignition Delay in a Single-particle Coal Combustion', *Combustion and Flame* **161**(7), 1900–1910.

Graham, J.,1997. Emissions and Efficiencies of Domestic Appliances Burning Various Fuels in South Africa, MSc Thesis, University of Cape Town, South Africa.

Graham, J. and Dutkiewicz, R.,1999. 'Assessing the Emissions and Cost Effectiveness of Traditional and Transitional Household Fuel Burning Appliances in South Africa', *Clean Air Journal* **10**(3), 13–21.

Grobbelaar, C., Asamoah, J. and Surridge, A.,1995. 'The Low-Smoke Coal Programme of the Department of Mineral and Energy Affairs', *Journal of Energy in Southern Africa* **6**(2), 79–82.

Grobbelaar, C. and Surridge, A.,1995. 'The Manufacture and Combstion of Low-smoke Coal', *Journal of Energy in Southern Africa* **6**(2), 83–86.

Grubor, B. and Manovic, V.,2002. 'Influence of Non-uniformity of Coal and Distribution of Active Calcium on Sulphur Self-rentention by Ash: A Case Study of Lignite Kolubara', *Energy and Fuels* **16**, 951–955.

Grubor, B., Manovic, V. and Arsic, B.,1999. Influence of Combustion Conditions and Coal Characteristics on Self-rentention of SO_2 by Ash Itself, *in* 'Proceedings of the Mediterreanian Combustion Symposium', pp. 866–877.

Gryglewicz, G. and Jasienko, S.,1992. 'The Behavior of Sulphur Forms during Pyrolysis of Low-rank Coals', *Fuel* **71**, 1225–1229.

Gulia, S., Nagendra, S. S., Khare, M. and Khanna, I.,2015. 'Urban Air Quality Management - A Review', *Atmospheric Pollution Research* **6**(2), 286 – 304.

Gulyurtlu, I., Abelha, P., Gregori, A., Garcia-Garcia, A., Boavida, D., Crujeira, A. and Cabrita, I.,2004. 'The Emissions of VOCs during Co-Combustion of Coal with Different Waste Materials in a Fluidised Bed', *Energy and Fuels* **18**, 605–610.

Gupta, R.,2007. 'Advanced Coal Characterisation: A Revew', *Energy and Fuels* **21**, 451–460.

Hancox, P. and Gotz, A.,2014. 'South Africa's Coalfields - A 2014 Perspective', *International Journal of Coal Geology* **132**, 170 – 254.

Hao, Y., Zhang, Q., Zhong, M. and Li, B.,2015. 'Is There Convergence in Per Capita SO_2 Emissions in China? An Empirical Study Using City-level Panel Data', *Journal of Cleaner Production* **108, Part A**, 944 – 954.

Hattingh, B.,2012. Product Evaluation and Reaction Modelling for the Devolatilizaton of Large Coal Particles, Master's thesis, North West Univeristy, South Africa.

Hittle, L., Sharkley, A., Houalla, H., Proctor, A., Hercule, D. and Morsi, B.,1993. 'Determination of Sulfur Forms on Coal Surfaces by X-ray Photoelectron Spectroscopy.', *Fuel* **72**, 771–773.

Hlatshwayo, T.,2008. The Partition Behaviour and the Chemical Speciation of Selected Trace Elements in a Typical Coal Sample duing Pyrolysis, Msc thesis, North West Univeristy, South Africa.

Hoets, P.,1995. 'The Acceptability of Three Coal-based Low-smoke Fuels in Evaton', *Journal of Energy in Southern Africa* **6**(2), 97–107.

Hoets, P.,1996. User Acceptability of Low-smoke Fules, Low-smoke Fules Programme 1995/6, Soweto, Technical report, Department of Minerals and Energy.

Holland, M., Cadle, A., Pinheiro, R. and Falcon, R.,1989. 'Depositional Environments and Coal Petrography of the Permian Karoo Sequence: Witbank Coalfield, South Africa', *International Journal of Coal Geology* **11**(2), 143 – 169.

Horsfall, W.,1994. Low-smoke Fuel from Discards, Report to the Department of Minerals and Energy Affairs, Department of Minerals and Energy.

Howard, J. and Essenhigh, R.,1967. 'Mechanism of Solid-particle Combustion with Simultaneous Gas-phase Volatiles Combustion', *Symposium (International) on Combustion* **11**(1), 399 – 408.

Hu, Y., Naito, S. and Kobayashi, N. an dHasatani, M.,2000. 'CO_2, no_x and SO_2 Emissionsfrom the Combustion of Coal with High Oxygen Concentration Gases', *Fuel* **79**, 1925–1932.

Huffman, G. and Huggins, F.,1984. Reaction and Transformations of Coal Mineral Matter at Elevated Temperature, *in* 'Preprints of Symposia, Division of Fuel Chemistry', Vol. 29, American Chemical Scociety, Washiongton DC, pp. 56–67.

Ibraimo, M., Annegarn, H. and Pemberton-Pigott, C.,2014. Modelling of Bottom-Lit Down-Draft BBDD Clean-Burning Coal Stove, *in* 'Proceedings of the Twenty-Second Domestic Use of Energy (DUE) Conference', Cape Peninsula University of Technology, Cape Town.

Ilic, M., Grubor, B. and Manovic, V.,2003. 'Sulphur Retention by Ash during Coal Combution. Part I. A Model of Char Particle Combution', *Journal of the Serbian Chemical Society* **68**(3), 171–182.

Inglesi, R. and Pouris, A.,2010. 'Forecasting Electricity Demand in South Africa: A Critique of Eskom's Projections', *Southern African Journal of Science* **106**, 50–53.

ISO19579:2006,2011. 'ISO 19579:2006 - Solid Mineral Fuels - Determination of Sulfur by IR Spectrometry. ed. 1.', Available online at `http://v-dbt-win1.nwu.ac.za/SANS/documents/SANS19579.pdf` Acessed 17 May 2017.

Jaecker-Voirol, A.,2000. VOC: Volatile Organic Compounds, *in* 'Pollutants from Combustion: Formation and Impacts on Atmospheric Chemistry', NATO Science Series C: Mathematical and Physical Sciences, Wiley, chapter 12, pp. 241–261.

Jeffrey, L.,2005. 'Characterisarion of the Coal Resource of South Africa', *The Journal of the South African Institute of Mining and Metallurgy* **105**(2), 95–102.

Jetter, J., Zhao, Y., Smith, K., Khan, B., Yelverton, T., DeCarlo, P. and Hays, M.,2012. 'Polluntant Emissions and Energy Efficiency under Controlled Conditions for Household Biomass Cookstoves and Implications for Metrics Useful in Setting International Standards', *Environmental Science and Technology* **46**(19), 10827–10834.

Jeuland, M., Pattanayak, S. K. and Bluffstone, R.,2015. 'The Economics of Household Pollution', *Annual Reviews of Resource Economics* **7**, 81–108.

Jiang, X., Huang, X., Liu, J. and Han, X.,2010. 'NO_x Emission of Fine- and Superfine- Pulverised Coal Combustion in O_2/CO_2 Atmosphere', *Energy and Fuels* **24**, 6307–6313.

Johnson, J. and Glarborg, P.,2000. Sulphur Chemistry in Combustion I: Sulphur in Fuels and Combustion Chemistry, *in* 'Polluntants from Combustion: Formation and Impact on Atmo-

spheric Chemistry', Pollutants from Combustion: Formation and Impacts on Atmospheric Chemistry, Springer, Netherlands:Dordrecht, chapter 13, pp. 263–282.

Kaitano, R.,2007. Characterisation and Reaction Kinetics of High Ash Chars derived from Inertinite-rich Coal Discards, PhD Thesis, North West University, South Africa.

Kalenga, P.,2011. Determination and Characterisarion of Sulphur in South African Coal, MSc Theis, University of the Witwaterstrand, South Africa.

Kampa, M. and Castanas, E.,2008. 'Human Health Effects of Air Pollution', *Environmental Pollution* **151**(2), 362 – 367. Proceedings of the 4th International Workshop on Biomonitoring of Atmospheric Pollution (With Emphasis on Trace Elements).

Kankaria, A., Nongkynrih, B. and Gupta, S.,2014. 'Indoor Air Pollution in India: Implications on Health and Its Control.', *Indian Journal of Community Medicine* **39**(4), 203–207.

Kelemen, S. and George, G.N. Gorbaty, M.,1990. 'Direct Determination and Quatifiation of Sulphur Forms in Heavy Peteroleum and Coals: 1. The X-ray Photoelectron Spectroscopy (XPS) Approach.', *Fuel* **69**, 939–944.

Khandelwal, M., Hill Jr, M., Greenough, P., Anthony, J., Quill, M., Linderman, M. and H.S., U.,2016. 'Why Have Improved Cook-stove Initiatives in India Failed?', *World Development* **92**, 13 – 27.

Kim, H. and Chun, W.,1998. 'The Particle Size Effect on the Pollutant Formation in Pulverised Coal Combustion', *Environental Engineering Research* **3**(1), 21–29.

Kim, S., Kang, Y., Lee, H., Kim, J. and Hong, S.,2011. 'Characteristics of Fundamental Combstion and NO_x Emmision Using Various Rank Coals', *Journal of the Air and Waste Management Association* **61**, 254–259.

Kimemia, D.,2009. Biomass Alternative Urban Energy Economy: Case of Setswetla, Alexandra Township, Gauteng, MSc Thesis, University of Johannesburg, South Africa.

Kimemia, D., Annegarn, H., Makonese, T., Molapo, V. and Tobinson, J.,2010. Characterisation of Domestic Biomass Combustion Technologies Used in Setswetla, Alexandra Township, Gauteng, *in* 'Proceedings of the Domestic Energy Use (DUE) Conference', Cape Peninsula University of technology, Cape Town, South Africa., Cape Peninsula University of Technology, Cape Town.

Kimemia, D., Annegarn, H., Robinson, J., Pemberton-Pigott, C. and Malapo, V.,2011. Optimising the *Imbaula* Stove, *in* 'Proceedings of the 2011 Domestic Use of Energy (DUE) Conference'.

Kipruto, W.,2011. A Review of the Cook Stove Test Method and their Applicability in Small Scale CDM Cook Stove Projects, Technical report, United Nations Framework Convention on Climate Change, Bonn, Germany.

Kishore, V. and Ramana, P.,2002. 'Improved Cookstoves in Rural India: How Improved are they?: A Critique of the Perceived Benefits from the National Programme on Improved Chulhas (npic),', *Energy* **27**, 47–63.

Kituyi, E., Marufu, L., Huber, B., Wandinga, S., Jumba, I., Andeae, M. and Helas, G.,2001. 'Biofuels Consumption Rates and Patterns in Kenya', *Biomass and Bioenergy* **20**, 83–99.

Kök, M., Özbas, E., Hicyilmaz, C. and Karacan, O.,1997. 'Effect of Particle Size on the Thermal and Combustion Properties of Coal', *Thermochimica Acta* **302**, 125–130.

Kök, M., Özbas, E., Karacan, O. and Hicyilmaz, C.,1998. 'Effect of Particle Size on Coal Pyrolysis', *Journal of Analytical and Applied Pyrolysis* **45**, 102–110.

Kosowska-Golachowska, M.,2010. Coal Combustion, *in* 'Handbook of Combustion', Vol. 4: Solid Fuels, Wiley-VHC, chapter 5, pp. 171–216.

Krawczyk, E., Zajemska, M. and Wylecial, T.,2013. 'The Chemical Mechanism of SO_x Formation and Elimination in Coal Combstion Process', *Chemik* **67**(10), 856–862.

Kshirsagar, M. P. and Kalamkar, V. R.,2014. 'A Comprehensive Review on Biomass Cookstoves and a Systematic Approach for Modern Cookstove Design', *Renewable and Sustainable Energy Reviews* **30**, 580 – 603.

Kühn, M.,2015. Production of a Low-smoke Fuel via Low-temperature Pyrolysis, MEng Thesis, North West Univeristy, South Africa.

Kühn, M., Bunt, J., Neomagus, H., Piketh, S., Everson, R. and Coetzee, S.,2017. 'Coal-derived Low Smoke Fuel Asessment through Coal Stove Combustion Testing', *Journal of Analytical and Applied Pyrolysis* **126**, 158–168.

Kumar, A., Prasad, M. and Mashira, K.,2013. 'Comparitive Study of the Effect of Different Parameters on Performance and Emissions of Biomass Cook Stoves.', *Journal of Research in Engineering and Technology* **1**(3), 121–126.

Language, B., Piketh, S. J., Wernecke, B. and Burger, R. P.,2016. Householad Air Pollution in South African Low-income Settlements: A Case Study, *in* 'Air Pollution XXIV: Proceedings of the 24th International Conference on Modelling, Monitoring and Management of Air Pollution (AIR 2016)', Vol. 207 of *WIT Transactions on Ecology and The Environment*, WIT Press, pp. 227–236.

Le Roux, L.,2009. 'Reduction in Pollution using the Basa Njengo Magogo Methodology and Applicability to Low-smoke Fuels.', *Journal of Energy in Southern Africa* **20**(3), 3–10.

Le Roux, L., Cilliers, K. and Van Vuuren, D.,2004. Low-smoke Fuels: Standard Testing and Verification., Technical report, CSIR, Department of Mining Technology.

Levenspiel, O.,1999. *Chemical Reaction Engineering*, 3rd edn, Wiley.

Levy, A., Merryman, E. L. and Reid, W. T.,1970. 'Mechanisms of Formation of Sulfur Oxides in Combustion', *Environmental Science and Technology* **4**(8), 653–662.

Li, K. and You, C.,2010. 'Particle Combustion Model Simultaneously Considering a Volatile and Carbon Reaction', *Energy and Fuels* **24**, 4178–4184.

Li, Q., Benyon, P., Benfell, K., Bryant, G., Tate, A., Boyd, R., Harris, D. and Wall, T.,2009.

'Comparison of Pulverised Coal Combustion in Air and in O_2/CO_2 Mixtures by Thermogravimetric Analysis', *Journal of Analytical and Applied Pyrolysis* **85**, 521–528.

Li, Q., Jiang, J., Zhang, Q., Zhou, W., Cai, S., Duan, L., Ge, S. and Hao, J.,2016. 'Influences of Coal Size, Volatile Matter Content, and Additive on Primary Particulate Matter Emissions from Household Stove Combustion', *Fuel* **182**, 780 – 787.

Li, X. G., ma, B. G., Xu, L., Luo, Z. and Wang, K.,2007. 'Catalytic Effect of Metallic Oxides on Combustion Behavior of High Ash Coal', *Energy & Fuels* **21**(5), 2669–2672.

Liang, X., Wang, Q., Jiao, F., Chen, J., Ying, G., Namioka, T. and Nonomiya, Y.,2017. 'Influence of Inherent Moisture on the Formation of Particulate Matter during Low-Rank Coal Combstion', *Journal of Chemical Engineering of Japan* **50**(5), 351–357.

Linak, W., Miller, C. and Wendt, J.,2000. 'Comparison of Particle Size Distribution and Elemental Partitioning from the Combstion of Pulverised Coal and Residual Fuel Oil', *Journal of the Air and Waste Management Association* **50**, 1532–1544.

Linak, W. and Wendt, J.,1993. 'Toxic Metal Emissions from Incineration - Mechanism and Control', *Progress in Energy and Combustion Science* **9**, 145–185.

Lionel, T., Martin, R. and Brown, N.,1986. 'A Comparitive Study of Combustion in Kerosene Heaters', *Environmental Science and Technology* **20**, 78–85.

Liu, F., Li, W., Li, H. and Chen, B.,2007. 'Uneven Distribution of Sulfur and their Transformations during Pyrolysis', *Fuel* **86**, 360–366.

Liu, H., Feng, B., Lu, J. and Zhang, G.,2005. 'Coal Property Effects on N_2O and NO_x from Circulating Fluidised Bed Combustion of Coal', *Chemical Engineering Communications* **192**, 1482–1489.

Liu, J., Mauzerall, D. L., Chen, Q., Zhang, Q., Song, Y., Peng, W., Klimont, Z., Qiu, X., Zhang, S., Hu, M., Lin, W., Smith, K. R. and Zhu, T.,2016. 'Air Pollutant Emissions from Chinese Households: A Major and Underappreciated Ambient Pollution Source', *Proceedings of the National Academy of Sciences* **113**(28), 7756–7761.

Liu, X., Xu, M., Yao, H., Yu, D., Lv, D. and Zhou, K.,2008. 'The Formation of Particulate Matter during Combustion of Density Separated Coal Fractions', *Energy and Fuels* **22**, 3844–3851.

Liu, Y., Che, D. and Xu, T.,2002. 'Catalytic Reduction of SO_2 during Combustion of Typical Chinese Coals', *Fuel Processing Technology* **79**(2), 157–169.

Lloyd, P.,2014. 'The Energy Profile of a Low-income Urban Community', *Journal of Energy in Southern Africa* **25**, 75 – 80.

Lockwood, A., Welker-Hood, K .and Rauch, M. and Gottlieb, B.,2009. Coal's Assault on Human Health, Technical report, World Health Organisation. Available online at `http://www.psr.org/assets/pdfs/psr-coal-fullreport.pdf` Acessed: 22 March 2016.

Lombardi, F., Riva, F., Bonamini, G., Barbieri, J. and Colombo, E.,2017. 'Laboratory Protocols

for Testing of Improved Cooking Stoves (ICSs): A Review of State-of-the-art and Further Developments', *Biomass and Bioenergy* **98**, 321–335.

Lu, Z., Zhang, Q. and Streets, D.,2011. 'Sulfur Dioxide and Primary Carbonaceous Aerosol Emissions in China and India', *Atmospheric Chemistry and Physics* **11**, 9839–9864.

Ludwig, L., Marufu, T. L., Huber, B., Andeae, M. and Helas, G.,2003. 'Domestic Combustion of Biomass Fuels in Developing Countries: A Major Source of Atmospheric Pollutants', *Journal of Atmospheric Chemistry* **44**, 23–37.

Lui, X., Xu, M., Yu, D., Gao, X., Cao, Q. and Hao, W.,2007. 'Influenece of Mineral Matter on Emission of Particulate Matter during Coal Combustion', *Frontiers of Energy and Power Engineering in China* **1**(2), 213–217.

Mabahwi, N., Leh, O. and Omar, D.,2014. 'Human Health and Wellbeing: Human Health Effect of Air Pollution', *Procedia - Social and Behavioral Sciences* **153**, 221 – 229.

Makonese, T.,2011. Protocols for Thermal and Emissions Performance Testing of Domestic Fuels and Stoves., MPhil Thesis, University of Johannesburg, South Africa.

Makonese, T.,2015. Systematic Investigation of Smoke Emissions from Packed-bed Residential Coal Combustion Devices, PhD Thesis, University of Johannesburg, South Africa.

Makonese, T., Masekameni, D. and Annegarn, H.,2017b. 'Influence of Coal Properties on the Perfomance of Fixed-bed Coal-burning Braziers.', *Journal of Energy in Southern Africa* **28**(2), 40–51.

Makonese, T., Masekameni, D., Annegarn, H. and Forbes, P.,2015. 'Influence of Fire-Ignition Method and Stove Ventilation Rates on Gaseous and Particle Emissions from Residential Coal Braziers', *Journal of Energy in Southern Africa* **26**(4), 16–28.

Makonese, T., Masekameni, D., Annegarn, H. and Forbes, P.,2017. 'Emission Factors of Domestic Coal-burning Braziers', *South African Journal of Energy* **28**(40-51).

Makonese, T., Pemberton-Pigott, C., Robinson, J., Kimemia, D. and Annegarn, H.,2012. 'Performance Evaluation and Emission Characterisarion of Three Kerosense Stoves Using a Heterogeneous Testing Protocol HTP', *Energy and Sustainable Development* **16**, 344–351.

Makonese, T., Robinson, J., Pemberton-Pigott, C. and Annegarn, H.,2011. A Preliminary Comparison of Stove Testing Method betwen the Water Boiling Test and the Heterogeneous Testing Protocol, *in* 'Domestic Use of Energy Conference', Cape Peninsula Univeristy of Technology, Cape Town.

Mangena, S. and Korte, G.,2000. Development of a Process for Producing Low-smoke Fuels from Coal Discards., Technical report, CSIR Department of Mining Technology.

Marek, E. and Stanczyk, K.,2013. 'Case Studies Investigating Single Coal Particle Ignition and Combustion', *Journal of Sustainable Mining* **12**(3), 17–31.

Markos, J., Zajdlik, R., Remiarova, B. and Jelemensky, L.,2001. 'Experiment Study of Single Coal Char Particle Combustion Mechanism', *Chemistry Papers* **55**(6), 359–363.

Marlow, D., Niksa, S. and Kruger, C.,1992. 'Secondary Pyrolysis and Combustion of Coal Volatiles', *Symposium (International) on Combustion* **24**(1), 1251–1258.

Martin, W. I., Hollingsworth, J. W. and Ramanathan, V.,2014. Household Air Pollution from Cookstoves: Impacts on Health and Climate, *in* 'Global Climate Change and Public Health', Springer, chapter 13, pp. 237 – 255.

Masekameni, D.,2015. Perfomance Evaluation and Emissions Characterisation of Domestic Coal Combustion in Optimised Braziers (*imbaulas*), Master's thesis, Univeristy of Johannesburg, South Africa.

Masekameni, D., Makonese, T. and Annegarn, H.,2014. Optimisation of Ventilation and Ignition Method for Reducing Emissions from Coal-Burning *Imbaulas*, *in* 'Proccedings of the Twenty Second Conference on the Dometic Use (DUE)of Energy', Cape Peninsula University of Technology, Cape Town.

Masondo, L., Masekameni, D., Makonese, T., Annegarn, H., and Mohapi, K.,2016. 'Influence of Coal-particle Size on Emissions using the Top-lit Updraft Ignition Method', *The Clean Air Journal* **26**(1), 15 – 20.

Mastral, A., Callen, M. and Carcia, T.,1999. 'Polycyclic Hydrocarbons and Organic Matter Associated to Particulate Matter Emmitted from Atmospheric Fluidised Bed Coal Combstion', *Environmetal Science and Technology* **33**, 3177–3184.

Mathee, A.,2004. 'Indoor Air Pollution in Developing Countries: Recommendations for Research - Commentary on the Paper by Professor Kirk. R. Smith', Availabel on line. South African Medical Research Council: Pretoria.

Mathews, J. P., Hatcher, P. G. and Scaroni, A. W.,1997. 'Particle Size Dependance of Coal Volatile Matter: Is There a Non-maceral-related Effect', *Fuel* **76**(4), 359–362.

Matjie, R., French, D., Ward, C., Pistorius, P. and Li, Z.,2011. 'Behaviour of Coal Mineral Matter in Sintering and Slagging of Ash During the Gasification Process', *Fuel Processing Technology* **92**, 1426–1433.

Matjie, R. H., Li, Z., Ward, C. R., Kosasi, J., Bunt, J. R. and Strydom, C. A.,2015. 'Mineralogy of Furnace Deposits Produced by South African Coals during Pulverized-fuel Combustion Tests', *Energy and Fuels* **29**(12), 8226–8238.

Matjie, R., Li, Z., Ward, C., Bunt, J. and Strydom, C.,2016. 'Determination of Mineral Matter and Elemental Composition of Individual Macerals in Coals from Highveld Minds', *Journal of the South African Institute of Mining and Metallurgy* **116**, 169–180.

Matzakos, A.,1992. Fundamental Mechanisms of Coal Combustion, PhD Thesis, Rice University, U.S.A.

Mdluli, T.,2007. The Societal Dimensions of Domestic Coal Combustion: People's Perceptions and Indoor Aerosol Monitoring, PhD Thesis, University of Johannesburg, South Africa.

Miller, G. and Tillman, D.,2008. *Combustion Engineering Issues for Solid Fuel Systems*, Academic Press/Elsevier, Amsterdam.

Miller, J. and Bowman, C.,1989. 'Mechanism and Modelling of Nitrogen Chemistry in Combustion', *Progress in Energy and Combustion Science* **15**, 287–338.

Mitchell, E., Lea-Langton, A., Jones, J., Williams, A., Layden, P. and Johnson, R.,2016. 'The Impact of Fuel Properties on the Emissions from the Combustion of Biomass and other Solid Fuels in a Fixed Bed Domestic Stove', *Fuel Processing Technology* **142**, 115 – 123.

Molina, A. and Mondragon, F.,1998. 'Reactivity of Coal Gasification with Steam and CO_2', *Fuel* **77**, 1831–1839.

Morgan, P. A., Robertson, S. D. and Unsworth, J. F.,1986. 'Combustion Studies by Thermogravimetric Analysis: 1. Coal Oxidation', *Fuel* **65**, 1546–1551.

Morgan, P. A., Robertson, S. D. and Unsworth, J. F.,1987. 'Combustion Studies by Thermogravimetric Analysis: 2. Char Oxidation', *Fuel* **66**, 210–215.

Muller, C., Yu, H. and Zhu, B.,2015. 'Ambient Air Quality in China: The Impact of Particulate and Gaseous Pollutants on IAQ', *Procedia Engineering* **121**, 582 – 589.

Müller, M., Schnell, U. and Scheffknecht, G.,2013. 'Modelling the Fate of Sulphur during Pulverised Coal Combustion under Conventional and Oxy-fuel Conditions', *Energy Procedia* **37**, 1377–1388.

Naidoo, S., Piketh, S. and Curtis, C.,2014. 'Quantification of Emissions Generated from Domestic Burning Activities from Townships in Johannesburg', *Clean Air Journal* **24**(1), 34 –41.

Naz, S., Page, A. and Agho, K. E.,2016. 'Household Air Pollution and Under-five Mortality in India (1992–2006)', *Environmental Health* **15**(1), 54.

Nel, S.,2011. Catalytic Steam Gasification of Large Coal Particles, MEng Thesis, North West Univeristy, South Africa.

Ninomiya, Y., Zhang, L., Sato, A. and Dong, Z.,2004. 'Influence of Coal Particle Size on Particulate Matter Emissions and Its Chemical Species Produced during Coal Combustion', *Fuel Processing Technology* **85**, 1065–1088.

Nkosi, N., Piketh, S., Burger, R. and Annegarn, H.,2017. Variablity of Domestic Burning Habbits in the South African Highveld: A Case Study in the Kwadela Township, *in* 'Domestic Use of Energy Conference', Cape Peninsula University of Technology, Cape Town, South Africa.

NOVA Institute,2017. 'Basa Magogo Project', Available online at `http://www.nova.org.za/projects/basa-magogo.php` Accessed 24 February 2017.

Okolo, G. N.,2010. The Effects of Chemical and Physical Properties of Chars Derived from Inertinite-rich, High-ash Coals on Gasification Reaction Kinetics, MEng Thesis, North West Univeristy, South Africa.

Olivella, M., Palacios, J., Vairavamurthy, A., del Río, J. and de las Heras, F.,2002. 'A Study of Sulfur Functionalities in Fossil Fuels using Destructive- (ASTM and Py–GC–MS) and Non-destructive- (SEM–EDX, XANES and XPS) Techniques', *Fuel* **81**(4), 405–411.

Pemberton-Pigott, C.,2017. Unexpected Social Impacts og Greatly Improved Heating Stoves in Rural Kyrgzstan. Talk presented at the Domesticu use of Energy Conference, 3-5 April 2017, Cape Town, South Africa. (unbuplished).

Pemberton-Pigott, C., Annegarn, H. and Cook, C.,2009. Emission Reactions from Domestic Coal Burning: Practical Application of Combustion Principles, *in* 'Proceedings of the Domestic Use of Energy (DUE) Conference', Cape Peninsula University of Technology, Cape Town.

Pinetown, K., Ward, C. R. and van der Westhuizen, W.,2007. 'Quantitative Evaluation of Minerals in Coal Deposits in the Witbank and Highveld Coalfields, and the Potential Impact on Acid Mine Drainage', *International Journal of Coal Geology* **70**(1–3), 166 – 183.

Preble, C., Hadley, O., Gasgil, A. and Kirchstetter, T.,2014. 'Emissions and Climate-Relevant Optical Properties of Polluntants Emitted from a Three-Stone Fire and the Berkeley-Dafur Stove Tested under Laboratory Conditions', *Environmental Science and Technology* **48**(11), 6484–6491.

Pretorius, I., Piketh, S. and Burger, R.,2015. The Impact of the South African Energy Crisis on Emissions, *in* 'Air Pollution XXIII', Vol. 198 of *Transactions on Ecology and the Environment*, WIT Press, pp. 255–264.

Qase, N., Lloyd, P. and van Zyl, H.,2000. Intervention Potential for Low-smoke Fuels in the Coal Distribution Chain, Unpublished manuscript, University of Cape Town, Cape Town.

Querol, X., Fernandez-Turiel, J. L. and Lopez-Soler, A.,1995. 'Trace Elements in Coal and their Behavior During Combstion in a Large Power Station', *Fuel* **74**(3), 331–343.

Ramabuda, M.,2015. Gasification and Combstion Kinetics of Typical South African Coal Chars., Masters thesis, North West University, South Africa.

Robinson, J., Ibraimo, M. and Pemberton-Pigott, C.,2011. The Uncontrolled Cooking Test: Measuring Three-Stone Fire Performance in Northern Mozambique, *in* 'Proceedings of the 19th International Conference on Domestic Use (DUE) of Energy', Cape Peninsula University of Technology, Cape Town.

Roets, L.,2014. The Effect of Mineral Addition on the Pyrolysis Products Derived from Typical Highveld Coal, MEng Thesis, North West Univeristy, South Africa.

Rogers, D.,1995. 'Particulate and Gaseous Emission from a Low-smoke Stove using Three Low-smoke Fuels and One Domestic Coal', *Journal of Energy in Southern Africa* **6**(2), 87–92.

Rohra, H. and Taneja, A.,2016. 'Indoor Air Quality Scenario in India—An Outline of Household Fuel Combustion.', *Atmospheric Environment* **129**, 243–255.

Rosenvold, R. and Dubow, J.,1982. 'Thermal Analyses of Ohio Bituminous Coals', *Thermochimica Acta* **53**(3), 321–332.

Sami, M., Annamalai, K. and Wooldridge, M.,2001. 'Co-firing of Coal and Biomass Fuel Blends', *Progress in Energy and Combustion Scence* **27**, 171–214.

SANS-1111,2008. Coal-burning Appliances (Reduced Smoke Emission Types), South African National Standard, South Africa Bureau of Standards, Groenkloof, South Africa.

Schobert, H.,2013. *Chemistry of Fossil Fuels and Biofuels*, Cambridge University Press, New York.

Scorgie, Y.,2012. Urban Air Qaulity Management and Planning in South Africa, PhD Thesis, University of Johannesburg, South Africa.

Scorgie, Y., Burger, L. and Snowden, M.,2001. 'Assessing the Potential of Low-smoke Fuels in Addressing Air Pollution and Human Health Impacts due to Household Coal Burning Emmissions', *The Clean Air Journal* **10**(8), 6 – 16.

Scorgie, Y., Kneen, M., Annegarn, H. and Burger, L.,2003. 'Air Pollution in the Vaal Triangle - Quantifying Source Contributions and Identifying Cost-effective Solutions', *The Clean Air Journal* **13**(2), 5–18.

Scott, A.,2002. 'Coal Petrology and the Origin of coal Macerals: A Way Ahead', *International Journal of Coal Geology* **20**, 119–134.

Senior, C., Panagiotou, T. *et al.*,2000. Formation of Ultrafine Particulate Matter from Pulverised Coal Combustion, *in* 'Preprints of Symposia, Division of Fuel Chemistry', Vol. 45, American Chemical Scociety, Washiongton DC.

Sentorun, C., Haykiri-Acma, H. and Kucukbayrak, S.,1996. 'Effect of Mineral Matter on the Combustion Curve of Chars', *Thermochimica Acta* **277**, 65 – 73.

Shao, D., Hutchinson, E., Heidbrink, J., Pan, W. and Chou, C.,1994. 'Behavior of Sulphur During Coal Pyrolysis', *Journal of Analytical and Applied Pyrolysis* **30**, 91– 100.

Shen, X.,2009. Coal Combustion and Combustion Products, *in* 'Coal, Oil Shale, Natural Bitumen, Heavy Oil and Peat', Vol. 1, EOLSS Publications, pp. 319–339.

Shirazi, A. R., Bet-tin, O., Eklund, L. and Lindqvist, O.,1995. 'The Impact of Mineral Matter in Coal on its Combustion, and a New Approach to the Determination of the Calorific Value of Coal', *Fuel* **72**(2), 247–251.

Sloss, L.,2001. Organic compounds from coal utilisation, Technical report, IEA Coal Research. Available online at `http://www.iea-coal.org.uk/documents/81070/5426/Organic-compounds-from-coal-utilisation` Acessed 27 April 2017.

Smith, I.,1982. The Combustion Rates of Coal Chars: A Review, *in* 'Nineteenth Symposium (International) on Combustion', The Combustion Institute, pp. 1045–1065.

Smith, K. R.,1994. 'Health, Energy, and Greenhouse-gas Impacts of Biomass Combustion in Household Stoves', *Energy for Sustainable Development* **1**(4), 23 – 29.

Smith, K. R.,2014. 'In Praise of Power', *Science* **345**(6197), 603.

Smith, K. R., Frumkin, H., Balakrishnan, K., Butler, C. D., Chafe, Z. A., Fairlie, I., Kinney, P., T., K., Mauzerall, D. L., McKone, T. E., McMicheal, A. J. and Scheiner, M.,2013. 'Energy and Human Health', *Annual Reviews in Public Health* **34**.

Smith, K. R. and Mehta, S.,2003. 'The Burden of Disease from Indoor Air Pollution in Develop-

ing Countries: Comparison of Estimates', *International Journal of Hygiene and Environmental Health* **206**(4), 279 – 289.

Smith, K., Uma, R., Kishore, V., Lata, K., Madne, S., Rao, G., Zhang, J., Rasmussen, R., Khalil, M. and Thorneloe, S.,2000. Greenhouse Gases from Small-scale Combustion Devices in Developing Countries. Phase IIa: Household Stoves in India, U.S. EPA Report No. EPA-600/R-00-053, U.S. Environmental Protection Agency, Washington, DC.

Smoot, L. and Smith, P.,1985. *Coal Combustion and Gasification*, Plenum Press: New York.

Snyman, C. and Botha, W.,1993. 'Coal in South Africa', *Journal of African Earth Sciences (and the Middle East)* **16**(1), 171 – 180.

Solomon, P. and Hamblen, D.,1985. Pyrolysis, *in* H. Richard, ed., 'Chemistry of Coal conversion', SCHLOSBERG.

Solomon, P., Serio, M. and Suurberg, E.,1992. 'Coal Pyrolysis: Experiments, Kinetic Rates and Mechanisms', *Progress in Energy and Combustion Science* **18**, 133–220.

Sonibore, O., Ehinola, O., Egashira, R. and KeanGiap, L.,2005. 'An Investigation into the Thermal Decomposition of Nigerian Coal', *Journal of Applied Science* **5**(1), 104–107.

Sowazi, S. and Maake, R.,2001. Clean Energy Initiatives in South Africa: Qalabotja Micro-scale Experiment as a Case Study, *in* 'Domestic Use of Energy (DUE) Conference', Minerals and Energy Policy Centre, pp. 261–265.

Speight, J.,1994. *The Chemistry and Technology of Coal*, 2 edn, York: Marcel Dekker.

Speight, J.,2005. *The Handbook of Coal Analysis*, Vol. 166 of *Chemical Analysis: A Series of Monographs on Analytical Chemistry and its Applications*, 2 edn, Wiley-Interscience.

StatsSA,2012. Census 2011:p0301.4, Technical report, Statistics South Africa. Available online at `https://www.statssa.gov.za/publications/P03014/P030142011.pdf`.

Sternling, C. and Wendt, J.,1972. Kinetic Mechanisms Governing the Fate of Chemically Bound Sulphur and Nitrogen in Combustion, Technical Report Contract No. EHSD 71-45 (Task 14), U.S. Environmental Ptotection Agency, Washington, D.C.

Stopes, A. C.,1935. 'On the Petrology of Banded Bituminous Coal', *Fuel* **14**(1), 4–13.

Stopes, M. C.,1919. 'On the Four Visible Ingredients in Banded Bituminous Coal: Studies in the Composition of Coal, No. 1', *Proceedings of the Royal Society of London B: Biological Sciences* **90**(633), 470–487.

Stubington, J.,1984. 'Release of Volatiles from Large Coal Particles in a Hot Fluidised Bed', *Fuel* **63**(7), 1013–1019.

Svoboda, K., Cermák, J. and Vesely, V.,2000. No_x Chemistry and Emissions - I Heterogenous Reaction (no and no_2, *in* 'Pollutants from Combustion: Formation and Impacts on Atmospheric Chemistry', NATO Science Series C: Mathematical and Physical Sciences, Springer, Netherlands:Dordrecht, chapter 8, pp. 145–164.

Svoboda, K., Hartman, M. and Cermák, J.,2000. Combustion Mechanisms — Solid Phase, *in* 'Pollutants from Combustion: Formation and Impact on Atmospheric Chemistry', NATO Science Series C: Mathematical and Physical Sciences, Springer, Netherlands:Dordrecht, chapter 3, pp. 35–50.

Tait, H.,1993. Low-cost Low-smoke Reconstituted Fuel for Developing Areas, Short report (January 1993) on Briquette Production by Enertek, to the Department of Mineral and Energy Affairs, CSIR: Enertek, Pretoria, South Africa.

Tait, H. and Lekalakala, J.,1993. Optimisation of a Coal-based Low-cost, Low-smoke Reconstituted Solid Fuel., Final Report, ENER-C, CSIR Enertek, Pretoria. South Africa.

Tajwar, S., Saleemi, A., Ramzan, N. and Naveed, S.,2011. 'Improving Thermal and Combustion Efficiency of Gas Water Heater', *Applied Thermal Engineering* **31**, 1305–1312.

Taljaard, J.,1998. Indoor Air Quality in Qalabotjha, Technical report, CSIR and Enpro, Pretoria, South Africa.

Taylot, R.,2009. The Use of Laboratory Testing of Biomass Cookstoves and the Shortcomings of the Dominant U.S. Protocol., Master's thesis, Iowa State University, U.S.A.

Terblanche, P., Danford, I. and Pols, A.,1995. 'Comparative Evaluation of Human Exposure to Air Pollution from Low-smoke and Conventional Household Coal Usage', *Journal of Energy in Southern Africa* pp. 131–136.

Terblanche, P., Nel, C., Opperman, L. and Nyikos, H.,1993. 'Exposure to Air Pollution from Transitional Household Fuels in a South African Population.', *Journal of Exposure Analysis and Environment Epidemiology* **3**(1), 15–22.

Terblanche, P., Opperman, L., Nel, R. and Pols, A.,1993b. 'Prevelance of Respiratory Illnesses in Different Regions of South Africa', *Clean Air Journal* **8**(8), 18–20.

Tissari, J., Lyyränen, J., Hytönen, K., Sippula, O., Tapper, U., Frey, C., Saanio, K., Pennanen, A., Hillamo, R., Salonen, R., Hitvonen, M. and Jokiniemi, J.,2008. 'Fine Particle and Gaseous Emissions from Normal and Smouldering Wood Combustion in a Conventional Masonry Heater', *Atmospheric Environment* **42**, 7862–7873.

Tomeczek, J. and Palugniok, H.,2002. 'Kinetics of Mineral Matter Transformations during Coal Combustion', *Fuel* **81**, 1251–1258.

TSI,2004. Combustion Analysis Basics: An Overview of Measurements, Methods and Calculations usedd in Combstion Analysis, techreport, TSI Incorporated. avilable online at `https://www.google.co.za/url?sa=t&source=web&rct=j&url=http://www.tsi.com/uploadedFiles/_Site_Root/Products/Literature/Handbooks/CA-basic-2908175.pdf&ved0ahUKEwjCyMzPv_fWAhwJAMKHYZDXQFggoMAA&usg=AOcVaw2sHfJnqbncG80GW0CfujXm` Acessed 17 October 2017.

Uski, O.,2014. Toxicological Effect of Fine Partiles form Small-scale Biomass Combstion, PhD Thesis, University of Eastern Finland, Finland.

Vamvuka, D. and Woodburn, E.,1998. 'A Model of the Combustion of a Single Small Coal Particle using Kinetic Parameters Based on Thermogravimetric Analyses', *Internationa Journal of Energy Research* **22**, 657–670.

van der Merwe, G.,2011. The Influence of Particle Size and Devolatilisation Conditions on the CO_2 Gasification of Highveld Coal, MEng Thesis, North West Univeristy, South Africa.

van Dyk, J., Benson, S., Laumb, M. and Waanders, B.,2009. 'Coal and Coal Ash Characterisation to Understand Mineral Transformations and Slag Formation', *Fuel* **88**, 1057–1063.

van Horen, C., Nel, R. and Terblanche, P.,1996. 'Indoor Air Pollution from Coal and Wood use in South Africa: An Overview', *Energy for Sustainable Development* **3**(1), 38–40.

van Krevelen, D.,1981. *Coal: Typography-Chemistry-Physics-Constitution*, Elsevier, Amsterdam.

van Niekerk, A., Holm, D., Hugo, J., Mokoena, L. and van Niekerk, W.,1994. Report: Trial Runs, Three Low-smoke Fules, Kagiso, Technical report, NOVA Institute.

van Niekerk, A., Swanepoel, P. and Kornelius, G.,1999. 'New Possibilities to Improve Air Quality in Low Income Housing and Reduce Greenhouse Gasses', *The Clean Air Journal* **10**(4), 21–27.

van Niekerk, D., Pugmire, R., Solum, M., Painter, P. and Mathews, J.,2008. 'Structural Characterization of Vitrinite-rich and Inertinite-rich Permian-aged South African Bituminous Coals', *International Journal of Coal Geology* **76**(4), 290 – 300.

van Niekerk, W.,2006. 'From Technology Transfer to Participative Design: A Case Study of Pollution Prevention in South African Townships', *Journal of Energy in Southern Africa* **17**(3), 58 – 64.

Varey, J. E., Hindmarsh, C. J. and Thomas, K.,1996. 'The Detection of Reactive Intermediates in the Combustion and Pyrolysis of Coals, Chars and Macerals', *Fuel* **75**(2), 164 – 176.

Vargas-Moreno, J., Callejon-ferre, A., Perez-Alonso, J. and Velazquez-Marti, B.,2012. 'A Review of the Mathematical Models for Predicting the Heating Value of Biomass Materials', *Renewable and Sustainable Energy Reviews* **16**(5), 3065–3083.

Vassilev, S. V. and Vassileva, C. G.,1996. 'Occurrence, Abundance and Origin of Minerals in Coals and Coal Ashes', *Fuel Processing Technology* **48**(2), 85 – 106.

Vejahati, F., Xu, Z. and Gupta, R.,2010. 'Trace Elements in Coal: Associations with Coal Minerals and their Behavior During Coal Utilization - A Review', *Fuel* **89**, 904–911.

VITA,1985. Testing the Efficiency of Wood-burning Cookstoves : International Standards., Technical report, Volunteers in Technical Assistance, VA.

von Holt, S.,1992. An Investigation into Column Floatation of South African Coals, MSc Thesis, University of Cape Town, South Africa.

Vorres, K. S.,1986. Chemistry of Mineral Matter and Ash in Coal: An Overview, *in* 'Mineral Matter and Ash in Coal', ACS Symposium Series; American Chemical Society, American Chemical Society: ACS, chapter 1, pp. 1–8.

Vovelle, C. and Delfau, J.,2000. Formation of Aromatics in Combustion Systems, *in* 'Polluntants form Combstion: Formation ad Impact on Atmospheric Chemistry', NATO Science Series C: Mathematical and Physical Sciences, Wiley, chapter 10, pp. 183–2014.

Wagner, N. J. and Hlatshwayo, B.,2005. 'The Occurrence of Potentially Hazardous Trace Elements in Five Highveld Coals, South Africa', *International Journal of Coal Geology* **63**(3–4), 228 – 246.

Wagner, N., Schoonraad, P., Swanepoel, P., van Niekerk, A., Scholtz, C., Kornelius, G., Julies, A., Pretorius, O., Wassemerman, J. and Muller, A.,2005. Results of Domestic Smoke Reduction Programme at eMbalenhle (Mpumalanga) and Zamdela (Free State), *in* 'Proceedings of the National Association for Clean Air (NACA) Annual Conference', pp. 29–30.

Wang, J., Lou, H. H., Yang, F. and Cheng, F.,2016. 'Development and Performance Evaluation of a Clean-burning Stove', *Journal of Cleaner Production* **134, Part B**, 447 – 455. Special Volume: Green and Sustainable Innovation for Cleaner Production in the Asia-Pacific Region.

Wang, X., Watson, J. G., Chow, J. C., Gronstal, S. and Kohl, S. D.,2012. 'An Efficient Multipollutant System for Measuring Real-World Emissions from Stationary and Mobile Sources', *Aerosol and Air Quality Research* **12**, 145–160.

Ward, C. R.,2002. 'Analysis and Significance of Mineral Matter in Coal Seams', *International Journal of Coal Geology* **50**(1–4), 135 – 168.

Wendt, J.,1980. 'Fundamental Coal Combustion Mechanisms and Polluntant Formation in Furnaces', *Progress in Energy and Combustion Scence* **6**, 201–222.

Wenzel, M.,2006. 'Granny Shows the Way: Results from Implementing an Alternative Firelighting Method in Orange Farm', *Journal of Energy in Southern Africa* .

Wernecke, B., Language, B., Piketh, S. and Burger, R.,2015. 'Indoor and Outdoor Particulate Matter Concentrations on the Mpumalanga Highveld -A Case Study', *The Clean Air Journal* **25**, 12 –16.

White, R.,2015. Changes in Chemical and Physical Properties of South African Coal during Pyrolysis, MSc Thesis, North West University, South Africa.

WHO,2002. 'Addressing the Links between Indoor Air Pollution, Household Energy and Human Health', Online at `http://www.who.int/mediacentre/events/HSD_Plaq_10.pdf?ua=1` Accessed 23 February 2017.

WHO,2014. 'Burden of Disease from Houshold Air Pollution for 2012.'. Avalaible Online at `http://www.who.int/phe/health_topics/outdoorair/databases/FINAL_HAP_AAP_BoD_24March2014.pdf` Acessed 23 February 2017.

Wielgosinski, G.,2012. Pollutant Formation in Combstion Processes, *in* Z. Nawaz and S. Naveed, eds, 'Advances in Chemical Engineering.', InTech, pp. 292–324. avalibale through InTechOpen at `https://www.intechopen.com/books/advances-in-chemical-engineering/pollutants-formation-in-combustion-processes` Accessed 29 May 2017.

Wijayanta, A., Saiful, A., Nakaso, K. and Fukai, J.,2010. 'Detailed Reaction Mechanisms of Coal

Volatile Combustion: Comparison between Without Soot and With Soot Models.', *Journal of Novel Carbon Resource Scinces* **2**, 8–11.

Williams, H., Pourkashanian, M., Jones, J. and Skorupska, N.,2000. *Combustion and Gasification of Coal*, Taylor & Francis: New York.

Winter, F., Prah, M. and Hofbauer, H.,1997. 'Temperature in Fuel Particles Burning in a Fluidized Bed: The Effect of Drying, Devolatilisation, and Char Combustion', *Combustion and Flame* **108**, 302–314.

Xu, M., Yu, D., Yao, H., Liu, X. and Qiao, Y.,2011. 'Coal Aerosol-generagted Aerosols: Formation and Properties', *Proceedings of the Combustion Institute* **33**, 1681–1697.

Yang, C., Li, S., Song, W. and Lin, W.,2013. 'Pyrolysis Behaviour of Large Coal Particles in a Lab-scale Bubbling Fluidized Bed.', *Energy and Fuel* **27**, 126–132.

Yi, H., Niansu, H., Peishen, L., Jie, L., Wan, Y., Jin, Y., Yanan, Y. and Guolu, U.,2007. Characteristics and Evolution of Sulphur Functionalities in Coal and Sewage Sludge during Combstion, *in* 'Challenges of Power Engineering and Environment: Proceedings of the International Conference on Power Engineering', Vol. 2, Springer, pp. 169–173.

Yu, D., Xu, M., Sui, J., Liu, X., Yu, Y. and Cao, Q.,2005. 'Effect of Particle Size on the Proximate Composition and Combstion Properties', *Thermochimica Acta* **439**, 103–109.

Yu, Y., Xu, M., Yao, H., Yu, D., Qiao, Y., Sui, J., Liu, X. and Cao, Q.,2007. 'Char Characteristics and Particulate Matter Formation duirng Chinese Bituminous Coal Combustion', *Proceedings of the Combustion Institute* **31**, 1947–1954.

Zajdlik, R., Jelemensky, L., Remiarova, B. and Markos, J.,2001. 'Experimental and Modelling Investigation of Single Coal Particle Combsution', *Chemical Engineering Science* **56**(4), 1355–1361.

Zhang, J. and Morawska, L.,2002. 'Combustion Sources of Particles: 2 Emission Factors and Measurement Methods', *Chemosphere* **49**, 1059–1074.

Zhang, J., Smith, K., Ma, Y., Se, S., Jiang, F., Qi, W., Liu, P., Khalil, M., Rasmussen, R. and Thorneleo, S.,2000. 'Greenhouse Gases and Other Airborne Pollutants from Household Stoves in China: A Database for Emission Factors', *Atmospheric Environment* **34**, 4537–4549.

Zhang, L., Huang, J., Fang, Y. and Y., W.,2006. 'Gasification Reactivity and Kinetics of Typical Anthracite Chars with Steam and CO_2', *Energy and Fuels* **20**, 1201–1210.

Zhou, C., Zhao, J., Li, X. and Shi, R.,2016. 'Effects of Catalyst on Combustion Reactivity of Anthracite and Cosl Char wit Low Combustibility at Low/High eating Rate', *Journal of Thermal Analysis and Calorimetry* **126**, 1469–1480.

Zhou, H., Huang, Y., Mo, G., Liao, Z. and Cen, K.,2013. 'Conversion of Fuel-N to N_2O and NO_x during Coal Combstion in Combustor of Different Scale', *Chinese Journal of Chemical Engineering* **21**(9), 999–1006.

Zhu, M., Zhang, H., Tang, G., Liu, Q., Lu, J., Yue, G., Wang, S. and Wan, S.,2009. 'Igni-

tion of Single Coal Particle in a Hot Furnace under Normal- and Micro-gravity Condition', *Proceedings of the Combustion Institute* **32**(2), 2029–2035.

Zhu, W., Song, W. and Lin, W.,2008. 'Effect of the Coal Particle Size on Pyrolysis and Char Reactivity for Two Types of Coal and Demineralized Coal', *Energy and Fuels* **22**, 2482–2487.

Zielke, C. W., Lebowitz, H., Struck, R. and Gorin, E.,1970. 'Sulphur Removal during Combustion of Solid Fuels in a Fluidised Bed of Dolomite', *Journal of the Air Pollution Control Association* **20**(3), 164–169.

Zygourakis, K.,2000. Mechanism and Optimisation of Coal Combustion, Final Technical Report Sumitted to the Department of Energy DE-GF22-96PC96214, Department of Chemical Engineering, Rice University.

Appendices

Appendix A

Coal And LSF Characterisation

A.1 Float and Sink Analysis Results

Float and sink analyses were performed by SGS Laboratories.

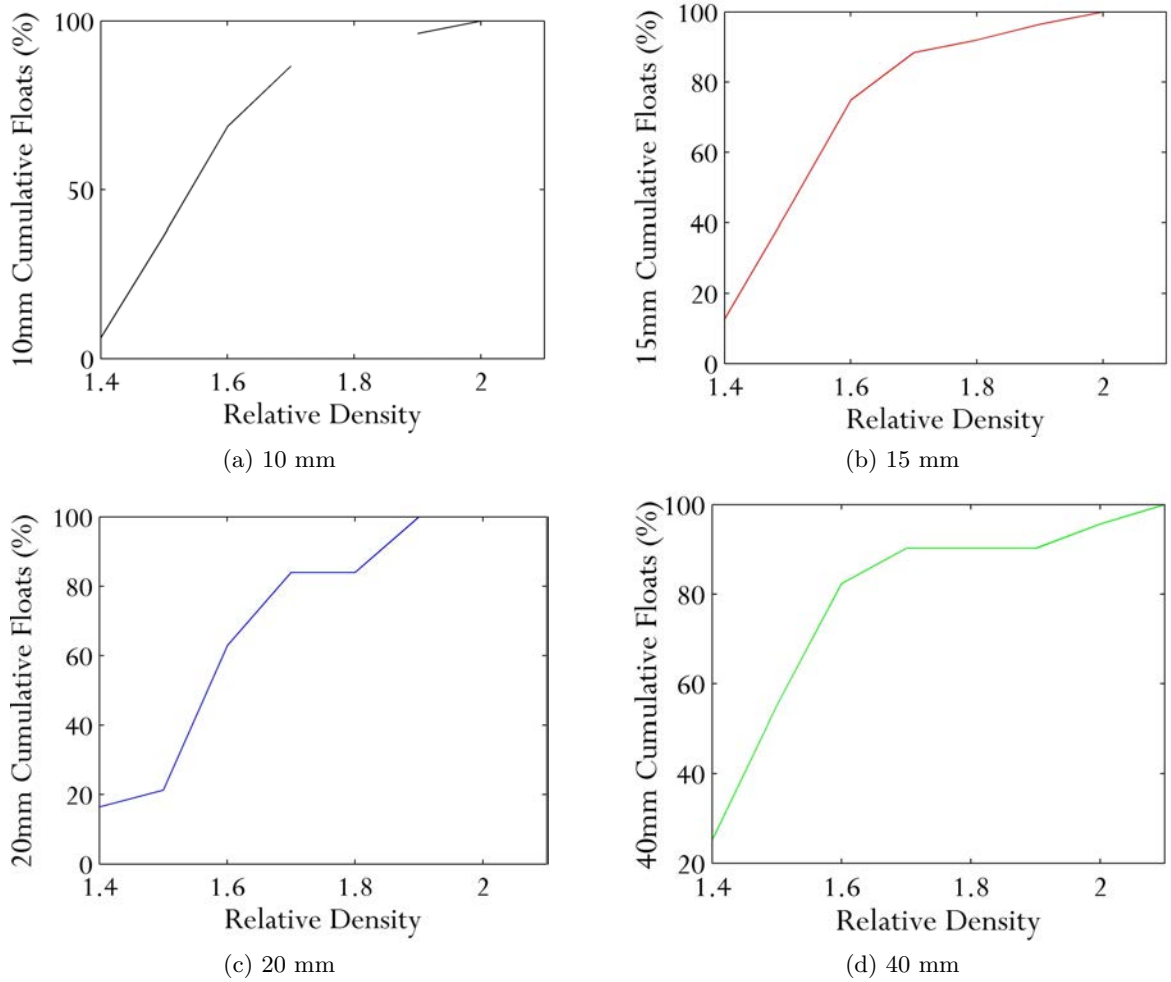

(a) 10 mm

(b) 15 mm

(c) 20 mm

(d) 40 mm

Figure A.1: Densimtric curves for all the size fractions

The aim of the sink and float analysis was to determine which size fraction would yield the

largest "homogenised" sample for the calibration of instruments. Figure B.3 shows that all the size fractions had at least 60% of the particle reporting to the desired relative density range of 1.4-1.6. However, taking into account the abundance of the fractions according to the PSD, the 30 mm particles were chosen. Based on these results, it can be argued that the parent sample may have been dry cleaned, removing shale and rock as well as particles with higher densities. The low sulphur (especially of pyritic sulphur) content of the parent coal sample is consistent with this theory.

A.2 Chemical Analyses Results and Conversions

The results obtained from the proximate and ultimate analysis are reported on an air dry basis as this is the state at which the coal is most stable, however, for discussions and comparison, other bases are preferred. Table A.1 provides the untreated results from these analyses.
Conversion to the different bases were done as suggested by Speight [2005]. in the following equations, X is any property determined by conventional means, M is moisture, A is ash, S is sulphur, MM is mineral matter, FC is fixed carbon, and VM is volatile mater.

To convert to a dry basis (d.b), the moisture is eliminated from the total mass:

$$X_{d.b} = X_{a.d} * \frac{100}{100 - M_{a.d}}$$

To convert to dry, ash free basis (d.a.f) from the a.d results, both the moisture and the ash are eliminated

$$X_{d.a.f} = X_{d.b} * \frac{100}{100 - A_{d.b}}$$

In order to use the calorific value for the determination of the rank of the coal, the Parr formula is used to determine the mineral matter which is then excluded to express the properties on a dry, mineral matter free basis (dmmf),

$$MM = 1.08A + 0.5S$$

then

$$X_{dmmf} = X_{d.b} * \frac{100}{100 - MM}$$

For the determination of FC and VM on a dmmf v=basis, it is assumed that 50% of the sulphur is released during the VM tests and should therefore not be conted as part of the organic VM

$$FC_{dmmf} = \frac{100(FC_{d.b} - 0.15S)}{100 - (M + MM)}$$

and

$$VM_{dmmf} = 100 - FC_{dmmf}$$

Table A.1: Chemical analyses results on an air-dried basis

	Parent Coal	MixedCoal	15Coal	20Coal	30Coal	40Coal	MixedLSF	15LSF	20LSF	30LSF	40LSF
Proximate Analysis (d.a.f)											
% Inherent moisture content	2.6	3.10	2.20	2.30	2.30	2.20	1.00	0.60	0.70	0.70	0.60
% Ash content	24.0	24.10	26.80	23.40	23.30	25.60	28.60	33.30	25.70	30.50	32.80
% Volatile Matter	24.4	28.50	24.30	23.90	25.90	27.20	9.10	9.80	9.50	10.90	12.40
%Fixed carbon (by calculation)	49.0	44.30	46.70	50.40	48.50	45.00	61.30	56.30	64.10	57.90	54.30
Ultimate Analysis (d.a.f)											
e % Carbon Content	58.0	56.86	55.70	59.30	58.10	55.80	61.18	57.90	65.40	59.40	57.20
% Hydrogen Content	3.23	3.36	2.96	3.18	3.17	3.05	1.93	1.51	1.71	1.56	1.79
% Nitrogen Content	1.39	1.33	1.38	1.44	1.43	1.37	1.49	1.44	1.59	1.56	1.36
% Oxygen Content (by calculation)	10.47	10.18	8.26	9.86	9.84	8.22	4.96	3.65	3.75	6.01	2.58
Forms of Sulphur											
% Pyritical Sulphur	0.06										
% Sulphatic Sulphur	0										
% Organic Sulphur	0.31										
% Total sulphur	0.37	1.16	2.15	1.08	1.85	3.84	0.84	1.61	0.58	0.33	3.71
Gross Calorific Value (MJ/kg)	22.84	22.13	21.88	23.19	23.16	21.93	23.24	21.84	24.48	22.00	21.84
Crucible Swelling Number (CNS)	0										
Calculated Properties											
Fuel ratio	2.0	1.6	1.9	2.1	1.9	1.7	6.7	5.7	6.7	5.3	4.4
Atomic H/C ratio	0.7	0.7	0.6	0.6	0.7	0.7	0.4	0.3	0.3	0.3	0.4
Atomic O/C ratio	0.1	0.1	0.1	0.1	0.1	0.1	0.1	0.0	0.0	0.1	0.0

A.3 ASTM Rank Classification

The rank classification of each fuel was determined using the ASTM D388 standard, making use of the % FC and % VM. Table A.2 shows the results. Fixed carbon (FC) and volatile matter (VM) composition are given on a dry mineral-matter free basis. In the case of the LSFs, the standard indicates that for coals with % FC >69 %, the FC classification is to be used, regardless of what the CV classification yields.

Table A.2: Rank Classification by ASTM D388 Standard

	Fixed Carbon		Volatile Matter		Calorific Value	
	[%]	Rank	[%]	Rank	[MJ/kg]	RanK
Parent Coal	66.1		33.9		13 194	
Comp Coal	59.9		40.1		12 674	
15mmCoal	64.3		35.7		12 873	B and C
20mmCoal	67.1	A	32.9	B	13 171	
30mmCoal	67.2		35.9		13 005	
40mmCoal	65.5		39.6		13 404	
CompChar	90.2		13.4		14 300	
15mmChar	89.7		15.6		14 339	
20mmChar	90.1	B	13.4	C	14 464	B and C
30mmChar	87.3		16.4		14 042	
40mmChar	87.4		19.9		13 816	

A=semianthracite, B=High Volatile A Bituminous, C=Low Volatile Bituminous

A.4 Mineral Matter Diffractograms

Figure A.2 shows the chromatograph used to determine the mineral matter of the parent coal showing the number of counts on the y-axis.

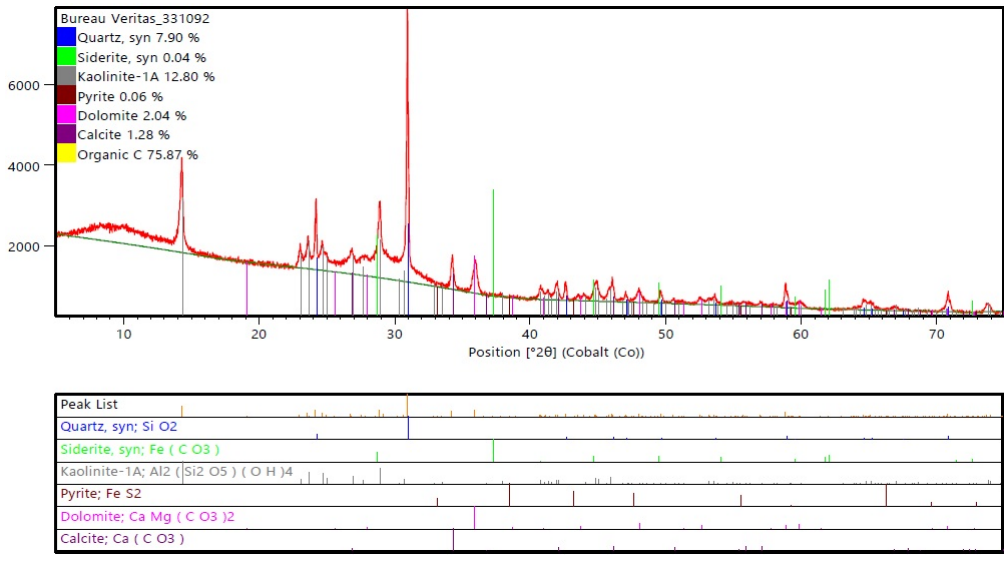

Figure A.2: Parent Coal Sample XRD Chromatograph

Appendix B

Thermogravimetric Analyses Repeatability Curves

Each experiment was repeated until at least two profiles were obtained. The average of the runs is then reported.

B.1 Pyrolysis Repeatability Curves

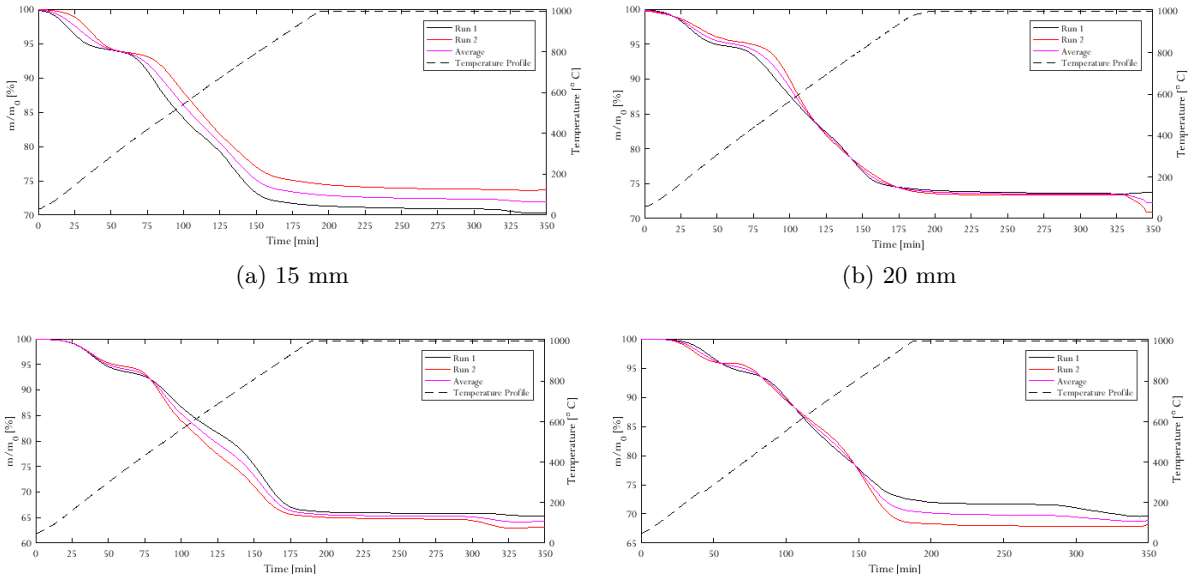

(a) 15 mm

(b) 20 mm

(c) 30 mm

(d) 40 mm

Figure B.1: Repetition results of pyrolysis experiments

B.2 Coal Combustion Repeatability Curves

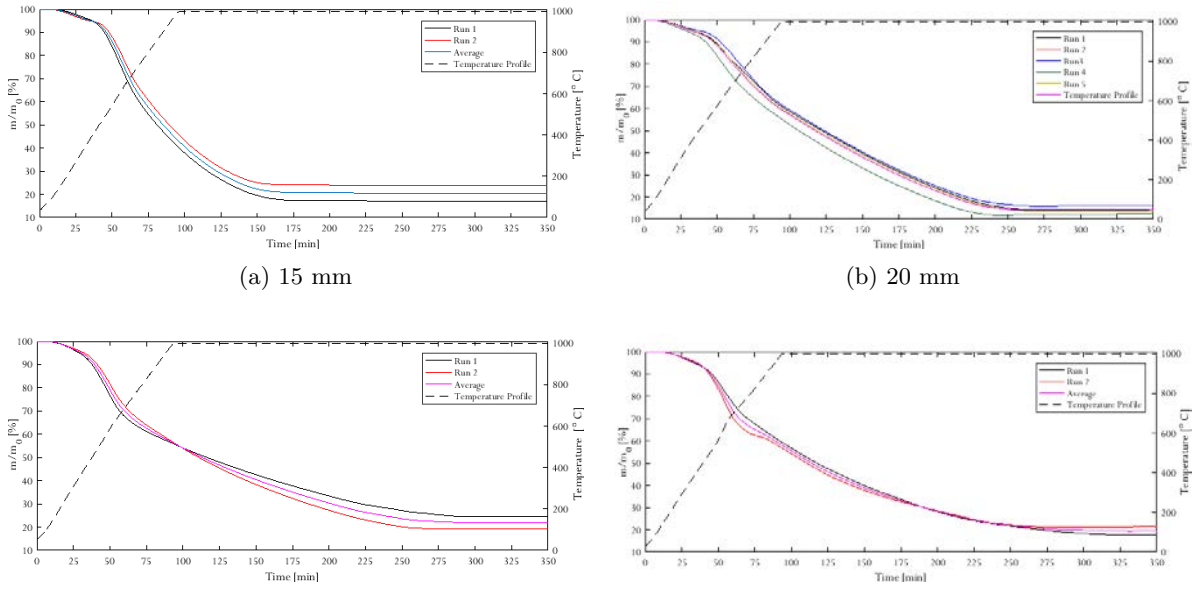

(a) 15 mm

(b) 20 mm

(c) 30 mm

(d) 40 mm

Figure B.2: Repetition results of coal combustion experiments

B.3 LSF Combustion Repeatability Curves

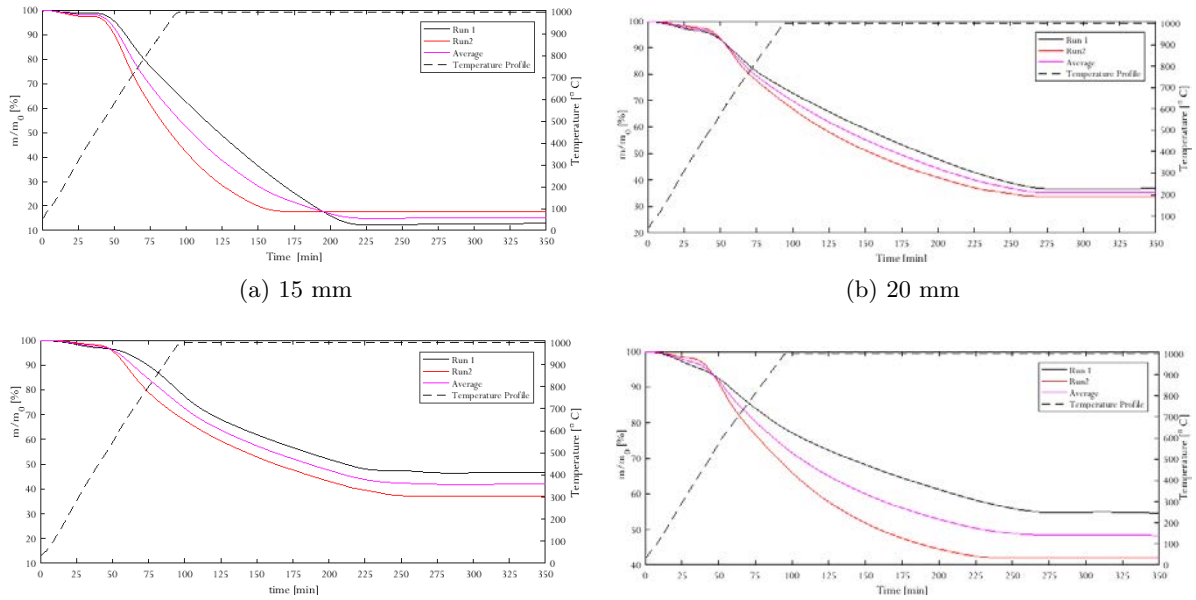

(a) 15 mm

(b) 20 mm

(c) 30 mm

(d) 40 mm

Figure B.3: Repetition results of coal combustion experiments

Appendix C

Combustion Tests: Calibrations and Quality Control

Auxiliary information regarding the experimental setup and data processing for the combustion tests is shown in this Appendix.

C.1 MATLAB^{TM} Script for Emission Concentration Conversions

The gas anaysers report emissions values on in units of ppm (NO_x, CO, SO_2) and vol% (O_2, CO_2). In order to determine the amount in gram, for the determination of emission factors, the HTP does a series of computations for each task segment, employing the measured emission concentrations, fuel characteristics and the stoichiometry of the formation of each pollutant. These calculations were adapted into a MATLAB^{TM} executable script in order to express the EFs as a curve spanning the entire length of the test. The input is a text file containing the measured emission in ppm (and mg for PM), the moisture-, hydrogen- and oxygen composition, as well as the gross calorific and lower heating value of the fuel and the output is a text file containing the EF curve (g/kf or g/MJ) for each pollutant

```
function EmissionFactors = efcurves(Moist,Hyd,Oxy, GCV,LHV)
%computatons to convert the measured ppm concentrations of pullutants to g
%and then to determine the EF on a mass or energy yielded basis. Tests in
%[] brackets indicate the cells on the HTP spreadsheet where the relavant
%data can be found or where the calculation is perfomed.
%Moist = fuel moisture  [Fuels!C16]
%Hyd = fuel hydrogen    [Fuels!C19]
%Oxy =  fuel oxygen     [Fuels!C29]
%GCV =  fuel GCV        [Fuels!C30]
%LHV =  fuel LHV        [Fuels!C26]

EFCurve = importdata('EFCurve.txt','\t',1);  %imports the input file
Time = EFCurve.data(:,1);                    %extract each ppm column
```

```
CO2 = EFCurve.data(:,2);
SO2 = EFCurve.data(:,3);
NOx = EFCurve.data(:,4);
CO = EFCurve.data(:,5);
PM = EFCurve.data(:,6);          %mg
MassCons = EFCurve.data(:,7);    %kg
NetHeatRel = EFCurve.data(:,8); %MJ

%step 1: mass element detected in each gas [Perfomance!C66]
CO2_det = CO2.*12;
SO2_det = SO2.*32;
NOx_det = NOx.*12;
CO_det  = CO.*12;

%step 2: determine teh mass of combustible material (C,S,N) in detected gas
%ash and CNS corrected mass [Perfomance!C68]
CorretedMassCons = MassCons.*(LHV/GCV);
%Mass of combustibles in consumed fuel [Perfomance!C69]
MassCombustibleElements = CO2_det + SO2_det + NOx_det + CO_det;

%step 3: estimation of gas plume mass (incl H and O)
Orig_Moist = (Moist/100)*(GCV/LHV);   %[Perfomance!K75]
Orig_Oxy = (Oxy/100)*(GCV/LHV);       %[Perfomance!L75]
EstimatedTotalEmission = MassCombustibleElements./(1 - Orig_Moist -...
    Orig_Oxy - ((Hyd/100)*(GCV/LHV))); %[Perfomance!C70]

%step 4: mass of each pollutant emistted
Orig_CO2 = CO2_det./EstimatedTotalEmission;              %[Perfomance!C76]
MassCO2_Emitted = (CorretedMassCons.*Orig_CO2)./(12*44); %[Performance!C77]

Orig_SO2 = SO2_det./EstimatedTotalEmission;              %[Perfomance!D76]
MassSO2_Emitted = (CorretedMassCons.*Orig_SO2)./(32*64); %[Performance!D77]

Orig_NOx = NOx_det./EstimatedTotalEmission;              %[Perfomance!E76]
MassNOx_Emitted = (CorretedMassCons.*Orig_NOx)./(14*30); %[Performance!E77]

Orig_CO = CO_det./EstimatedTotalEmission;              %[Perfomance!G76]
MassCO_Emitted = (CorretedMassCons.*Orig_CO)./(12*26); %[Performance!G77]

%step5 determine the EF by dividing by mas or energy
EFCO2_mass = MassCO2_Emitted./MassCons;
EFSO2_mass = MassSO2_Emitted./MassCons;
EFNOx_mass = MassNOx_Emitted./MassCons;
```

```
EFCO_mass = MassCO_Emitted./MassCons;
EFPM_mass  = PM./MassCons;

EFCO2_energy = MassCO2_Emitted./NetHeatRel;
EFSO2_energy = MassSO2_Emitted./NetHeatRel;
EFNOx_energy = MassNOx_Emitted./NetHeatRel;
EFCO_energy = MassCO_Emitted./NetHeatRel;
EFPM_energy = PM./NetHeatRel;

dlmwrite('EF_OutputR1.txt',[Time EFCO2_mass EFSO2_mass EFNOx_mass ...
    EFCO_mass EFPM_mass EFCO2_energy EFSO2_energy EFNOx_energy ...
    EFCO_energy EFPM_energy])
```

C.2 Gas Analyser Calibration Gas Certificates

Calibration gases for the two gas analysers were supplied by Air Liquide South Africa. Gases were specified to be within the range of typical household emission concentrations as well as within the limits of the instruments. The analysis certificates are photographed and shown in Figure C.1

Figure C.1: Calibration gas analysis certificates as supplied by Air Liquide.

C.3 Gas Supply System Calibration

Figure C.2 shows the complete ignition gas supply system.

Figure C.2: Ignition Gas Supply system

The rotameter was calibrated using a bubble flow meter. For this calibration, the outlet of the rota meter is connected to a open-ended cylindrical tube of known volume with a soap solution at the bottom. The rotameter is set to a specific set point and the flowing gas causes a bubble to form and traverse the length of the cylinder. The time taken for a single bubble to travel through a known volume is measured and Equation C.3 can be used to determine the exact flow at each set-point of the flow meter; where y is the volume covered by the bubble and t is the time taken to do so.

$$Q\ (\text{mL.min}^{-1}) \ = \ 60\text{x}\left[\frac{\text{y (mL)}}{\text{t (sec)}}\right] \tag{C.1}$$

A calibration curve is constructed by taking such readings for several set point. Figure C.3 shows typical calibration curves. Gas was fed at a flow rate of 4.5-5 normal litres per minute.

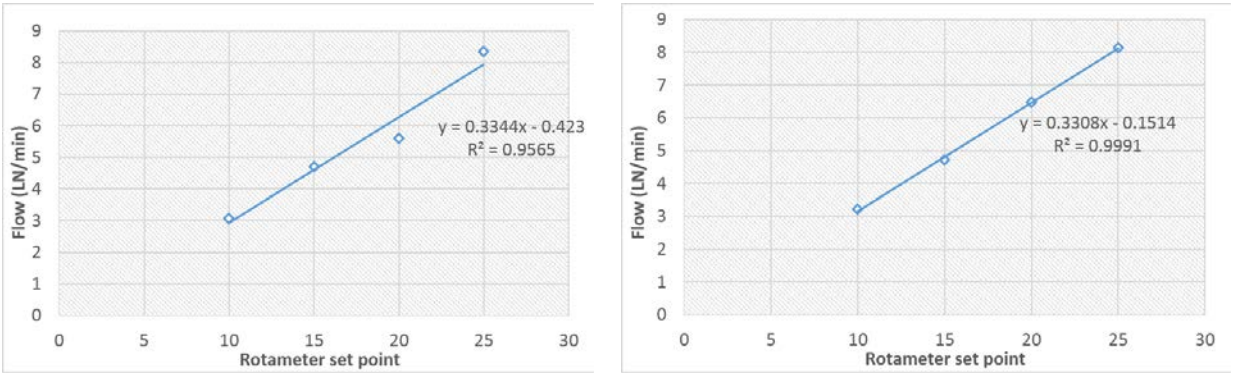

(a) Calibration Curve 1

(b) Calibration Curve 2

Figure C.3: Typical LPG Rotameter Calbration Curves

Appendix D

Combustion Tests: Results and Discussion

Further information and graphs pertaining to the results of the combustion tests will be shown in this Appendix.

D.1 Water Boiling and Ignition Times Standard Errors

The time series plots for the water boiling procedure of each of the fuels is shown in figure **??** along with the relative lengths of each of the three task segments. Table D.1 contains the results for all 30 experiments and their standard error, while Table D.2 shows the same information for the ignition times.

Table D.1: All Fuels: Water Boiling Times and Standard Error Calculation

	Run No	Boiling Time [min]			Mass Evaporated [g]				Run No	Boiling Time [min]			Mass Evaporated [g]		
		Pot 1	*Pot 2*	*Cooking*	*Pot 1*	*Pot 2*	*Cooking*			*Pot 1*	*Pot 2*	*Cooking*	*Pot 1*	*Pot 2*	*Cooking*
15mmCoal	1	27.37	29.22	56.59	0.00	20.00	20.00	**15mmLSF**	1	37.78	38.62	76.40	0.00	0.00	0.00
	2	44.00	38.67	82.67	0.00	0.00	0.00		2	25.01	30.01	55.02	0.00	20.00	20.00
	3	18.10	25.75	43.85	0.00	100.00	100.00		3	51.52	45.92	97.44	60.00	60.00	120.00
	Ave	29.82	31.21	61.04	0.00	40.00	40.00		Ave	31.39	34.32	65.71	20.00	26.67	46.67
	Std Dev	13.12	6.69	19.79	0.00	52.92	52.92		Std Dev	9.03	6.09	15.12	34.64	30.55	64.29
	Std Error	9.28	4.73	13.99	0.00	37.42	37.42		Std Error	6.39	4.31	10.69	24.49	21.60	45.46
20mmCoal	1	19.75	22.80	42.55	0.00	20.00	20.00	**20mmLSF**	1	27.00	19.17	46.17	0.00	0.00	0.00
	2	26.67	21.83	48.50	0.00	0.00	0.00		2	23.80	32.23	56.03	0.00	20.00	20.00
	3	29.00	24.87	53.87	0.00	100.00	100.00		3	21.58	16.33	37.91	0.00	0.00	0.00
	Ave	25.14	23.17	48.31	0.00	40.00	40.00		Ave	24.13	22.58	46.70	0.00	6.67	6.67
	Std Dev	4.81	1.55	5.66	0.00	52.92	52.92		Std Dev	2.72	8.48	9.07	0.00	11.55	11.55
	Std Error	3.40	1.10	4.00	0.00	37.42	37.42		Std Error	1.93	6.00	6.41	0.00	8.16	8.16
30mmCoal	1	20.83	21.67	42.50	120.00	20.00	140.00	**30mmLSF**	1	28.70	19.01	47.71	0.00	0.00	0.00
	2	25.17	24.00	49.17	0.00	20.00	20.00		2	33.75	19.80	53.55	0.00	20.00	20.00
	3	16.57	16.83	33.40	0.00	0.00	0.00		3	21.55	16.67	38.22	0.00	0.00	0.00
	Ave	20.86	20.83	41.69	40.00	13.33	53.33		Ave	28.00	18.49	46.49	0.00	6.67	6.67
	Std Dev	4.30	3.66	7.92	69.28	11.55	75.72		Std Dev	6.13	1.63	7.74	0.00	11.55	11.55
	Std Error	3.04	2.59	5.60	48.99	8.16	53.54		Std Error	4.33	1.15	5.47	0.00	8.16	8.16
40mmCoal	1	25.67	18.92	44.59	0.00	0.00	0.00	**40mmLSF**	1	23.75	24.67	48.42	20.00	20.00	40.00
	2	20.53	18.42	38.95	0.00	20.00	20.00		2	21.17	22.50	43.67	20.00	20.00	40.00
	3	30.00	21.58	51.58	0.00	0.00	0.00		3	19.00	23.92	42.92	0.00	20.00	20.00
	Ave	25.40	19.64	45.04	0.00	6.67	6.67		Ave	21.31	23.70	45.00	13.33	20.00	33.33
	Std Dev	4.74	1.70	6.33	0.00	11.55	11.55		Std Dev	2.38	1.10	2.98	11.55	0.00	11.55
	Std Error	3.35	1.20	4.47	0.00	8.16	8.16		Std Error	1.68	0.78	2.11	8.16	0.00	8.16
CompCoal	1	23.22	30.92	54.14	0.00	0.00	0.00	**CompLSF**	1	27.67	26.37	54.04	0.00	0.00	0.00
	2	15.92	20.08	36.00	20.00	0.00	20.00		2	35.08	25.08	60.16	0.00	0.00	0.00
	3	11.75	16.83	28.58	0.00	0.00	0.00		3	22.75	17.25	40.00	40.00	0.00	40.00
	Ave	16.96	22.61	32.29	6.67	0.00	6.67		Ave	28.50	22.90	51.40	13.33	0.00	13.33
	Std Dev	5.81	7.38	5.25	11.55	0.00	11.55		Std Dev	6.21	4.94	10.34	23.09	0.00	23.09
	Std Error	4.11	5.22	3.71	8.16	0.00	8.16		Std Error	4.39	3.49	7.31	16.33	0.00	16.33

Table D.2: All Fuels: Ignition Times and Standard Error Calculation

	Run No	Ignition Gas		Ignition Time		Run No	Ignition Gas		Ignition Time
		Mass [g]	*Flow Rate [L.min]*	*[min]*			*Mass [g]*	*Flow Rate [L.min]*	*[min]*
15mmCoal	1	0.68	3.92	45.32	**15mmLSF**	1	0.48	4.93	23.95
	2	0.80	3.92	53.58		2	0.64	4.93	33.25
	3	0.94	3.92	51.00		3	0.30	4.26	23.58
	Ave	0.81	3.92	49.97		Ave	0.47	4.70	26.93
	Std Dev	0.13	0.00	4.23		Std Dev	0.17	0.39	5.48
	Std Error	0.08	0.00	2.44		Std Error	0.10	0.22	3.16
20mmCoal	1	0.66	4.59	36.00	**20mmLSF**	1	0.36	3.92	25.33
	2	0.54	4.59	44.50		2	0.52	4.93	23.58
	3	0.58	4.93	33.25		3	0.56	4.93	26.25
	Ave	0.59	4.70	37.92		Ave	0.48	4.59	25.05
	Std Dev	0.06	0.19	5.86		Std Dev	0.11	0.58	1.36
	Std Error	0.04	0.11	3.39		Std Error	0.06	0.33	0.78
30mmCoal	1	0.44	5.09	30.00	**30mmLSF**	1	0.32	4.93	15.25
	2	0.40	4.93	34.00		2	0.26	4.93	17.00
	3	0.44	4.93	24.30		3	0.34	4.93	14.15
	Ave	0.43	4.98	29.43		Ave	0.31	4.93	15.47
	Std Dev	0.02	0.10	4.87		Std Dev	0.04	0.00	1.44
	Std Error	0.01	0.06	2.81		Std Error	0.02	0.00	0.83
40mmCoal	1	0.22	4.76	10.75	**40mmLSF**	1	0.30	3.92	29.83
	2	0.36	4.93	15.63		2	0.40	4.93	23.25
	3	0.26	4.93	11.83		3	0.32	4.93	15.78
	Ave	0.28	4.87	12.74		Ave	0.34	4.59	22.95
	Std Dev	0.07	0.10	2.56		Std Dev	0.05	0.58	7.03
	Std Error	0.04	0.06	1.48		Std Error	0.03	0.33	4.06
CompCoal	1	0.44	4.43	26.92	**CompLSF**	1	0.26	3.92	24.25
	2	0.46	4.26	25.72		2	0.50	4.93	25.23
	3	0.58	4.93	29.58		3	0.60	4.93	29.67
	Ave	0.49	4.54	27.41		Ave	0.45	4.59	26.38
	Std Dev	0.08	0.35	1.98		Std Dev	0.17	0.58	2.89
	Std Error	0.04	0.20	1.14		Std Error	0.10	0.33	1.67

D.2 Mass Consumption Rates

The normalised mass remaining for all the fuels are shown in Figure D.1 The % normalised masses untreated (ash content not accounted for) mass for each of the fuels are shown in FigureD.1. These are given on a % basis as the fuel loading was not the same for all the fuels.

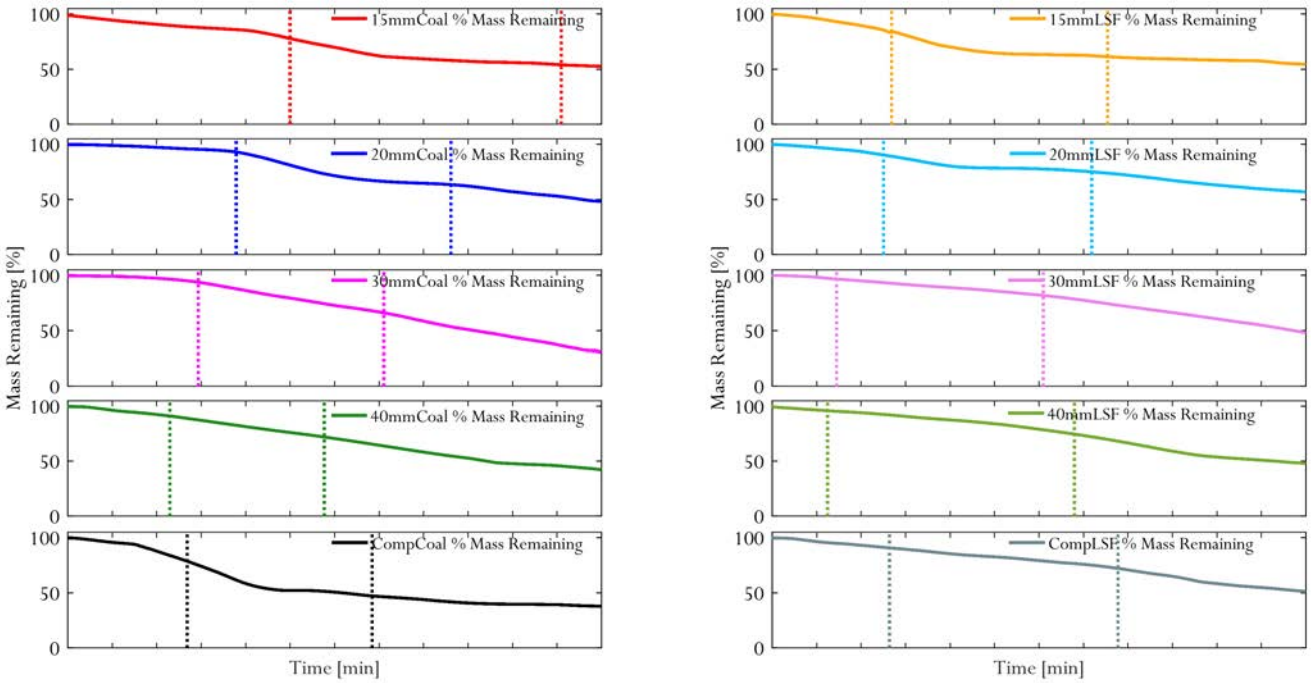

Figure D.1: Normalised Mass [%] Remaining.

D.3 Heat Curves

The following plots show the differences between the total heat released form combustion and (a) the total usable heat delivered, the total heat delivered as (b) cooking energy, and (c) radiant heat. Tables D.3 and D.4 show the energy and power output results for all 30 experiences along with the determination of standard errors.

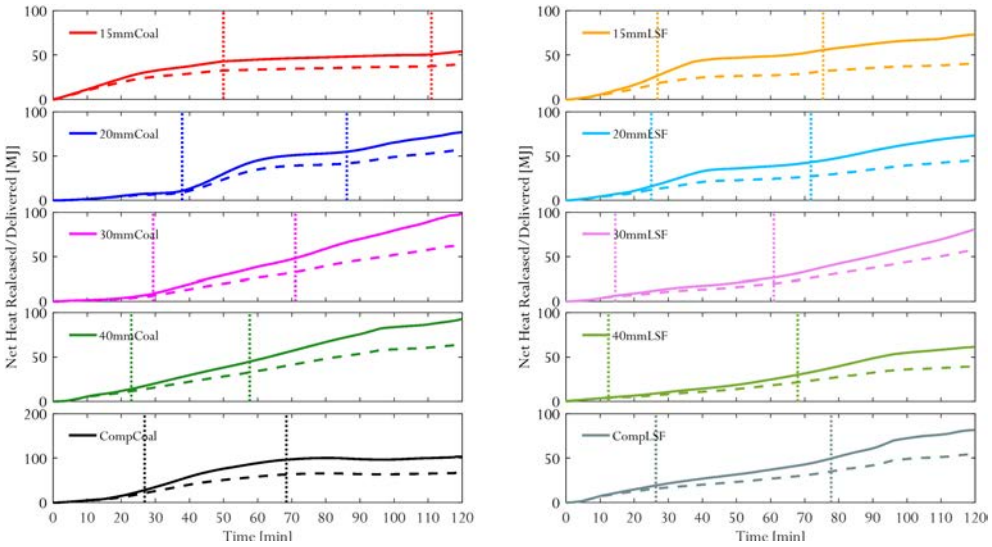

(a) Combustion Heat Released and Net Usable Heat Delivered

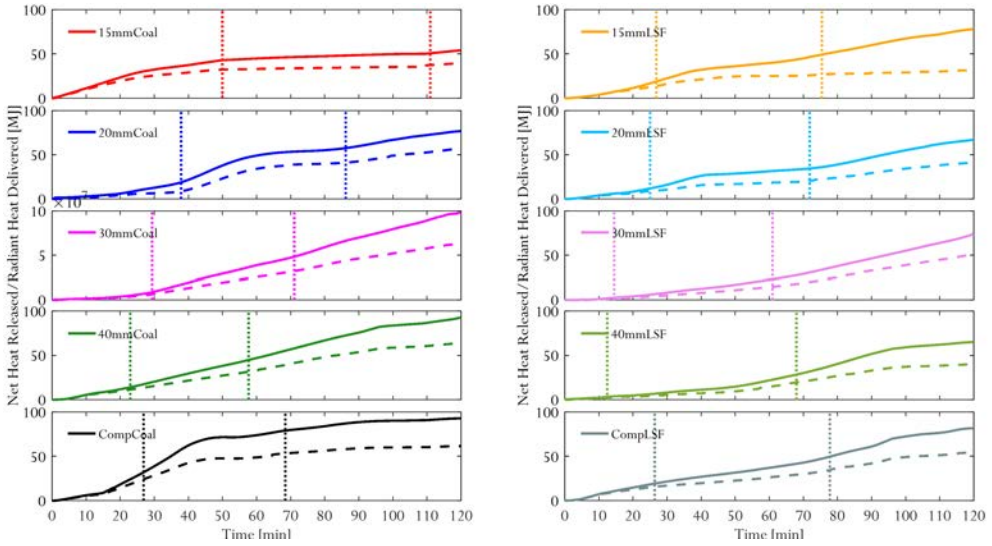

(b) Combustion Heat Released and Net Radiant Heat Delivered

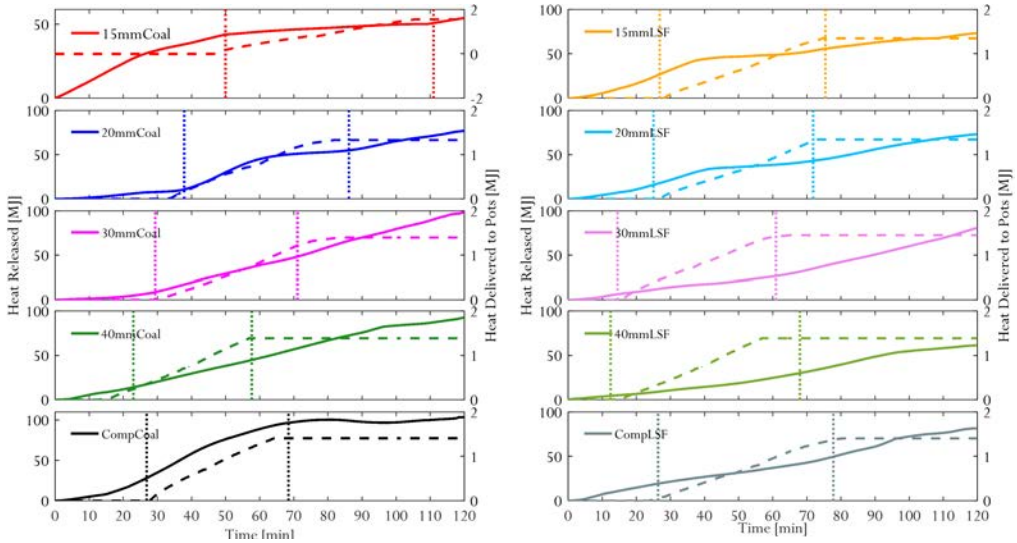

(c) Combustion Heat Released and Net Cooking Heat Delivered

Figure D.2: Total Combustion Heat Released and Net Usable Heat Delivered, the solid lines show the total heat released through combustion and the dashed lines show the (a) net usable heat delivered for(b) heating, and (c) cooking

Table D.3: Coals: Error Calculations for Thermal Properties

	Run No	Heat [MJ]				Power [kW]		
		Yielded	*Radiant*	*Cooking*	*Delivered*	*Fire*	*Heating*	*Cooking*
15mmCoal	1	54.67	38.80	1.60	40.40	7.50	5.3	0.42
	2	56.52	33.20	1.27	34.47	6.70	3.9	0.25
	3				0.00			
	Ave	55.60	36.00	1.44	37.44	7.10	4.60	0.34
	Std Dev	1.31	3.96	0.23	4.19	0.57	0.99	0.12
	Std Error	0.93	2.80	0.17	2.97	0.40	0.70	0.09
20mmCoal	1				0.00			
	2	50.58	37.70	1.50	39.20	7.00	5.2	0.47
	3	76.70	49.20	1.30	50.50	10.60	6.8	0.39
	Ave	63.64	43.45	1.40	44.85	8.80	6.00	0.43
	Std Dev	18.47	8.13	0.14	7.99	2.55	1.13	0.06
	Std Error	13.06	5.75	0.10	5.65	1.80	0.80	0.04
30mmCoal	1	110.20	64.10	1.40	65.50	15.20	8.8	0.48
	2	96.16	64.40	1.40	65.80	13.20	8.9	0.45
	3	89.37	59.70	1.20	60.90	12.30	8.2	0.56
	Ave	98.58	62.73	1.33	64.07	13.57	8.63	0.50
	Std Dev	10.62	2.63	0.12	2.75	1.48	0.38	0.06
	Std Error	6.13	1.52	0.07	1.59	0.86	0.22	0.03
40mmCoal	1	54.21	38.50	1.40	39.90	7.50	5.3	0.53
	2	67.61	45.90	1.40	47.30	9.30	6.3	0.56
	3	63.05	34.20	1.40	35.60	8.70	4.7	0.44
	Ave	61.62	39.53	1.40	40.93	8.50	5.43	0.51
	Std Dev	6.81	5.92	0.00	5.92	0.92	0.81	0.06
	Std Error	3.93	3.42	0.00	3.42	0.53	0.47	0.04
CompCoal	1	90.61	62.60	1.40	64.00	12.50	8.6	0.38
	2	93.11	61.70	1.40	63.10	12.80	8.5	0.63
	3	114.68	73.30	1.40	74.70	15.80	10.1	0.78
	Ave	99.47	65.87	1.40	67.27	13.70	9.07	0.60
	Std Dev	13.23	6.45	0.00	6.45	1.82	0.90	0.20
	Std Error	7.64	3.73	0.00	3.73	1.05	0.52	0.12

Table D.4: LSFs: Error Calculations for Thermal Properties

	Run No	Heat [MJ]				Power [kW]		
		Yielded	*Radiant*	*Cooking*	*Delivered*	*Fire*	*Heating*	*Cooking*
15mmLSF	1	61.58	28.60	1.30	29.90	8.50	3.9	0.28
	2	55.39	32.90	1.40	34.30	7.60	4.5	0.40
	3	84.05	51.90	1.30	53.20	11.60	7.1	0.55
	Ave	58.49	30.75	1.33	39.13	9.23	5.17	0.41
	Std Dev	4.38	3.04	0.06	12.38	2.10	1.70	0.14
	Std Error	2.53	1.76	0.03	7.15	1.21	0.98	0.08
20mmLSF	1	66.19	40.70	1.40	42.10	9.10	5.6	0.49
	2	67.23	41.50	1.40	42.90	9.30	5.7	0.48
	3	85.67	52.90	1.30	54.20	11.80	7.3	0.55
	Ave	73.03	45.03	1.37	46.40	10.07	6.20	0.51
	Std Dev	10.96	6.82	0.06	6.77	1.50	0.95	0.04
	Std Error	6.33	3.94	0.03	3.91	0.87	0.55	0.02
30mmLSF	1	84.08	60.20	1.40	61.60	11.60	8.30	0.48
	2	66.70	45.00	1.40	46.40	9.20	6.20	0.48
	3	81.80	59.10	1.30	60.40	11.30	8.1	0.53
	Ave	77.53	54.77	1.37	56.13	10.70	7.53	0.50
	Std Dev	9.45	8.48	0.06	8.45	1.31	1.16	0.03
	Std Error	5.45	4.89	0.03	4.88	0.75	0.67	0.02
40mmLSF	1	87.26	59.00	1.50	60.50	12.00	8.1	0.51
	2	101.54	70.40	1.40	71.80	14.00	9.7	0.54
	3	92.11	65.90	1.40	67.30	12.70	9.1	0.53
	Ave	93.64	65.10	1.43	66.53	12.90	8.97	0.53
	Std Dev	7.26	5.74	0.06	5.69	1.01	0.81	0.02
	Std Error	4.19	3.32	0.03	3.28	0.59	0.47	0.01
CompLSF	1	80.47	53.20	1.50	54.70	11.10	7.3	0.45
	2	70.25	44.10	1.40	45.50	9.70	6.1	0.41
	3	94.46	65.60	1.40	67.00	13.00	9	0.51
	Ave	81.73	54.30	1.43	55.73	11.27	7.47	0.46
	Std Dev	12.15	10.79	0.06	10.79	1.66	1.46	0.05
	Std Error	7.02	6.23	0.03	6.23	0.96	0.84	0.03

D.4 Pollutant Emission Factors

The time series plots for the CO, CO_2, and PM EF are shown below and the full suite of species identified from the VOC analysis are presented in Tables D.5 and D.6

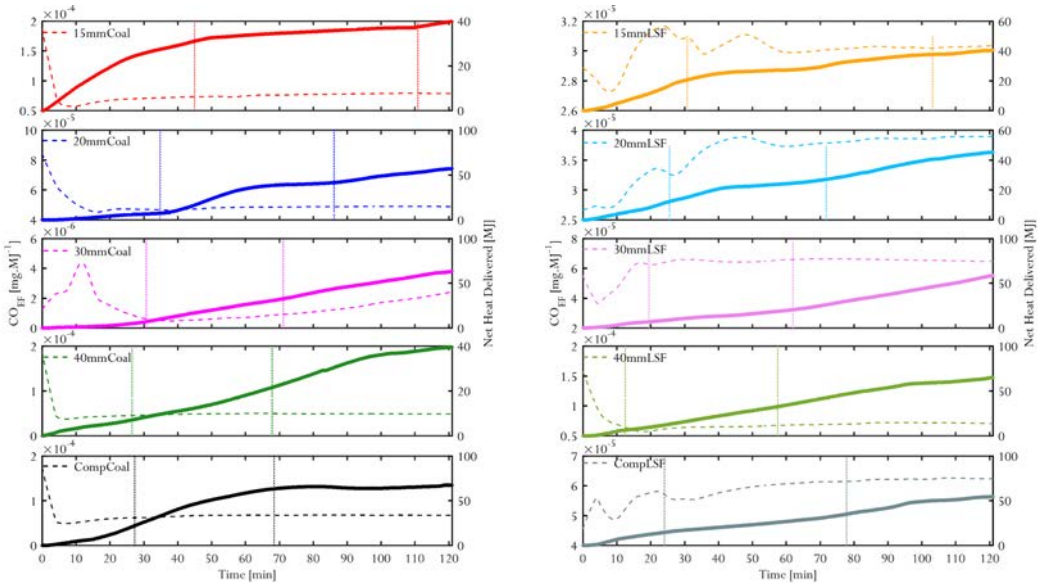

Figure D.3: Time series plots of the CO [g/MJ] emission factors. The EFs are shown as the dashed lines against the left-hand side axes and the solid lines along the right-hand side axes are the net heat delivered for cooking and heating.

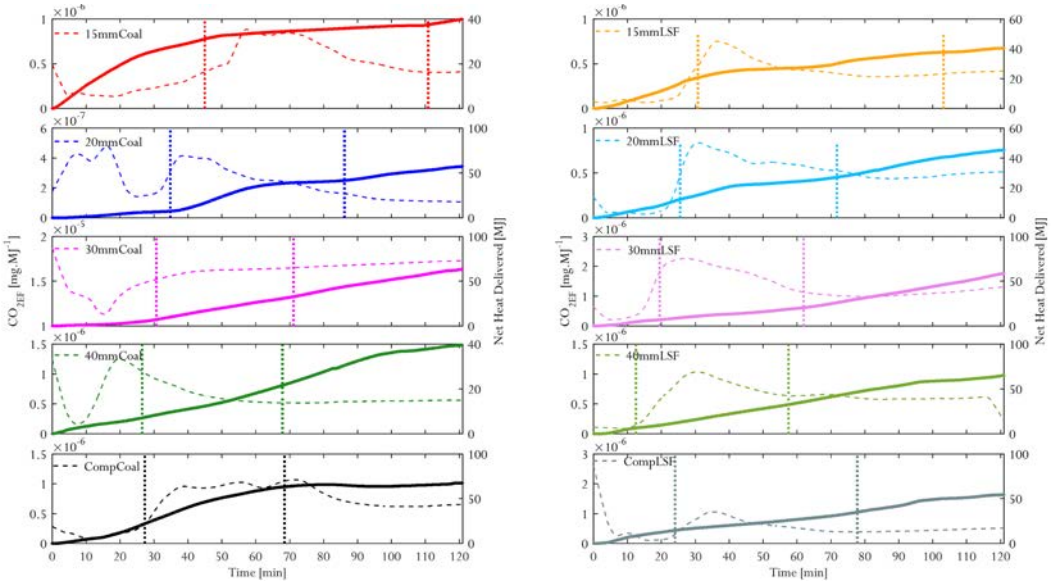

Figure D.4: Time series plots of the CO_2 [g/MJ] emission factors. The EFs are shown as the dashed lines against the left-hand side axes and the solid lines along the right-hand side axes are the net heat delivered for cooking and heating.

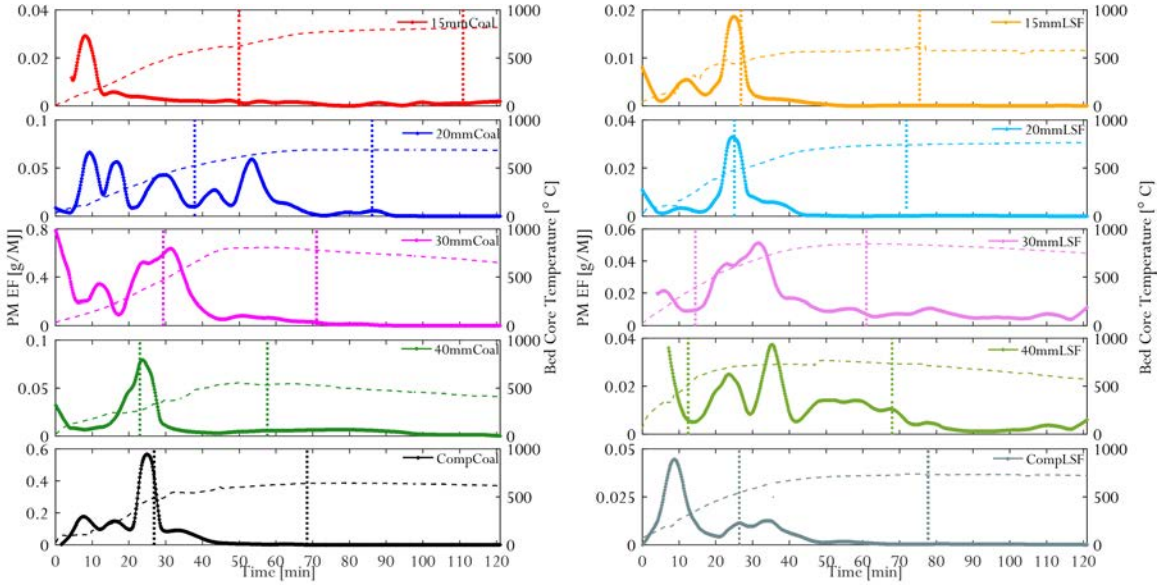

Figure D.5: Time series plots of the PM_{EF} [g/MJ] emission factors. The EFs are shown as the dashed lines against the left-hand side axes and the solid lines along the right-hand side axes are the bed core temperatures.

Table D.5: Coal Fuels VOC Analysis Results [total mg detected]

	15mmCoal	**20mmCoal**	**30mmCoal**	**40mmCoal**	**CompCoal**
Acetone	23.426	2.674	102.557	0.480	2.630
Pentane	77.400	4.941	223.048	1.637	6.648
Hexane	24.639	2.816	87.958	0.794	2.081
Methylethylketone	12.584	1.496	53.042	0.309	1.313
Ethyl Acetate	1.715	0.165	12.642	0.163	0.163
Chloroform	1.472	0.141	4.221	0.140	0.140
1,1,1-Trichloroethane	1.419	0.136	4.071	0.135	0.135
1,2-Dichloroethane	7.067	0.678	20.270	0.673	0.670
Isopropyl Acetate	0.947	0.091	2.717	0.090	0.090
Benzene	80.946	14.807	601.284	5.436	20.807
Cyclohexane	3.124	0.342	12.016	0.106	0.325
Carbon Tetrachloride	3.139	0.301	9.003	0.299	0.298
Isooctane	0.508	0.049	2.387	0.048	0.099
Heptane	15.882	2.056	62.766	0.250	1.474
Trichloroethylene	4.246	0.408	12.177	0.404	0.403
1,4-Dioxane	6.153	0.591	17.648	0.586	0.584
Propyl acetate	1.571	0.151	4.507	0.150	0.149
Methyl Isobutyl Ketone	2.021	0.194	5.796	0.192	0.192
Toluene	46.709	7.177	249.090	1.000	6.880
Isobutyl Acetate	0.657	0.063	1.883	0.063	0.062
Tetrachloroethylene	2.651	0.254	10.049	0.252	0.301
1,2-Dibromoethane	4.527	0.435	12.985	0.431	0.429
Butyl Acetate	3.589	0.344	10.292	0.342	0.340
Chlorobenzene	2.001	0.192	5.740	0.191	0.190
Ethylbenzene	3.909	0.632	21.590	0.125	0.610
m+p-Xylene	7.914	1.316	43.480	0.241	1.154
Styrene	1.476	0.213	9.556	0.126	0.290
o-Xylene	3.273	0.442	16.144	0.118	0.423
Nonane	3.369	0.485	15.173	0.137	0.368
Cumene	0.380	0.043	1.133	0.026	0.039
Propylbenzene	1.211	0.132	4.414	0.115	0.120
1,3,5-Trimethylbenzene	0.629	0.073	3.020	0.060	0.063
1,2,4-Trimethylbenzene	0.865	0.095	4.772	0.082	0.096
Decane	1.083	0.125	6.871	0.110	0.133
Limonene	2.648	0.254	7.594	0.252	0.251
1,2-Dichlorobenzene	1.721	0.165	4.937	0.164	0.163
Naphthalene	1.342	0.129	4.613	0.128	0.127
Naphthas*	43.854	7.038	243.833	1.290	4.271

Table D.6: LSFs VOC Analysis Results [total mg detected]

	15mmCoal	**20mmCoal**	**30mmCoal**	**40mmCoal**	**CompCoal**
Acetone	0.585	0.560	14.221	0.879	0.879
Pentane	1.744	3.151	38.167	3.591	3.591
Hexane	0.765	0.763	11.670	0.884	0.884
Methylethylketone	0.314	0.329	5.640	0.440	0.440
Ethyl Acetate	0.163	0.163	2.970	0.162	0.162
Chloroform	0.140	0.140	2.139	0.139	0.139
1,1,1-Trichloroethane	0.135	0.135	2.063	0.134	0.134
1,2-Dichloroethane	0.673	0.672	10.273	0.670	0.670
Isopropyl Acetate	0.090	0.090	1.377	0.090	0.090
Benzene	8.579	9.259	212.600	11.652	11.652
Cyclohexane	0.105	0.105	1.623	0.133	0.133
Carbon Tetrachloride	0.299	0.298	4.563	0.297	0.297
Isooctane	0.048	0.048	0.738	0.048	0.048
Heptane	0.184	0.226	4.682	0.329	0.329
Trichloroethylene	0.404	0.404	6.171	0.402	0.402
1,4-Dioxane	0.586	0.585	8.944	0.583	0.583
Propyl acetate	0.150	0.149	2.284	0.149	0.149
Methyl Isobutyl Ketone	0.192	0.192	2.938	0.191	0.191
Toluene	0.939	1.153	33.346	2.225	2.225
Isobutyl Acetate	0.063	0.062	0.954	0.062	0.062
Tetrachloroethylene	0.252	0.380	6.111	0.305	0.305
1,2-Dibromoethane	0.431	0.430	6.581	0.429	0.429
Butyl Acetate	0.342	0.341	5.216	0.340	0.340
Chlorobenzene	0.191	0.190	2.909	0.190	0.190
Ethylbenzene	0.096	0.121	3.257	0.214	0.214
m+p-Xylene	0.194	0.212	6.730	0.469	0.469
Styrene	0.126	0.126	1.993	0.154	0.154
o-Xylene	0.094	0.097	2.320	0.186	0.186
Nonane	0.117	0.128	2.570	0.158	0.158
Cumene	0.026	0.026	0.402	0.031	0.031
Propylbenzene	0.115	0.115	1.761	0.115	0.115
1,3,5-Trimethylbenzene	0.060	0.060	0.947	0.063	0.063
1,2,4-Trimethylbenzene	0.082	0.082	1.258	0.082	0.082
Decane	0.099	0.100	1.681	0.106	0.106
Limonene	0.252	0.252	3.849	0.251	0.251
1,2-Dichlorobenzene	0.164	0.164	2.502	0.163	0.163
Naphthalene	0.128	0.128	1.951	0.127	0.127
Naphthas*	1.071	1.153	24.860	1.461	1.461